Seagrass wrack dynamics in Geographe Bay, Western Australia

April 2010

CE Oldham
PS Lavery
K McMahon
C Pattiaratchi
TW Chiffings

AUSTRALIA ECU EDITH COWAN UNIVERSITY
THE UNIVERSITY OF WESTERN AUSTRALIA
Achieve International Excellence
DHI

Clients Department of Transport Shire of Busselton	**Client's representative** James Holder
Project title Seagrass wrack dynamics in Geographe Bay, Western Australia.	**Project No** DPI 1062/07
Authors Carolyn Oldham (UWA) Paul Lavery (ECU) Kathryn McMahon (ECU) Charitha Pattiaratchi (UWA) Tony Chiffings (DHI)	**Date** April 30th 2010
	Approved by Carolyn Oldham
Key words Geographe Bay Seagrass wrack Marine biogeochemistry Hydrodynamics	☒ Open ☐ Internal ☐ Proprietary
Distribution Department of Transport: James Holder Shire of Busselton: Oliver Darby, Sharon Woodford-Jones UWA, ECU, DHI: Team Leaders	**No of Copies** Electronic

TABLE OF CONTENTS

LIST OF FIGURES

LIST OF TABLES

1.1 The Port Geographe problem

Geographe Bay is a large embayment located approximately 200 km to the south of Perth (Figure 2.1). The shallow waters of the bay support extensive seagrass beds (0-14 m) that contribute large volumes of wrack to the local beaches (wrack being seagrass and algal material "cast ashore"). This occurs predominantly during the winter period. In Geographe Bay the wrack is largely made up of seagrass leaves from the two dominant species occurring within the Bay (see Section 2).

The movement of wrack onto the beaches of Geographe Bay has been observed to usually commence with the first winter storms in May. The wrack then continues to accumulate throughout the winter with most of the wrack being removed from the beaches in late winter and early spring.

Along most of the coast, the wrack that collects on the beaches does not unduly affect the people who live closeby. However at Port Geographe, a proportion of the wrack moving onshore is permanently trapped on the western side of the western training wall of the Port Geographe harbour and marina estate; the wrack deposition banks often extend along the beach more than a kilometre to the west of the training wall (Figure 1.1). The Port Geographe harbour entrance was constructed in 1996/97 and consists of two training walls extending 200 m seawards, perpendicular to the coast and into about four metres of water. To the east of the training walls are two groynes that hold pocket beaches. The large volumes of sand and wrack collecting in this vicinity, and the physical intervention needed to remove this material annually, have become major environmental issues that are impacting severely on the amenity of the area for local residents. The mechanical equipment used to remove the sand and wrack also has major impacts due to the use of heavy earthmoving machinery on the beach, loss of beach access, noise, fumes from engines and the release of hydrogen sulfide (H_2S) gas within the wrack. The recent bypassing operation has established that each year, up to 100,000 cubic metres of wrack arrives and is trapped on the shore to the west of Port Geographe.

a) b)

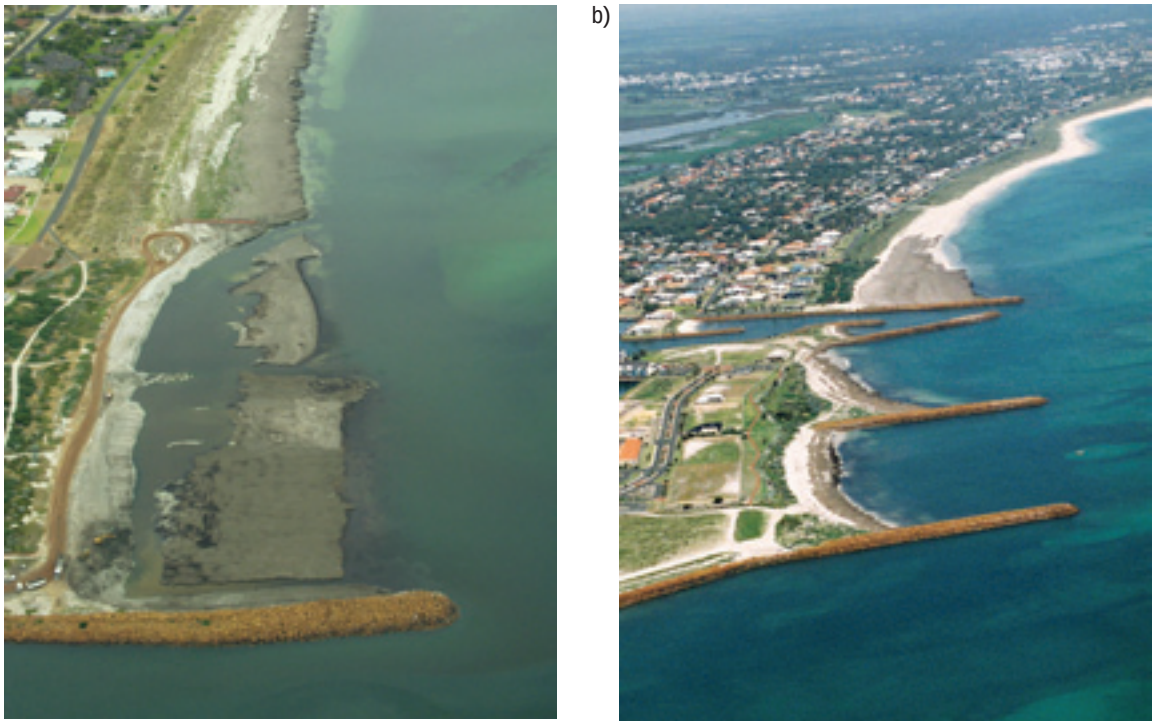

Figure 1.1 Typical accumulation of wrack a) adjacent to the west training wall and b) Moonlight Bay.

The conditions of environmental approval imposed on the Port Geographe development by the State Government required the developer, Tallwood Nominees, to manage the seagrass wrack and sand that collects at and around the harbour entrance. The western training wall or groyne was, in fact, designed to capture sand as it moved from west to east along the beaches, so it could be mechanically bypassed to ensure no likelihood of the beaches to the east being starved of sand. It was originally estimated that 50,000 m^3 per year of sand would be bypassed eastwards in the vicinity of Port Geographe through littoral transport processes. Since the construction of the Port Geographe groynes, smaller volumes of sand have been bypassed each year as a result of limited funds supplied by the developer and technical difficulties created by the trapping of seagrass wrack amongst the sand. This led to beach erosion at Wonnerup Beach, on the eastern side of the port, as well as further accumulation of seagrass wrack to the west and at times accumulation in the port entrance channel.

Early management attempts involved the piles of wrack that collected on the beach being covered with sand, which only further increased the problems as the wrack decomposed and gave off H_2S gas. More recently, the sand and wrack have been mechanically bypassed to Wonnerup Beach, initially by truck and, in the last four years, through both trucking and a pumping system. These management activities involved a major quarrying operation each year with bulldozers, excavators, loaders, dump trucks and pumps working on the beach for at least three months every winter/spring. They have a direct impact on those residents who live nearby, and a further loss of amenity for those who want to use the beach.

When this study started, few details were known of the wrack lifecycle and the processes leading to wrack deposition onto the beach and its subsequent removal. Consequently strategies to reduce the accumulation of wrack on the beach were different to identify. For example, it was not known to what extent the seagrass beds of the bay contributed to the wrack on the beach nor what processes detached leaves or whole plants and moved them ashore. A key question then was what happens to the wrack that is washed from the shore late in winter? Does it remain offshore, move further up the coast or stored relatively close to the beach, only to be brought back again next year? As significant bypassing of the wrack at Port Geographe had only been in operation for five years it was not known if this had been a period of catch up, moving older seagrass stored offshore, or were these levels normal and allowance has to be made for the bypassing of 100,000 m^3 annually?

This study was aimed at improving knowledge of the seagrass in Geographe Bay, and the movement of seagrass wrack within the natural system, with the objective of minimising the need for any physical intervention to remove wrack annually from the beach on the western side of the western training wall at Port Geographe. If practicable, this information then could be used either for analysing options for physical changes to the Port Geographe groynes and/or improving the existing management systems used for sand and wrack bypassing operations.

1.2 The brief from Department of Transport

The Request for Services No. DPI 1062/07, of which this report is a final product, required the research to address a number of tasks. The details for these tasks are provided below:

a. Define a baseline of the existing wrack dynamics at locations within Geographe Bay to allow the Port Geographe situation to be understood within the context of the whole bay,

b. Identify the seagrass species and the biological cycle contributing to the generation of wrack by identify the main species contributing to the supply of wrack; the proportions of each species within the wrack; the mechanisms whereby, and timeframes within, which plants or parts of plants break free from the parent and become available for transportation within the ocean,

c. Identify the properties of the wrack and the impact of these properties on the mechanism for movement of the wrack in its various stages of decomposition, beginning when fresh foliage is detached from the plant, to a point where it has decayed to small particles that can no longer be washed up on the beach,

d. Describe the lifecycle of wrack once the leaf and rhizome material is moving within the water column in terms of how it is stored offshore, is transported around the bay, and is stored onshore,

e. Determine the natural mechanisms, which bring wrack onto the beach, and subsequently remove it and determine where it travels and how fast as well as the influence of wind and ocean generated movements on these,

f. Identify management mechanisms which would improve the natural removal of wrack from the beaches at Port Geographe including a review of M J Paul and Associates Pty Ltd [2005] and make comment on the alternatives for changes to the groyne and entrance structures, and the present bypassing processes. Consideration of alternative recommendations on techniques for managing the wrack including a review of the orientation of beaches to determine whether there is a controlling point at which wrack stranded on the beach will no longer be removed by ocean forces, and

g. Recommend any further work that is needed to improve the understanding of seagrass wrack movement in Geographe Bay in order for effective management decisions to be made at Port Geographe.

At the completion of the services provide a comprehensive report providing all data collected for the project, the analysis of the data and other research, and outcomes (in response to all matters defined within Section 2, Part A 'Specification').

The critical importance of sand bypassing with respect to the Port Geographe configurations has long been recognized, but was not included as part of the study reported here. In a separate study (utilizing the hydrodynamic model developed within the seagrass study) the Department of Transport requires that sediment modelling be undertaken for the preferred entrance configuration options at Port Geographe established within the Seagrass Study. In addition, the brief requires both seagrass wrack and sediment modelling to be done for Wonnerup Beach to establish preferred options for enhanced coastal protection.

The results from this separate sand transport study are to be reported to Department of Transport and Shire of Busselton in August 2010. It is then envisaged that the final conclusions and recommendations from both studies will be re-assessed and a single set of recommendations prepared.

At the commencement of the project, the Contract Authority set up a Steering Committee consisting of representatives of the Department for Planning and Infrastructure, Shire of Busselton, the developer of Port Geographe and the scientific Study team. The Steering Committee acted as a technical liaison group for the study and reviewed progress and direction of the study as it progressed.

1.3 How we have approached the problem

At the start of the Study there was a clearly identified annual cycle already established for wrack movement on and off the beaches. This cycle brings wrack to the beaches in early winter and removes it through the early weeks of spring. The mechanisms that cause these wrack movements are largely influenced by the physical properties of the wind, waves and surges occurring during storm conditions. A more detailed understanding of these mechanisms was required so that better predictions can be made about the behaviour of the wrack in circumstances where changes were planned affecting the configuration of the Port Geographe entrance structures and/or the beach orientation to the west.

The Study Team therefore proposed that numerical modelling form the basis for describing the hydrodynamic processes driving seagrass movement and accumulation in the bay. The intention was to provide a quantitative tool with which to assess management options, as well as an analytical tool for scientific purposes. The numerical modelling includes hydrodynamic and particle transport simulations. The particles within the model have been parameterised to mimic the behaviour of seagrass wrack. While both model elements must be validated, the hydrodynamic simulations can be validated against readily available data, whereas validation of the particle (seagrass) transport simulations is far more challenging.

In considering the practicalities associated with research over a two-year time period and annual funding constraints, it was decided to undertake the work in two stages consistent with the need for two field campaigns over the winter periods. In this way the results from Stage 1 (winter of year 1 - 2008) could be used to further refine the work planned in Stage 2 (year 2 - 2009) prior to it being undertaken.

In Stage 1 of this project, we collected much of the validation data for the seagrass particle transport: quantifying wrack deposition and removal from beaches, documenting hydrodynamic conditions when wrack deposition and erosion occurs and characterising wrack decomposition cycles. The results from this work were presented to the Steering Committee and Shire of Busselton Council in November 2008 and reported in March 2009 [*Lavery et al*., 2009].

Stage 1 of the Project aimed to:

- apply and validate hydrodynamic model MIKE 21 to Geographe Bay,
- characterise baseline conditions for specified Geographe Bay beaches and their seasonal wrack dynamics,
- understand the hydrodynamic conditions which control wrack deposition and erosion on beaches,
- use MIKE 21 to predict on/offshore movement of wrack, and
- characterise wrack properties on specified beaches over the decomposition cycle.

In Stage 2, we combined the results from Stage 1 with the established particle transport and hydrodynamic model to better understand Bay-wide movement of seagrass including establishing key biological parameters such as degradation rates, to test management scenarios and finally, to make recommendations.

Stage 2 of the Project aimed to:

- determine the likely catchment area for wrack generation using the hydrodynamic and transport models,
- conduct a field campaign offshore from Geographe Bay to determine the seagrass species composition and leaf turnover rates within the catchment area over an annual cycle,
- using field and laboratory experiments, determine the decomposition rate of wrack under a variety of conditions,
- refine the particle track module to include wrack settling and erosion rates,
- use the hydrodynamic model with the particle tracking module to simulate the generation, transport and dispersion of seagrass in Geographe Bay and also to simulate the deposition and erosion of seagrass wrack along Geographe Bay beaches, and
- use the hydrodynamic model and knowledge of seagrass movement and wrack decomposition cycles to assess possible management scenarios and make recommendations for improved management of seagrass wrack in Geographe Bay and at Port Geographe.

1.4 The report and how it is structured

This report addresses the findings from the two years of research by first setting out the background to the study (this Chapter). A regional, physical and biological context, including an initial conceptual model of the key processes being studied and modelled, is then provided in Chapter 2. Chapters 3 – 10 provide the scientific results from the two-year study. The final chapter provides a summary of the conclusions from the study and the management recommendation.

2.1 The physiography of Geographe Bay

Geographe Bay sits within the south-west of Western Australia as a large coastal embayment that extends from Cape Naturaliste to the west, past Busselton and around to Bunbury in the north-east (Figure 2.1). The bay has unusually sheltered waters, protected by the Cape from the predominant south-west swell. The bay is very shallow, with a bottom gradient of 2 m km^{-1} until about 15 m water depth. Some of the largest seagrass meadows in Western Australia are found in Geographe Bay.

The south-west region of Western Australia had a population of 152,000 in 2008; the Shire of Busselton had a population of 29,000 [*South West Development Commission*, 2009]. The area is dominated by agricultural and forestry activities, although tourism, weekend recreation and lifestyle residential also have a strong influence.

A network of agricultural drains were constructed during the 1950's to facilitate cattle and sheep farming, potato and lucerne crops. At this time loss of seagrass from the bay was observed, possibly due to increased sediment loads entering the bay.

The sandy soils of the Geographe Bay catchments have very low nutrient retention capacity [*McComb and Davis*, 1993] and as a consequence, high concentrations of nutrients enter the bay [*McMahon et al*., 1997; *McMahon and Walker,* 1998]. In the early 1990s there was concern that the nutrients entering the bay, from sources associated with agriculture and wastewater (225 tonnes of nitrogen and 34 tonnes of phosphorus per year) would negatively impact the marine environment, but at that time no impacts were detected [*McMahon et al.*, 1997].

Since the 1990's, the population of the shires surrounding Geographe Bay has increased markedly, as have the nutrient inputs (409 tonnes of nitrogen and 53 tonnes of phosphorus per year), more than would be required to produce the maximum biomass of seagrass in Geographe Bay [*McMahon and Walker*, 1998]. Recently benchmarking and preliminary impact studies have been undertaken [*Barnes et al.*, 2008]. Localised reductions in cover of *Posidonia* were reported in the bay, around Port Geographe and the Vasse Diversion Drain outlet. On a bay-wide scale, no change in seagrass cover was detected between 2004 and 2007 [*van Niel et al.*, 2009].

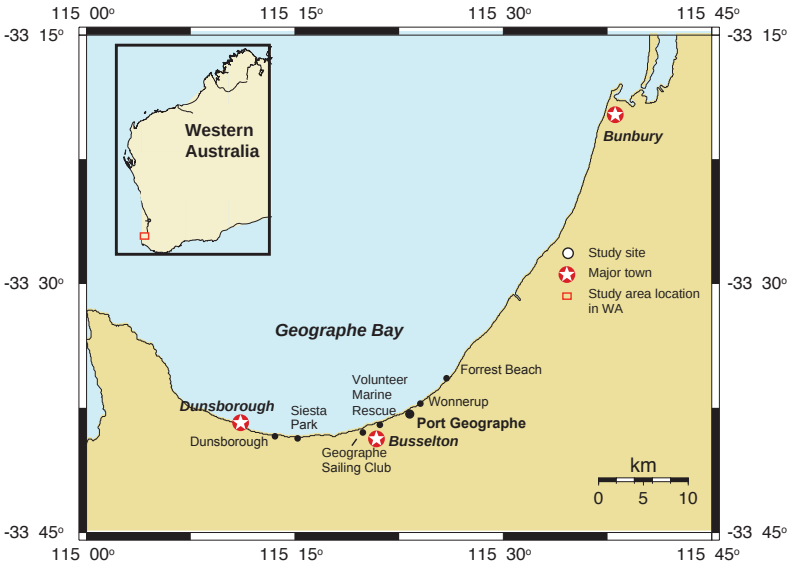

Figure 2.1 Key locations and sites used for this study. The site names are used throughout this report; note that the site "Volunteer Sea Rescue" is the Busselton Volunteer Sea Search and Rescue, and the site "Geographe Sailing Club" is the Geographe Bay Yacht Club.

2.2 Seagrass in Geographe Bay

Seagrasses are marine flowering plants; there are about fifty-five species world-wide with twenty-five species found in Australia, and nine found in Geographe Bay. Seagrasses are important components of near-shore habitats, providing food and shelter for a variety of organisms such as fish and crabs, stabilising sediments and filtering the water. Worldwide the economic value of the ecosystem services they provide, has been estimated at US$19,000 ha^{-1} yr^{-1}, an order of magnitude higher than estimated for coral reefs [*Costanza et al.*, 1997].

Seagrass meadows within Geographe Bay are recognized as a major biotope and form the predominant benthic habitat [*Walker et al.*, 1987]. Extensive meadows exist in the bay from 0 -15 m water depth, with sparser meadows extending down to 30 m water depth [*Barnes et al.*, 2008]. The two main genera of seagrass within the 0 - 15m depth range are *Posidonia* and *Amphibolis* (Figure 2.1) [*McMahon et al.*, 1997]. *Posidonia sinuosa* Cambridge and Kuo has greater than 60% coverage throughout the bay. *Amphibolis antarctica* (Labillardiere) Sonder and Ascherson ex Ascherson is the next most common seagrass species [*Walker et al.,* 1987]. *Amphibolis griffithii* is more common at greater depths. Other species present in the bay include *Posidonia angustifolia*, *Posidonia coriacea*, *Halophila ovalis*, *Syringodium isoetifolium*, *Zostera tasmanica* and *Thallasodendron pachyrhizum*.

The leaves of seagrasses are shed naturally and accumulate within the seagrass meadow. Generally *Posidonia sinuosa* produces about 2 – 3 leaves per plant per year, whilst the other most common species produce about 26 smaller leaves per plant in a year [*Marba and Walker*, 1999]. These shed leaves can be transported to the shore where they accumulate forming beach wrack [*McMahon et al.*, 1997].

Wrack has an important function, providing food and habitat for other organisms on the beach [*Ince et al.*, 2007], in the water near-shore [*Kirkman and Kendrick*, 1997] and for birds [*Dugan et al.*, 2003]. The wrack breaks down on the beach or is transported back into the water.

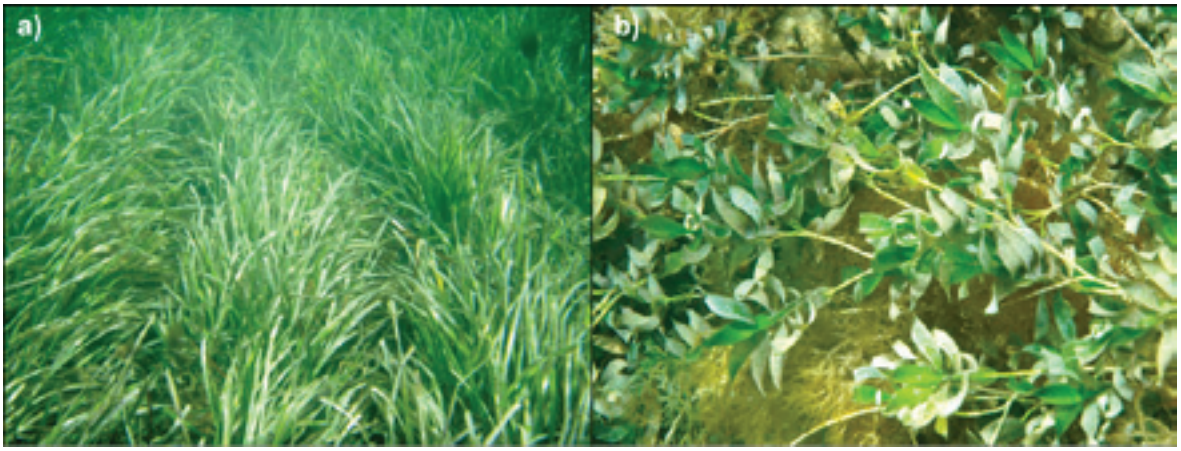

Figure 2.2 a) Meadow of *Posidonia sinuosa* b) Meadow of *Amphibolis antarctica*.

3 OCEANOGRAPHIC PROCESSES IN GEOGRAPHE BAY

3.1 Oceanographic processes

3.1.1 Bathymetry

Geographe Bay has relatively simple bathymetry with mostly gentle gradients. The nearshore area of the bay is characterised by submarine sand bars rising up to 2 m above the flat sea floor [*Fahrner and Pattiaratchi*, 1994]. Water depths gradually increase to 3-4 metres several hundred metres off shore, and then the seafloor slopes gently to the 30 m isobath some 15 km offshore. Beyond that, a very gently sloping platform with an average depth of 40 metres extends to the 50 m isobath some 75 km offshore of Bunbury. From Eagle Bay to the westward point of Cape Naturaliste the bathymetry becomes quite steep, dropping quickly to depths greater than 40 m. The only complexity in the otherwise simple bathymetry is the Naturaliste Reefs, which rise to the surface from a depth of approximately 40 m [*Fahrner and Pattiaratchi*, 1994].

3.1.2 Water level fluctuations

Many processes contribute to relative water levels in south-western Australia with timescales ranging from seconds to hundreds of years [*Pattiaratchi and Eliot,* 2008]. Some of the processes and their relative amplitude in the local region are outlined in Table 3.1. These processes are discussed throughout this section.

Table 3.1 Water level components in south-western Australia [*Pattiaratchi* and *Eliot*, 2008].

PROCESS	DURATION	REFERENCE
Wave action	2–20 seconds	Lemm (1996)
Tidal conditions	12–24 hours	Easton (1970)
Sea breezes	24 hours	Masselink & Pattiaratchi (2001)
Pressure systems (cycle)	1–10 days	Hamon (1966)
Continental shelf waves	3–10 days	Fandry et al. (1984)
Oceanic currents (Leeuwin current)	Seasonal	Pattiaratchi & Buchan (1991)
Oceanographic forcing	Years	Church et al. (2004)
Climate variability	Decades	Pariwono et al. (1986)
Climate change	10^3+ years	Wyrwoll et al. (1995)

3.2 Tides

Astronomic tides are the most widely recognised phenomena affecting water levels. These tides are the harmonic fluctuations of water level developed through the gravitational attraction from astronomic bodies (mainly the sun and moon). The tides measured at the Bunbury tide station are considered representative of the tides experienced along south-western Australia. The four largest constituents are associated with diurnal and semidiurnal effects of the sun and moon (Table 3.2). The relative position of the sun and moon develops a monthly cycle of enhanced (spring) and lowered (neap) tidal ranges as the principal constituents move in and out of phase.

Table 3.2 Principal tidal constituents for Bunbury.

CONSTITUENT	AMPLITUDE (M)	PERIOD (HR)	DESCRIPTION
K_1	0.173	23.93	Principal lunar diurnal constituent
O_1	0.120	25.82	Principal solar diurnal constituent
M_2	0.057	12.42	Principal lunar semidiurnal constituent
S_2	0.053	12.00	Principal solar semidiurnal constituent

South-western Australia experiences a mixed, micro-tidal, mainly diurnal climate, with an astronomic tidal range of 1.2 m. The daily tidal range varies biannually, with solstice tidal peaks occurring around December–January and June–July, producing a monthly tidal range that is about 20% higher than during equinoctial troughs during February–March and September–October. A large, seasonal mean water level signal also occurs, with a 0.22-m average annual range, peaking in June and lowest in November ([*Pariwono et al*., 1986; *Pattiaratchi and Buchan*, 1991]. The combined effect of the seasonal tidal cycle and annual mean sea level cycle produces short periods, which include high and low water levels during May–June and December–January, respectively.

Along south-western Australia, the tide's diurnal component has a range of 0.6 m, and the semidiurnal tide has a range of only 0.2 m. The semidiurnal tidal range is related to the lunar cycle, with the maximum tidal range occurring close to the full and new moons, and minimum tidal ranges occurring close to the lunar cycle's first and last quarters—the spring–neap cycle. Diurnal tides are related to the declination angle of the moon's orbital plane. The diurnal and semidiurnal tides oscillate at a frequency of 13.63 and 14.77 days, respectively. This phase difference, of 1.14 days, between the two tidal signals modulates the resultant tide over an annual cycle, causing the diurnal and semidiurnal tides that are in phase during the solstice (resulting in a maximum "spring" tidal range) and out of phase at the equinox (resulting in a minimum "spring" tidal range). This means the highest tidal range (the "spring" tide) does not always correspond with the full/new moon cycle.

During the solstice, when the diurnal and semidiurnal tides are in phase, the maximum tidal range corresponds with the full/new moon cycle; during the equinox, the maximum tidal range does not correspond with the full/new moon cycle. Mixed tides occur during "neap" tides closest to the equinox, with two high and low waters commonly observed over a tidal cycle. Hence, in a diurnal tidal system, such as along south-west Australia, definitions such as spring and neap tides do not always relate to phases of the moon, as is the case for semidiurnal tides.

Another consequence of the diurnal tides is the seasonal change in the times of high/low water. During the summer, the low water generally occurs between 4 am and 12 pm, depending on the phase of the moon, with high water in the evening. As summer progresses, the low water occurs earlier; as winter starts, the low water occurs later at night, becoming progressively earlier in the evening (with high water occurring in the morning).

Geographe Bay experiences a mixed, micro-tidal, mainly diurnal climate, with an astronomic tidal range of 1.2 m. The daily tidal range varies biannually, with solstice tidal peaks occurring around December–January and June–July, producing a monthly tidal range that is about 20% higher than during equinoctial troughs during February–March and September–October. A large, seasonal mean water level signal also occurs, with a 0.22 m average annual range, peaking in June and lowest in November [*Pariwono et al.*, 1986; *Pattiaratchi and Buchan*, 1991]. The combined effect of the seasonal tidal cycle and annual mean sea level cycle produces short periods, which include high and low water levels during May–June and December–January, respectively.

The tidal range in Geographe Bay is small (~ 0.5 m) due to an amphidromic point located offshore of Cape Naturaliste. The tides are mixed, both diurnal (one high and one low tide per day) and semi-diurnal (two high and two low tides per day). The soli-lunar diurnal (K1) and main lunar diurnal (O1) have amplitudes of 0.12 and 0.122 m respectively [*Noreika*, 1995]. The Australian National Tide Tables [*Australian Hydrographic Office*] has values for K1 and O1 of 0.12 and 0.18 m respectively for Busselton. These National Tide Tables also indicate that tidal magnitudes vary minimally through the area and are only offset in time on the order of minutes.

3.3 Atmospheric storm surges

Direct atmosphere-induced forcing on the ocean includes wind stress on the water surface and water level changes in response to barometric pressure variation. It is often hard to distinguish between these phenomena, as most synoptic systems generate geostrophic winds associated with the rotation of the pressure systems.

The relationship between pressure and water level is termed the inverse barometer effect, with lower pressures raising the water levels. A conventional estimate for response is that a 1-hPa pressure change develops a 1-cm water level change. However, this effect relates to only local-scale pressure variations, and reflects the deviation from regional-scale pressure behaviour. This relationship is not apparent over longer times, particularly seasonal shifts. Mean water levels and barometric pressures increase over winter in south-west Australia. Hence monthly means of water level and pressure are positively correlated, but detrended daily means are negatively correlated.

The effect of pressure system translation further complicates the relationship between barometric pressure and surface water level. Although Proudman [1953] found a theoretical relationship for the effect of system speed on the barometric surge, the effect of distance from the system centre was not defined. In south-western Australia, there are several types of synoptic storm systems, which can be centred anywhere up to a thousand kilometres from the coast. These systems include mid-latitude depressions, cutoff lows, troughs, extra-tropical highs, and occasional tropical cyclones [*Steedman and Craig*, 1983].

Winds blowing across the ocean surface create stress on the water. A portion of the transferred energy develops waves, with another portion contributing to the water column's motion. The coastal boundary, through which flow cannot pass, may restrict the nearshore currents. Hence onshore wind causes water to pile up at the shore; this is known as wind set-up. Offshore winds results in lower water levels near the shore. The significance of wind set-up was acknowledged for the south-west in the Australian National Tide Tables [*Australian Hydrographic Office*]. In Geographe Bay this effect is thought to be significant and of the same order as astronomic tides. Storm surge levels at Bunbury were found to occur with a range of 0.4 to 1.05 m in the period 1930 - 1980. Comparison of the tidal records at Bunbury and Busselton shows there is little difference in the water levels even for extreme events like cyclone Alby which resulted in a water level of 2.48 m above the chart datum [*Fahrner and Pattiaratchi*, 1994; *Wearne*, 2000].

Busselton water levels for 2008 are shown in Figure 3.1. A filter has been applied to show observed water levels, tidal components, and storm surges (72 hour filter). The frequency and height of the peaks in the plot of storm surges for 2008 indicates that July was a relatively stormy month while almost no storm events occurred in August, similar to the month of January.

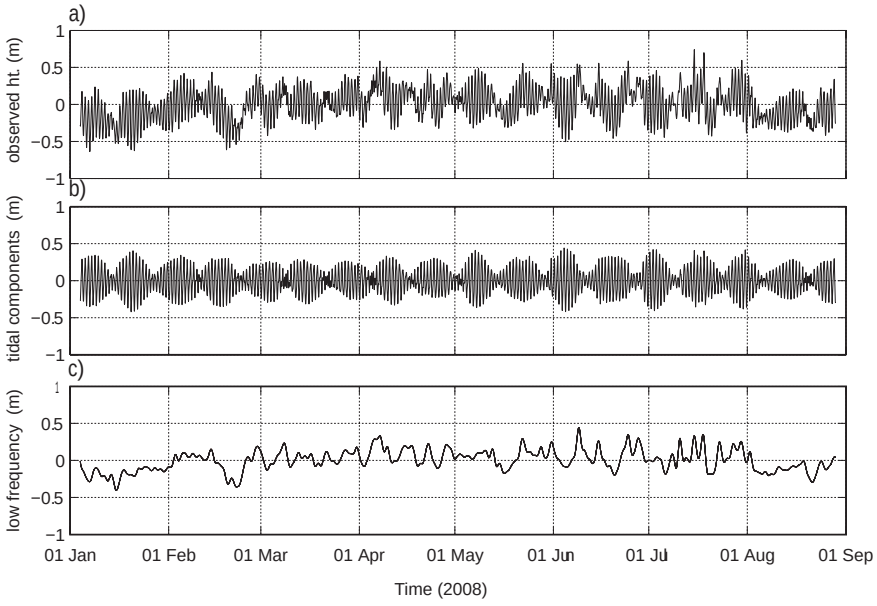

Figure 3.1 Time series of (a) observed; (b) tidal; and, (c) storm surges at Busselton during the period 1 Jan to 1 Sep 2008.

3.4 Coastal-trapped waves

The power spectra of sea level (Figure 3.2) indicates a broad peak in energy in the 'weather' band (5 - 20 days) and these are generally due to atmospheric effects. Closer examination and comparison of the tidal residuals with local meteorological data revealed a number of significant tidal residuals that were not fully explained by local synoptic conditions but were a combination of locally generated and remotely generated signals, the former through local changes in atmospheric pressure and local wind. The remote signal is characteristic of a long period coastally trapped shelf wave, travelling anti-clockwise relative to the Australian coast.

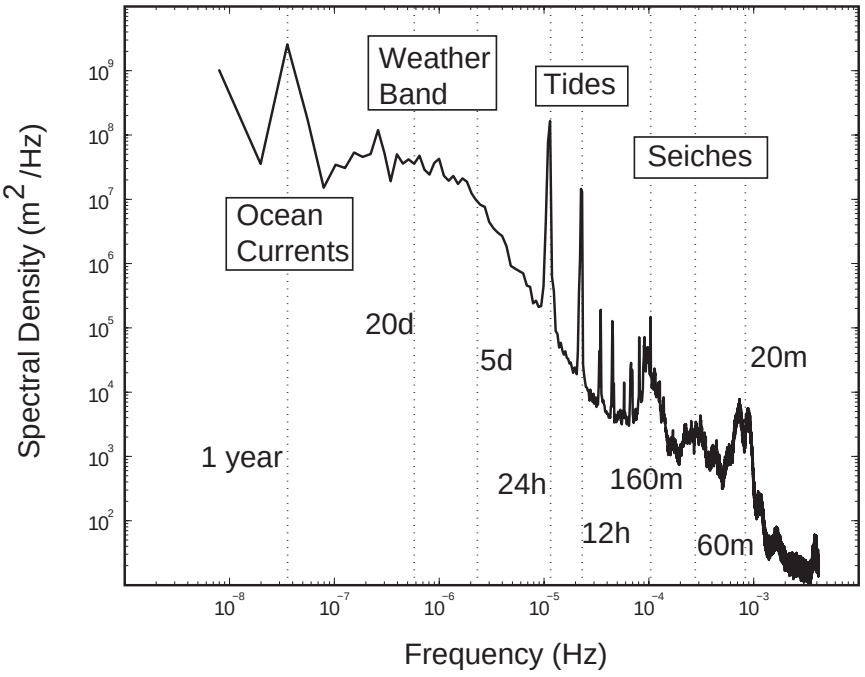

Figure 3.2 Spectra of water levels at Fremantle showing the different scales of variability.

A coastally trapped wave is defined as a wave that travels parallel to the coast, with maximum amplitude at the coast and decreasing offshore. Examples of these waves include continental shelf waves (CSWs) and internal Kelvin waves [*Le Blond* and *Mysak*, 1978] which are governed through vorticity conservation [*Huyer*, 1990]. Coastally trapped waves need a shallowing interface and may develop a range of modes according to the shelf structure [*Tang and Grimshaw*, 1995]. They travel with the coast to the left (right) in the southern (northern) hemisphere. Along the Australian coast, shelf waves propagate anti-clockwise relative to the landmass. All these wave types propagate along the coastal boundary, with the wave signal reducing in amplitude with distance offshore.

Continental shelf waves (CSWs) depend on only the cross-shelf bathymetry profile and the vertical density profile controls the structure of an internal Kelvin wave [*Huyer*, 1990]. The alongshore component of wind stress usually generates CSWs, which are active along the Western Australian coast, that were first reported by Hamon [1966]. Provis and Radok [1979] demonstrated that these waves propagate anti-clockwise along the south coast of the Australian continent over a maximum distance of 4000 km at speeds of 5–7 m s^{-1}.

Along the Western Australian coastline, the continental shelf waves are generated through the passage of mid-latitude low-pressure systems and tropical cyclones. The continental shelf waves can be identified from the sea level records by low-pass filtering (i.e. removal of the tidal component). An example is shown on Figure 3.3 for tidal records from Geraldton, Fremantle and Albany. Several CSWs with amplitudes ranging from 0.1 to 0.5 m can be identified. For example, between days 290 and 295, an increase of ~0.5 m in the sub-tidal water level was observed at Geraldton. The same variation in water level signal was seen at Fremantle and Albany, and could be attributed to the passage of

a CSW. The correlation coefficients between sub-tidal water levels at these three locations were all greater than 0.8, despite observations being several hundred kilometres apart. The propagation time of the CSW between Geraldton and Fremantle was 23 hours, and between Fremantle and Albany it was 17 hours, yielding a mean propagation speed of ~500 km day^{-1} (~ 6 m s^{-1}). The period of the continental shelf wave range between 3 - 10 days and corresponds to the passage of synoptic systems from west to east across the Western Australian coastline.

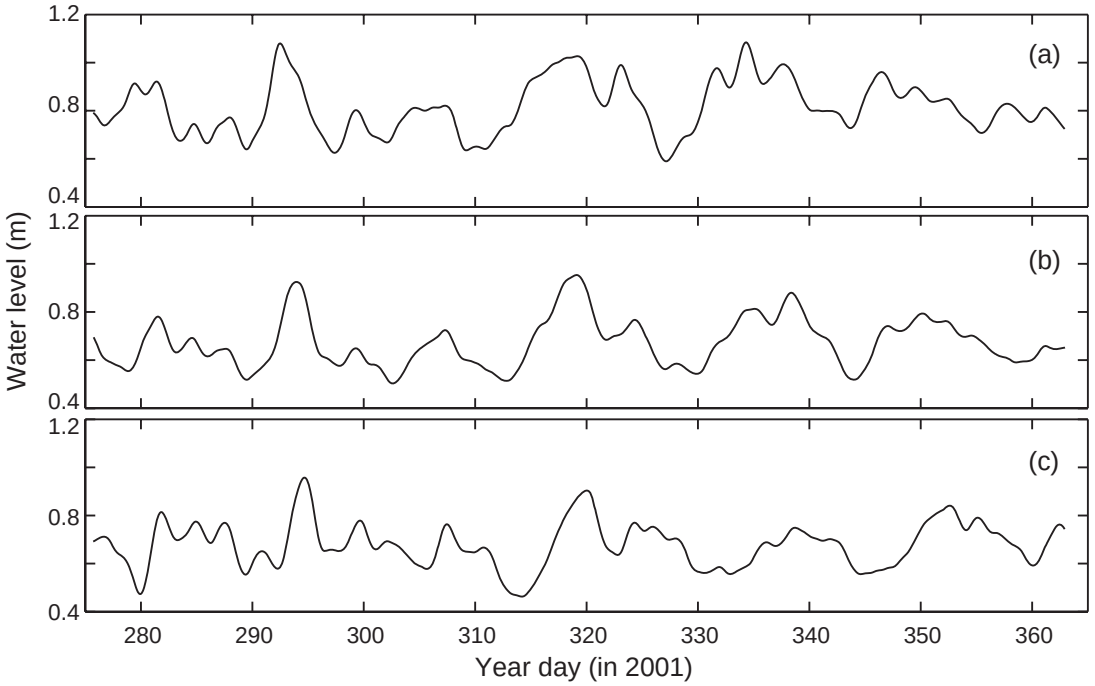

Figure 3.3 Low-frequency water levels at (a) Geraldton, (b) Fremantle, and (c) Albany for days 275 to 365 in 2001 showing the presence of continental shelf waves (from O'Callaghan *et al.* [2007]).

Tropical cyclones are intense low pressure systems which form over warm ocean waters at low latitudes and are associated with strong winds, torrential rain and storm surges (in coastal areas). They may cause extensive damage as a result of strong winds and flooding (caused by either heavy rainfall and/or coastal storm surges). The impacts of tropical cyclones on the north-west region of Australia are well known with several severe cyclones impacting this region over the past few years. The most noticeable impacts of these cyclones are normally restricted to the region of impact of the cyclone, and hence the direct effect of cyclones on south-western Australia is rare. Fandry *et al*. [1984] identified 1 to 2 m amplitude peaks in sea level propagating southwards with speeds ranging between 400 - 600 km day^{-1}. These were associated with tropical cyclones travelling southward and were attributed to a resonance phenomenon when speeds of the southward component of the cyclone speeds were close to the southward propagating continental shelf wave.

Sea level records at Fremantle indicate remote forcing due to tropical cyclones. Comparison between the low frequency component of sea level records along the west and south coasts of Western Australia with the occurrence of tropical cyclones in the North-West shelf region has revealed that every tropical cyclone, irrespective of its severity and path, generated a southward propagating sea level signal or a continental shelf wave [*Eliot and Pattiaratchi*, submitted]. The wave can be identified in the coastal sea level records, initially as a decrease in water level, 1 - 2 days after the passage of the cyclone and has a period of about 10 days. As an example, water level record at Fremantle for the period 1 - 19 December 1995 is shown on Figure 3.4. Tropical cyclone Frank was declared as a category 1 cyclone on 7 December and developed into a category 4 cyclone by 11 December and crossed the coastline near Carnarvon on 12 December. The evidence of the continental shelf wave becomes evident on 8 December when the water level starts to decrease and reaches a minimum level on 10 December and a maximum peak on 14 December. The wave height (trough to crest) was 0.55 m, higher than the tidal range during this time (Figure 3.4).

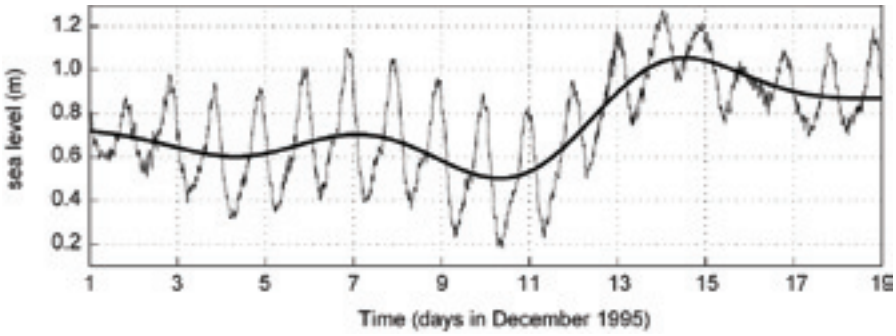

Figure 3.4 Sea level record at Fremantle (thin black line) during December 1995 showing the low-frequency water level variation (thick-line) induced by Tropical Cyclone Frank.

3.5 Currents

3.5.1 The Leeuwin Current

The major oceanic-scale forcing along the Western Australian coast is due to the Leeuwin Current, a poleward eastern boundary current. The Leeuwin Current is a shallow (< 300 m), narrow band (< 100 km wide) of warm, lower salinity water of tropical origin, which flows southward, mainly above the continental slope from Exmouth to Cape Leeuwin [*Church et al.*, 1989; *Ridgway and Condie*, 2004; *Smith et al.*, 1991]. The maximum flow of the current is located at the 200 m isobath. At Cape Leeuwin it pivots eastward, spreads onto the continental shelf and flows towards the Great Australian Bight. It is now accepted that the Leeuwin Current signature extends from North West Cape to Tasmania as the longest boundary current in the world [*Ridgway and Condie*, 2004].

There is general consensus that the driving force of the Leeuwin Current is an alongshore geopotential gradient (also called steric height gradient). The source of the Leeuwin Current water is the Indian Ocean from the west, with a component from the North West continental shelf, which originates from the Pacific Ocean. The south-east trade winds in the Pacific Ocean drive the South Equatorial Current westwards advecting warm surface waters towards Indonesia. This results in the flow of warm, lower salinity water from the western Pacific Ocean through the Indonesian Archipelago into tropical regions of the Indian Ocean. The warmer, lower salinity, lower density water in the north-east Indian Ocean and colder, higher salinity, higher density water off south-western Australia results in a surface slope of ~4 x 10^{-7} (from north to south), relative to the surface 0 – 300 dB level, between latitudes 15 and 35° S. This corresponds to a sea level difference of 0.55 m between North West Cape and Cape Leeuwin. From October to March, the Leeuwin Current is weaker as it flows against the maximum southerly winds, whereas between April and August the current is stronger as the southerly winds are weaker [*Godfrey and Ridgway*, 1985]. This is reflected in the mean sea level at Fremantle. Here the sea level is higher between April and August when the Leeuwin Current is stronger (lower wind stress) and lower between October and January when the current is weaker (high wind stress). Thus although the Leeuwin Current flows all year round, it exhibits a strong seasonality, with the stronger flows occurring during the winter (May to July). The location of the 'core' of the current also changes seasonally; in winter the core of the current is pushed close to the 200 m contour by the westerly winds, whereas in summer the southerly wind stress pushes the current offshore (Figure 3.5).

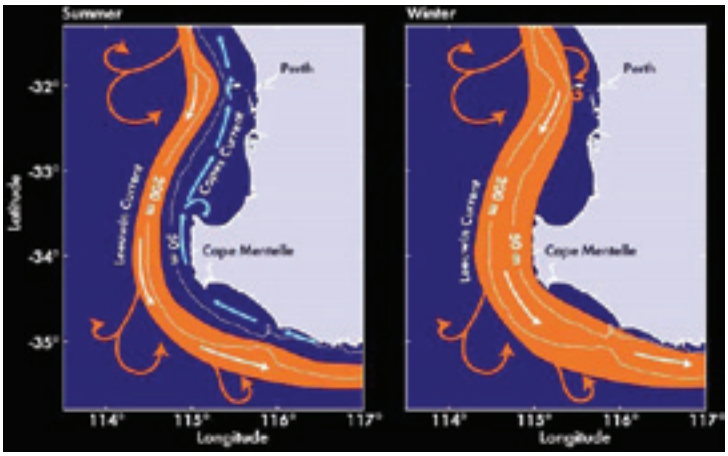

Figure 3.5 Schematic of surface currents off south-western Australia; during the summer the northward flowing Capes Current is located on the inner shelf and bounded offshore by the Leeuwin Current. In winter the Leeuwin Current is located farther inshore [*Hansen*, 1984].

3.5.2 The Capes Current

Pearce and Pattiaratchi [1999] defined the Capes Current as a cool inner shelf current, originating from the region between Capes Leeuwin (34° S) and Naturaliste, which moves towards the equator along the south-western Australian coast in summer and extends northwards past the Abrolhos Islands. The Capes Current seems to be well established around November, when winds in the region become mostly southerly because of the strong sea breezes [*Pattiaratchi et al.*, 1997] and continues until about March when the sea breezes weaken. Gersbach *et al*. [1999] showed the Capes Current source water was from upwelling between Capes Leeuwin and Naturaliste, which was augmented by water from the south to the east of Cape Leeuwin.

Gersbach *et al*. [1999] described the dynamics of the Capes Current, off Cape Mentelle. The continental shelf in Australia's south-west comprises a step structure, with an inner shelf break at 50 m and an outer shelf break at 200 m [*Pearce and Pattiaratchi*, 1999]. This bathymetry influences the circulation, especially in the summer. In the summer, the alongshore wind stress overwhelms the alongshore pressure gradient on the inner shelf (depths < 50 m), moving surface layers offshore, upwelling colder water onto the continental shelf, and pushing the Leeuwin Current offshore (Figure 3.6). Here, the Capes Current is present on the inner shelf and bounded offshore by the Leeuwin Current on the lower shelf, with upwelling occurring over the inner shelf break [*Gersbach et al.*, 1999]. Numerical model results showed a wind speed of 7.5 ms^{-1} was sufficient to overcome the alongshore pressure gradient on the inner continental shelf [*Gersbach et al.*, 1999]. The Leeuwin Current strengthens in the winter, and, in the absence of wind stress, migrates closer inshore, flooding upper and lower terraces [*Pearce and Pattiaratchi*, 1999].

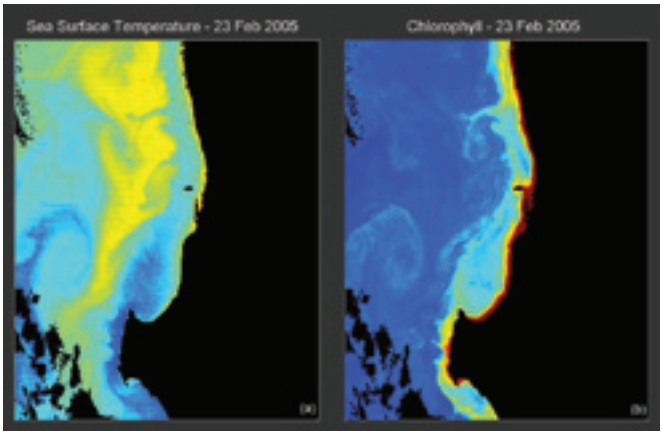

Figure 3.6 Ocean colour images off south-western Australia showing the sea surface temperature and the upwelling of cold water onto the Capes Current with the associated high chlorophyll a concentration.

Although the Capes Current extends from Cape Leeuwin to past the Abrolhos Islands, the most intense upwelling, and therefore the highest concentration of surface chlorophyll a (Figure 3.6), occurs between Capes Naturaliste and Leeuwin, as the winds are strongest along this section of the coast compared with the north.

3.6 The wind field

The weather systems along south-western Australia are dominated by anti-cyclonic high-pressure systems with periodic tropic and extra-tropical cyclones (mid-latitude depressions) and local seasonal sea-breezes [*Eliot and Clarke*, 1986]. Anticyclones move to the east and pass the coast every 3-10 days [*Gentilli*, 1972]. The seasonal movement of the high-pressure systems across the south-west of Western Australia, contributes to the strong seasonality in the wind regime (Figure 3.7). The location of the anti-cyclonic band migrates from around 38°S in summer, generating mainly offshore winds, to around 30°S in winter, producing mainly onshore winds [*Gentilli*, 1972]. Tropical cyclones track down from the northwest coast infrequently during late summer and can have a significant impact on the coastline [*Eliot and Clarke*, 1986; *Lemm*, 1996].

Sea breezes, which are stronger during the summer dominate the coastal region including the Mentelle sub-basin, with offshore (westward) winds in the morning and strong (up to 15 m s^{-1}) sea breezes commencing around noon and weakening during the night [*Pattiaratchi et al.*, 1997]. Unlike the 'classic' sea breeze, these sea breezes blow parallel to the coastline; their onset is rapid, initial velocities are relatively high, and the surface currents respond almost instantaneously [*Masselink and Pattiaratchi*, 2001].

During winter, the region is subject to the passage of frontal systems, and ~30 storm events are experienced [*Lemm et al.*, 1999]. During the passage of a frontal system, the region is subject to strong winds (up to 25 – 30 m s^{-1}) initially from the north-west, and then over 12 – 16 hours changing to westerlies and then south-westerlies. The south-westerly winds gradually weaken over two to three days, and calm, cloud-free conditions prevail for another three to five days before the passage of another frontal system.

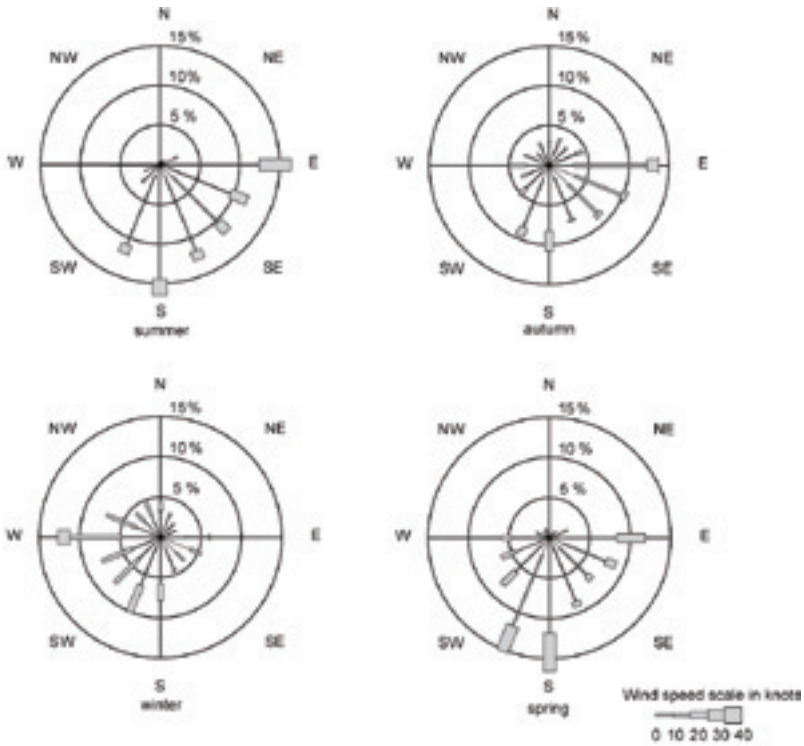

Figure 3.7 Wind roses from Cape Naturaliste constructed using data recorded in 2006 and 2007 (two years) showing the seasonal variation in the wind field.

3.7 Wave climate

The surface gravity waves reaching the Geographe Bay study area are a combination of swell developed in the Indian and Southern Oceans and locally generated wind waves [*Fahrner and Pattiaratchi*, 1994]. The wave climate therefore is dominated by these two types of waves.

South-west swells are refracted around Cape Naturaliste and arrive at different sections of the Western Australian coast with varying heights and angles. Geographe Bay is well protected from these swell waves by Cape Naturaliste, with gradually increasing exposure from south to north. The swell waves typically have periods of 10 - 14 s and heights (within the bay) of up to 2 m in winter but generally less than 1m in summer.

Wind waves generated by local winds are short-crested with periods of 5 - 10 s. Wave direction is strongly dependent upon wind direction. Geographe Bay is well exposed to these waves during north-westerly winter storms or cyclonic events. Wind wave heights can become quite large during winter, but are generally less than 1 metre in summer [*Fahrner and Pattiaratchi*, 1994].

The wave refraction diagram (Figure 3.8) demonstrates the wave shadowing effect of Cape Naturaliste on the predominant south-west swells as they refract into Geographe Bay. In the diagram, wave rays represent wave energy approaching from the south-west. At Cape Naturaliste the wave rays spread out as they are refracted toward the coast. Constant wave energy is maintained between wave rays, but distance between wave rays varies along the coast. Busselton is located within the zone where a unit of wave energy is spread over a large distance, resulting in a low wave climate most of the year. During winter storms, when waves approach from the west or north-west, Cape Naturaliste does not provide this protection and larger waves reach the shore at the base of Geographe Bay.

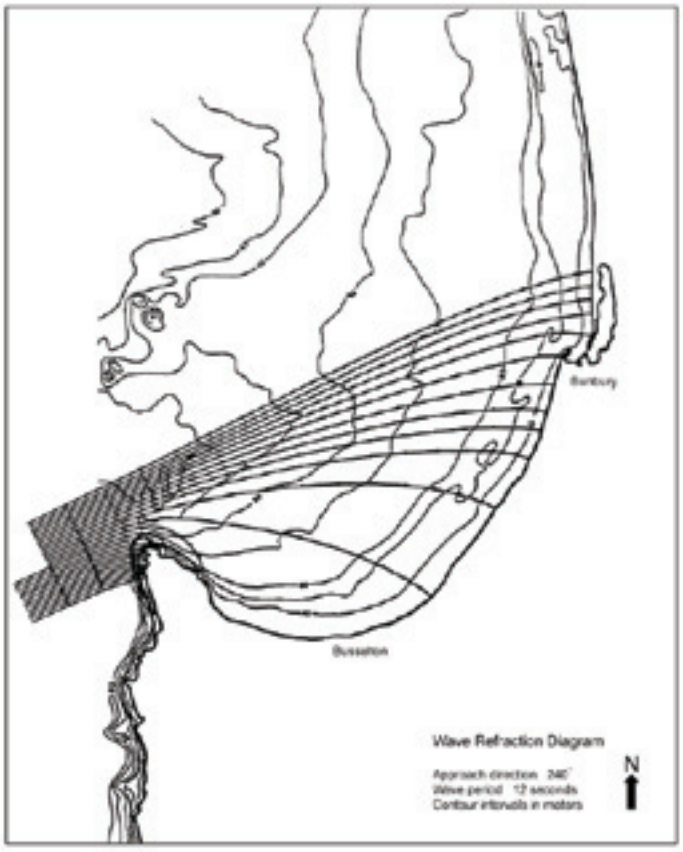

Figure 3.8 Wave refraction diagram for Geographe Bay.

4 WRACK GENERATION

4.1 Spatial and temporal variation in wrack generation

A primary requirement for understanding the lifecycle of seagrass in Geographe Bay is determining the sources of wrack, the rate of wrack generation and whether the rate of generation varies between locations and at different times of the year.

4.1.1 Objective

To determine the distribution and composition of seagrass in Geographe Bay and the rate of wrack generation by *Posidonia sinuosa* and *Amphibolis antarctica* in autumn and winter.

4.1.2 Methods

4.1.2.1 Seagrass cover in Geographe Bay

The area of seagrass meadows in Geographe Bay was determined from previous mapping studies [*van Niel et al.*, 2009] that were verified by ground-truthing during this two-year project. To calculate wrack generation rates, four zones were delineated within the broader area, according to depth (5 m or 10 m) and latitude across the bay (Siesta Park and Forrest Beach). In each of the four zones, the area of both seagrass meadows and unvegetated sediments were calculated using ESRI ArcGIS 9.3 software (Figure 4.1).

Seagrass species composition within the zones was estimated from a number of sources [*Barnes et al.*, 2008; *Walker et al.*, 1995; *Walker et al.*, 1987]. While the surveys of Walker *et al.* [1987] and [1995] are dated, they sampled the seagrass meadows randomly from Eagle Bay to Leschenault Inlet, and across 1993-1994, making these data the most comprehensive and representative surveys of seagrass undertaken in Geographe Bay. The more recent study of Barnes *et al.* [2008] included only locations where *P. sinuosa* was present, so is not fully representative of the species composition in Geographe Bay. Walker *et al.* [1995] and Barnes *et al.* [2008] used a number of common sites, which showed generally consistent species composition despite the two studies being undertaken 15 years apart. Based on the consistency at the common sites, we used the data from Walker *et al.* [1995] to characterize the seagrass composition in the study area.

4.1.2.2 Seagrass shoot density and biomass

Seagrass shoot density and biomass of *P. sinuosa* and *A. antarctica* were determined at two locations (Siesta Park, Forrest Beach, Table 4.1) and at two water depths (5, 10m) on 14-17 April and 11 August 2009. At each site, areas dominated by *P. sinuosa* and *A. antarctica* were identified and within each area, all above-ground biomass was collected from ten 20 x 20 cm quadrats. Samples were stored frozen and processed on return to the laboratory. For *P. sinuosa*, the number of shoots and leaves per shoot were counted, and for *A. antarctica*, the number of stems counted. Samples were then dried at 60°C for 24 hours to determine dry weight (DW).

Table 4.1 GPS coordinates of the four sites used for shoot density, biomass and wrack generation studies.

SITE	DEPTH (M)	EASTING	NORTHING
Forrest Beach	5	50 H 0353582	6280864
Forrest Beach	10	50 H 0342501	6282348
Siesta Park	5	50 H 0336571	6275712
Siesta Park	10	50 H 0336006	6277434

This study presents the first estimates for reported wrack generation rates for Geographe Bay. Wrack can be generated through:

a. Whole leaf shedding (*P. sinuosa* only);

b. Partial leaf loss through necrosis and erosion of leaf tips (*P. sinuosa* only);

c. Stem removal (*A. antarctica* only); and,

d. Complete shoot removal (*P. sinuosa* only).

Following sampling and data analysis, estimates for partial leaf loss (b) and complete shoot removal (d) were abandoned due to irreconcilable differences in shedding estimates. In any event, partial leaf loss rates were captured within the whole leaf shedding rate estimates. Consequently, wrack generation was estimated from whole leaf shedding (*P. sinuosa*) (a) and *A. antarctica* shoot removal (c). Wrack generation was estimated at the two locations and depths described above (Table 4.1), in autumn (14 April – 8 May) and winter (14 – 29 July) 2009. Due to storm activity prohibiting recovery of samples, in particular at the Forrest Beach 5m site, estimates of leaf turnover times was conducted again from 29 July and from 11 September.

a. Whole leaf shedding (*P. sinuosa*)

To determine rates of wrack generation by leaf shedding, shoot tagging was undertaken to estimate leaf extension rates and, based on the size of the leaf, estimates of leaf turnover time. At time zero (T_0) approximately 40 - 50 shoots of *P. sinuosa* were tagged at each site and depth. A central picket with a sub-surface buoy was installed in the middle of the *P. sinuosa* meadow; a large peg with flagging tape was placed ~ 2-3 m from the central star picket in four random directions. Approximately 15 shoots were then tagged in very close proximity to the peg. Each shoot was tagged with a leather punch just above the leaf sheath, and the number of leaves per shoot and length of each leaf within the shoot, were measured with a ruler to the nearest 0.5 cm. A numbered cable tie was placed at the base of the tagged shoot so that measurements could be matched at time one (T_1). At T_1, tagged shoots were collected and leaf extension, leaf length and leaves per shoot measured.

b. Stem removal (*A. antarctica*)

To determine rates of wrack generation by stem removal (generally through storm damage) tagging of stems was undertaken. At T_0, approximately 80 stems of *A. antarctica* were tagged at each site and depth. A central picket with a sub-surface buoy was installed in the middle of the *A. antarctica* meadow. A large peg was placed ~ 4 m from the central star picket, and then 4 permanent quadrats pegged, evenly spaced and ~ 1 m apart. Within each quadrat, stems were counted and marked with plastic garden wire at their base. At T_1, tagged stems were re-counted to assess change in stem density, and any untagged stems (new growth) also noted. These plots were then revisited for the winter tagging.

To convert wrack generation estimates into biomass, an average weight of each seagrass species was taken. The mean dry weight of stems (stem plus leaves) collected for shoot density was used for *A. antarctica*. For *P. sinuosa*, a leaf length by weight regression was calculated from leaves collected in the winter productivity samples.

4.1.3 Results

4.1.3.1 Seagrass cover in Geographe Bay

Van Niel *et al*. [2009] mapped seagrass cover from Peppermint Beach north of Capel River (S 33°30'59.6", E 115°30'49.6") to Eagle Bay (S 33°25'23.5", E 111°58'05.6"). In 2007, within this area there were approximately 8,725 ha of seagrass meadow and 3,628 ha of unvegetated sediment. Forrest Beach at 10 m water depth had the greatest cover of both *P. sinuosa* and *A. antarctica*, while Forrest Beach at 5 m water depth had the least cover of *P. sinuosa* and Siesta Park had the least cover of *A. antarctica* (Figure 4.1, Table 4.2).

Table 4.2 Estimates of seagrass area in the four zones used to determine wrack generation rates (see Figure 4.1).

REGION	SITE	% COVER			
(Barnes *et al*. 2008)	(Walker *et al*. 1995)	*P. sinuosa*	*A. antarctica*	Sand	Total seagrass
Western		65 ± 9	24 ± 7	2 ± 1	91 ± 4
	Toby's inlet	66 ± 7	21 ± 5	12 ± 2	88 ± 2
	Dunsborough	44 ± 9	17 ± 6	27 ± 8	73 ± 8
Central		74 ± 9	18 ± 10	4 ± 2	91 ± 2
	Busselton Jetty	87 ± 9	10 ± 6	4 ± 3	96 ± 3
	Buayanup Drain	91 ± 5	3 ± 2	4 ± 2	96 ± 2
Eastern		49 ± 8	28 ± 7	1 ± 1	87 ± 5
	Forrest Beach	13 ± 2	29 ± 3	11 ± 3	88 ± 4
	Vasse/ Wonnerup	79 ± 16	3 ± 1	3 ± 2	97 ± 2

4.1.3.2 Seagrass species composition

The composition of seagrass recorded by Walker *et al.* [1995] was generally consistent with that of Barnes *et al*. [2008] though the latter noted lower *P. sinuosa* and higher *A. antarctica* cover than Walker *et al*. [1995] in the central region (Table 4.3). Overall, *P. sinuosa* dominated throughout Geographe Bay, ranging from 44 ± 9 % cover at Dunsborough to 91 ± 5% cover at Buayanup Drain. Forrest Beach was the only site showing a significant cover of *A. antarctica* (29 ± 3 % cover).

Table 4.3 Comparison of species composition and cover from Walker *et al*. (1995) and Barnes *et al*. (2005)

SITE	AREA (ha)			% VEGETATED
	Total	*P. sinuosa*	*A. antarctica*	
Siesta Park 5 m	3494.1	1704.6	280.1	58.5
Forrest Beach 5 m	2211.7	1150.3	373.2	66.1
Siesta Park 10 m	3353.5	1609.3	267.1	54.6
Forrest Beach 10 m	5234.2	2818.9	883.6	69.7
Total	**14473.5**	**7283.1**	**1804.0**	

For further estimates of wrack generation (see below) cover data from Walker *et al*. [1995] (Table 4.3) were aligned with zones delineated for the current investigation (Figure 4.1). As Walker *et al*. [1995] did not measure difference in percent cover by depth, data are assumed equal for 5 m and 10 m depths.

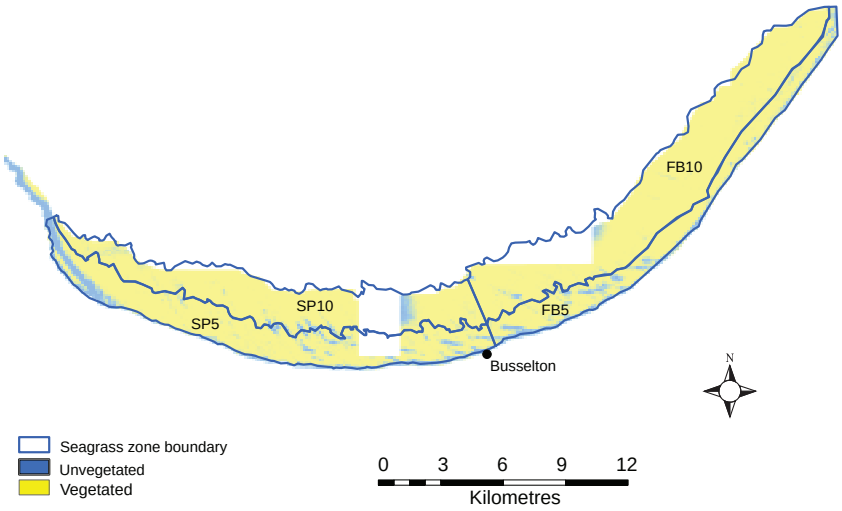

Figure 4.1 Geographe Bay seagrass distribution. Areas bordered by blue indicate zoning for Siesta Park five and ten metre deep sites (SP 5 and SP 10) and Forrest Beach five and ten metre sites (FB 5 and FB 10) used for calculating wrack generation estimates.

4.1.3.3 Seagrass meadow shoot density

P. sinousa shoot density varied significantly ($p < 0.05$) among sites and at different times, ranging from 605 ± 61 shoots per m² (Forrest Beach 5 m, July) to 1,453 ± 81 (Siesta Park 5 m, July; Figure 4.2). All sites except Forrest Beach 5 m had a greater shoot density in July than in April. The difference in shoot density among sites was not significant in April but in July Siesta Park 5 m had a significantly greater shoot density than all other sites.

As for *P. sinuosa*, the density of *A. antarctica* stems varied significantly among sites and times (ANOVA, $p < 0.05$), ranging from 188 ± 39 m^{-2} (Siesta Park 5 m, July) to 580 ± 83 m^{-2} (Forrest Beach 5 m, April; Figure 4.2). In April, Forrest Beach 5 m had a significantly greater shoot density than all other sites. In July, no difference was detected between sites, but at this time Forrest Beach 5 m had a significantly lower shoot density than in April.

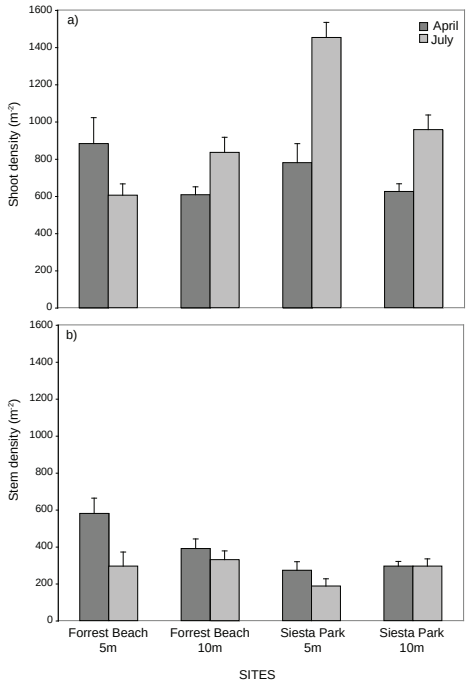

Figure 4.2 Results of shoot and stem density estimates for Forrest Beach five and ten metre sites (FB 5 m and FB 10 m) and Siesta Park five and ten metre sites (SP 5 m & SP 10 m) collected in *P. sinuosa* and *A. antarctica* seagrass meadows.

The range of *P. sinuosa* shoot density observed in this study was larger than that observed in some earlier studies (Table 4.4), though the mean shoot densities were comparable. Barnes *et al*. [2008] reported larger mean shoot densities but that study selectively sampled *P. sinuosa* sites whereas the other studies used random sampling methods that allowed for meadows with some *A. antarctica*, probably accounting for the lower *P. sinuosa* densities. Given the general comparability of our density estimates with earlier estimates, it is appropriate to use these in further estimation of the wrack generation rates.

Table 4.4 Comparison of mean shoot density estimates of *P. sinuosa* collected from Geographe Bay in the present investigation to those of Barnes *et al*. [2008] and *UWA* [2008].

SHOOT DENSITY	CURRENT STUDY		BARNES *ET AL*. 2008	UWA 2008
	April 2009	July 2009		
mean	725 ± 47	963 + 61	1210 ± 64	723 ± 19
min	250	350	783	625
max	1625	1900	1917	792

Mean *P. sinuosa* leaf lengths and growth rates varied between sites and times (Table 4.5). Mean leaf lengths ranged from 214.5 + 18.8 mm at Forrest Beach 10 m in July, up to 511.7 + 14.8 mm at Forrest Beach 5 m in May. In all cases, mean maximum leaf lengths were greater in May than in July. Mean leaf extension rates also varied between times and sites, ranging from 0.9 + 0.1 mm day^{-1} at Siesta Park 5 m in May, to 2.0 + 0.2 mm day^{-1} at Siesta Park 5m in July. Leaf extension rates were generally lower in May than in July ranging 0.9 + 0.1 mm day^{-1} at Siesta Park 5 m water depth, to 2.0 + 0.26 mm day^{-1} at Forrest Beach 10 m water depth.

Table 4.5 *P. sinuosa* leaf length and growth characteristics, collected from Forrest Beach and Siesta Park at 5 and 10 m water depth in May and July, 2009.

	MAY				JULY			
	Forrest Beach		Siesta Park		Forrest Beach		Siesta Park	
	5m	**10m**	**5m**	**10m**	**5m**	**10m**	**5m**	**10m**
Leaf extension (mm d^{-1})	1.3 ±.2	1.1 ±.4	0.9 ±.1	1.3 ±.2	1.5 ±.1	2.0 ±.3	2.0 ±.2	1.3 ±.1
Max leaf length (mm)	511.7 ±14.8	330.1 ±20.5	347.2 ±12.5	409.6 ±20.9	271.3 ±19.7	214.5 ±18.8	226.2 ±11.5	245.3 ±18.1
Days to lose 1 leaf	376.2	296.6	323.2	305.6	179.7	106.51	110.8	184.90
Leaf mass (g DW)	0.19	0.12	0.12	0.15	0.10	0.08	0.08	0.09

4.1.3.4 Wrack generation rates and biomass

Daily wrack generation rates for *P. sinuosa* are a function of the shoot density at a site and the rate of leaf turnover, where leaf turnover is defined as the average leaf length divided by the average daily leaf extension rate. Due to the differences in leaf lengths and leaf extension rates, *P. sinuosa* leaf shedding rate varied across sites and times, generally being greater in July than May and ranging from 3.4 to 16.1 leaves m^{-2} day^{-1} at Forrest Beach 5 m and Siesta Park 5 m, respectively (Table 4.6). For *A. antarctica*, wrack generation is a function of the loss of whole stems from a meadow.

Stem removal rates were measured directly as the change in stem density over ~ 20 days and also varied between sites and times, but with no consistent pattern. *A. antarctica* stem removal rate ranged from approximately 0.4 to 3.8 stems m^{-2} day^{-1} at Forrest Beach 5 and 10 m sites respectively.

Due to differences in daily wrack generation rates across time, the total biomass of *P. sinuosa* and *A. antarctica* wrack generated in one year is expressed as a range. May wrack generation rates represent the end of spring though autumn growth pattern (~ 2/3 of the year), while the July rates represent winter and spring (1/3 year). The total net biomass of wrack generated annually would likely fall within these estimates.

Based on May wrack generation rates, approximately 16,900 t. of *P. sinuosa* and 15,700 t of *A. antarctica* wrack would be generated in one year, giving a total of 32, 600 t DW (Table 4.6). The total amount of wrack generated within each region was similar, with the exception of *A. antarctica* at Forrest Beach 10 m (10,000 t DW yr^{-1}), which was estimated to have generated five times the amount of *A. antarctica* wrack generated in each of the other regions. The total wrack estimated to be produced based on July wrack generation rates (35,200 t DW yr^{-1}), is similar to May, however, the proportions of *P. sinuosa* and *A. antarctica* differs (approximately 21,300 t DW yr^{-1} *P. sinuosa* compared to 14,000 t DW yr^{-1} *A. antarctica*).

Table 4.6 Estimates of *P. sinuosa* whole leaf shedding and *A. antarctica* stem removal for Forrest Beach and Siesta Park at 5 and 10 m depth in May and July, 2009.

	P. SINUOSA WHOLE LEAF SHEDDING		*A. ANTARCTICA* STEM REMOVAL		TOTAL
	(leaves $m^{-2}d^{-1}$)	t (DW). y^{-1}	(stems $m^{-2}d^{-1}$)	t (DW). y^{-1}	
May					
Siesta Pk 5 m	4.5	4053.4	0.9	2091.6	6145.07
Forrest Bch 5 m	3.4	2595.9	0.9	1935.1	4531.04
Siesta Pk 10 m	5.3	4717.1	1.2	1606.4	6323.46
Forrest Bch 10 m	4.4	5572.3	2.5	10031.0	15603.30
Total		16938.8		15664.1	32602.88
July					
Siesta Pk 5 m	16.1	5800.1	0.9	7324.5	13124.59
Forrest Bch 5 m	7.2	4468.5	3.8	3142.5	7611.05
Siesta Pk 10 m	4.1	1569.9	2.1	2029.5	3599.45
Forrest Bch 10 m	9.7	9467.3	0.4	1449.2	10916.51
Total		21305.8		13945.8	35251.59

4.1.4 Significance of results

The wrack generation studies were designed to clarify where and how much wrack is generated annually, so that this information could be applied in wrack particle transport models. There were spatial and temporal variations in species composition, shoot density and leaf turn-over rates. Consequently different regions within Geographe Bay contribute differently to the wrack generation (in terms of leaf biomass), at different times of the year.

Annually, it is estimated that 32,600 to 35,200 tonnes of seagrass wrack is generated from the nearshore seagrass meadows to a depth of 10m, those meadows most likely to contribute wrack to the Port Geographe area. Although the total amount of wrack estimated to be produced varies little with time, the relative proportion of *P. sinuosa* to *A. antarctica* varies between May and July.

Based on May rates of wrack generation, wrack generated across Geographe Bay would consist approximately 52% *P. sinuosa* and 48% *A. antarctica*. The production of *P. sinuosa* wrack would occur relatively evenly across the bay, but the majority of *A. antarctica* wrack (~ 64%) is likely to originate from the Forrest Beach 5 m region.

Based on July rates of wrack generation, approximately 60% of the wrack produced would be *P. sinuosa* and 40% *A. antarctica*. The higher contribution of *P. sinuosa* at this time is likely to reflect the higher estimated leaf turn-over for this period. The greatest proportion of *P. sinuosa* wrack generated in this period is likely to occur from Forrest Beach 10 m; this wrack that is less likely to be trapped west of the Port Geographe Marina given the location of Forrest Beach east of the marina and the predominantly easterly longshore drift of wrack. However, large volumes of wrack are also predicted to come from the Siesta Park sites, which would likely be the source of wrack that eventually is trapped by the Port Geographe marina.

The spatial patterns in wrack generation were used in developing the wrack particle transport model, specifically by determining the locations for 'seeding' the model with *P. sinuosa* and *A. antarctica* particles according to the measured wrack generation for different regions. This determined the initial conditions for the model. Hydrodynamic forces subsequently caused movement and accumulation of wrack throughout Geographe Bay, including Port Geographe.

5 WRACK PARTICLE TRANSPORT

Once generated, wrack is transported through and out of Geographe Bay, including a substantial accumulation at Port Geographe. Understanding the processes that influence the transport of seagrass wrack is a priority for modelling the distribution of wrack accumulations. Relatively little was known at the commencement of this study about the physical properties of wrack and how the wrack interacted with hydrodynamic forces. This section reports on work designed to fill this knowledge gap. The work addressed:

- the timing and conditions under which wracked is exported from the meadows (and subsequently becomes available for transport to the beaches or removed from the system by other processes), and
- the physical properties of wrack that influence its transport in the water column (i.e. the form of wrack accumulations, settling velocity and critical shear stress).

5.1 Transport of wrack out of seagrass meadows under different weather conditions

A portion of the wrack produced in offshore seagrass meadows eventually deposits on the beaches of Geographe Bay. Observations suggest that this is not a continual process, rather it is confined to the late-autumn and winter period. This suggests that the export of wrack from the meadows may be coupled to the hydrodynamic conditions experienced during winter and, if so, this needed to be reflected in the model to predict the timing and subsequent fate of seagrass wrack.

5.1.1 Objective

To investigate the movement of wrack out of seagrass meadows under different weather conditions.

5.1.2 Methods

Export of wrack from meadows was estimated by comparing the biomass of wrack within meadows over defined periods, and correcting for the net generation of wrack expected over the same period. Wrack biomass in seagrass meadows was estimated at two sites (Forrest Beach, Siesta Park) in two depths (5m, 10m) on five occasions (15 April, 4 May, 3 June, 7 July and 21 July 2009). At each site and depth, all wrack was manually collected from 10 randomly located 50 x 50 cm quadrats and the dry weight determined in the laboratory. The average daily net change in wrack biomass (g DW m^{-2} d^{-1}) in the seagrass meadow between each sample occasion was then calculated for each site and depth. Net export was determined by correcting for the expected generation of wrack over the same period, based on data reported in the previous section of this report (Section 4).

5.1.3 Results

5.1.3.1 Changes in wrack biomass in seagrass meadow

The change in biomass of wrack in the meadows followed a general pattern of increasing loss of biomass from autumn through winter (Figure 5.1), though sites further to the east of Geographe Bay (Forrest Beach) showed losses earlier in the year than the more westerly Siesta Park sites.

During the first (autumn) sampling period (15 April - 4 May), wrack biomass declined at Forrest Beach sites (Figure 5.1) with the daily net change at 5 m depth (-4.6 g m^{-2} d^{-1}) twice that of the 10 m depth (-2.1 g m^{-2} d^{-1}; Figure 5.2). In contrast, at the Siesta Park sites located further west, wrack biomass increased at a rate of 3.0 g m^{-2} d^{-1} (5 m) and 1.6 g m^{-2} d^{-1} (10 m site).

The first major storm event of the winter period occurred in late May, during the second sampling period. Between 4 May and 3 June, the rate of change in wrack biomass at Forrest Beach sites remained negative, though less so than the

previous period (-0.3 and -0.7 g m^{-2} d^{-1} at 5 and 10m sites respectively; Figure 5.2). At Siesta Park sites, the shallower meadow (5m) showed a net loss of biomass (-6.1 g m^{-2} d^{-1}) while the 10 m site recorded an accumulation of 2.2 g m^{-2} d^{-1}.

By the third sample period (3 June – 7 July), daily wrack change at all sites was negative. Siesta Park sites had the greatest rates of decline (-1.9 and -4.9 g m^{-2} d^{-1}) at 5 and 10 m sites respectively. In the final sample period, between 7 and 21 July, there were relatively small standing crops of wrack remaining in the meadows and the changes in biomass were negligible relative to all previous sampling periods (-0.2 and 0.1 g m^{-2} d^{-1}).

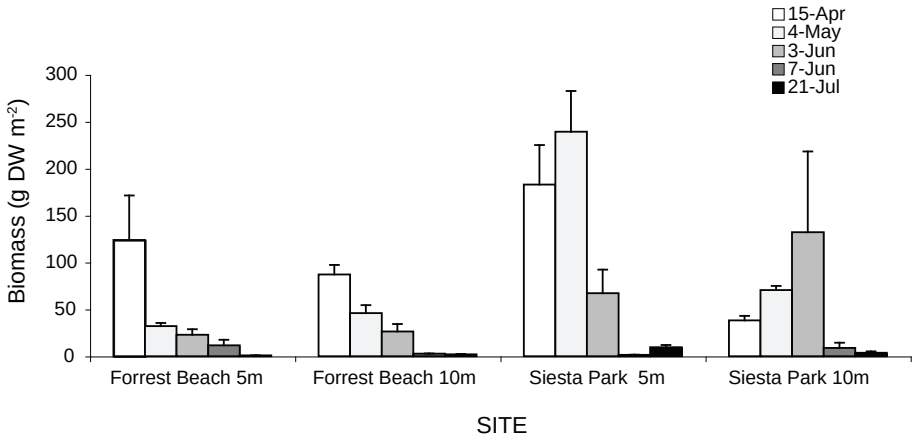

Figure 5.1 Seagrass wrack biomass in 5 and 10 m deep seagrass meadows at Forrest Beach (FB) and Siesta Park (SP) during autumn and winter 2009.

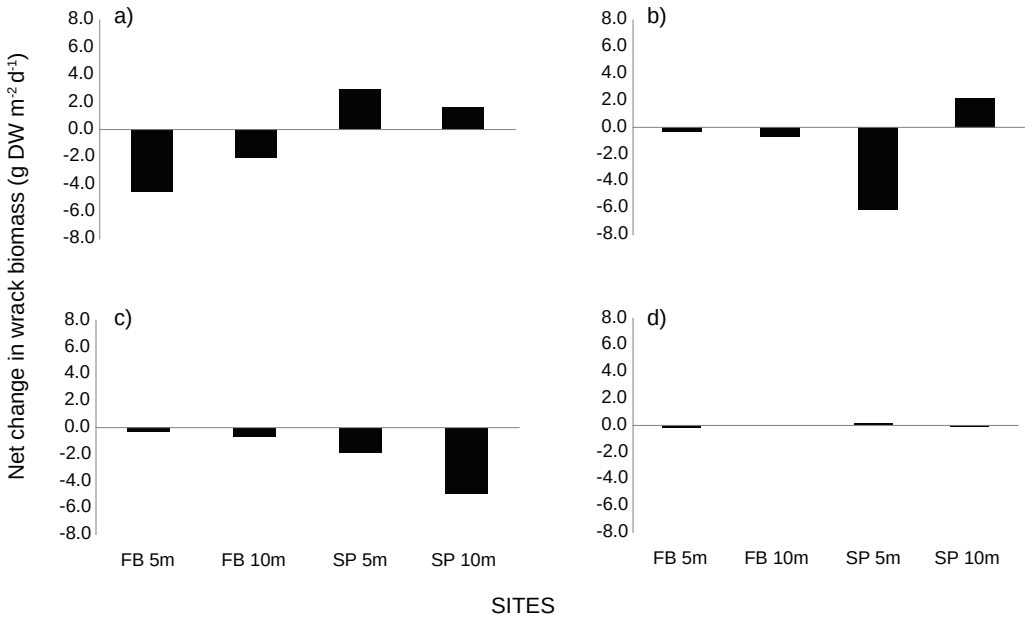

Figure 5.2 Daily net change in wrack biomass at Forrest Beach (FB) and Siesta Park (SP) seagrass meadows during autumn and winter sampling periods in 2009.

5.1.4 Significance of results

The generally negative trend in wrack biomass following storm activity suggests that storms are a key mechanism in removing wrack from the seagrass meadow. Wrack biomass appears to accumulate over the summer period and is then rapidly lost from meadows during the first few significant storm events of the year. These observations of loss from meadows correlate well with the appearance of wrack on adjacent beaches (see Section 6). Visual observations by divers suggest that increasing water movement at the surface of the seagrass canopy suspends the wrack in the water column, where it moves with the local currents as a high density of individual leaves, rather than the wrack moving along the seabed in larger aggregates.

There was spatial variation in the change in wrack biomass. Sites to the north-east of the bay (Forrest Beach) declined in the autumn period (between 15 April and 4 May), while those to the south-west (Siesta Park) showed export at the commencement of the winter period (between 4 May and 3 June). This appears to reflect exposure to storm-driven waves and swell. Forrest Beach has greater exposure to the southwest storm and swell conditions typical of summer and autumn. Hence, it is likely to be affected more significantly by these weather patterns earlier in the year than Siesta Park to the west. However, as storm direction moves more north-westerly, typical of winter frontal systems, the Siesta Park region would also be exposed, most likely accounting for the wrack export observed in June and July.

There was also variation in biomass change with depth. Shallow sites (5 m) initially declined more significantly than deeper sites (10 m). This is likely to be a consequence of higher exposure to wave and currents at 5 m, than at lower depths.

This information assists in validating the wrack transport model predictions, following the simulation of currents driven by frontal weather systems. It also indicates that Geographe Bay has two principle states with respect to wrack accumulations:

- a spring-summer-autumn accumulation period when wrack builds up in offshore regions, and
- an autumn-winter period when annual wrack production is exported from the meadow and is available for transport shorewards.

5.2 Wrack form during transport

Once exported from meadows, wrack is available for transport elsewhere in Geographe Bay. In modelling that transport, it was critical to understand the forms in which wrack exists and moves. Anecdotal evidence suggested wrack was moved as large aggregations, rolling along the seabed in bedload transport, though other observations were of these forms rapidly disaggregating under increased water velocities with the wrack then being transported as individual leaves. These two scenarios present quite different 'particles' to be parameterised within the particle transport model.

5.2.1 Objective

To investigate the form of wrack accumulations in the offshore unvegetated habitat, in order to better understand the movement of wrack between the seagrass meadow and the beach and to inform the parameterisation of the particle transport model.

5.2.2 Methods

As part of bay-wide surveys (Section 6) manta tows were conducted at six unvegetated sites in Geographe Bay (Dunsborough, Siesta Park, Geographe Bay Yacht Club, Port Geographe, Wonnerup and Forrest Beach) at two times of the year (18 and 19 May and 27 and 28 July). Due to poor weather conditions, sampling at Dunsborough, Siesta Park and the Geographe Bay Yacht Club was abandoned in May.

Along each manta tow transect, visual estimates were made from the shore to the edge of the seagrass meadow, running perpendicular to the shoreline and approximately 500 m apart. Every 1.0 m the presence / absence of wrack was recorded, and classified as thin, thick, fine, or 'cigar' (Figure 5.3).

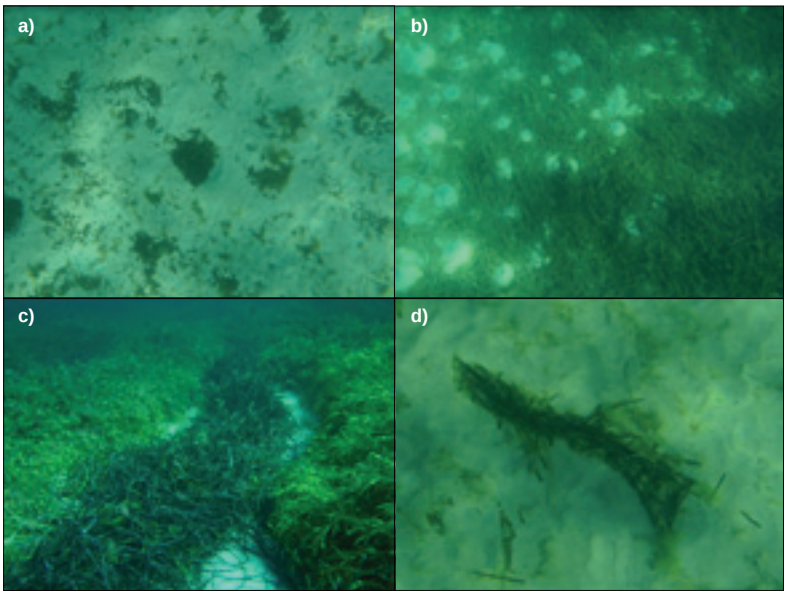

Figure 5.3 Wrack forms used in the classification of off-shore accumulations. a) fine b) thin c) thick and d) cigar.

5.2.3 Results

In May, at Wonnerup and Port Geographe, wrack was generally in the form of fines (95% and 86% respectively; Figure 5.4), while at Forrest Beach it was more evenly distributed between thick (29%) and thin (38%) forms and fines (25%). In July, wrack was found predominately as thin forms at Port Geographe and Dunsborough or as fines at all other sites. On no occasion at any site were significant amounts of the linear forms, referred to as cigars, found.

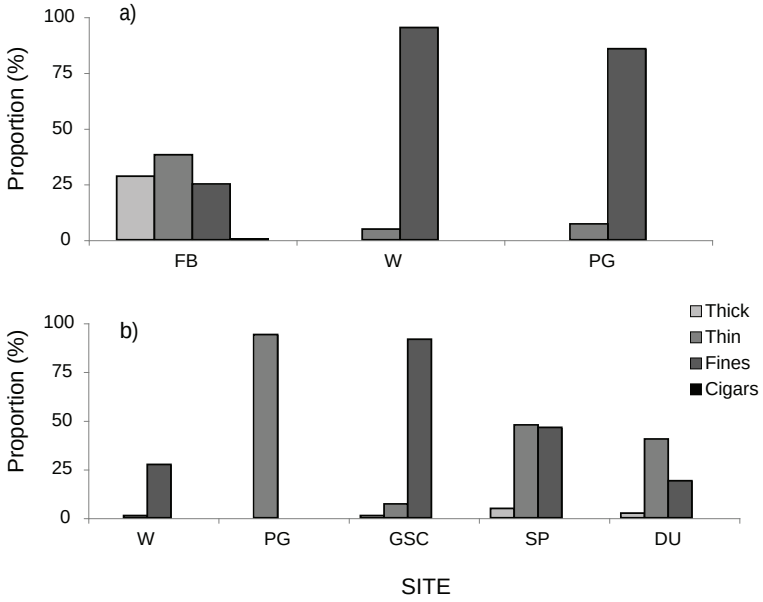

Figure 5.4 Proportion of wrack in different forms at six unvegetated sand sites in Geographe Bay.

5.2.4 Significance of results

The loose arrangement of wrack leaves in 'thin' and 'fine' forms suggests that when wrack is moving between the seagrass meadow and the beach, it is likely to be as a high density of individual particles (leaves), as opposed to being clumped or bound together. This was consistent with the earlier observation by divers that as swell- and wind-driven water movement increased wrack was suspended in the water column and moved as a high density of individual leaves, rather than the wrack moving along the seabed in larger aggregates.

There is no evidence to support the anecdotal suggestion that most wrack moves along the seabed as rolling aggregates. This limits the possibility of trapping these aggregates in depressions or channels to prevent their movement towards shore and Port Geographe.

To accurately reflect wrack dynamics, the particle transport model was constructed around the behaviour and movement of individual leaves, as opposed to larger aggregations or clumps of wrack. Subsequent model development focused on the two major forms of seagrass particles, individual *Posidonia sinuosa* leaves and individual *Amphibolis antarctica* stems with leaves attached to them.

5.3 Physical properties of beach wrack

The physical properties of wrack are important determinants of its behaviour in two respects:

- the transport of wrack, both within the water column as well as on and off beaches, and
- the biogeochemical transformations of wrack, including its decomposition and the generation of H_2S.

Studies were conducted to determine the properties of wrack with respect to both transport and biogeochemistry. In this section, the properties of wrack relevant to transport in the water column are reported: the settling velocity of wrack particles and the critical shear stress. The physical properties relevant to wrack accumulations on the beach and their biogeochemical transformation are presented in Section 7.

5.3.1 Objective

To determine the settling velocity and critical shear stress for resuspension of *Posidonia sinuosa* leaves and *Amphibolis antarctica* shoots.

5.3.2 Methods

5.3.2.1 Settling Rate

The settling velocity was determined for fresh and aged seagrass particles, soaked over different durations. Seagrass particles used were: *P. sinuosa* leaves of 3 sizes (small: 0.6-0.7 x 4.0 cm; mid: 0.6-0.8 x 10.0 cm; large: 0.6-0.8 x 30 cm), *A. antarctica* stems; *A. antarctica* leaves; and *A. antarctica* shoots (stem + leaf). Fresh seagrass particles were collected from Geographe Bay 24 hours prior to commencing the experiment and stored at 4°C. Aged seagrass particles were collected six weeks prior to commencing the experiment and dried at ambient room temperature.

Initial trials indicated that following a period of drying, a proportion of leaves floated on re-wetting, but that the proportion decreased as the re-wetting period increased. Since this could be critical in determining the behaviour of particles that have been drying on a beach and are subsequently moved offshore, we tested the effect of different soaking times on the sinking rate of dried particles. Particles were soaked in seawater for 0, 2, 8, 16 and 28 hours. The settling velocity was determined by placing the sample under the surface of the water in a 2 m high column filled with seawater at 16°C. The time taken for each sample to travel over a 20.0 cm distance was recorded and this was converted to a settling velocity (m min^{-1}). Twenty replicates of each wrack type were used.

5.3.2.2 Critical shear stress of wrack

Seagrass particle re-suspension experiments were conducted in a 20 m flume (Figure 5.5) filled with freshwater and operated under uni-directional flow conditions. Water depth in the flume averaged 35 cm and the flume width was 60 cm. A net was installed at the downstream end of the flume to allow retrieval and re-use of the seagrass particles. A flow straightener was installed in the upstream end of the flume.

Figure 5.5 The 20 m recirculating flume with a water depth of 35 cm.

Selected fresh *A. antarctica* branches (Figure 5.6), fresh *P. sinuosa* leaves (Figure 5.7) and dried *P. sinuosa* leaves were trimmed to approximately 10 cm in length and all epiphytes, fauna and inorganic particles removed. Three replicate groups of each particle type were collected; in each group there were 10 particles. All particles were soaked in freshwater for 24 hours before the experiments, and then stored in freshwater between experiments. The particle groups containing *P. sinuosa* fresh leaves were discarded after four days and replaced with leaves recently collected from Perth beaches.

Figure 5.6 Typical *Amphibolis antarctica* branches used for the flume resuspension experiments.

Figure 5.7 Typical *Posidonia sinuosa* leaves (fresh and dried) used for the flume resuspension experiments.

Resuspension experiments were conducted at six different water velocities. Flume water velocities were controlled by adjusting an inflow valve and also a sluice gate to control outflow. Velocity profiles were measured for each experiment. A SontekTM micro-acoustic doppler velocimeter (ADV) was positioned at 5 depths through the water column, measuring water 3D velocities at 2 Hz. The flume water was seeded with SphericalTM 110P8 glass spheres (mean diameter 11 – 18 microns, density 1.1 g cm^{-3}) to ensure signal to noise ratios > 5 dB. The velocities were averaged over a 3 – 5 minute period.

For each experiment, the 10 particles were individually placed on the bottom of the flume and released. The time for each particle to travel 6 m (or 2 m at the very low water velocities) was recorded and particle velocities calculated. On reaching the net at the end of the flume, all particles were retrieved; each of the three replicate groups was released three times into the flume. During transport along the flume, particles move up and down through the water column; at times many became stuck on the bottom of the flume and then were dislodged and moved again along the flume. The particle velocities recorded used total transport timescales, irrespective of whether part of this time was spent stationary.

5.3.3 Results

5.3.3.1 Wrack settling velocity

The settling velocity of wrack ranged from 0.36 – 3.59 m min^{-1} (Figure 5.8). *A. antarctica* stems and *A. antarctica* stems + leaves settled faster than the other wrack components (range: 1.28 – 3.59 m min^{-1}), regardless of aging, though the aged stems and stems + leaves required at least 2 hours of soaking before they would sink. There was little difference in the mean sinking rate of *P. sinuosa* leaves of different lengths or ages, ranging from 0.36 – 2.24 m min^{-1} but generally between 1.0 and 2.0 m min^{-1}. Generally, *P. sinuosa* leaves, whether fresh or aged, sank at a slightly faster rate after soaking for 28 hours than leaves that had not been soaked. The effect of soaking time on the sinking rate of *A. antarctica* particles was less clear.

The proportion of leaves that floated varied between seagrass species, among ages of seagrass and as a function of the time the wrack had been soaking (Figure 5.8). In the case of *P. sinuosa,* fresh leaves (regardless of length) floated if they had been not been soaked; for long leaves about 80% floated. With increased soaking time there was a steady decline in the proportion of fresh *P. sinuosa* leaves floating. About 20 % of fresh leaves floated during the first 8 hours of soaking, declining to less than 5 % after 16 hours. With aged leaves, 70-85 % floated without soaking but all sank after 2 hours of soaking.

An insignificant proportion of fresh *A. antarctica* stems and stems+leaves floated. About 20 % of fresh *A. antarctica* leaves floated without soaking, but this declined to negligible after 16 hours of soaking. In stark contrast, 100% of aged *A. antarctica* stems and stems + leaves floated if they had not been soaked. Following 2 hours soaking, 65% of stems + leaves sank but stems were more resistant to sinking and required 8 hours of soaking for half to sink and even after 28 hours soaking, approximately 15 % of remained floating.

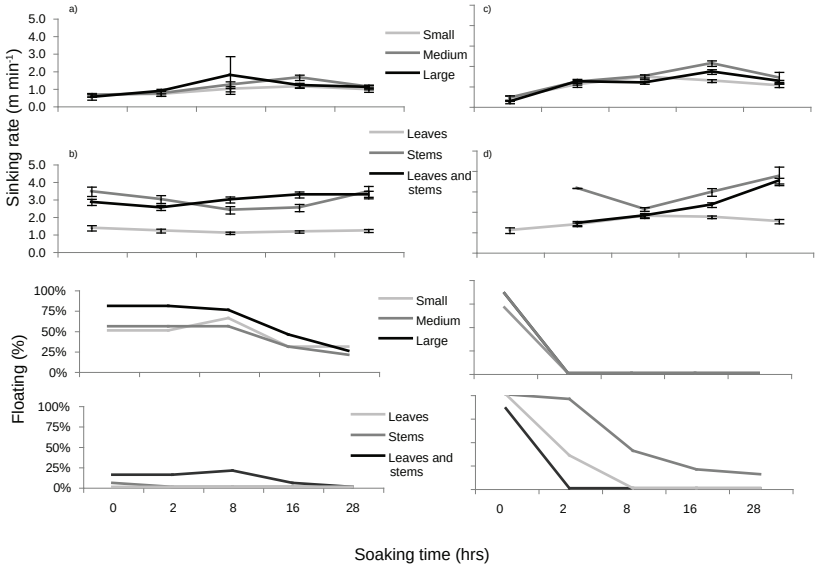

Figure 5.8 Settling rates of different aged seagrass leaves and/or stems, soaked between zero and 28 hours.

5.3.3.2 Re-suspension of wrack

The free stream velocities across the five experiments ranged from 0.06 – 0.39 m s^{-1} and the boundary layer thickness varied from 0.03 – 0.15 m (Figure 5.9). The free stream velocity was defined as the water velocity above the boundary layer and which was constant with depth.

The *A. antarctica* and dried *P. sinuosa* particles began to move once free stream water velocities exceeded 0.06 m s^{-1}. The fresh *P. sinuosa* particles began to move once the free stream velocities > 15 cm s^{-1}. All particle velocities were less than free stream water velocities across all experiments; on average the particle velocities were approximately 70 % of the free stream velocities (Figure 5.10).

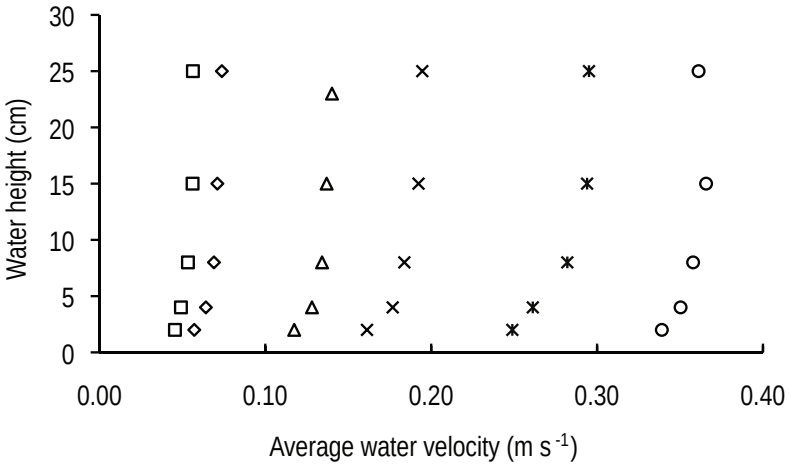

Figure 5.9 Water velocity profiles from the six re-suspension experiments. The different symbols represent water velocities in different experiments.

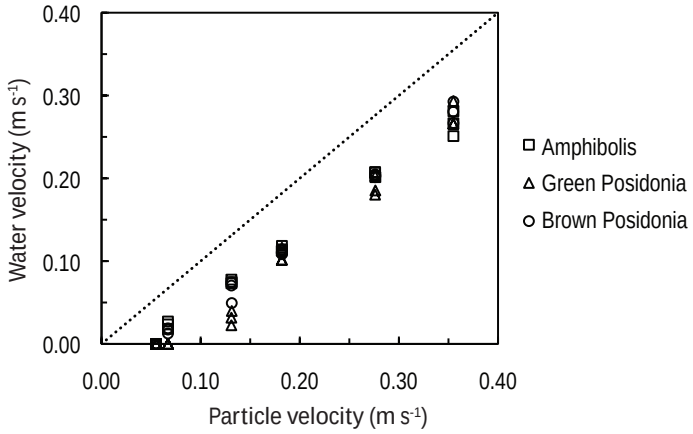

Figure 5.10 Comparisons of free stream water velocity and particle velocity, for each of the particle types.

5.3.4 Significance and application of the results

For simplicity, seagrass wrack was parameterised as spherical particles. We present below the parameterization of particle transport in the x- and z-directions (z is positive upwards). The change in particle position in the x-direction dx_p (m), at water height z (m) after timestep, Δt (s), was given by:

$$dx_p = U_h \Delta t + U_s \Delta t + a\sqrt{6 E_h \Delta t} \qquad \textbf{Eq. 5-1}$$

where U_h is the horizontal water velocity in the x-direction (m s^{-1}) at water height and is calculated from the hydrodynamic model using Eq. 5-1 and U_s is a Stokes drift velocity (m s^{-1}). The last term in Eq. 5-1 describes turbulent diffusion of the particle using a random walk formulation, where a is a normally distributed random number and Eh is a constant horizontal eddy diffusivity (0.0005 m^2 s^{-1}). The horizontal water velocity U_h experienced by a particle at height z_p above the seabed, is given by:

$$U_h = U_o \frac{\log_{10}\left(\frac{z_p}{z_o}\right)}{\log_{10}\left(\frac{0.37h}{z_o}\right)} \qquad \textbf{Eq. 5-2}$$

where U_O is the depth-averaged water velocity (m s^{-1}) output from the hydrodynamic model, h is the total height of the water column (m) and z_O is the roughness lengthscale (m).

The roughness lengthscale z_O may be estimated from *in situ* roughness elements, such as ripples, as:

$$z_0 = \frac{2H_r^2}{3L_r} \qquad \textbf{Eq. 5-3}$$

where H_r is the ripple height and L_r is the ripple wave length (Van Rijn, 1993). Over seagrass meadows there are minimal roughness elements, however ripples of approximately 0.06 m height and 4 m wavelength were observed over bare sand in Geographe Bay. An appropriate roughness length for the Geographe Bay seabed was therefore estimated as 0.01 m.

Stokes drift is caused when wave-induced horizontal orbital velocities decrease closer to the seabed (van Rijn 1989); U_s is a second-order mean Lagrangian velocity in the direction of wave propagation. In the offshore environment, Stokes drift velocities become insignificant, however closer to shore, they can be significant and should be estimated from linear wave theory as:

$$U_s = \frac{1}{8}\omega k H^2 \frac{\cosh(2k(s-h))}{\sinh^2(kh)} \qquad \textbf{Eq. 5-4}$$

where ω is angular frequency (radians s^{-1}), E_v is wavenumber (radians m^{-1}), H is the wave height (m) and s is the distance to the free surface(m).

The change in particle position in the z-direction, dz_p (m), after timestep, Δt (s), was given by:

$$dz = a\sqrt{6E_v\Delta t} + w_s\Delta t \qquad \textbf{Eq. 5-5}$$

where w_s is the particle settling velocity (m s^{-1}) and E_h is a constant vertical eddy diffusivity (0.0005 m^2 s^{-1}). We assumed that vertical advective velocities were negligible.

The particle settling velocity, w_s, was estimated from the particle settling experiments and was a function of exposure to air. After drying the seagrass particles became positively buoyant. The particles became negatively buoyant after soaking in water for 24 hours. As we anticipated that the particles would spend some time stranded on the beach and drying out, this dynamic behaviour was incorporated into the model. When first in contact with high water levels, the dried particles float and can be transported offshore; over a period of 24 hours, they become progressively more negatively buoyant (assuming a linear progression). After 24 hours of continuous soaking, they achieved the settling velocities given in Figure 5.8.

Once settled to the seabed, the particles will be resuspended only when the hydrodynamic conditions are sufficiently energetic. As described above, *Amphibolis* and dried *Posidonia* particles were resuspended once the free stream velocities exceeded 0.06 m s^{-1}. Fresh *Posidonia* particles were resuspended once the free stream velocities exceeded 0.15 m s^{-1}. However we expect that the critical free-stream velocities required for particle resuspension under laboratory conditions will be different to those required in the field. Specifically, the roughness length scale will likely differ significantly, and this in turn impacts on the critical water velocities. So instead of using free-stream or depth-averaged velocities as a critical threshold, we used a critical shear stress, which normalizes the roughness length scale with the total water height:

$$\tau_{critical} = \frac{U_0^2\kappa^2}{\ln^2(0.37h/z_0)} \qquad \textbf{Eq. 5-6}$$

where κ is the Von Karman constant (0.4). The critical free-stream velocities measured in the laboratory were converted into critical depth-averaged velocities. An effective laboratory z_0 was then estimated from the intercept of u(z) vs ln(z) to be approximately 0.001 m and h was 0.3 m. Inserting these variables into Eq. 5-6, we obtained = 3 x 10^{-5} N m^{-2} for *Amphibolis* and dried Posidonia, and $\tau_{critical}$ = 8 x 10-5 N m^{-2} for fresh *Posidonia* particles. These critical bottom shear stresses could be directly applied in the particle model.

The current-induced bottom shear stress, τ, experienced by a particle at the seabed was estimated by substituting the appropriate depth-averaged velocities (now obtained from the hydrodynamic model), total water height and the field roughness (0.01 m) into Eq. 5-6. When this bottom shear stress exceeded the critical shear stress, the particle will be resuspended. Once resuspended, only turbulent transport could increase the particles' height in the water column (see Eq. 5-1).

6 WRACK ACCUMULATION

Once exported from meadows, wrack is available for transport, predominantly as suspended individual leaves or shoots. At the commencement of the project, the fate of the wrack was unclear. While it was understood that some was deposited on beaches and that a significant amount accumulated at Port Geographe, it was not clear what proportion of the wrack generated from meadows this represented and where wrack may accumulate prior to arrival at Port Geographe. Understanding the distribution of wrack and any temporal shifts in this distribution may provide insights into management options, such as interception of wrack or timing of beach management activities.

This section reports the results of the investigations into the spatial and temporal trends in wrack accumulation in Geographe Bay. Section 6.1 addresses the distribution of wrack accumulations on beach and sub-tidal habitats in Geographe Bay, as well as trends in the total wrack biomass accumulated annually. Sections 6.2 provides qualitative and quantitative spatial and temporal variations in beach wrack. Section 6.3 presents the temporal and spatial variation in beach morphometry. Section 6.4 discusses composition of wrack accumulations on the beach and how these vary over time.

6.1 Distribution of wrack accumulations in Geographe Bay

6.1.1 Objective

To quantify the mass and distribution of wrack in Geographe Bay at different times of the year.

6.1.2 Methods

The biomass of wrack was assessed in three habitats throughout Geographe Bay: beach, un-vegetated sub-tidal sediment and seagrass meadow. The assessments were conducted in autumn and winter to identify any temporal differences in the distribution of wrack and to confirm the hypothesis developed from the 'Wrack Generation' studies that wrack accumulates offshore during spring, summer and early autumn and is transported inshore during the first autumn/winter storms (see Section 5.1).

Sampling of the three habitats was conducted in each of six regions in Geographe Bay: Forrest Beach, Dunsborough/Quindalup, Siesta Park, Geographe Sailing Club, Port Geographe, Wonnerup and Forrest Beach. Sampling was conducted on 19 and 20 May and 27 & 28 July. In the beach habitat, additional samples were collected at the Geographe Volunteer Marine Rescue outpost on 3 June 2009. On some occasions, weather prevented sampling of the sub-tidal habitats (detailed below).

6.1.2.1 Beach habitat

Bay-wide wrack volume and biomass estimates were made at the seven beach sites on the dates given above and opportunistically on 3 to 4 June 2009, following a storm event. At each site, five 200 m long transects were established parallel to the shoreline, approximately 30 m apart. At the start and end of each transect, the width [m] of the beach from the first dune to the waterline was recorded, to define the sampling area. The length, width and height of all wrack accumulations in each sampling area was estimated using tape measures and, for continuous wrack bands, the percentage of cover recorded. At approximately 20 m distance from the start of each transect, a sample of wrack was collected in a standard 1 L container for bulk density and biomass measurements, ensuring the wrack was not compacted during sampling. The density of that sample was assumed to be representative of all wrack in the sample area. Samples were dried to a constant mass and weighed in the laboratory.

6.1.2.2 Un-vegetated sub-tidal habitat

To provide an estimate of cover of wrack on the un-vegetated sediment, a random stratified survey approach was used. Manta tows were initially conducted at each site, from the shore to the edge of the seagrass meadow, perpendicular

to the shoreline and approximately 500 m apart. Every metre, the presence/absence of wrack was recorded by visual assessment and classified as absent, thin, thick, fine or cigar.

Representative wrack accumulations identified from the manta tows were then quantitatively sampled. Four 20 m transects were laid out from a central position at each site. Every 1.0 m a photograph was taken along each transect and substrate type (*P. sinuosa*, *A. antarctica*, *Halophila*, sand) and wrack type (thin, thick, fine, cigar) recorded. For each wrack type found on each transect, a sample was taken with a 20 x 20 cm quadrat and dried in the laboratory to determine dry weight.

Due to storms, Dunsborough/Quindalup, Siesta Park and Geographe Sailing Club could not be sampled in autumn (May sample dates) and Forrest Beach could not be sampled in winter (July). To calculate bay-wide estimates of wrack accumulation, averages have been used from sampled sites in place of missing data.

6.1.2.3 Seagrass meadow

At each site, four 20 m transects were laid out randomly from a central position within the seagrass meadow and wrack samples were collected as per sampling in the unvegetated habitat (see above). Due to storms, Dunsborough/ Quindalup, Siesta Park and Geographe Sailing Club were not be sampled in May. All sites were sampled in July. To calculate bay-wide estimates of wrack accumulation, averages were used in place of missing data.

6.1.3 Results

6.1.3.1 Wrack volume on beaches

The bio-volume of wrack (volume of wrack per m^2) varied among sites and times (Figure 6.1). Before the storm period (19 May) the mean bio-volume, averaged over all beaches, was $2.48 \times 10^{-3} \pm 1.72 \times 10^{-3}$ m^3 m^{-2}, though this varied by about 4 orders of magnitude across the sites, from $7.43 \times 10^{-6} \pm 1.53 \times 10^{-6}$ m^3 m^{-2} at Geographe Sailing Club to $1.30 \times 10^{-2} \pm 1.06 \times 10^{-2}$ m^3 m^{-2} at Siesta Park. After the storm period, in early June, the bio-volume averaged across all sites increased, to $9.49 \times 10^{-2} \pm 2.86 \times 10^{-2}$ m^3 m^{-2}, ranging from $2.00 \times 10^{-4} \pm 1.43 \times 10^{-4}$ m^3 m^{-2} at Wonnerup to 0.35 ± 0.05 m^3 m^{-2} at Port Geographe.

By late July, the volume of wrack an average across all sites was $2.31 \times 10^{-1} \pm 0.71 \times 10^{-1}$ m^3 m^{-2}, ranging $1.59 \times 10^{-5} \pm 1.11 \times 10^{-5}$ m^3 m^{-2} at Quindalup to 1.31 ± 0.37 m^3 m^{-2} at Port Geographe.

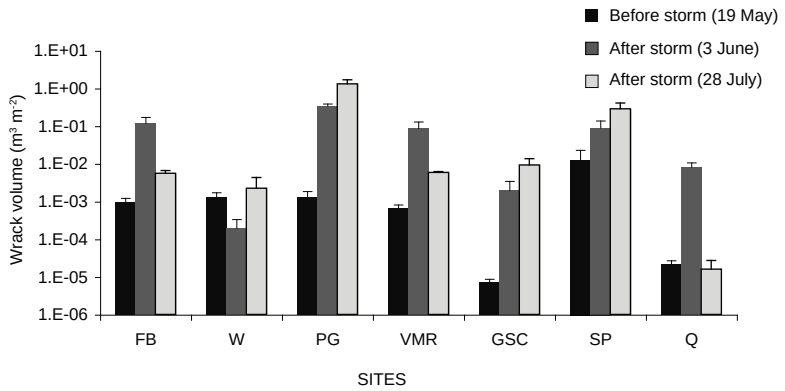

Figure 6.1 Volume of wrack at beach sites in Geographe Bay before and after an early storm event in 2009.

6.1.3.2 Wrack biomass on beaches

In May, wrack biomass in the beach habitat was generally three to five orders of magnitude lower than in either the seagrass meadow or un-vegetated habitat (Table 6.1). Among beach sites, there was considerable variation in mean biomass, ranging from $5.8 \times 10^{-6} \pm 2.3 \times 10^{-6}$ kg DW m^{-2} at Geographe Sailing Club to $2.7 \times 10^{-3} \pm 1.9 \times 10^{-3}$ kg m^{-2} at Siesta Park.

In July, wrack biomass per square meter was still generally lowest in the beach zone, though not at all sites, and had increased by orders of magnitude at several sites (Table 6.1). Siesta Park (0.30 ± 0.19 kg m^{-2}) and Port Geographe (0.37 ± 0.10 kg m^{-2}) had the greatest wrack biomass per unit area of all sites and habitats. Wrack biomass in the un-vegetated zone and seagrass meadow were generally similar among sites and lower in July than in May, by between one and three orders of magnitude.

Table 6.1 Wrack biomass in beach and sub-tidal habitats at sites throughout Geographe Bay during May and June 2009 (n.d. = no data).

BIOMASS (KG M^{-2})						
	Dunsb'rgh	Siesta Park	Geo. Sailing Club	Port Geographe	Wonnerup	Forrest Beach
May						
Beach	$7.2 \times 10^{-6} \pm 2.6 \times 10^{-6}$	$2.7 \times 10^{-3} \pm 1.8 \times 10^{-3}$	$5.8 \times 10^{-6} \pm 2.6 \times 10^{-6}$	$4.4 \times 10^{-4} \pm 1.4 \times 10^{-4}$	$4.6 \times 10^{-4} \pm 2.0 \times 10^{-4}$	$2.5 \times 10^{-4} \pm 0.9 \times 10^{-4}$
Unveg.	n.d.	n.d.	n.d.	0.28 ± 0.01	0.29 ±0.01	0.24 ± 0.06
Seagrass	n.d.	n.d.	0.21 ±0.08	0.25 ±0.03	0.20 ±0.05	0.03 ± 0.02
July						
Beach	$3.2 \times 10^{-6} \pm 2.1 \times 10^{-6}$	0.30 ±0.19	$1.5 \times 10^{-3} \pm 0.7 \times 10^{-3}$	0.37 ±0.10	$6.5 \times 10^{-4} \pm 4.9 \times 10^{-4}$	$1.2 \times 10^{-3} \pm 0.3 * 10^{-4}$
Unveg.	0.06 ±0.03	0.11 ±0.07	$1.3 \times 10^{-2} \pm 1.7 \times 10^{-3}$	$9.4 \times 10^{-2} \pm 3.6 \times 10^{-3}$	$1.6 \times 10^{-2} \pm 1.2 \times 10^{-2}$	n.d.
Seagrass	$2.0 \times 10^{-2} \pm 1.1 \times 10^{-2}$	$2.2 \times 10^{-3} \pm 7.1 \times 10^{-4}$	$7.3 \times 10^{-2} \pm 4.2 \times 10^{-5}$	$4.6 \times 10^{-2} \pm 5.2 \times 10^{-3}$	$9.5 \times 10^{-3} \pm 7.8 * 10^{-4}$	$1.3 \times 10^{-2} \pm 6.6 \times 10^{-4}$

Where wrack was present in sub-tidal unvegetated habitat, the biomass per unit area was generally higher than in seagrass meadow. However, not all unvegetated habitat contained wrack. Manta tows in May indicated that 51 - 86% of the unvegetated, sub-tidal sediment between the shoreline and seagrass meadows had some wrack cover (Table 6.2). In July, percent cover ranged from 43.8 % at Dunsborough to 82 % at Forrest Beach. In contrast, all seagrass meadow habitat contained some wrack cover. The total wrack biomass for each region was then calculated by multiplying the average biomass per square metre of habitat containing wrack by the total area containing wrack. Where samples could not be collected due to weather conditions, averages were used from other sites at that time.

Table 6.2 Proportion of unvegetated, sub-tidal habitat at Geographe Bay sites with wrack cover in May and July 2009. (n.d. = no data).

% COVER OF WRACK AT SITE						
	Dunsborough	Siesta Park	Geo. Sailing Club	Port Geographe	Wonnerup	Forrest Beach
May	n.d.	n.d.	n.d.	70.0%	51.0%	86.0%
July	43.8%	86.3%	68.8%	81.3%	51.3%	82.0%

6.1.3.3 Regional wrack biomass accumulation

In May, an estimated 21,836 tonnes of wrack was present in the study area, more than 99 % of which was in the seagrass meadows and unvegetated sub-tidal habitats. Only 1.31 ± 0.21 tonnes was present on the beaches (Figure 6.2,), the majority at a single beach (Siesta Park; ~ 1.06 ± 0.74 t). Note that these beach mass estimates exclude the Port Geographe marina itself. Offshore, wrack accumulations were relatively evenly distributed across the six regions.

In July, the total biomass of wrack found on beaches (again excluding Port Geographe marina itself) had increased to 202.33 ± 26.47 t (Figure 6.2), more than a 150-fold increase relative to May. The majority (117.64 ± 73.72 t) occured at Siesta Park and Port Geographe (83.66 ± 22.18 tonnes), with the biomass at other sites ranging from 0.002 ± 0.001 t at Dunsborough to 0.50 ± 0.14 t at Forrest Beach. The total biomass of wrack in the un-vegetated sub-tidal habitat (2,319.40 ± 177.19 t) and seagrass meadows (2,116.24 ± 175.40 t) was considerably lower than in May, though still substantially higher than the mass found on beaches.

Wrack biomass (t)	May	July
Beach	1.3 ± 0.2	202.3 ± 26.5
Unvegetated	7,939.5 ± 209.7	2,319 ± 176.2
Vegetated	13,895.1 ± 519.6	2,116.2 ± 175.4
Total	21,835.9	4,638.0

Area (sq. km)	DU	SP	GSC	PG	W	FB
Beach	0.51	0.39	0.31	0.22	0.1	0.41
Unvegetated	67.2	91.5	92.7	41.4	21.7	58.1
Vegetated	121.2	199.9	138.1	82.3	83.9	269.3

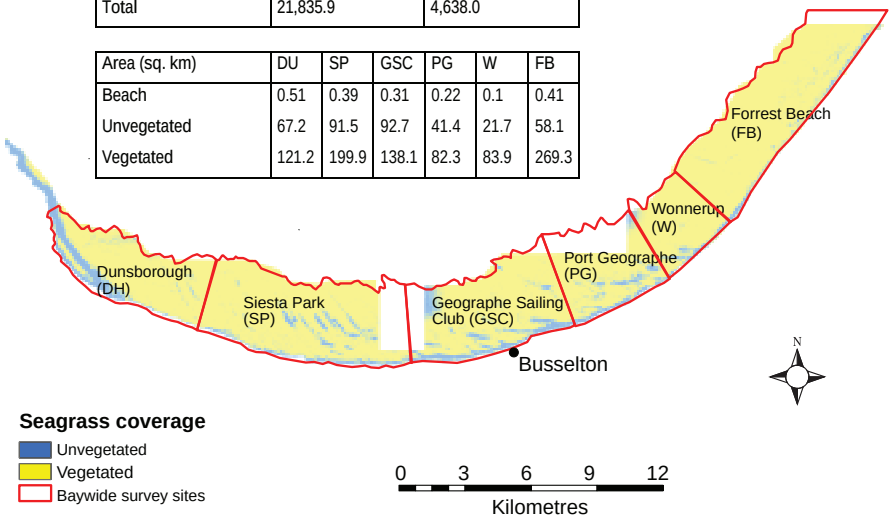

Figure 6.2 Estimates of total wrack biomass on beaches and in seagrass meadows and unvegetated sub-tidal areas to 10 m depth in Geographe Bay (seagrass coverage data by van Niel *et al.* [2009]). These data exclude accumulations within 1.5 km west of the Port Geographe marina western groyne and the pocket beaches within the marina.

6.1.3.4 Wrack accumulation estimates for Geographe Bay Marina West

The total mass of wrack accumulated in Port Geographe was defined as that present on the pocket beaches and in the area up to 1 km west of the western groyne at Port Geographe. Estimates of the volume of wrack bypassed from Port Geographe were obtained from the annual beach monitoring reports compiled by the Port Geographe developer. These estimates were summarised by M J Paul & Assoc. P/L for 2004-2007 (M J Paul & Associates P/L 2008) and unpublished estimates were provided for 2008 by Dr Stuart Barr of Shore Coastal, acting on behalf of the Shire of Busselton. The volume of seagrass removed annually was in the order of 90,000 – 150,000 m^3. Using the volume to biomass estimates derived in this study, these volumes equate to approximately 4,400 – 7,300 tonnes of wrack, the upper estimate being for 2009.

By late July, 7,300 tonnes of wrack was estimated to have accumulated at Port Geographe, which equates to 97% of all the wrack estimated to be on beaches throughout the Geographe Bay study area at that time (Figure 6.3). This equates to 33% of all the wrack estimated to have accumulated in offshore habitats up to the end of May 2009 and prior to the first storms that moved wrack shoreward. The remaining 67% was located either in the offshore seagrass meadows (9.7%), unvegetated sub-tidal habitat (10.6%), other beaches (0.9%) or elsewhere (45.8% or 9,901 t, Figure 6.3). The unaccounted 'elsewhere' fraction could include wrack transported offshore, that moving past Port Geographe and exported eastwards towards Bunbury or losses to decomposition.

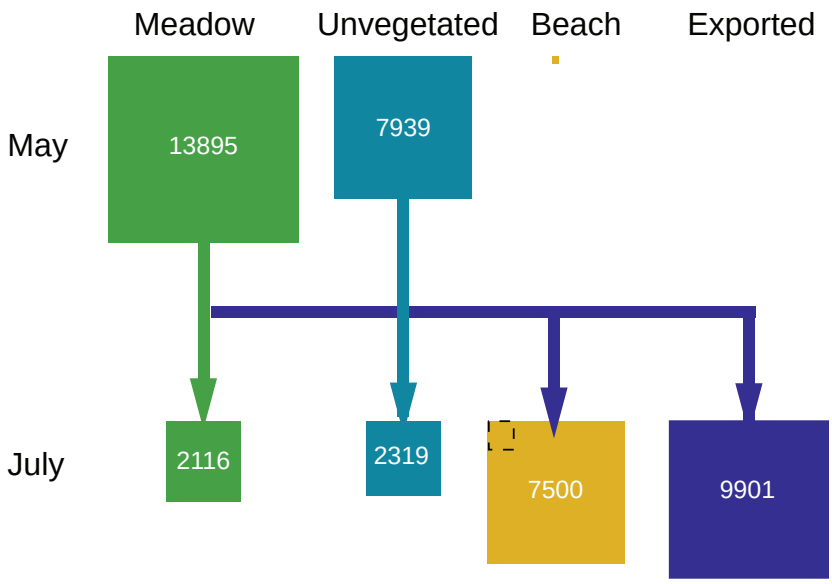

Figure 6.3 Mass balance for wrack in offshore and beach habitats of Geographe Bay, including Port Geographe. (The yellow "Beach" box represents all beaches. The dashed box within "Beach" represents all beaches other than Port Geographe.)

6.1.4 Significance of results

Wrack accumulations are not uniformly distributed in Geographe Bay. In autumn, the greatest accumulation of wrack was in the seagrass meadow and unvegetated habitats sub-tidal habitat. During this period, less than 1% of the wrack in the bay was accumulated on the beach.

Following storm events in June, there was a greater bio-volume of wrack at most beach sites. This is consistent with the findings of the wrack export from meadows studies (Section 5.1) that storms are responsible for removing wrack from the seagrass meadow in autumn, and depositing it on beaches in winter. Subsequent sampling towards the end of July indicated that wrack bio-volumes on some beaches declined, suggesting that storms are also responsible for the transport of wrack off some beaches. The amount of wrack accumulated in the seagrass meadow and un-vegetated habitat had also declined significantly by July.

While the amount of wrack on beaches had increased over 150-fold by July compared to May, it was distributed unevenly, with Siesta Park and Port Geographe having proportionally much greater biomass than all other beach sites. These results are consistent with anecdotal evidence. It is also consistent with our own observations (reported in Section 6.2) of highly heterogeneous accumulations on beaches, both in space and time.

Together, these results are consistent with the conceptual model of Geographe Bay in which wrack is predominantly stored offshore during spring, summer and autumn and is then transported inshore during late autumn and winter storms. Once inshore, wrack is deposited onto and transported off beaches and while it is in the shallow nearshore

waters it is available to be transported by longshore currents. This suggests a mechanism for the highly heterogeneous and transient accumulations of wrack observed along the beaches (see Sections 6.2). In natural circumstances, we might expect the wrack to gradually move in an easterly direction, periodically accumulating but then being removed from beaches. The Port Geographe marina traps about 97% of all wrack on the beaches in July, and about 33% of the wrack present in the study area in May. It is the major winter store of wrack in the bay and prevents the normal dispersal mechanisms that otherwise produce relatively small wrack accumulations that are very patchy in space and time.

6.2 Temporal and spatial variation in beach wrack

Anecdotal accounts and observations suggested that the naturally occurring wrack accumulations on beaches are patchy in time and space. Consequently, under natural conditions, wrack tends not to accumulate for extended periods on any one beach. Understanding any relationship between weather patterns and the movement of wrack onto and off beaches was a key aim of the project. To gain this understanding, it was first necessary to characterize the variation in beach accumulations over time and among beaches.

6.2.1 Objective

To determine the temporal and spatial variation in wrack abundance on Geographe Bay beaches over an autumn-winter period.

6.2.2 Approaches

The amount of wrack on beaches was assessed in two ways:

- Qualitative assessment. The qualitative approach allowed a spatially extensive and frequent analysis of wrack accumulation on beaches throughout Geographe Bay. Photographic images were recorded approximately daily at 14 beaches throughout Geographe Bay from 1 May – 1 October 2008 using cameras, or via webcams at two additional sites. The volume of wrack on the beach was then categorized using a visual assessment of each image and the changes in wrack accumulation analysed for each beach.
- Quantitative assessment. To provide a more detailed assessment of changes in wrack abundance on beaches, the volume and biomass of wrack was measured directly at a sub-set of three beaches from April to December.

6.2.3 Qualitative assessment of wrack abundance on beaches

Volunteers from the local community were recruited to take photographs of 14 beaches across Geographe Bay (Table 6.3). The sites were selected to cover a broad spatial scale and to include beaches with potentially different accumulation patterns due to offshore features or orientation. Photographs were taken from a standard position on the beach, in both directions running parallel with the coastline. The start and end date of monitoring at the different volunteer sites varied, but most sites were monitored between June and September. At the Volunteer Marine Rescue building and the Geographe Sailing Club, webcams were installed and set to record images at six minute intervals. For webcam data, the clearest image of each day was chosen for analysis. The webcams regularly stopped communication so there are many gaps in the data.

Table 6.3 Sites used in the qualitative and quantitative assessments of spatial and temporal variations in beach wrack.

SITES	GPS LOCATION	START DATE	END DATE	GROYNE PRESENT
Volunteer Imagery sites				
Wonnerup East (WE)		1/5/2008	11/9/2008	No
Wonnerup	S33° 37.639’ E115° 23.826’	1/5/2008	1/9/2008	West end

Moonlight Bay		1/5/2008	30/9/08	Both ends
Port Geo. Groyne (PGW)	S33° 37.872' E115° 23.268'	9/5/2008	27/8/08	East end
Guerin St	S33° 38.075' E115° 22.822'	12/5/2008	14/8/08	No
998 Geographe Bay Rd (998)	S 33° 38.219' E115° 22.307'	9/5/2008	13/9/08-	No
Vol. Marine Rescue (VMR)	S 33° 38.503' E115° 21.249'	10/6/2008	15/9/08	No
Busselton Jetty (BJ)	S33° 38.653' E115° 20.689'	3/5/2008	29/9/08	No
High St (H)	S33° 38.877' E115° 20.151'	18/6/08	16/9/08	No
Bower St (B)	S33° 39.195' E115° 18.839'	22/5/08	30/9/08	No
Dolphin Rd (DR)	S33° 39.282' E115° 18.127'	6/6/2008	29/7/08	X No
Abbey (A)	S33° 39.382' E115° 16.308'	13/5/08	1/10/2008	Both ends
Quindalup (Q)	S33° 39.210' E115° 13.565'	1/5/2008	31/7/08	No
Dunsborough (D)		22/5/08	13/8/08	No
Web cam sites				
Volunteer Marine Rescue	S33° 38.532' E115° 21.128'	6/6/2008	22/9/08	
Geographe Sailing Club	S33° 38.975' E115° 19.888'	20/6/08	2/9/2008	
Quantitative sites	Start of transect			
Forrest Beach (FB)	S33° 38.975' E115° 19.888'	22/4/08	11/12/2008	
Vol. Mar. Res. (VMR)	S33° 38.532' E115° 21.128'	22/4/08	11/12/2008	
Geographe Sailing Club (GSC)	S33° 38.975' E115° 19.888'	22/4/08	11/12/2008	

All images were analysed to provide a classification of the amount of wrack on the beach using a qualitative scale (Table 6.4). This qualitative scale was converted into volume and biomass estimates using matched photo and biomass/volume data collected at seven beaches on 19 May, 3 June and 28 July 2009. At each beach and time, four 200m long transects were established, photographed and images analysed using the qualitative scale defined above. At the same time, the volume of wrack on each transect was estimated by a rapid assessment approach described below. The mean biovolumes for size classes in the qualitative scale ranged from $5.13 \times 10^{-4} \pm 0.96 \times 10^{-4}$ m^3 m^{-2} for class 3, to 0.79 ± 0.31 m^3 m^{-2} for class 8 (Table 6.4). In general, each increase in the qualitative scale corresponded to approximately one order of magnitude increase in wrack volume, with the exceptions of classes 6 and 7 which showed little difference.

Table 6.4 Qualitative scale used to classify wrack accumulations on Geographe Bay beaches, and the mean volume of wrack corresponding to each class.

SCALE	DESCRIPTION	BIOVOLUME [m^3m^{-2} ± SE]
0	Photography not commenced	n.a
1	No image	n.a
2	No wrack	n.a
3	Thin cover (~ < 0.1 m high) covering < 10% of beach width	$(5.13 \pm 0.96) \times 10^{-4}$
4	Thin cover (~ < 0.1 m high) covering 10-50% of beach width	$(6.52 \pm 1.40) \times 10^{-3}$
5	Thin cover (~ < 0.1 m high) covering > 50% of beach width	$(4.36 \pm 2.80) \times 10^{-2}$
6	Thick cover (<1 m high) small aggregations separated by sand	$(1.28 \pm 0.36) \times 10^{-1}$
7	Thick cover (<1 m high) small aggregations thin wrack between them	$(1.69 \pm 0.31) \times 10^{-1}$
8	Thick cover (<1 m high) continuous aggregations	$(7.96 \pm 3.13) \times 10^{-1}$
9	Thick cover (>1 m high) with continuous aggregations	n.a.

The amount of wrack on beaches within Geographe Bay varied spatially and temporally (Table 6.5). Averaged across all sites, beaches scored a Qualitative Scale 5 (thin cover less than 10 cm high covering > 50% of beach; Table 6.4 and Table 6.5). Sites to the west of Geographe Bay had higher than mean scores (5-6) while sites in the central portion of the bay had lower than mean scores (3-4). The highest values occurred at sites in closer proximity to the Port Geographe development, reaching 8.5 at the Port's western groyne, and the lowest scores were for beaches east of Port Geographe (Wonnerup and Wonnerup East) which had mean values of 2.9 and 3.4, respectively.

Across a subset of sites with the most regularly recorded imagery (Wonnerup East, Wonnerup West, Guerin St, 998 Geographe Bay Rd, Busselton Jetty, Bower St and Dunsborough) and without groynes, there was a trend of increasing variation in the amount of wrack on the beaches from May to August (Figure 6.4). While there was no obvious trend in median or lower percentiles, the maximum amounts of wrack observed increased, from 6 in May to 7 in June and reaching a maximum of 9 in late July and early August (Figure 6.4). Thus, the variability in wrack increases as winter progresses with peak wrack accumulations occurring from July onwards.

Table 6.5 Amount of wrack on beaches in Geographe Bay during autumn-winter 2009. Wrack volume was classified from 1 to 9 as per the qualitative scale of assessment (Table 6.4), Data are averaged over the sampling period, however does not include the Guerin St site, which was influenced by wrack from the Port Geographe development.

SITE	WRACK ABUNDANCE (AS PER QUALITATIVE CLASSIFICATION SCALE)			
Ordered from west (top) to east (bottom)	Mean ± se (n)	Percentiles		
		Median	75th	90th
Dunsborough	5.0 ± 0.07 (162)	5	6	6
Quindalup	6.3 ± 0.12 (73)	7	7	7
Abbey	6.3 ± 0.21 (81)	7	8	8
Dolphin Rd	3.9 ± 0.12 (48)	4	4	4
Bower St	4.2 ± 0.05 (250)	4	4	6
Geographe Sailing Club	4.0 ± 0.15 (64)	4	4	6
High St	3.8 ± 0.04 (127)	4	4	4
Busselton Jetty	3.8 ± 0.06 (216)	4	4	4
Vol. Marine Rescue	4.0 ± 0.03 (185)	4	4	4
Vol. Marine Rescue (web cam)	3.6 ± 0.06 (78)	4	4	4
998 Geographe Bay Rd	5.7 ± 0.08 (247)	6	7	7
Guerin St	6.4 ± 0.16 (128)	7	7	9
Port Geographe Groyne	8.5 ± 0.06 (206)	9	9	9
Moonlight Bay	5.8 ± 0.15 (117)	6	7	8
Wonnerup	2.9 ± 0.13 (56)	3	3	4
Wonnerup East	3.4 ± 0.07 (110)	4	4	4
All sites with groynes	6.7 ± 0.13 (277)	7	9	9
All sites without groynes	4.3 ± 0.03 (1487)	4	4	6
ALL SITES	5.0 ± 0.04 (2148)	4	6	8

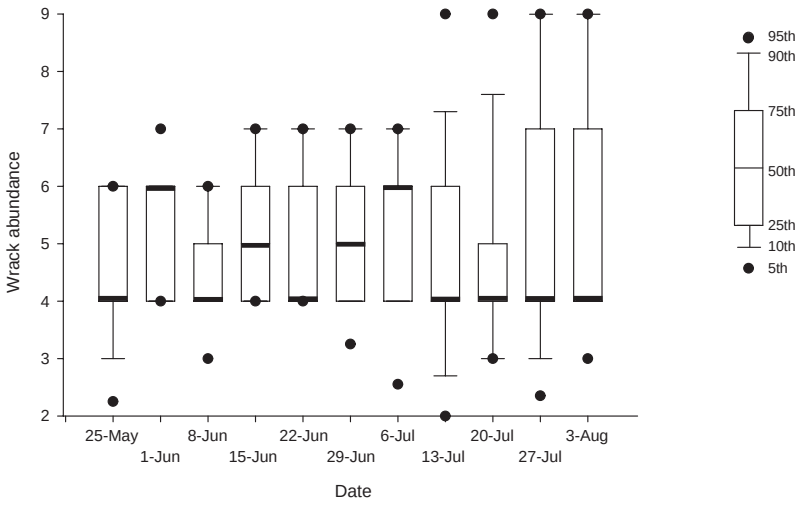

Figure 6.4 Percentile plots of wrack abundance over time (weekly intervals) at sites without groyne structures (Wonnerup East, Wonnerup West, Guerin St, 998 Geographe Bay Rd, Busselton Jetty, Bower St and Dunsborough.

Despite these overall trends, there were contrasting site-specific patterns in wrack accumulation (Figure 6.5 - Figure 6.7). Dunsborough, Quindalup and Bower St had the maximum accumulations in May and early June (scores of 6 -7) reducing to 4 in July and for the rest of the sampling period (Figure 6.5). Sites close to Port Geographe (998 Geographe Bay Rd, Guerin St and Port Geographe Groyne, Figure 6.5) and Abbey had increasing accumulations of wrack over the sampling period. There were generally low amounts of wrack (< 4) at Wonnerup West, Busselton Jetty and Volunteer Marine Rescue, with peaks (6 - 7) but only for a short duration, indicating a short residence time of wrack on the beach (Figure 6.5 and Figure 6.7). Finally the Port Geographe beaches had large accumulations of wrack but were highly variable (Figure 6.6).

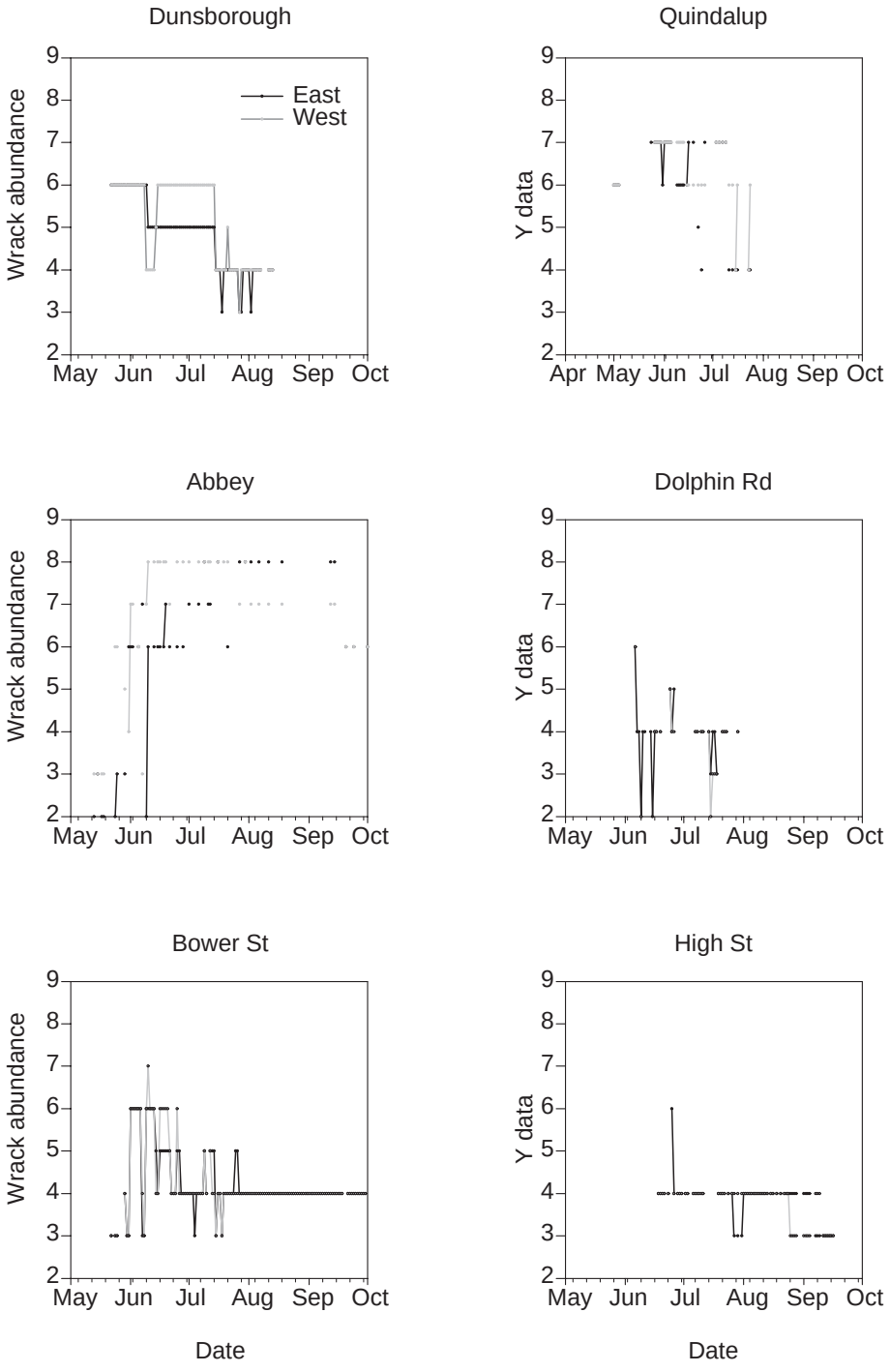

Figure 6.5 Wrack abundance scores (qualitative scale) over time (daily intervals) at sites in Western Geographe Bay. See Table 6.4 for explanation of wrack abundance scores.

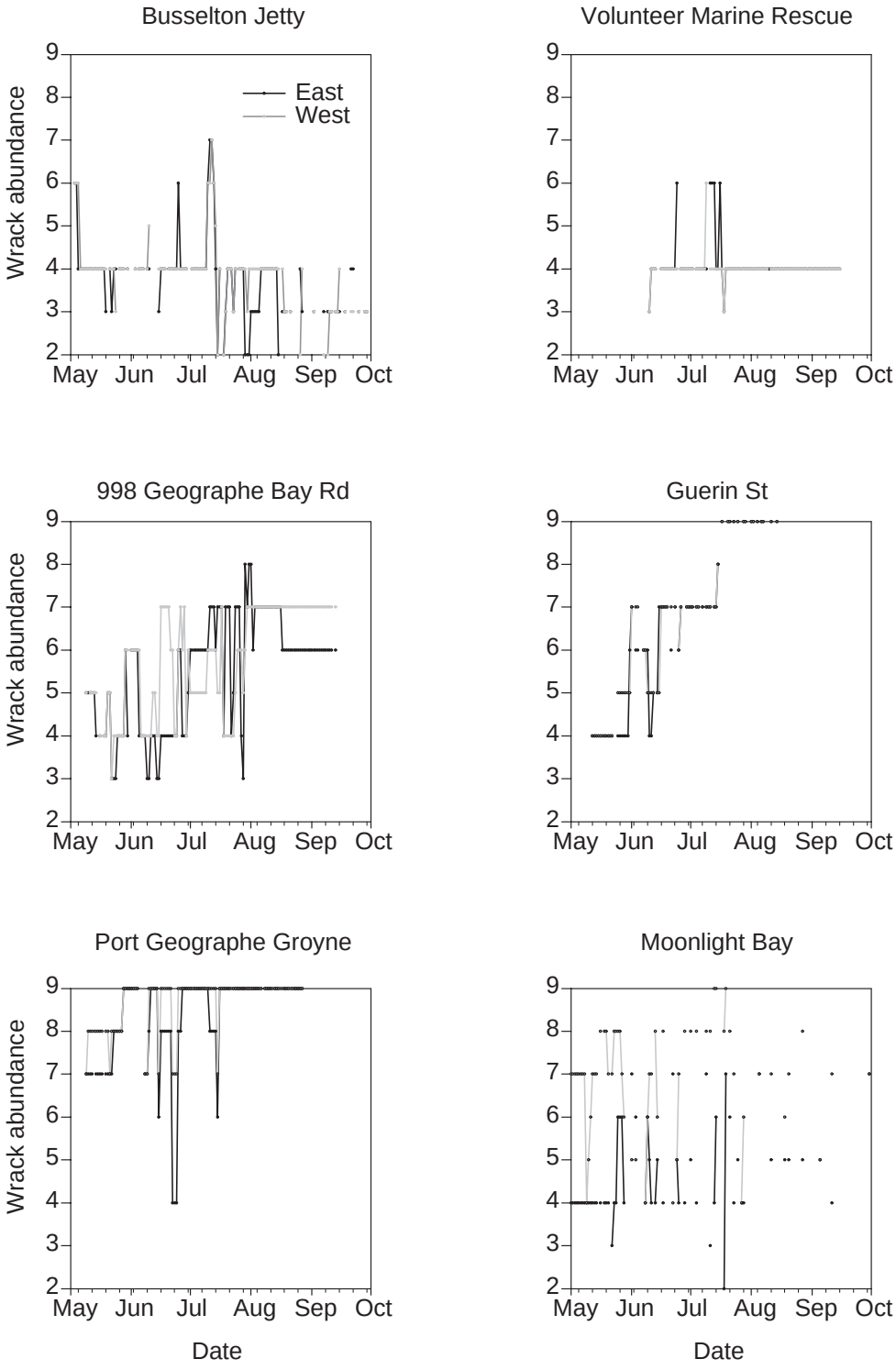

Figure 6.6 Wrack abundance scores (qualitative scale) over time (daily intervals) at sites in central Geographe Bay. See Table 6.4 for explanation of wrack abundance scores.

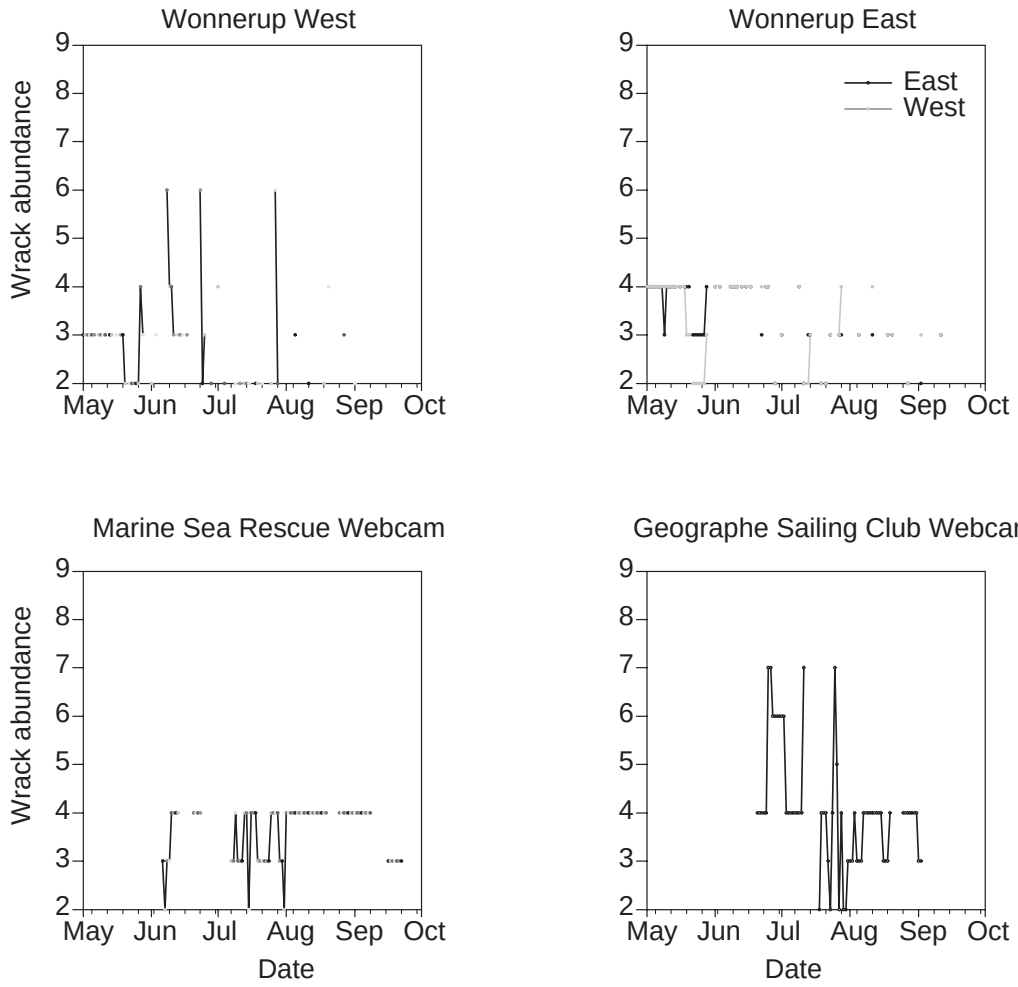

Figure 6.7 Wrack abundance scores (qualitative scale) over time (daily intervals) at sites in eastern Geographe Bay and the two web cam sites. See Table 6.4 for explanation of wrack abundance scores.

6.2.4 Quantitative assessment of wrack abundance on beaches

The amount of wrack on beaches was quantitatively assessed using two approaches:

- three sites were surveyed 10 times over the year from 22 April – 11 December to estimate the volume of wrack on the beach.
- three sites were surveyed 5 times over the year from 19 May – 20 October to estimate the biomass of beach wrack both above and below the beach surface.

6.2.4.1 Wrack volume

The volume of wrack on a 200 m stretch of beach was estimated at Forrest Beach, Volunteer Marine Rescue and Geographe Sailing Club, on ten occasions, between 22 April and 12 December 2008. These sites were considered representative of natural wrack accumulations within ~ 10 km of Port Geographe. April and May were considered the pre-accumulation, June – August the accumulation period and September – December the post accumulation period. The volume was estimated from the shoreline to the edge of the vegetation along a 200 m stretch of beach. The length, width and height of aggregations were recorded, summed and the volume expressed as m^3 of wrack per m^2 of beach.

There was some spatial and temporal variation in the volume of wrack on beaches in Geographe Bay (Figure 6.8 and Figure 6.9). For the three standard sites, the greatest volume was observed at Forrest Beach, once during the pre-

accumulation period (7.5 x 10^{-2} m^3 m^{-2}) and once during the accumulation period (3.4 x 10^{-2} m^3 m^{-2}). The maximum volume at Volunteer Marine Rescue was 1.05 x 10^{-2} m^3 m^{-2} and at Geographe Sailing Club was 8.4 x 10^{-3} m^3 m^{-2}, both during the accumulation period. Disregarding the peaks at Forrest Beach, the average volume of wrack on the beaches was greater during the accumulation period, 5.74 x 10^{-3} m^3 m^{-2} in comparison to the pre-accumulation (1.49 x 10^{-3} m^3 m^{-2}) and post-accumulation (0.53 x 10^{-3} m^3 m^{-2}) periods. These volumes were equivalent to some of the lowest amounts of wrack observed on the beaches in Geographe Bay where image analysis was done during the study period, ~ 3 - 4 from the qualitative scale, equivalent to a thin cover of wrack (< 10 up to 50 % of the width of the beach).

6.2.4.2 Wrack biomass

The biomass of wrack was estimated at the same three beaches as volume estimates, on five occasions between 19 May and 22 October 2008. Within each 200 m stretch of beach, four transects were established running perpendicular from the shoreline to the primary dune vegetation. On each transect, a standard volume of wrack was sampled from an accumulation considered representative of those along the transect. Samples were taken from the surface of each wrack accumulation and at the surface of the underlying sediment (surface: 1 000 cm^3; sediment: 196 cm^3 to 10 cm depth). The samples were sieved to remove sand and other debris leaving only wrack, which was dried at 60°C and weighed. Biomass was expressed as kg DW m^{-3}, and converted to biomass kg DW m^{-2} based on the volume of surface wrack present on the beach for each sampling occasion.

Table 6.6 Sampling dates for quantitative assessment of wrack volume and biomass on Forrest Beach, Volunteer Marine Rescue and Geographe Sailing Club beach sites.

DATE	SEASON	VOLUME	BIOMASS
22 April 2008	Pre-accumulation	Y	
20 May 2008	Pre-accumulation	Y	Y
9 June 2008	Accumulation	Y	
23 June 2008	Accumulation	Y	Y
22 July 2008	Accumulation	Y	
13 August 2008	Accumulation	Y	Y
27 August 2008	Accumulation	Y	
22 September 2008	Post-accumulation	Y	Y
20 October 2008	Post-accumulation	Y	
11 December 2008	Post-accumulation	Y	Y

The biomass of wrack sitting on the beach surface (i.e. excluding buried material) ranged from 0.001 – 3.64 kg m^{-2} at the three sites over the year (Figure 6.9). The biomass was greater in the accumulation period (mean = 0.28 kg m^{-2}) compared to the pre- (mean = 0.06 kg m^{-2}) and post-accumulation (mean = 0.03 kg m^{-2}) periods. The biomass of wrack buried to 10 cm ranged from 0 - 4.65 kg m^{-2} (Figure 6.9) and it too was higher in the accumulation period (mean = 0.41 kg m^{-2}), than the pre- (mean = 0.29 kg m^{-2}) and post-accumulation (mean = 0.04 kg m^{-2}) periods.

On a number of occasions wrack was observed buried 15 - 45 cm under the sediment surface as a thick layer ~ 10-15 cm thick. On these occasions the biomass of wrack was typically higher than was observed in the top 10 cm layer of sediment, ranging from 2.73 to 3.43 kg m^{-2} or 39 – 49 kg m^{-3}.

Forrest Beach

Volunteer Marine Rescue

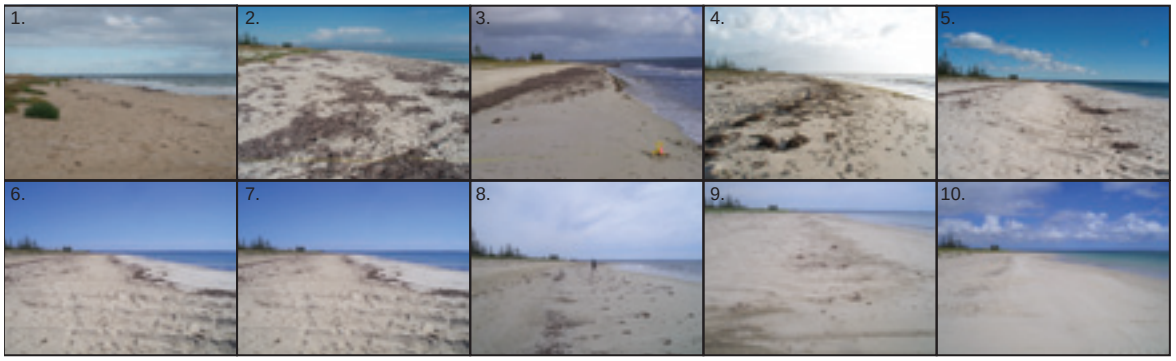

Geographe Sailing Club

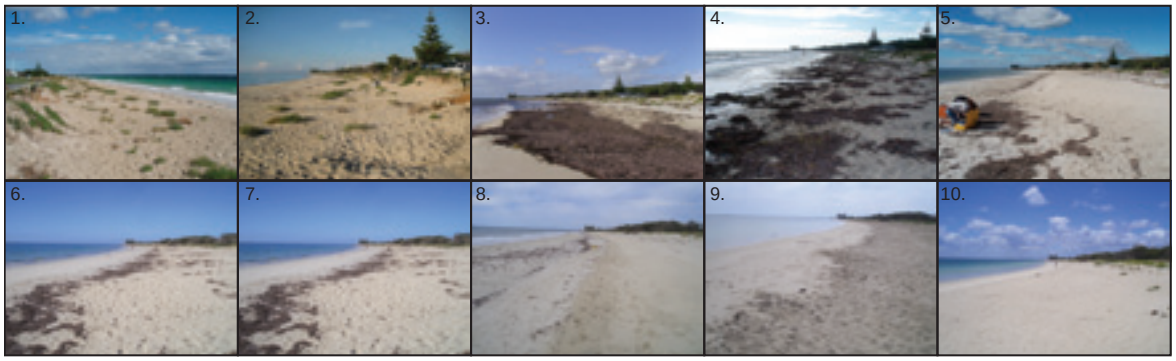

Figure 6.8 Photographs of wrack accumulations on the 10 sampling occasions in 2008, at each of the three quantitative assessment beaches: 1) 22 April; 2) 20 May; 3) 9 June; 4) 23 June; 5) 22 July; 6) 13 August; 7) 27 August, 8) 22 September; 9) 20 October; 10) 11 December.

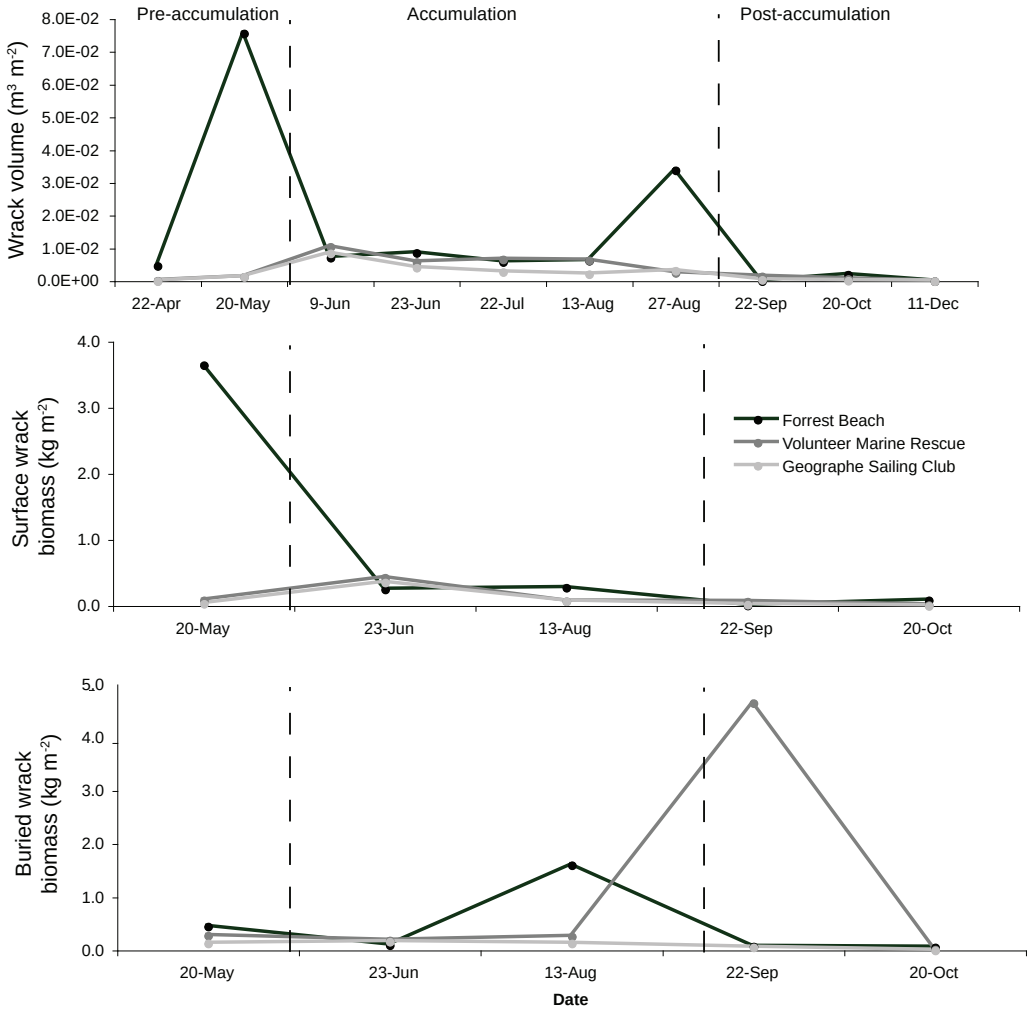

Figure 6.9 Wrack volume and biomass (surface and buried) at three beach sites from April-May to October 2008.

6.2.5 Significance of results

The accumulation of wrack on Geographe Bay beaches is highly variable with time and among beaches. This is indicative of complex processes resulting in the frequent deposition and removal of wrack from beaches. The results highlighted the need to incorporate off-shore movement of wrack accumulations into the particle transport model.

Despite the highly variable nature of wrack accumulations, beaches generally had more wrack on them during the accumulation period (July – August). These findings are consistent with our conceptualisation of wrack dynamics in Geographe Bay, whereby wrack is exported from offshore seagrass meadows in early winter into the near-shore zone. Once in the inshore zone, wrack is continually moving between the beaches and the nearshore waters and, while in the nearshore waters, transported in long-shore currents. Presumably, it is the wrack removed from the beaches and carried in longshore transport that ultimately accumulates at Port Geographe.

Beaches with groynes generally had more wrack than those without groynes. Sites close to Port Geographe had the most wrack, followed by Quindalup and Abbey Beach. Sites north-east of Port Geographe groyne had the least wrack. These findings are consistent with groynes interfering with the natural processes responsible for removal of wrack from beaches and along the shore. However, we cannot discount that there may be other factors influencing wrack accumulation at some of these sites.

Wrack biomass on the surface of the beach ranged from 0.001 – 3.64 kg m^{-2} (avg: 0.37 kg m^{-2}) but on occasions significantly more could be buried as deep as 45 cm below the sediment surface in bands 10 – 15 cm thick. This highlights the potential for loss of wrack from the system through burial, but also the potential for wrack to subsequently be released during beach erosion events. It also indicates that wrack may be buried deep in sediments where the bio-geochemical conditions could favour anoxic decomposition and the possible release of hydrogen sulfide, methane and other gases.

The biomasses and volumes of wrack recorded at the three quantitative assessment sites are not indicative of the larger accumulations that can occur on some Geographe Bay beaches. The aggregations observed here averaged 6.7 x 10^{-3} m^3 m^{-2}, considerably less than those recorded at Port Geographe, estimated to be 3.75 m^3 m^{-2} over a 2 km stretch [*DPI*, 2007].

6.3 Temporal and spatial variation in beach morphometry

The previous section indicated that wrack is not only deposited on beaches of Geographe Bay but that it can be rapidly removed from those beaches and become available for long-shore transport and re-deposition on other beaches. This process occurs on daily to weekly timescales, resulting in highly patchy and temporally variable beach wrack accumulations. Presumably, it is the longshore movement of wrack that has been removed from beaches that ultimately results in the large accumulations at Port Geographe. A potentially important determinant of the ability of wrack to accumulate on beaches is the beach morphometry. Once deposited, however, wrack can alter beach morphometry and may affect the subsequent deposition of more wrack or the removal of wrack from the beach. To improve the understanding of wrack accumulation and transport on and off beaches, and any relationship to beach morphometry, beach morphometry was assessed across the winter accumulation period.

6.3.1 Objective

To determine the temporal and spatial dynamics in beach width and slope over an annual cycle in Geographe Bay, to improve understanding of wrack accumulation and transport on and off beaches.

6.3.2 Materials and methods

Three sites (Forrest Beach, Volunteer Marine Rescue, Geographe Sailing Club) were surveyed on 10 occasions between 22 April – 11 December 2008 to estimate the beach slope and width. April and May were considered the wrack pre-accumulation period, June - August the accumulation period and September – December the post accumulation period.

At each site four transects (Table 6.7) were run perpendicular to shore along a 200m stretch of beach from the edge of the dune vegetation to ~ 5 horizontal metres into the water. The relative height along the transect was measured with a Dumpy level and staff and referenced to a 'Reference location,' which was a solid substrate not likely to alter height over the course of the study, in turn referenced to a Landgate Control Point with a known height above sea level (AHD). The location of dune vegetation, edge of seawater, high water mark and the position of wrack along each transect were noted.

Table 6.7 GPS coordinates for the reference locations and the start of each beach morphometry transect at each site (WGS 84), and the name and coordinates of the Landgate control points used to relate the transects to standard AHD (m).

SITES	TRANSECT 1	TRANSECT 2	TRANSECT 3	TRANSECT 4	REFERENCE LOCATION	CONTROL POINT
Forrest Beach (FB)	S33°38.975' E115°19.888'	S33°35.175' E115°26.927'	S33°35.204' E115°26.905'	S33°39.003' E115°19.761'	S33°35.247' E115°26.909'	SSM HB 17 (3.794m) 355448.000 6 281312.000
Volunteer Marine Rescue (VMR)	S33°38.532' E115°21.128'	S33°38.515' E115°21.214'	S33°38.521' E115°21.170'	S33°38.532' E115°21.128'	S33°38.543' E115°21.250'	BUS 47 (3.040m) 333833.4884 1152116.9227
Geographe Sailing Club (GSC)	S33° 38.975' E115°19.888'	S33°38.982' E115°19.865'	S33°38.982' E115°19.865'	S33°39.003' E115°19.761'	S33°38.999' E115°19.828'	BS 01109 (2.945m) 345097.703 6275237.443

Beach slope was calculated from the edge of the dune vegetation and from the high water mark to 0 m AHD. Width of the beach was calculated from 0 m AHD and from the water's edge to the start of the dune vegetation. The average beach profile from each site at each time was also plotted.

6.3.3 Results

The slope of the beach (dune vegetation to 0 m AHD) varied over the year and among sites, ranging from 4.0 – 7.8 cm m^{-1} (or 1:13 – 1:25; Figure 6.10). VMR and GSC both showed fluctuating beach slope over the study period with no clear trends. Forrest Beach had the most consistent slope over the year ranging from 5.5-6.0 cm m^{-1} (1:17 – 1:18).

The slope of the beach from the high water mark to the 0 AHD could not be calculated when the high water mark was not visible. This slope measure (from high water mark) followed a similar pattern to the other slope measure (from dune vegetation), but tended to be slightly more extreme; at the maximum slopes it was slightly steeper and at the minima less steep (Figure 6.10).

Beach width varied over the year and among sites, ranging from 20 – 45 m from the edge of the dune vegetation to 0 m AHD (Figure 6.10). At Forrest Beach the minimum beach width occurred in the pre-accumulation period (28 m) and the maximum in late July during the accumulation period (42 m). At the Volunteer Marine Rescue site minima were observed in late April (pre-accumulation) and mid-August (accumulation) at ~ 22 m, with the maximum in early June at 40 m. At Geographe Sailing Club the minimum was observed in late June (26 m) during the accumulation period and the maximum (45 m) in late September in the post-accumulation period.

The location of wrack on the beaches varied among times but was similar at all beaches. In the pre-accumulation period, if wrack was present it was located between the current water level and the high water mark (Figure 6.11). During the accumulation period wrack extended beyond the high-water mark and in August was spread over larger portions of the beach. By December no wrack was present on the beaches.

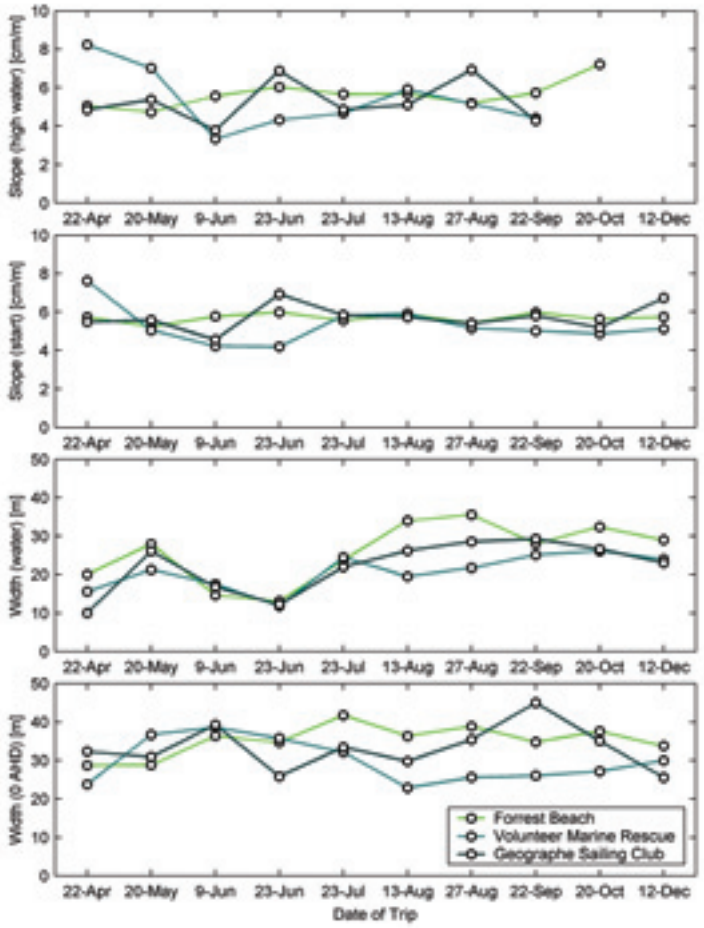

Figure 6.10 Beach slope (high-water mark to 0 m AHD and start of dune vegetation to 0 m AHD) and width (start of dune vegetation to water level at time of sampling and dune vegetation to 0 m AHD) at three beaches in Geographe Bay. At some times (12 December and 20 October at Volunteer Marine Rescue and Geographe Sailing Club) the high water mark was not visible so the slope from the high water mark to 0 AHD could not be calculated.

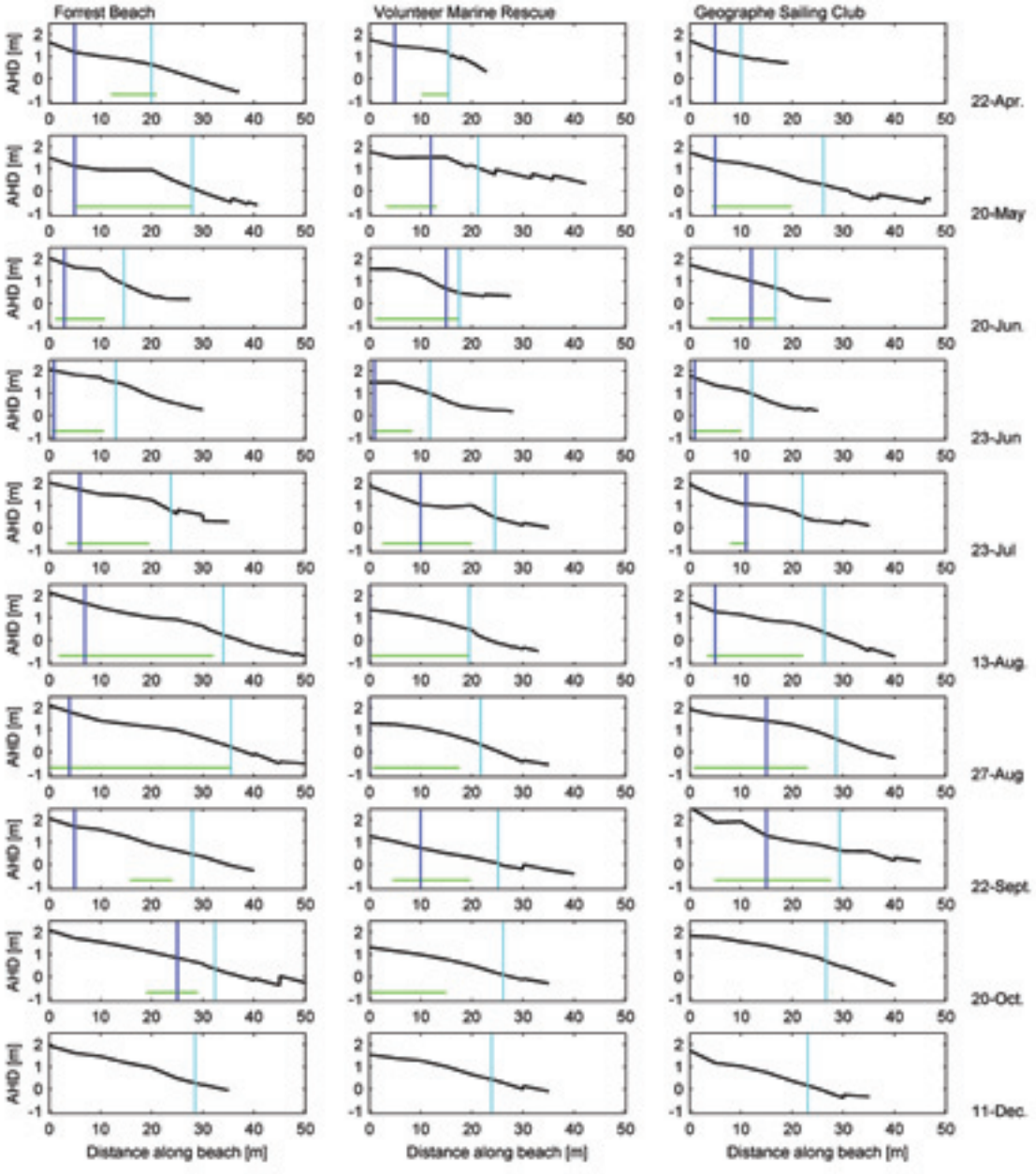

Figure 6.11 Beach morphometry referenced to 0 m AHD with the profile (black line), high-water mark (dark blue line), water level (light blue line) and location of wrack (green line) at the three main study sites in Geographe Bay over the year, 22 April to 12 December 2008. Each graph is an average of 4 profiles. 0 distance on the x-axis is the start of the dune vegetation.

6.3.4 Significance of results

Beach slope and width will affect the accumulation and movement of wrack onto and off beaches. Both features varied through the year and among sites, but not in any constant fashion. The most eastern site, Forrest Beach had the most consistent slope over the year. At the Volunteer Marine Rescue site the slope declined, increased and then remained steady. Geographe Sailing Club was the most variable. These differences among sites may be related to the near-shore bathymetric features, however, there is no detailed bathymetry near these standard sites so it is not possible to confirm this.

Of direct relevance to modelling of on- and off-shore wrack movement:

- beach slope (dune vegetation to 0 AHD) ranged from 4.0 – 7.8 cm m^{-1} (~1:13 – 1:25). These are similar to previous measurements (Aug 1976 to Oct 1979) of the beach slope (edge of bitumen to 0 AHD) in Geographe Bay, 3 – 7 cm m^{-1} (~1:14 – 1:33);
- beach width (start of dune vegetation to 0 AHD) ranged from 20 – 45 m;
- where there are large accumulations of wrack, the wrack may directly alter the beach profile (slope and width) and the boundary conditions for modelling; and,
- the water level on the beach was frequently 15 - 20 horizontal linear m above 0 AHD but at times up to 25 horizontal linear m above 0 AHD, indicating that there were frequent opportunities for wrack to be transported on and off the beach.

Where appropriate, these basic beach parameters have been applied in the particle transport model.

6.4 Composition of beach wrack

Wrack accumulations can be comprised of a variety of different seagrass and algal material. The composition affects a number of important aspects of wrack dynamics. These include physical and biogeochemical characteristics, such as: particle density, which affects the transport of wrack to the beach; bulk density of the beach accumulations, which may affect the re-mobilisation of wrack; tensile strength, which affects the ability to pump wrack in by-passing operations; the dissolved oxygen profile through wrack banks, which affects decomposition and gas evolution; and the rate of decomposition, which is a loss term for wrack.

As a pre-requisite for understanding the types of particles to incorporate into the particle transport model and in order to understand the likely behaviour of beach accumulations, the composition of beach wrack was determined.

6.4.1 Objective

To determine the temporal and spatial variation in the composition of beach wrack accumulations.

6.4.2 Methods

The composition of wrack was determined by two approaches:

- collecting wrack at three sites on five occasions over an annual cycle, and
- on a single occasion, collecting wrack from accumulations of different ages and sizes from the same three sites.

6.4.2.1 Composition of small wrack accumulations over an accumulation period

Samples to assess temporal and spatial variation in wrack composition were collected at the three standard sites, Forrest Beach, Volunteer Marine Rescue and Geographe Sailing Club on 19 - 22 May, 9 - 11 June, 12 - 15 August, 22 - 25 September and 20 - 22 October. May was considered the wrack pre-accumulation period, June - August the accumulation and September the post-accumulation period.

At each site and time, four replicate wrack accumulations were sampled. Within each replicate, two zones were sampled: surface wrack and sediment below the wrack. About 0.001 m^3 of wrack was collected from the surface with a quadrat and from the sediment with a core (Figure 6.12). Wrack was rinsed to remove sand and sorted into categories (Table 6.8) and age of wrack. Age was defined as either old (no green leaves) or new (green leaves or stem). An earlier experiment showed that moist leaves above the surface of the sediment turned brown within 2 weeks (*P. sinuosa*) or 2 - 4 weeks (*A. antarctica*), whereas buried leaves turned brown within 2 - 8 weeks (*P. sinuosa*) or 2 - 4 weeks (*A. antarctica*). Wrack was spun in a salad spinner for two cycles to remove excess water and the fresh weight recorded.

Figure 6.12 Methods to collect samples for above- and below-ground wrack composition. Above-ground samples were collected from within a 0.25 x 0.25 x 0.1 m area (a) and below-ground samples were taken with a core (b) and then sieved to remove sand (c). All samples were processed in the laboratory (d).

Table 6.8 Classification of beach wrack samples used in the composition analyses.

TYPE	AGE
P. sinuosa leaves	Old or New
P. sinuosa rhizomes & roots	na
A. antarctica stems without leaves	Old
A. antarctica stems with leaves	Old or New
A. antarctica rhizomes & roots	na
Macroalgae	na
Other	na

6.4.2.2 Composition of large wrack accumulations

The standard sites generally contained small wrack aggregations, < 0.5 m high. In order to characterize larger wrack accumulations, one-off sampling was conducted on 24th - 26th July 2008 at three sites with large accumulations. Siesta Park had aggregations > 1 m high and which had been present for more than twelve weeks. Guerin St had aggregations also > 1 m high but which had been present for six weeks. Abbey Beach had accumulations between 0.5-1m high which had been present for six weeks (Figure 6.13).

At each site four replicate accumulations were measured and within each replicate, four zones were sampled: Surface, at the top of the accumulation; Mid, midway between the top of the saturated zone and the surface; Saturated, the wrack at the top of the saturated zone; and Sediment, in the sediment below the wrack (Figure 6.14). The sampling was as for small wrack accumulations (see above).

Figure 6.13 Sites sampled with large wrack accumulations. (a) Siesta Park, (b) Guerin St, (c) Abbey Beach.

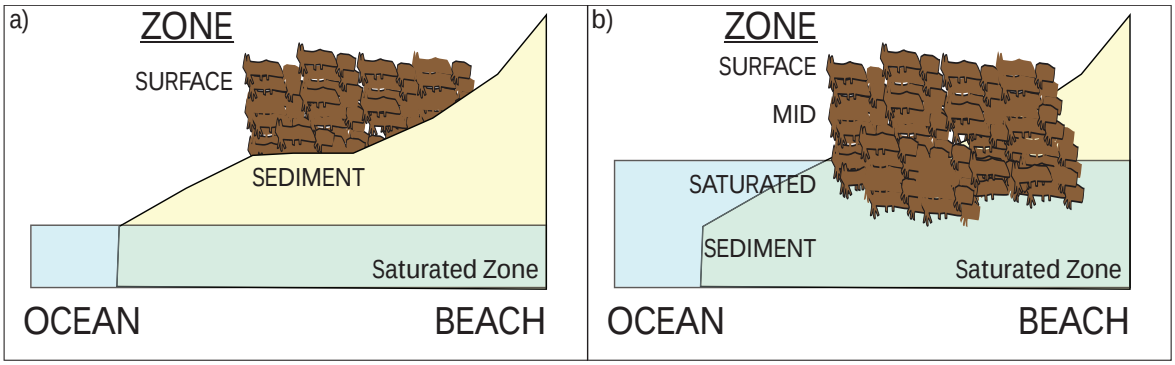

Figure 6.14 Depiction of sampling zones within a) small wrack accumulations and b) large wrack accumulations.

6.4.3 Results

6.4.3.1 Composition of small wrack accumulations over a year

P. sinuosa seagrass was the dominant component of beach wrack, both at the surface of small accumulations (avg: 55 %; max: 91 %) and buried in the sediment (avg: 82 %; max: 100%; Figure 6.15). The proportion of *A. antarctica* and algae in the surface beach wrack increased from an average of 5 % *A. antarctica* and 8 % algae in the pre-accumulation period up to an average of 31 % and 16 % respectively in the accumulation period. Greater proportions of *A. antarctica* and algae were also detected early in the post-accumulation period (late September). Generally the proportion of *A. antarctica* and algae buried in the sediment was also greater in the accumulation period. The general patterns in composition at each site were similar, though the amount of *A. antarctica* varied among sites (Figure 6.15).

Most of the above-ground seagrass wrack observed on the beaches (overall avg: 76 %) and buried in the sediment (overall avg: 96 %) was brown in colour (Figure 6.16), indicating the wrack had been on the beach for at least 2 - 8

weeks. A greater proportion of new material was present during the accumulation period (avg: 26 %) and in late September in the early stages of the post-accumulation period.

At all sites, the majority of the wrack was composed of above-ground seagrass material such as leaves and stems (overall avg: 94%; Figure 6.17). Below-ground material (rhizomes and roots) was not detected in the pre-accumulation period but was observed during the accumulation period, in both surface wrack and buried in the sediment, though always less than 10% of the mass. Below-ground material was most abundant in wrack in the early post-accumulation period (late September), with the maximum observed at Volunteer Marine Rescue in the sediment (40 %).

'Other' material observed in wrack included fauna, such as sponges and ascidians, and sticks and dead shells. In the surface wrack 'Other' material category never exceeded 2 % of the mass and in the sediment was generally less than 4 % DW, but on some occasions was 25 – 98 %, and this was generally due to dead shells and low amounts of plant material.

6.4.3.2 Composition of large wrack accumulations

Large accumulations of wrack generally had similar composition, age and source of seagrass wrack as small aggregations (Figure 6.15 - Figure 6.18). Older accumulations had less algae than new accumulations, and more below-ground material (Figure 6.18).

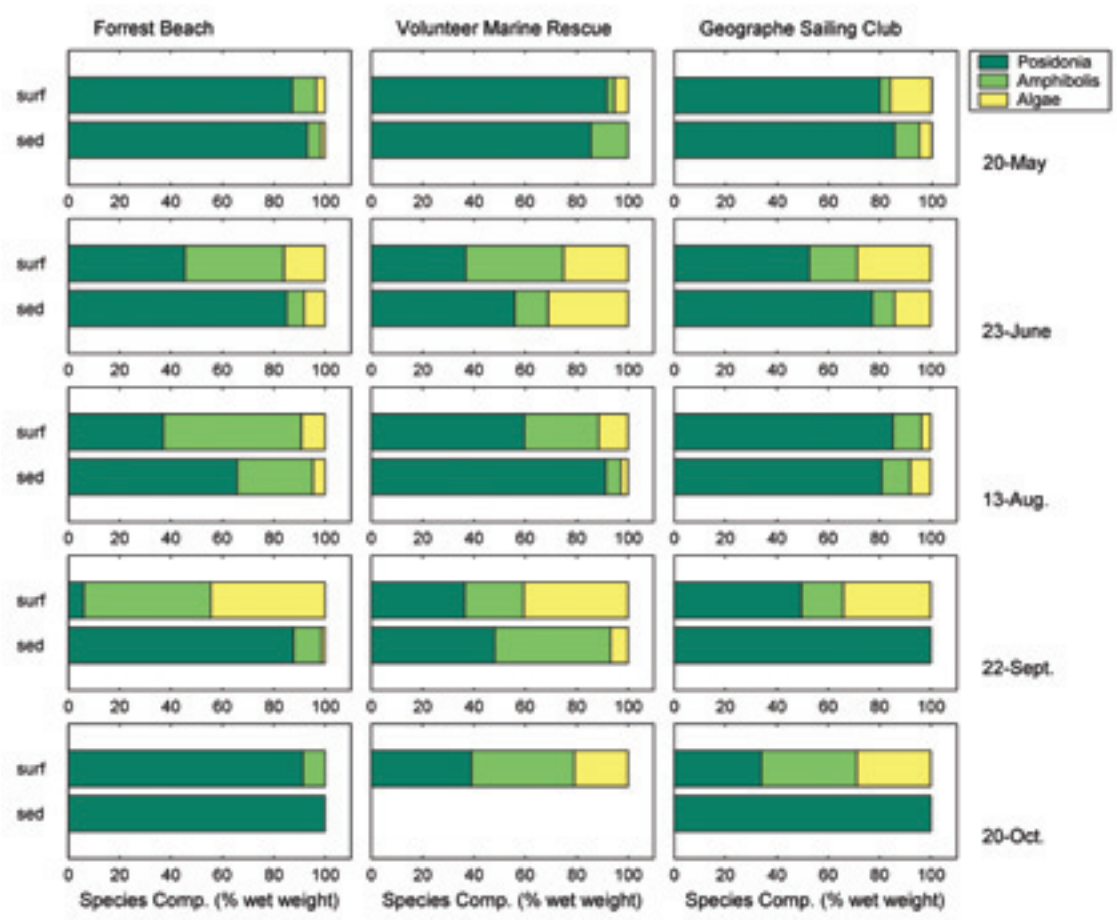

Figure 6.15 Wrack composition (% wet weight) at the three standard sites over the year. Note no wrack was present in the sediment at Volunteer Marine Rescue on 20 October and the 'Other' category was not included in the graphs. May = pre-accumulation period, Jun-Aug = accumulation period, Sept-Oct = post-accumulation period.

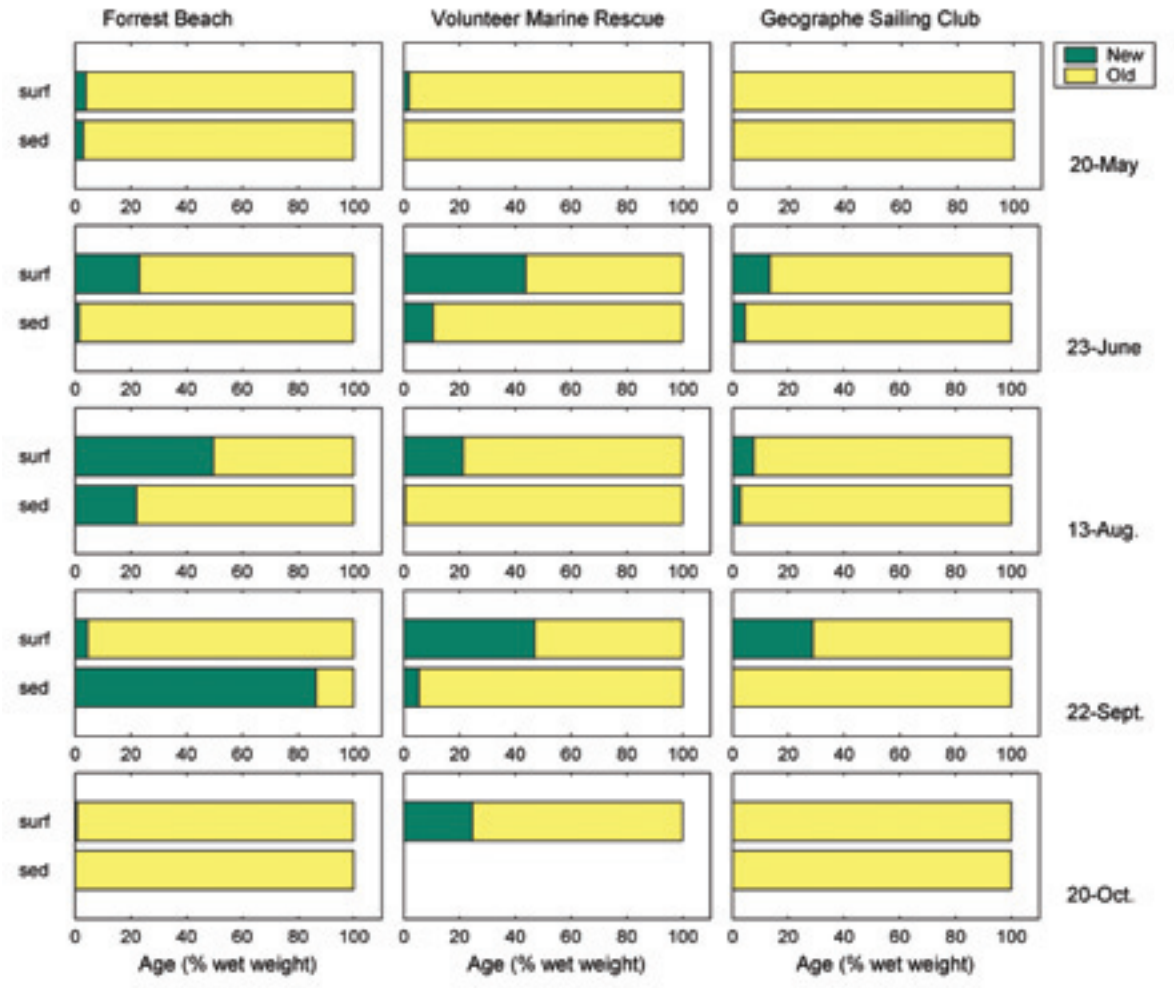

Figure 6.16 Age composition (% wet weight) of above-ground seagrass wrack at the three standard sites over the year. Note no wrack was present in the sediment at Volunteer Marine Rescue on 20 October.
May = pre-accumulation period, Jun-Aug = accumulation period, Sept-Oct = post-accumulation period.

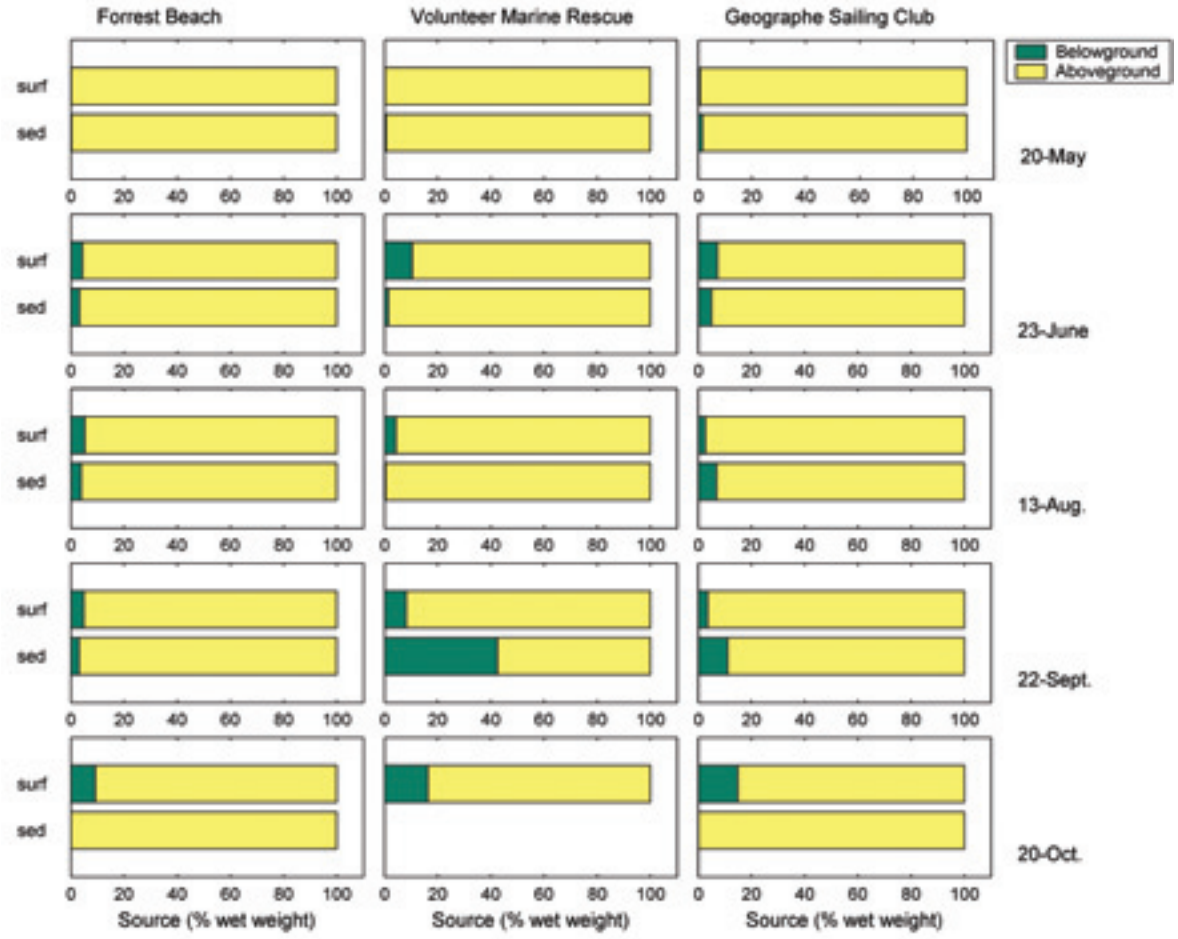

Figure 6.17 Source composition (% wet weight) of above (leaves and stems) or below-ground (rhizomes and roots) of seagrass wrack at the three standard sites over the year. Note no wrack was present in the sediment at Volunteer Marine Rescue on 20 October. May = pre-accumulation period, Jun-Aug = accumulation period, Sept-Oct = post-accumulation period.

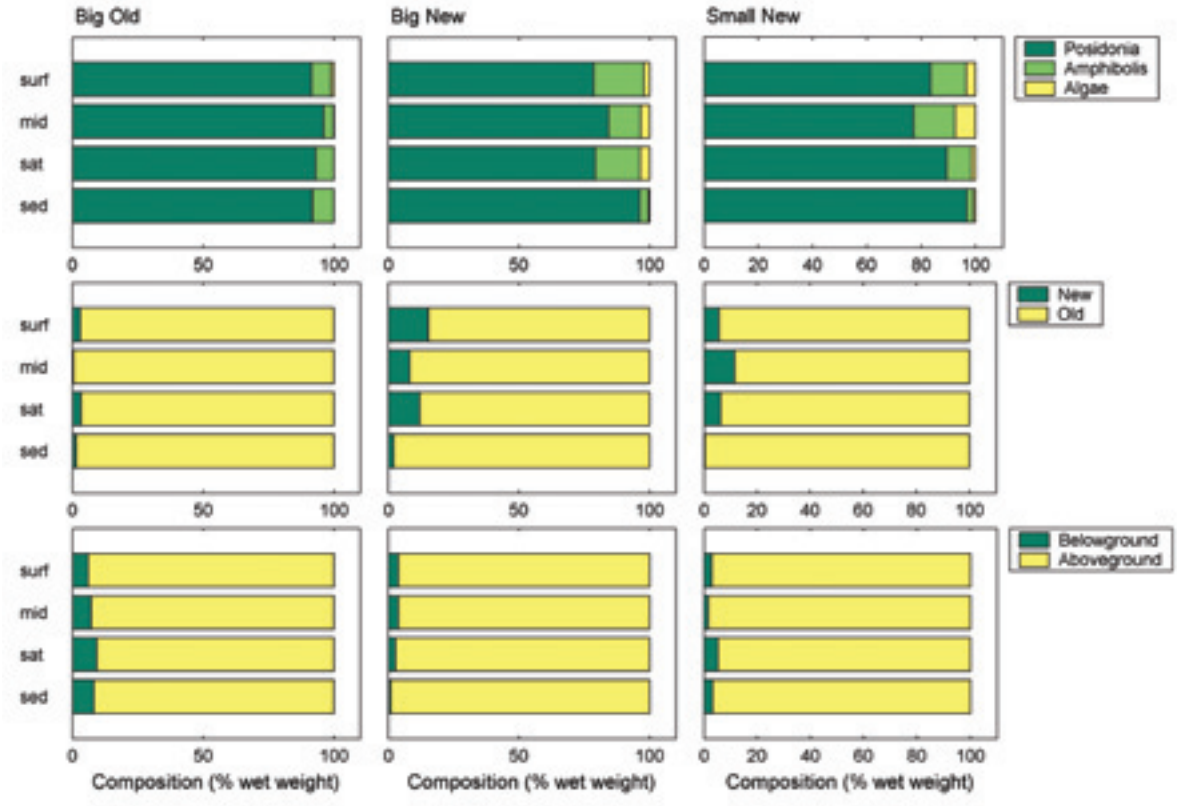

Figure 6.18 Wrack type (top), seagrass wrack age (middle) and source composition (bottom, % wet weight) from large wrack accumulations from a once-off sampling. Big Old is Siesta Park, Big New is Guerin St and Small New is Abbey.

6.4.4 Significance of results

Seagrass meadows in Geographe Bay are extensive, growing from ~ 2 m down to 30 m depth, and the shallow meadows (0 - 14 m) have the greatest density and most consistent cover [*Walker et al.*, 1987]. From Dunsborough to Vasse-Wonnerup estuary the sediment is predominantly sandy and covered with seagrass. Further north, there is some low and high relief reef [*McMahon et al.*, 1997]. The dominant seagrass in the shallow waters is *P. sinuosa*, with ~ 70% cover, and *A. antarctica* and *A. griffithii* are the next most common [*Walker et al.*, 1987] with larger meadows of *A. antarctica* located around Dunsborough [*McMahon et al.*, 1997].

P. sinuosa was the dominant component of beach wrack, reflecting its dominance in the waters of Geographe Bay. In the pre-accumulation period, it comprised 80 – 90 % of beach wrack, higher than the 70% cover observed in Geographe Bay, indicating that at this time of year it was more likely to be washed ashore than other seagrass species. *P. sinuosa* shoots produce 2 - 3 leaves per year, with the maximum biomass and leaf density in summer [*Marba and Walker*, 1999; *McMahon et al.*, 1997], and at the end of summer the oldest leaf is shed from the plant. Therefore, it is very likely that *P. sinuosa* leaves will be detached from the adult plant and be free in the water to be washed up on the beach during the pre-accumulation period.

The composition of beach wrack changes over the year. During winter and early spring (accumulation period) there was more new material and a higher proportion of algae. At this time it is likely that the stronger winds and wave energy could dislodge fresh seagrass material from meadows and algae from reefs.

There was a higher proportion of *A. antarctica* in beach wrack during winter (accumulation period), increasing from an average of 5 to 31 % which is close to the cover of *A. antarctica* in Geographe Bay, ~ 30 %. However, the proportion of *P. sinuosa* was much lower (~ 53 %) than would be predicted by its cover in Geographe Bay (70 %). This indicates that at this time of year *A. antarctica* and *P. sinuosa* are likely to be removed from meadows, but it is more common for *P. sinuosa* to be removed earlier in the year. *A. antarctica* has a vertical stem from which clusters of leaves arise. A new leaf is produced from a cluster every ~ 14 days and these stay on the plants for about 3 months [*Marba and Walker*, 1999]. So the smaller leaves of *A. antarctica* are shed more regularly over the year compared to the leaves of *P. sinuosa*. However, the stems of *A. antarctica* live for about two years and generally break off from the underground rhizome only when the wave energy is higher, typically in winter.

Beach wrack was mostly above-ground seagrass material. No below-ground material was observed in the pre-accumulation period, indicating that the energy was not high enough to dislodge below-ground material at this time. Below-ground material was present during the accumulation and post-accumulation period. In *P. sinuosa* seagrass meadows ~50-93% of biomass is below-ground [*Collier*, 2006; *Walker et al.*, 1991], but on the beach it comprised less than 12 % of the *P. sinuosa* wrack. In *A. antarctica* meadows ~ 7 – 20 % of biomass is below-ground [*Mackey et al.*, 2007; *Walker et al.*, 1991] and on the beaches 5 – 31 % of *A. antarctica* was below-ground material. Thus, above ground material is preferentially removed from *P. sinuosa* meadows, whereas for *A. antarctica* both above- and below-ground material is being dislodged from the meadow in roughly the proportions they occur in meadows. Again, this is consistent with *A. antarctica* being removed in high energy periods when whole plants are removed.

The composition of wrack accumulations was largely consistent irrespective of size. Consequently, differences in the physical and bio-geochemical characteristics of banks are unlikely to be due to differences in composition of the wrack and more likely related to the size and morphology of the banks.

With respect to modelling and management:

- the nature of the material in wrack accumulations changed over the year but was predominantly the leaves of *P. sinuosa*,
- the proportion of *A. antarctica* stems may be significant at some times and could affect mechanical aspects of wrack management such as by-passing, and
- subsequent modelling focused on two types of particles: *P. sinuosa* leaves and whole shoots (stem + leaves) of *A. antarctica*.

6.5 Physical properties of beach wrack accumulations

The physical properties of wrack are important determinants of its behaviour in two respects:

- the transport of wrack, both within the water column as well as on and off beaches, and
- the biogeochemical transformations of wrack, including its decomposition and the generation of H_2S

A range of studies was conducted to determine the properties of wrack with respect to both transportation and biogeochemistry. In this section, the properties of wrack relevant to its biogeochemical behaviour on beaches are reported.

6.5.1 Objective

To determine the physical characteristics of wrack accumulations on beaches, and the changes in these characteristics with age, in order to provide understanding of biogeochemical processes.

6.5.2 Methods

The physical conditions of wrack were determined by three approaches:

a. *in situ* measures of wrack (including bulk density, porosity, moisture content, percent of pore volume filled with water and particle size) at three standard sites, five times over an annual cycle,

b. in situ measures of wrack (including bulk density, porosity, moisture content, percent of pore volume filled with water and particle size) at three sites with large wrack accumulations once off, and

c. experiments to determine the physical properties of key components of wrack found on beaches in Geographe Bay (such as density, length to width ratios, brittleness, colour, moisture content and tensile strength, and how these parameters change with age).

6.5.2.1 Physical characteristics of small wrack accumulations over a year

Wrack characteristics were determined at Forrest Beach, Volunteer Marine Rescue and Geographe Sailing Club (see Table 6.3). Measures were taken in a subset of the ten occasions on which wrack volume and beach morphometry were assessed: 19 - 22 May, 9 - 11 June, 12 - 15 August, 22 - 25 September, 20 - 22 October.

At each site and time, four replicates accumulations were measured and within each replicate, two zones were sampled: surface wrack located at the top of the wrack accumulation; and sediment, the area immediately below the sediment-air interface below the wrack; Figure 6.19). On most occasions, the wrack was < 0.5 m high, however on one occasion at Forrest Beach the wrack was greater than 0.5 m high and buried into the sediment where it was in contact with a saturated zone. At this time, samples were taken at the surface, midway between the top of the saturated zone and the surface, in the saturated zone and in the sediment below the wrack.

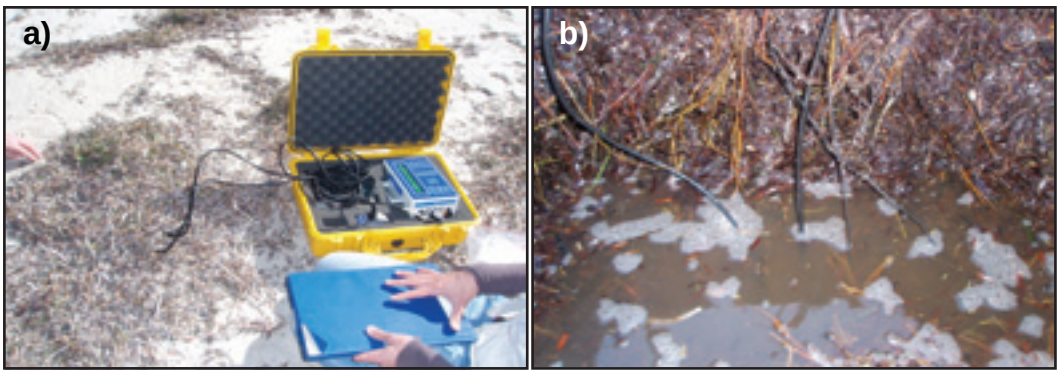

Figure 6.19 Sampling physical conditions of wrack in the surface (left) and saturated (right) zones.

Samples for bulk density, porosity, moisture content and percent of pore volume filled with water at time of collection were collected from surface, mid and saturated zones (Figure 6.19) with a container (1L, 15.4 x 9.3 cm surface area) and in the sediment zone with a core (48 mm diameter to 10 cm depth, 196 cm^3). Samples were sealed in the field to ensure no moisture loss and processed in the laboratory. The wet samples were weighed and then water added up to 1 L (mid and saturated zone samples) or 196 cm^3 (sediment zone samples) and reweighed. Samples were then dried to a constant mass and re-weighed.

The measures were calculated as follows:

$$\Psi = \frac{M_{dry}}{V_{total}} \qquad \textbf{Eq. 6-1}$$

$$\theta = \frac{M_{added} - M_{dry}}{\rho V_{total}} \qquad \textbf{Eq. 6-2}$$

$$\eta = \frac{M_{wet} - M_{dry}}{\rho V_{total} \phi} \qquad \textbf{Eq. 6-3}$$

where ψ is the bulk density of the sample including sand (kg m^{-3}), M_{dry} is mass of dried sample (kg), M_{wet} is the mass of wet sample (kg), M_{added} is the mass of water added (kg), V_{total} is total sample volume (m^3), ϕ is the porosity of the sample (% of volume), ρ is the density of seawater (kg m^{-3}), θ is the moisture content (%) of the sample, and η is the saturated pore volume (%). An additional measure of bulk density where sand was not included in the calculation, was estimated based on the samples collected for particle size. M_{dry} was wrack only, no sand.

For particle size analysis, samples were separated by flotation sieving into sinking (sand) and floating (wrack) components, and then into two size classes by sieving with standard pore size sieves a: > 1 mm, and b: 0.1 - 1 mm. Each component was dried to a constant weight and weighed.

6.5.2.2 Physical characteristics of large accumulations of wrack

The three sites usually had small aggregations of wrack, < 0.5 m high. A second one-off sampling was conducted to target larger aggregations of wrack between 24 - 26 July 2008. Three sites were selected: Siesta Park where the aggregations were > 1 m high and wrack had been present for more than twelve weeks; Guerin St where the aggregations were also > 1 m high and wrack had been present for six weeks; and Abbey Beach where the aggregations were 0.5 m high and had been present for six weeks.

At each site, four replicates where measured and within each replicate four zones were sampled, at the surface of the wrack, midway between the top of the saturated zone and the surface, in the saturated zone and in the sediment below the wrack.

6.5.2.3 Physical properties of key wrack components

The density, length to width ratios, brittleness, colour, moisture content and tensile strength of fresh and aged wrack were determined. Fresh *P. sinuosa* leaves, *A. antarctica* stems and leaves, and epiphytic algae (*Laurencia*) were collected from meadows and beach wrack, and *P. sinuosa* leaves and *A. antarctica* stem and leaves that had passed through the pump in the by-pass operations. Five replicate samples of each type were collected.

Two types of aging were assessed, 'in air' (the material was exposed to air on moist sediment) and 'buried' (under moist sediment and not exposed to air). Measurements for 'in air' aging were taken at time 0 (15/8/08), 2 weeks (29/8/08), 4 weeks (12/9/08) and 8 weeks (10/10/08). Measurements for buried aging were taken at Time 0 (4/9/08) and 4 weeks (6/10/08). Samples for tensile strength measures were aged for 10 weeks.

Density (g DW cm^{-3}) was calculated from the volume of the plant material using length x width x height for *P. sinuosa* and *A. antarctica* leaves, length x diameter for *A. antarctica* stems and bio-volume of algae. Material was then dried to a constant weight (DW). Length-to-width ratios were calculated from these data.

Brittleness of stems and leaves was assessed with a folding test. Leaves or stems were folded to determine if the material remained intact (not brittle), deformed in part (brittle) or completely snapped (very brittle). Colour of the leaf, stem or thallus, for algae, was determined by visual observation. Moisture content was measured by difference in weight after drying.

Tensile strength measures were carried out at CSIRO Textile and Fibre Technology, Victoria on an Instron Series 5500R machine with calibrated 100N load cell. Testing was performed in a room with constant temperature (20°C ± 0.5°C) and relative humidity (65 % ± 3 %). Samples were secured using pneumatic tensile grips of dimension 20 x 20 mm. Cross-head speed was 7.5 mm min^{-1} with an initial gauge length of 15 mm. Specimen thickness was measured using a digital micrometer with a tolerance of 0.004 mm and samples were wiped clean with a damp cloth to remove any residual salt or sand that may have interfered with thickness measurements. Due to the slender dimensions of the *P. sinuosa* leaf, the leaf was sectioned into 50 mm sections starting from 40 mm above the base of the leaf. These sections formed the replicate specimens for each leaf under test. For the *A. antarctica* stems, the diameter of each stem specimen was measured with the micrometer with the assumption that the cross-section was circular. Sectioning began from start of stem base at 50 mm intervals. Measurements were taken on 3 - 4 samples of *P. sinuosa* leaves and *A. antarctica* stems that were fresh, aged for ten weeks and of unknown age from beach wrack. For each leaf or stem at least four measures were taken and averaged for that replicate.

6.5.3 Results

6.5.3.1 Bulk density, porosity and moisture content in small aggregations

The mean bulk density (including sand) of small aggregations of surface wrack was 166 kg m^{-3} (range 76 - 411 kg m^{-3}), with no consistent differences among sites (Table 6.9). Surface wrack without sand in the accumulation had a considerably lower bulk density (mean = 48 kg m^{-3}; range 0.04 - 91 kg m^{-3}). Bulk density of the sediment below the wrack was considerably higher (mean = 1 214 kg m^{-3} ; range = 710 - 1 402 kg m^{-3}), due to the high sand content. There was no correlation between the volume of wrack on the beach and the bulk density in these small aggregations.

Average porosity of surface wrack across all sites and times was 74% (range 57 – 85%), and 35% in sediment (range 22 – 87%). Porosity was generally lower at the end of the accumulation period and during the post-accumulation period, although this was not the case at Geographe Sailing Club (Table 6.9).

Mean moisture content of surface wrack was 9 % by volume (range 1 – 17%), and in the sediment, 20% by volume (range 2 – 81%). There were large variations between sites and times indicating the variable moisture content. Minima were observed at most sites in the post-accumulation period (Table 6.9). Moisture content may also be estimated as the percentage pore volume filled with water; if the sediments were saturated at time of collection then moisture content would be 100%. Surface wrack had on average 13% moisture content (range 1 – 23%) and sediments 49% (range 7 – 100%).

6.5.3.2 Bulk density, porosity and moisture content in large aggregations

Large aggregations of wrack had similar properties to small aggregations, although there were some differences (Table 6.10). Bulk density of accumulations, including the sand component was, on average, lower than that observed in thin accumulations. This reflected the smaller amount of sand per unit volume incorporated into large wrack piles compared to thin layers, which were in direct contact with the sediment surface.

Within large accumulations, older piles had greater bulk density than younger piles of the same size, indicating an increase in bulk density with age of wrack accumulation. Bulk density of wrack without sand was also on average greater in the larger aggregations compared to the small aggregations, highlighting a greater compaction of wrack.

Within larger accumulations, the bulk density without sand generally increased from the smaller to larger accumulations and with age in the surface and mid-zone of the wrack piles. There was also more wrack incorporated into the underlying sediments below larger piles. The porosity of large aggregations of wrack (average 78 % by volume) was similar to small aggregations (average 74 % by volume), and in the sediment the porosity of large aggregations was slightly higher (45 % by volume) than small aggregations (35 % by volume).

Moisture content of the surface zone of large aggregations was similar to that of small aggregations (10 – 11 % vs. 9 %), whereas within larger aggregation older accumulations tended to have slightly higher moisture content than younger aggregations (12 vs. 9 %). Moisture content of the sediment was greater in large compared to small aggregations (45 % vs. 20 %). The percent of pore volume filled with water in the surface zone was similar between large and small aggregations (13 %), although within large aggregations the older piles had greater values than the newer piles (16 % vs. 12 %). In the sediment large aggregations were always saturated so that the percent of pore volume filled with water was 100 % compared to an average of 49 % in the small aggregations.

Table 6.9 Bulk density, porosity and moisture content of wrack at three standard sites over an annual cycle.

	DATE	FORREST BEACH		VOLUNTEER MARINE RESCUE		GEOGRAPHE SAILING CLUB		DATE AVERAGE	
		SURF	SED	SURF	SED	SURF	SED	SURF	SED
Bulk density (kg m^{-3})									
wrack + sand	19-May	158 ± 17	1205 ± 24	123 ± 20	1402 ± 72	411 ± 141	1315 ± 51	231	1307
	24-Jun	156 ± 38	1188 ± 81	198 ± 89	1215 ± 32	116 ± 27	1294 ± 40	157	1232
	12-Aug	118 ± 29	1014 ± 78	89 ± 13	1331 ± 164	92 ± 36	1352 ± 89	100	1232
	22-Sep	353 ± 74	1263 ± 38	180 ± 42	1320 ± 45	156 ± 44	710 ± 38	230	1098
	22-Oct	103 ± 17	1177 ± 81	161 ± 78	1252 ± 51	76 ± 21	1168 ± 26	113	1199
	Site avg	178	1169	150	1304	170	1168	166	1214
wrack	19-May	48 ± 10	4 ± 1	66 ± 9	3 ± 1	49 ± 7	1.2 ± 0.5	55	3
	24-Jun	34 ± 3	0.9 ± 0.3	41 ± 6	1.7 ±0.5	42 ± 1	1.5 ± 0.3	39	1
	12-Aug	44 ± 9	15 ± 8	46 ± 8	2.4 ± 1.5	35 ± 3	1.2 ± 0.5	42	6
	22-Sep	91 ± 18	0.6 ± 0.2	58 ± 15	0.2 ± 0.1	42 ± 5	0.5 ± 0.2	64	5
	22-Oct	71 ± 9	0.6 ± 0.3	17 ± 5	0.2 ± 0.2	26 ± 7	0.04 ± 0.03	38	0.3
	Site avg	58	4	46	1.4	39	1	48	3
Porosity	19-May	81 ± 2	35 ± 1	82 ± 2	37 ± 7	57 ± 9	33 ± 5	73	35
(% vol.)	24-Jun	71 ± 3	29 ± 2	77 ± 4	35 ± 3	74 ± 1	34 ± 1	74	33
	12-Aug	79 ± 3	37 ± 2	79 ± 3	23 ± 8	81 ± 1	30 ± 1	80	30
	22-Sep	61 ± 2	30 ± 1	68 ± 6	32 ± 1	76 ± 2	87 ± 5	68	50
	22-Oct	69 ± 5	36 ± 6	73 ± 4	22 ± 2	85 ± 1	30 ± 1	76	29
	Site avg	72	33	76	30	75	43	74	35
Moisture	19-May	17 ± 1	35 ± 1	13 ± 3	9 ± 7	10 ± 3	6 ± 5	13	17
content	24-Jun	10 ± 2	21 ± 3	12 ± 1	16 ± 4	17 ± 4	26 ± 1	13	21
(% vol.)	12-Aug	6 ± 3	15 ± 4	7 ± 2	14 ± 8	4 ± 1	13 ± 5	6	14
	22-Sep	10 ± 2	11 ± 5	13 ± 2	24 ± 2	10 ± 3	81 ± 5	11	39
	22-Oct	8 ± 2	12 ± 7	1 ± 1	2 ± 3	1 ± 1	4 ± 1	3	6

	Site avg	10	19	15	11	8	26	9	20
Pore	19-May	21 ± 1	100 ± 0	16 ± 4	19 ± 12	18 ± 3	15 ± 9	18	45
volume	24-Jun	15 ± 2	72 ± 13	16 ± 2	45 ± 9	23 ±6	78 ± 4	18	65
filled	12-Aug	7 ± 4	41 ± 10	9 ± 2	72 ± 6	5 ± 2	44 ± 15	7	52
with water	22-Sep	17 ± 4	38 ± 15	20 ± 5	74 ± 2	13 ± 4	93 ± 2	17	68
(%)	22-Oct	12 ± 2	27 ± 12	1 ± 1	7 ± 17	1 ± 1	12 ± 1	5	15
	Site avg	14	55	12	43	12	48	13	49

Table 6.10 Bulk density, porosity and moisture content in four zones of large accumulations of wrack at three sites in July 2008. * these values are higher due to large amounts of sand in saturated zone.

MEASURE	ZONE	SIESTA PARK	GUERIN ST	ABBEY	
		LARGE OLD	LARGE NEW	SMALL NEW	AVERAGE
Bulk density (kg m^{-3})					
wrack + sand	Surface	100 ± 19	52 ± 13	79 ± 6	77
	Mid	93 ± 14	59 ± 6	65 ± 9	72
	Saturated	63 ± 11	75 ± 14	208 ± 83*	115
	Sediment	1107 ± 76	1056 ± 14	1411 ± 37	1191
wrack	Surface	69 ± 4	56 ± 3	54 ± 7	69
	Mid	83 ± 3	70 ± 4	54 ± 8	69
	Saturated	49 ± 11	53 ± 2	105 ± 16	69
	Sediment	16 ± 10	14 ± 1	5 ± 2	12
Porosity (% volume)	Surface	76 ± 1	79 ± 1	79 ± 1	78
	Mid	76 ± 1	80 ± 1	78 ± 1	78
	Saturated	77 ± 1	77 ± 1	69 ± 4	74
	Sediment	45 ± 2	54 ± 1	37 ± 1	45
Moisture (% volume)	Surface	12 ± 1	9 ± 1	9 ± 2	10
	Mid	12 ± 2	12 ± 2	10 ± 2	11
	Saturated	77 ± 1	77 ± 1	69 ± 4	74
	Sediment	45 ± 2	54 ± 1	37 ± 1	45

Pore volume with water (%)	Surface	16 ± 1	12 ± 1	12 ± 2	13
	Mid	16 ± 2	15 ± 2	13 ± 2	15
	Saturated	100 ± 0	100 ± 0	100 ± 0	100
	Sediment	100 ± 0	100 ± 0	100 ± 0	100

6.5.3.3 Particle size distribution in small aggregations

In small wrack accumulations, the dominant component of wrack was fine sediment (>0.1 & < 1 mm in size; Table 6.11). In the surface wrack this component ranged from 37 – 83% DW of the wrack. The next most common component of surface wrack was large floating material (> 1 mm), which comprised mostly of seagrass and algae, ranging from 17 – 58% DW. The fine component of floating wrack ranged from 0.07 - 1.3% DW. In the sediment, sand consistently accounted for more than 98% of DW. There were no consistent temporal or spatial patterns in the particle size distribution of wrack accumulations, indicating no clear seasonal patterns or variation among beaches.

6.5.3.4 Particle size distribution in large aggregations

Large wrack aggregations had higher proportions of floating fractions in the surface zone compared to small aggregations (Table 6.12) and lower sand volume. The most dominant component in the surface zone was large floating (> 1 mm) which accounted for 95-99% of DW. In the sediment, the distribution of components was similar to small wrack aggregations with > 98% DW in the fine sinking fraction (Table 6.12).

The mid and saturated zones were generally similar to the surface zone in the particle size distribution, but there was more fine sand, up to 26% of DW, incorporated into the wrack compared to the surface zone, which had <1% DW (Table 6.12).

Among different large wrack accumulations there were slight differences in the particle size distribution. Piles greater than 1 m had more fine floating wrack than piles ~ 0.5 m high, and older piles also had more fine floating material than younger large piles (Table 6.12).

Table 6.11 Particle size distribution of small accumulations of wrack on the surface of the beach and buried in the sediment at the three standard sites over the year. Wrack was separated into organic floating components mostly plant material and sand and other sinking components, such as shells into two size categories > 1mm and > 0.1 – 1mm.

DATE	TYPE	SIZE (mm)	FORREST BEACH		VOLUNTEER MARINE RESCUE		GEOGRAPHE SAILING CLUB	
			SURF %	SED %	SURF %	SED %	SURF %	SED %
19-May	Float	>1	31 ± 7.0	0.30 ± 0.07	58 ± 13	0.13 ± 0.07	17 ± 6.0	0.07 ± 0.03
	Float	0.1 – 1	0.27 ± 0.06	0.05 ± 0.02	0.10 ± 0.02	0.05 ± 0.03	0.13 ± 0.04	0.02 ± 0.01
	Sink	>1	0.41 ± 0.06	1.1 ± 0.46	0.02 ± 0.02	0.69 ± 0.65	0.06 ± 0.04	0.08 ± 0.05
	Sink	0.1 – 1	68 ± 6.5	98 ± 0.45	42 ± 13	99 ± 0.66	83 ± 11	99 ± 0.04

24-June	Float	>1	18 ± 4.7	0.05 ± 0.02	26 ± 7.4	0.15 ± 0.05	44 ± 8.1	0.08 ± 0.03
	Float	0.1 – 1	0.52 ± 0.17	0.02 ± 0.0	0.11 ± 0.03	0.01 ± 0.0	0.42 ± 0.06	0.04 ± 0.03
	Sink	>1	0.04 ± 0.01	0.08 ± 0.06	0.03 ± 0.03	0.04 ± 0.03	0.01 ± 0.0	0.08 ± 0.07
	Sink	0.1 – 1	81 ± 4.8	99 ± 0.05	74 ± 7.5	99 ± 0.06	56 ± 8.1	99 ± 0.05
12-Aug	Float	>1	54 ± 9.0	1.4 ± 0.75	68 ± 12	0.17 ± 0.13	50 ± 13	0.09 ± 0.05
	Float	0.1 – 1	0.37 ± 0.22	0.19 ± 0.16	0.21 ± 0.08	0.05 ± 0.02	1.3 ± 0.4	0.01 ± 0.01
	Sink	>1	0.45 ± 0.28	0.87 ± 0.72	0.04 ± 0.03	0.38 ± 0.12	0.29 ± 0.23	0.17 ± 0.15
	Sink	0.1 – 1	45 ± 9.1	98 ± 0.8	37 ± 13	99 ± 0.22	49 ± 14	99 ± 0.17
22-Sept	Float	>1	22 ± 3.7	0.03 ± 0.02	43 ± 15	0.77 ± 0.74	39 ± 17	0.03 ± 0.01
	Float	0.1 – 1	0.07 ± 0.02	0.02 ± 0.01	0.42 ± 0.20	0.11 ± 0.11	0.25 ± 0.04	0.01 ± 0.01
	Sink	>1	0.64 ± 0.12	0.43 ± 0.19	0.05 ± 0.01	0.32 ± 0.14	0.58 ± 0.22	0.00 ± 0.00
	Sink	0.1 – 1	77 ± 3.8	99 ± 0.21	57 ± 15	99 ± 0.84	60 ± 17	99 ± 0.01
22-Oct	Float	>1	54 ± 6.8	0.02 ± 0.01	25 ± 10	0.01 ± 0.01	58 ± 10	0.0 ± 0.0
	Float	0.1 – 1	0.55 ± 0.17	0.03 ± 0.02	0.13 ± 0.07	0.01 ± 0.01	0.20 ± 0.12	0.0 ± 0.0
	Sink	>1	0.06 ± 0.03	0.06 ± 0.02	2.0 ± 1.7	0.05 ± 0.03	3.1 ± 1.5	0.15 ± 0.14
	Sink	0.1 – 1	45 ± 6.9	99 ± 0.01	73 ± 11	99 ± 0.05	38 ± 11	99 ± 0.14

Table 6.12 Particle size distribution in four zones of large aggregations of wrack at three sites in July 2008. Wrack was separated into organic floating components mostly plant material; sand; and other sinking components, such as shells into two size categories > 1mm and > 0.1 – 1mm.

ZONE	TYPE	SIZE (mm)	BIG OLD	BIG NEW	SMALL NEW
			SIESTA PARK %	GUERIN ST %	ABBEY %
Surface	Float	>1	95 ± 0.7	98 ± 0.24	99 ± 0.18
	Float	0.1 – 1	3.8 ± 0.44	2.3 ± 0.24	0.99 ± 0.17
	Sink	>1	0.07 ± 0.05	0.02 ± 0.02	0.05 ± 0.05
	Sink	0.1 – 1	1.0 ± 0.35	0.01 ± 0.01	0.36 ± 0.36

Mid	Float	>1	96 ± 1.2	74 ± 13	99 ± 0.19
	Float	0.1 – 1	3.4 ± 1.4	3.0 ± 0.95	1.1 ± 0.09
	Sink	>1	0.05 ± 0.02	0.13 ± 0.07	0.00 ± 0.00
	Sink	0.1 – 1	0.36 ± 0.13	23 ± 13	0.13 ± 0.13
Saturated	Float	>1	77 ± 10	70 ± 15	84 ± 4.6
	Float	0.1 – 1	5.0 ± 1.9	2.9 ± 1.0	2.3 ± 0.35
	Sink	>1	1.7 ± 1.5	0.41 ± 0.18	0.58 ± 0.33
	Sink	0.1 – 1	16 ± 10	26 ± 15	13 ± 4.3
Sediment	Float	>1	1.1 ± 0.93	0.96 ± 0.15	0.21 ± 0.03
	Float	0.1 – 1	0.51 ± 0.2	0.37 ± 0.03	0.16 ± 0.06
	Sink	>1	0.53 ± 0.17	0.47 ± 0.16	0.12 ± 0.03
	Sink	0.1 – 1	98 ± 1.0	98 ± 0.27	99 ± 0.08

6.5.3.5 Effect of age on physical properties of wrack

Generally, algae were the least dense wrack material, followed by *P. sinuosa* leaves, *A. antarctica* leaves and then, the most dense, *A. antarctica* stems (Table 6.13). Fresh *P. sinuosa* leaves and *A. antarctica* stems were less dense than wrack found on the beach, whereas fresh algae was more dense than beach wrack, and there was no difference in *A. antarctica* leaves.

Ageing affected the density of wrack, but not in a consistent way among species. With aging 'in air', fresh *P. sinuosa* leaves increased in density from 0.24 g DW cm^{-3} reaching maximums of 0.4 g DW cm^{-3} after 4 weeks (Figure 6.20). There was only a slight increase in density when the leaves were buried for 4 weeks (0.2 to 0.23 g DW cm^{-3}). *A. antarctica* leaves declined in density after 2 weeks of 'in air' aging (from 0.55 to 0.2 g DW cm^{-3}), but by 8 weeks the density had increased again to 0.4 g DW cm^{-3} (Figure 6.21). After 4 weeks of aging, buried leaves decreased slightly in density. *A. antarctica* stems showed different patterns in density with aging (Figure 6.20). Density decreased with age in both 'in air' and buried treatments, from 2.4 g DW cm^{-3} to about 1.8 g DW cm^{-3}.

The length to width ratio of fresh *P. sinuosa* leaves was greater than wrack on the beach, which was greater than by-passed wrack, indicating a general reduction in length from fresh, to beach wrack, to by-passed wrack. In contrast, the length to width ratio of fresh *A. antarctica* leaves was lower than wrack on the beach and by-passed wrack. The lower ratio was due to narrower leaves from beach wrack and wrack that had been by-passed rather than any change in length, which was unaffected by bypassing (Table 6.13).

Fresh seagrass material was generally green in colour, changing to brown on the beach. Fresh material was not brittle but *P. sinuosa* and *A. antarctica* leaves from beach wrack were brittle, as were *A. antarctica* stems after they were by-passed (Table 6.13). *P. sinuosa* leaves turned brown after 2 weeks aging 'in air' and black after 4 weeks. Buried leaves were slower to change colour: by 2 weeks 20% of leaves were brown, at 4 weeks 60% black and by 8 weeks all were black. *A. antarctica* stems aged 'in air' took 8 weeks to all turn black; at 4 weeks only 1/5 were black. Buried stems also took 8 weeks to turn black; at 4 weeks 3/5 were black and at 6 weeks 4/5.

Table 6.13 Physical properties of different wrack types collected fresh from meadows, from beach wrack or after passing through the bypassing pump. Mean ± stdev.

	WRACK SPECIES	WRACK TYPE		
		FRESH	ON BEACH	OUT OF PUMP
Density (g DW cm^{-3})	*P. sinuosa* leaf	0.242 ± 0.074	0.343 ± 0.135	0.301 ± 0.072
	A. antarctica stem	2.42 ± 0.76	3.22 ± 0.81	2.41 ± 0.40
	A. antarctica leaf	0.552 ± 0.160	0.544 ± 0.197	0.587 ± 0.066
	Algae	0.141 ± 0.061	0.088 ± 0.045	-
L/W ratio	*P. sinuosa* leaf	70.1 ± 10.3	19.7 ± 14.5	7.24 ± 2.25
	A. antarctica leaf	4.63 ± 0.42	7.29 ± 1.51	6.90 ± 0.34
Colour	*P. sinuosa* leaf	Green	Brown	Brown
	A. antarctica stem	Cream	Dark brown	Dark brown
	A. antarctica leaf	Green	Green-Brown	Green
	Algae	Red	Red-white	-
Brittleness	P. sinuosa leaf	Not brittle	Very brittle	Very brittle
	A. antarctica stem	Not brittle	Not brittle	Variable
	A. antarctica leaf	Not brittle	Variable	Not brittle
	Algae	Not brittle	Not brittle	-
Moisture content (%)	P. sinuosa leaf	-	47 ± 43	72 ± 5
	A. antarctica leaf	-	55 ± 23	60 ± 7
	Algae	-	93 ± 2	-

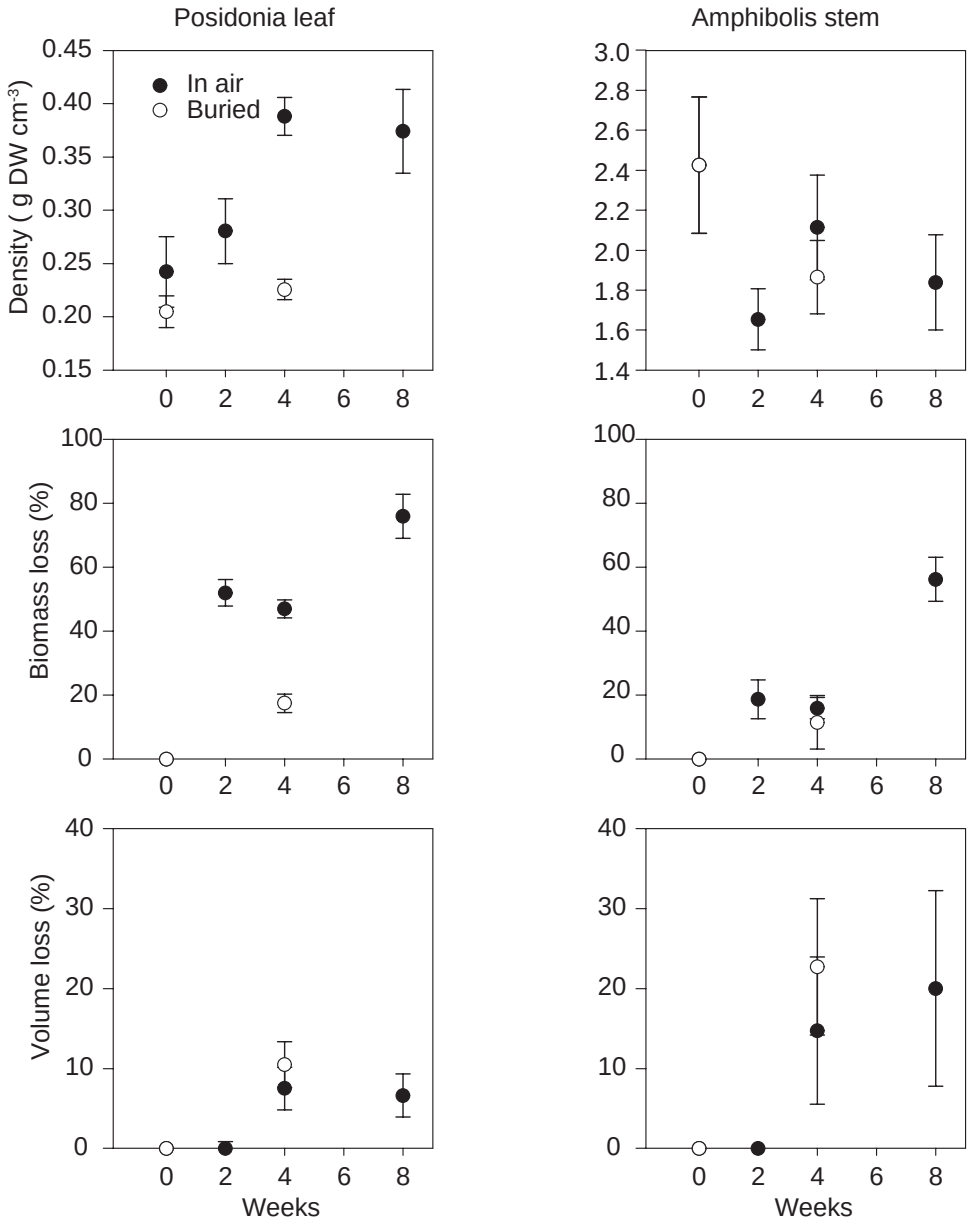

Figure 6.20 Change in density, biomass and volume of *P. sinuosa* leaf and *A. antarctica* stem wrack with age when exposed to air on moist sediment or when buried under moist sediment.

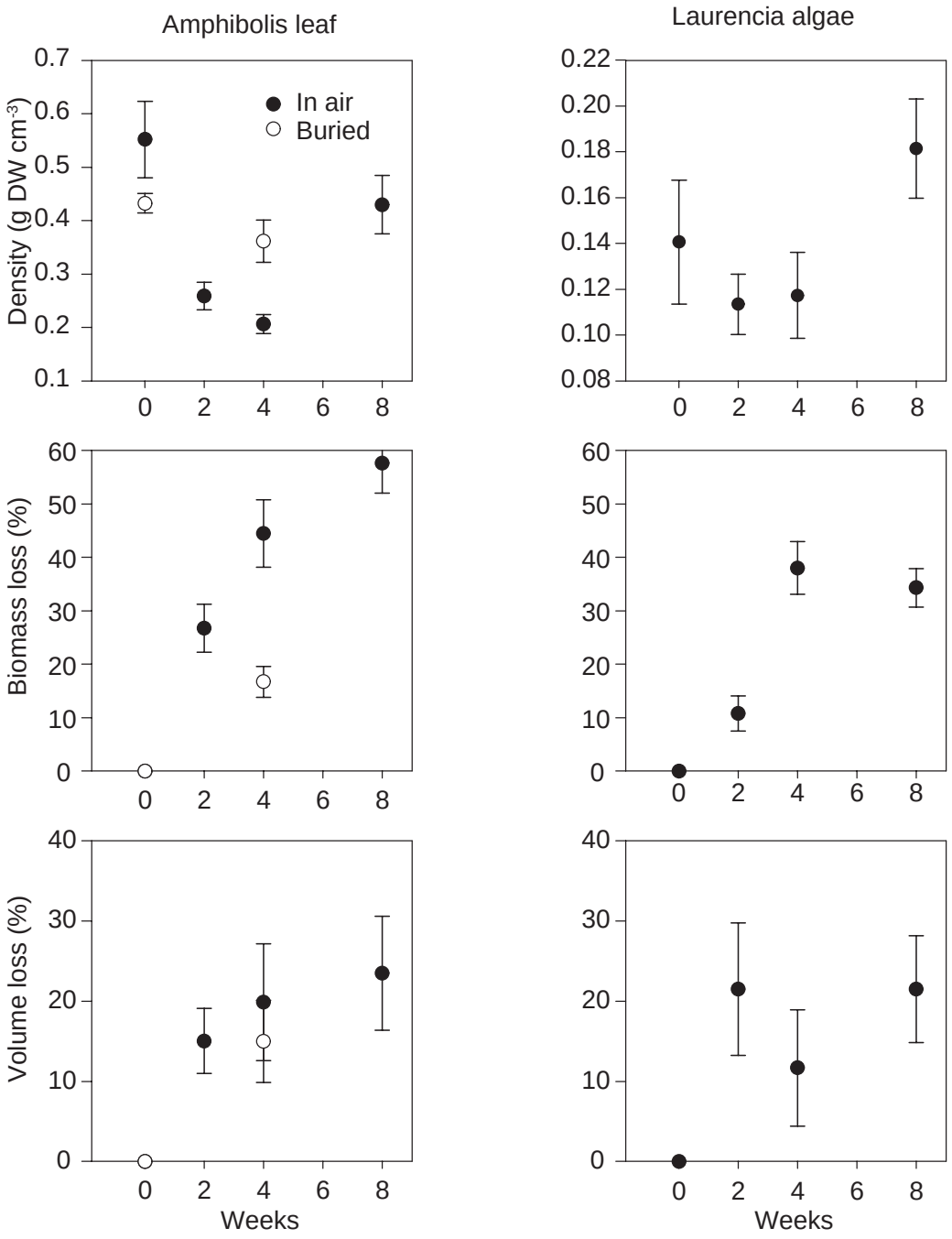

Figure 6.21 Change in *A. antarctica* leaf and *Laurencia* wrack with age when exposed to air on moist sediment or when buried under moist sediment.

6.5.3.6 Tensile strength

Both fresh *A. antarctica* stems and stems of unknown age sampled from the beach had higher tensile strength than *P. sinuosa* leaves under similar conditions (Table 6.14). However, after 10 weeks aging on wet sediment, the tensile strength of fresh *A. antarctica* stems had declined and was lower than *P. sinuosa* leaves, which had not changed. The maximum tensile strengths for both *A. antarctica* stems and *P. sinuosa* leaves was observed in dried material collected from the beach: 33 mPa for *A. antarctica* and 25 mPa for *P. sinuosa.*

Table 6.14 Tensile strength (Stress as mPa) of different aged seagrass leaves or stems.

	FRESH	AGED 10 WEEKS	UNKNOWN AGE FROM BEACH
P. sinuosa leaves	19.5 ± 1.1 (3)	19.0 ± 1.6 (4)	25.1 ± 3.5 (3)
A. antarctica stems	25.2 ± 3.4 (3)	10.4 ± 2.6 (4)	33.0 ± 7.6 (4)

6.5.4 Significance of results

The bulk density of beach wrack accumulations will influence its transport off beaches following initial deposition and is influenced by the size and age of wrack accumulations. Small, thin piles of wrack have the greatest bulk density compared to large wrack accumulations due to the greater proportion of sand worked into the wrack accumulation (37 – 83% DW vs. < 1% DW). However, excluding the contribution of sand, large wrack accumulations have a greater bulk density than small, thin piles of wrack, reflecting some compaction of the wrack and drying, which increases the specific density of individual wrack particles formed from leaf material. In larger accumulations (> 0.5 m high) older accumulations have higher bulk density than younger accumulations. This is likely due to the increase in density of *P. sinuosa* leaves, the dominant component of wrack, with aging.

With greater bulk density (without sand), more energy would be required to transport wrack accumulations off the beach. It is likely that when wrack becomes saturated with water at high tide or with storm surges, sand is washed out and only the bulk density of the wrack (without sand) would be important to consider for transport of the wrack off the beach. Therefore smaller, thin aggregations of wrack, with their lower bulk density (without sand) than large aggregations, are likely to be transported off beaches when the water level reaches above the aggregations and then drops, washing the wrack back into the ocean. Settling rate experiments (see Section 5.3.2.1) indicated that leaves that have dried on the beach have a greater probability of floating on re-wetting, further contributing to their movement offshore on inundation. Larger accumulations of wrack would require more energy to be removed from the beach. The beach profiles (Section 6.3) regularly showed that the high water mark reached above the height where small, thin piles of wrack occur. However, with larger aggregations (> 1 m high) the water level is unlikely to move above the height of the aggregations, so a combination of water level increases and wave energy would be required to disrupt these large aggregations and remove the wrack from the beach. Under this situation, older aggregations would require greater energy to disrupt than newer aggregations.

The particle transport model has incorporated a function to allow for the increase in bulk density of wrack with time it is resident on a beach. The model therefore incorporates the need for higher energy events to remove wrack accumulations from the beach. It also incorporates the initial positive buoyancy of re-wetted wrack, which aids in the removal of wrack under high water conditions.

The particle size distribution of wrack aggregations gives an indication of the decomposition state of the wrack. With greater age the size of wrack particles decreases. In large aggregations (> 0.5 m high) that have a greater residence time on the beach, there were clear differences in the particle size distribution. More fine fractions of wrack were present compared to small, thin aggregations (1 - 3.8% DW vs. <1% DW), deeper piles had more fines than shallow piles, and older piles (~ 12 weeks) had more fines than younger (~ 6 weeks). This demonstrates the physical breakdown of wrack in large aggregations and the potential for differences in the release of nutrients to fuel bacterial activity and changes in porosity, which could affect oxygen diffusion into the wrack. Both these factors would influence the rate and types of decomposition occurring in the banks which, in turn affects the rate of breakdown and removal of wrack and the types and amount of gases, including H_2S, liberated (addressed further in Section 7).

The tensile strength of wrack is relevant to the bypassing of wrack material through mechanical pumps. At the request of the Project Steering Committee, the tensile strengths have been determined for different components of wrack. The maximum tensile strengths were for dried material that had been on the beach for an unspecified period of time. These samples were stronger than either fresh samples or samples that had been aged on wet sediment. The greater tensile strength of samples from the beach is most likely due to their drying, which did not occur in any other sample. If tensile strength is a factor in diminishing pumping efficiency, then it may be desirable to pump freshly deposited material or accumulated wrack that has been re-wetted, and to reduce the amount of *Amphibolis* stems in the material, possibly through mixing of different batches of wrack.

7 WRACK DEGRADATION & H_2S PRODUCTION

Increased degradation is potential means of losing wrack from Geographe Bay. This section provides an assessment of the physical and chemical processes relevant to the degradation and decomposition of wrack in Geographe Bay. Degradation is a general term that encompasses many processes, including the bacterial decomposition of wrack, physical fragmentation by grazers and wave action, and photo-oxidation. Of particular relevance to the accumulations at Port Geographe is bacterial decomposition, because of the associated release of gas by-products.

Under oxic conditions, the main by-product of decomposition is carbon dioxide (CO_2), an odourless gas. Under anoxic conditions, a range of gaseous by-products occur, including methane and hydrogen sulfide (H_2S), the latter being particularly noxious and an identified management issue at Port Geographe. At the commencement of the study, a number of assumptions were made regarding the decomposition of wrack and generation of H_2S:

1. in order for microbial decomposition to occur, bacteria require access to a source of carbon. It was assumed that the wrack itself would be main source of carbon to bacteria, through the leaching of dissolved organic carbon and the production of fine particulate carbon. This needed to be confirmed as the underlying sediments might contain sufficient carbon to support decomposition and H_2S production even in the absence of wrack;
2. it was assumed that the wrack itself would be an important barrier to oxygen diffusion into the wrack and underlying sediments, thus facilitating anoxia and H_2S production; and
3. it was assumed that the source of sulphur in H_2S liberated from wrack was sulphate contained in seawater and present in the saturated zone of the wrack accumulations and underlying sediment porewaters.

The studies summarised in this section addressed the decomposition processes occurring in wrack to understand both the removal of wrack from the system and the conditions under which H_2S might be produced in wrack accumulations. Section 7.1 presents the physical characteristics of beach wrack that are relevant to decomposition and which will influence whether the accumulations are oxic or anoxic. Section 7.2 investigates wrack degradation rates on the beach, in the surf zone, and in un-vegetated and vegetated marine habitats. Section 7.3 presents the results of studies into the nutrient content, release of organic carbon from wrack and its bioavailability for heterotrophic bacteria, including sulphate-reducing bacteria. Section 7.4 reports the results of experiments and field observations on the release of H_2S from wrack under different conditions.

7.1 Physico-chemical characteristics of beach wrack relevant to decomposition

7.1.1 Objective

To determine the physical characteristics of wrack on beaches and how these change with age in order to provide relevant information on wrack decomposition.

7.1.2 Methods

The physical characteristics of wrack relevant to understanding decomposition were determined by two key approaches;

1. in-situ measurements of wrack accumulations at three sites over an annual cycle, capturing a range of accumulation types, from small to large; and
2. in-situ detailed profiling of wrack at three sites with large wrack accumulations on a single occasion.

Wrack samples were collected while assessing the spatial and temporal variation in beach wrack accumulations (Section 6.2). A full account of the sampling design is presented in that earlier section.

Temperature (˚C), redox potential (mV) and salinity (ppt) were profiled through the wrack accumulations with a TPS 90-FLMV probe and oxygen (% saturation) with a OxyGuard Polaris Dissolved Oxygen meter. In small accumulations (< 20 cm) the probe was inserted from the top of the accumulations. In deeper accumulations, a vertical face was cut into the wrack accumulation and the probe inserted horizontally into the accumulation, to record parameters 10 cm in from the exposed face. Redox potential and salinity were only recorded if the zone was saturated with water.

7.1.3 Results

7.1.3.1 Physical characteristics of small aggregations

At the three standard sites (Forrest Beach, Volunteer Marine Rescue and Geographe Sailing Club) surface wrack temperatures varied over the year with site average minima of 13.3 ± 0.3°C in winter to maxima of 24.9 ± 1.2°C in spring (Table 7.1). Sediment temperatures were generally 1°C lower, ranging from 13.1 ± 0.8°C to 24.0 ± 0.4°C. There was little variation among sites.

Oxygen concentrations in the surface wrack and sediment were generally around 100% saturation, except at Forrest Beach on those occasions when maximum wrack volume occurred (Table 7.1). At Forrest Beach on the 21st May 2008 surface wrack was ~ 0.5 m high and in contact with the saturated zone. At this time in the saturated zone there was 20 ± 7% oxygen saturation and redox was 151 ± 5 mV, whilst in the sediment under the wrack dissolved oxygen was 7 ± 1% saturation and redox was 99 ± 10 mV.

On a number of occasions wrack was observed buried 15 – 45 cm under the sediment surface (Forrest Beach - 13th August; Volunteer Marine Rescue and Geographe Sailing Club- 22nd August). The conditions around this buried wrack pile differed to the overlying sediment. Dissolved oxygen was lower, at 20 – 30% saturation and redox potential was lower, at -291 to -71 mV. Underneath this wrack layer was a saturated zone where dissolved oxygen was around 12% saturation, redox potential -352 to -225 mV and salinity similar to seawater, 32 ppt. The sediment under this water layer was even more depleted in oxygen (2 % saturation) and had lower redox potential (-366 to -277 mV) and salinity was brackish 12 ppt, indicating some freshwater input from groundwater.

Measurements of the saturated zone were collected at the three standard sites in September and October when the saturated zone ranged from 20-70 cm below the sediment surface and was not in contact with wrack (Table 7.2). The dissolved oxygen readings were less than the surface sediment and the redox potential varied among times: in September it was negative, ranging from -239 to -117 mV, whereas in October it was 78-134 mV.

Table 7.1 Temperature (°C) and dissolved oxygen (% saturation) in small wrack aggregations at standard sites over an annual cycle. Dissolved oxygen supersaturation (i.e. > 100 %) is typically found where intense photosynthesis is occurring.

DATE	ZONE	FORREST BEACH		VOLUNTEER MARINE RESCUE		GEOGRAPHE SAILING CLUB	
		Temp (°C)	D.O (% sat.)	Temp (°C)	D.O (% sat.)	Temp (°C)	D.O (% sat.)
19th May	Surface	18.5 ±0.8	97 ± 1	18.8 ± 0.6	87 ± 0.2	20.5 ± 0.3	97 ± 0.3
	Sediment	16.4 ± 0.2	7 ± 0.8	19.0 ± 0.7	87 ± 1.6	20.2 ± 0.2	95 ± 0.6
24th June	Surface	14.8 ± 0.2	100 ± 0.7	18.0 ± 0.2	103 ± 3.3	14.1 ± 0.2	104 ± 2.2
	Sediment	14.5 ± 0.2	96 ± 3.4	17.3 ± 0.3	102 ± 2.6	14.9 ± 1.1	103 ± 1.5
12th Aug	Surface	15.0 ± 0.9	112 ± 1.5	16.5 ± 0.6	115 ± 0.7	16.7 ± 0.1	115 ± 0.6
	Sediment	13.3 ± 0.3	65 ± 28	15.7 ± 0.7	114 ± 0.3	16.1 ± 0.1	113 ± 0.2
22nd Sep	Surface	13.3 ± 0.7	103 ± 3.4	16.5 ± 0.8	104 ± 2.3	15.6 ± 0.3	95 ± 5
	Sediment	13.1 ± 0.8	102 ± 3.0	16.9 ± 0.9	105 ± 2.1	15.6 ± 0.4	95 ± 5

Table 7.2 Physico-chemical characteristics in the saturated zone of small wrack accumulations (20 – 70 cm under the sediment surface).

SITES	DATE	DEPTH BELOW SEDIMENT (CM)	DISSOLVED OXYGEN (% SAT.)	REDOX POTENTIAL (MV)	SALINITY (PPT)	TEMP (°C)
Forrest Beach	22nd Sept	40 - 60	35 – 65	-239 to -141	11 – 22	13
	22nd Oct	45 - 60	35 - 45	90 – 117	nd	20
Volunteer Marine Rescue	22nd Sept	20 - 30	20 – 50	-158 to -117	18 -25	13
	22nd Oct	40 - 55	30 – 60	93 - 130	nd	19
Geographe Sailing Club	22nd Sept	20	20 -60	-222 to -185	14 - 19	14
	22nd Oct	60 - 70	15 - 40	78 - 134	nd	19

7.1.3.2 Physical characteristics of large aggregations

The oxygen saturation was lower in larger banks than small banks. In the sediment and saturated zone of wrack piles > 1 m high, oxygen was consistently 0% saturation, and was depleted through the mid-zone (40 – 80% saturation) and, at times, the surface zone (80 – 100% saturation) (Figure 7.1 and Figure 7.2). In the smaller of the large aggregations, ~ 0.5 m high the oxygen was depleted in the sediment and saturated zones (0-60%), and also in the mid zone (80-100%) but not in the surface zone (Figure 7.3).

Temperatures in the large wrack accumulations ranged from 11 - 24°C (Figure 7.1 and Figure 7.2), within the range found in the smaller accumulations. However, in any given period, small banks had lower temperatures, reflecting the heat generation and insulating properties of large wrack accumulations. There were differences in the temperature profile from the surface of the wrack to the sediment. The greatest variation of 4 - 7°C was observed in the large, old wrack piles (Figure 7.1), with 1 - 3°C variation in the large, new piles (Figure 7.2) and only 1 °C in the small, new piles (Figure 7.3).

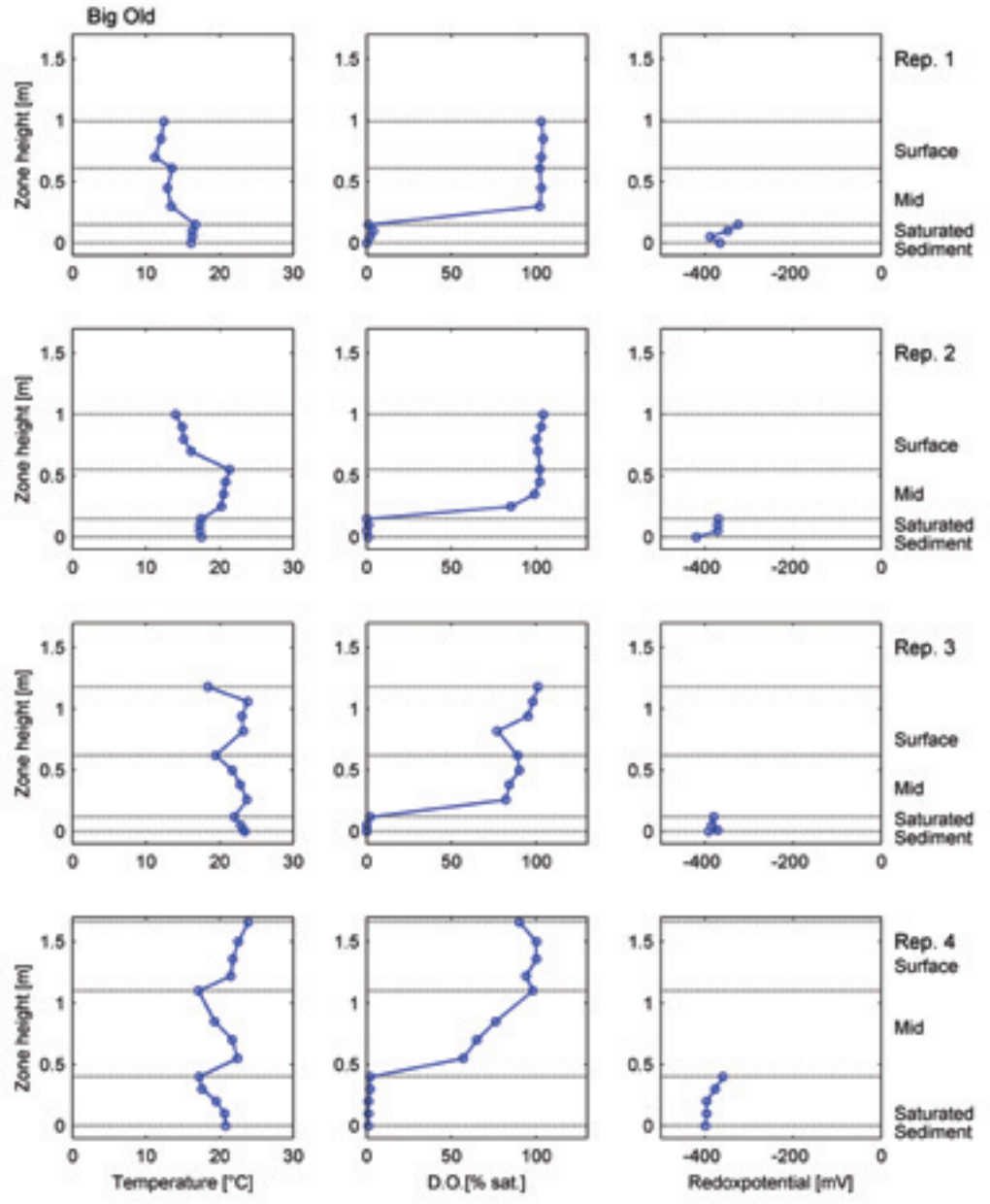

Figure 7.1 Physical profiles of temperature, dissolved oxygen and redox potential through large, old beach wrack accumulations. Each row of graphs represents one replicate wrack pile. NB: redox potential was only measured in the saturated zone.

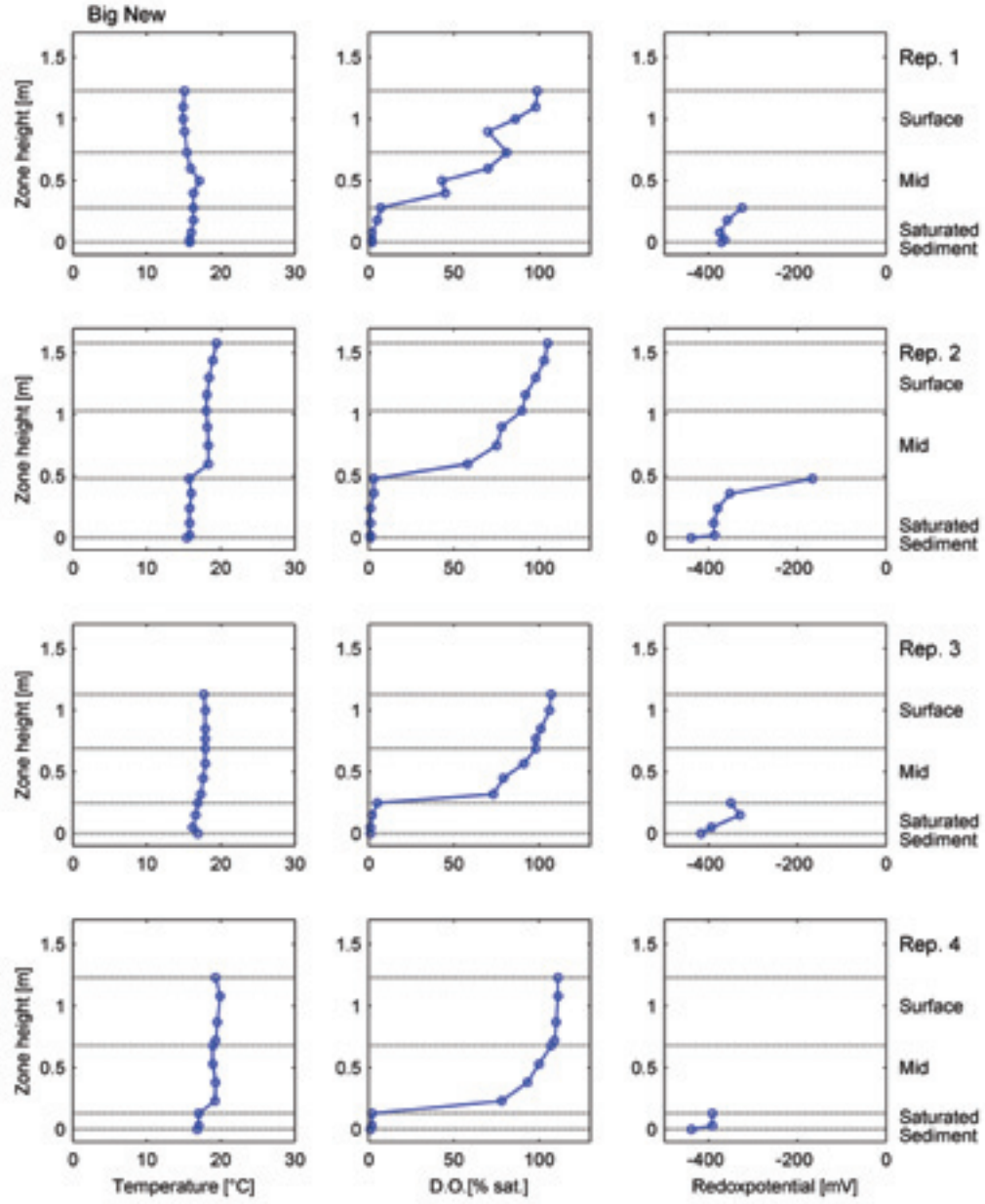

Figure 7.2 Physical profiles of temperature, dissolved oxygen and redox potential through large, new wrack accumulations. Each row of graphs represents one replicate wrack pile. NB: redox potential was only measured in the saturated zone.

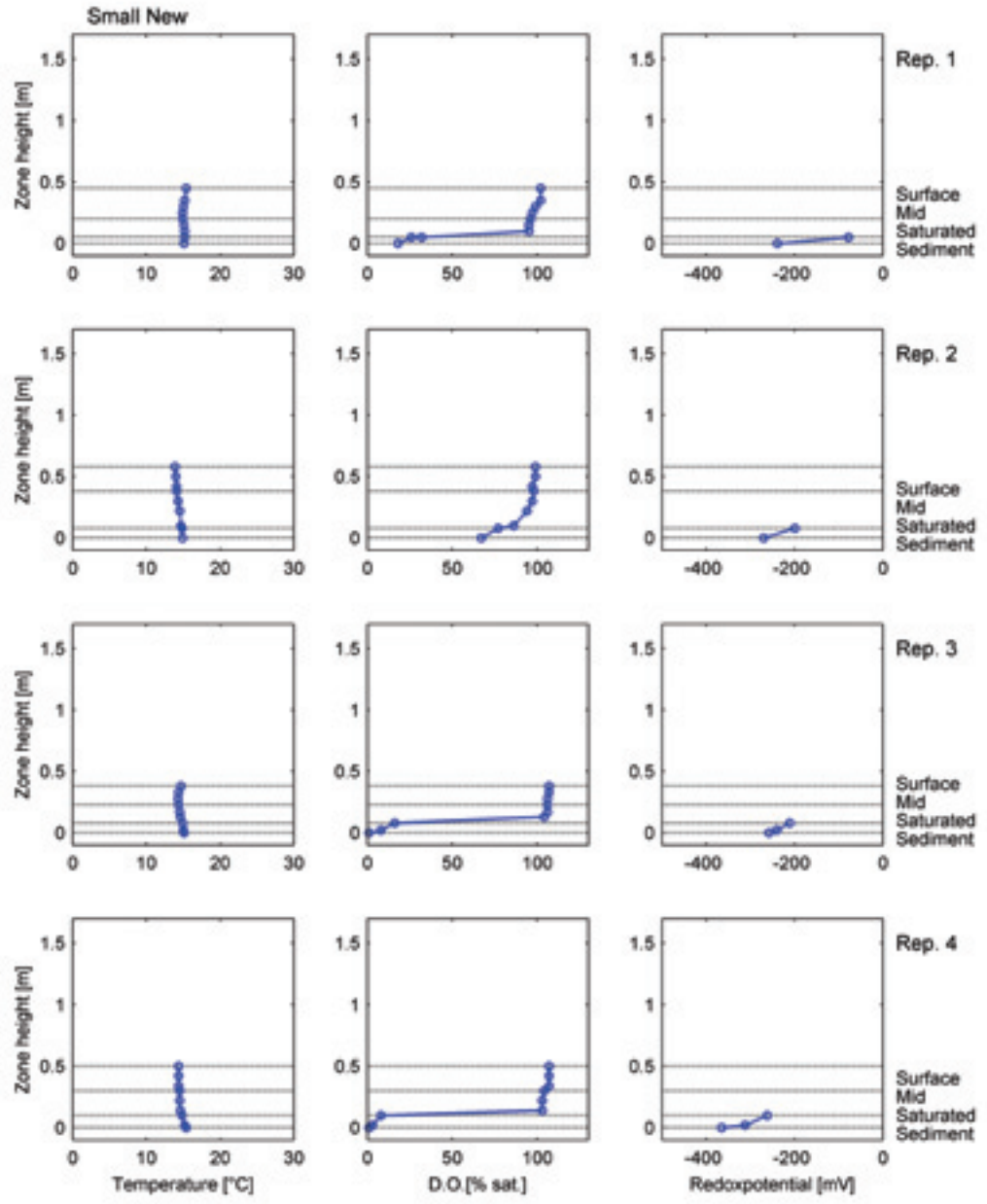

Figure 7.3 Physical profiles of temperature, dissolved oxygen and redox potential through small, new wrack accumulations. Each row of graphs represents one replicate wrack pile. NB: redox potential was only measured in the saturated zone.

7.1.4 Significance of results

Understanding the physical conditions of wrack and how these change with age is important for understanding the likely decomposition processes occurring within wrack accumulations. When oxygen is present throughout the wrack accumulations, decomposition will be predominantly aerobic, producing carbon dioxide (CO_2). Under hypoxic or anoxic conditions anaerobic decomposition will occur. Depending on the redox potential, bacteria will utilize different substrates as electron acceptors, liberating different gases as by-products of decomposition. Sulphate reduction and

hydrogen sulfide (H_2S) production occurs between -300 to 0 mV, and methane production (CH_4) from -350 to -100 mV; Figure 7.4).

Based on the redox potentials measured in the accumulations, H_2S production is likely to be associated with larger wrack accumulations (>0.5 m high) and when the wrack is in contact with the saturated zone. In these accumulations, (H_2S could accumulate within the wrack piles and flux out of the wrack through diffusion or when the accumulations are disturbed, such as during by-passing operations or trampling by walkers and dogs.

Conditions suitable for H_2S production were also recorded around buried bands of wrack about 15 - 45 cm below the sediment surface and which were in contact with the saturated zones.

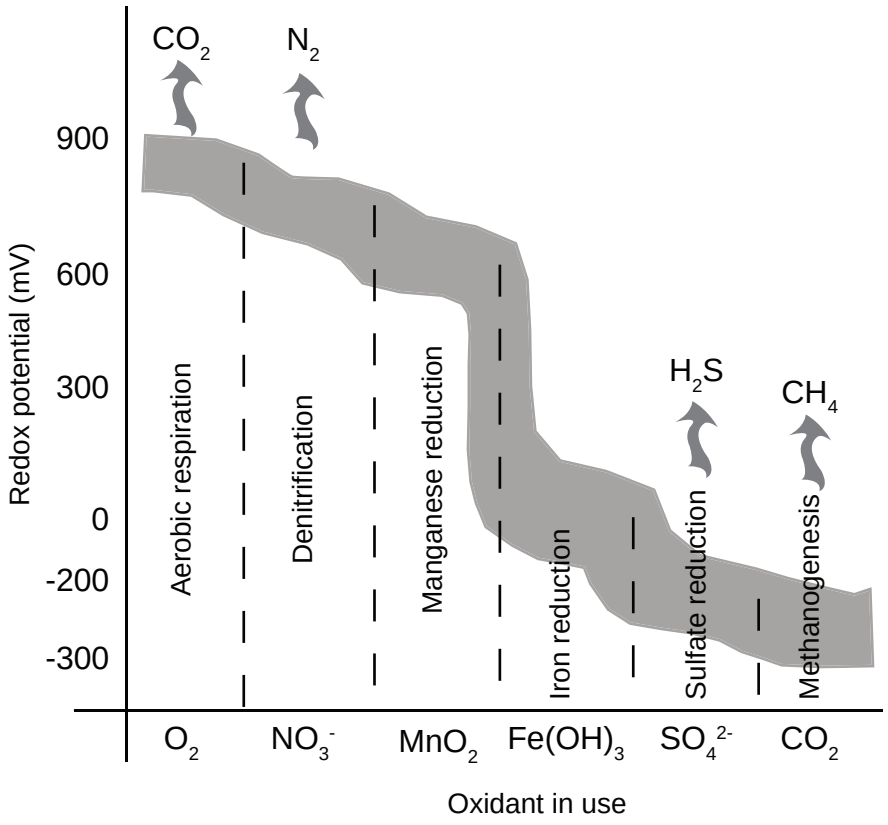

Figure 7.4 Redox potential dependent oxidation of compounds. Adapted from Hemond and Fechner [2000].

7.2 Wrack degradation rates

The degradation of wrack is a potentially important part of the wrack lifecycle to incorporate in the particle transport model. High rates of degradation coupled with low rates of transportation could see a significant loss of wrack before it reaches beaches. Conversely, under high rates of particle transport, such as those typical of winter in Geographe Bay, low rates of degradation may result in almost no loss of biomass due to degradation during passage from the offshore seagrass meadows to the beaches, including Port Geographe.

Degradation of intact seagrass particles is the result of biological and physical processes, including decomposition, consumption by macrofauna, photo-degradation and physical fragmentation. Published rates of degradation for seagrass material suggest that detached leaves take hundreds of days to be degraded [*Hansen*, 1984]. However, these rates were for material deposited on beaches where the opportunity for fragmentation and biological degradation may be less than in other habitats. No studies have examined the degradation rates of material while it is resident in the

seagrass meadows or un-vegetated marine habitat, where faunal consumption and microbial decomposition could be significant, or in the high-energy surf-zone where fragmentation due to wave action could reasonably be expected to be high.

7.2.1 Objective

To estimate the rate of wrack degradation in different habitats of Geographe Bay and at different times of year.

7.2.2 Materials and methods

Between 30 and 40 litter bags of fresh *P. sinuosa* (30 g FW) were placed in four different habitats (beach, surf, seagrass meadow and un-vegetated offshore sediment) at two times (16th April and 8th July 2009) and left to age for 2, 4, 8 and 12 weeks. At the start of each time, five samples of 30 g fresh *P. sinousa* were collected and dried to constant weight (7.0 and 7.22 g DW respectively) to determine the dry weight at the start of aging. After each aging period, four samples were collected in each zone and dried to constant mass to determine the change in mass over each period.

The beach zone was located just above the high tide mark (Figure 7.5) close to Port Geographe. The surf zone was placed at the same site in 0.3 m deep water. The vegetated and unvegetated zones were placed in 3.5 m depth, approximately 20 m apart from the edge of the seagrass meadow, approximately 1 km offshore. The April to June time period had low to moderate storm activity relative to the July to August time period.

Due to storm damage, the April trial was abandoned at four weeks for all zones other than the beach zone. Storm damage again led to the second trial being partially abandoned, but only for the surf zone after two weeks.

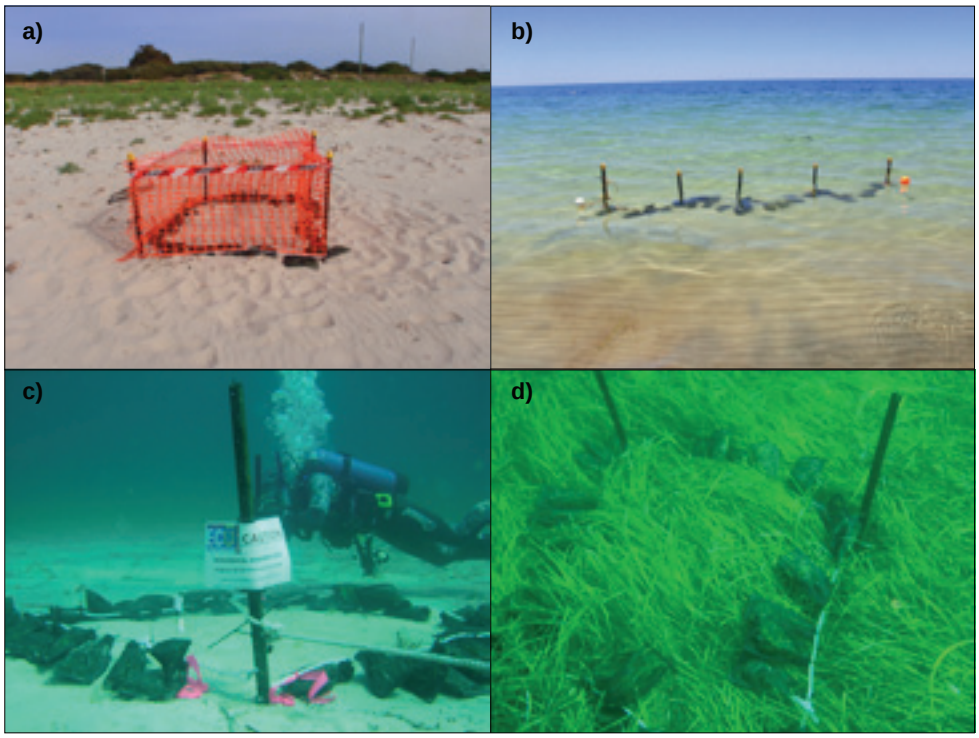

Figure 7.5 Seagrass degredation bags in the four habitats for which degredation rates were determined. a) Beach b) Surf-zone c) Unvegetated, d) Seagrass meadow.

7.2.3 Results

Wrack biomass declined in all degradation treatments, though the rate of change varied among times and habitats (Figure 7.6; Table 7.3). Beach zone had the lowest rates of degradation (2.0 ± 0.2 and 5.1 ± 1.1 g DW kg^{-1} d^{-1} in July and May, respectively), while the un-vegetated and vegetated habitats had the greatest, up to 14.8 g DW kg^{-1} d^{-1} (Table 7.3).

Degradation rates in July were significantly greater ($p > 0.05$) than in May for the un-vegetated and vegetated habitats, ranging from 11.3 + 0.2 to 14.8 ± 1.5 g DW kg^{-1} d^{-1} in July compared to 3.8 ± 0.2 to 8.7 ± 1.8 g DW kg^{-1} d^{-1} in May. However, the opposite trend occurred for the beach habitat, which had greater rates of degradation in May.

Corresponding to the degradation rates, the time required for wrack biomass to completely break down varied among habitats and between times (Table 7.3). In May, the time to complete degradation was longest on beaches (202 days), surf and un-vegetated habitats were similar at 189 and 194 days, respectively, and meadow had the quickest breakdown time, 130 days. In July, the time to completely break down was again longest on the beach (380 days) followed by surf zone (140 days) while un-vegetated and meadow habitats had similar times (76 and 79 days respectively), the fastest estimates for all habitats and times.

It is important to note that in all cases wrack decomposition bags in the surf zone were lost after 2 - 4 weeks due to the high-energy conditions destroying the experimental treatments. Consequently, the degradation rates are not strictly comparable to those of the other habitats. In fact, the degradation rates could potentially be much higher than the other habitats due to the fragmentation associated with such high-energy conditions.

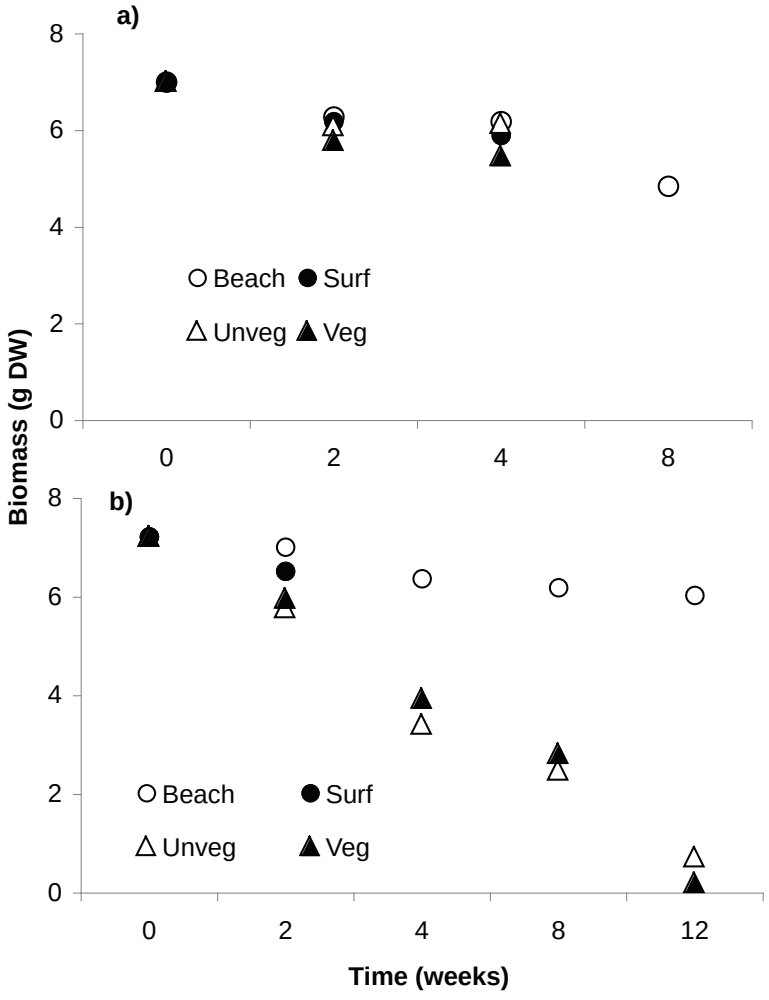

Figure 7.6 Biomass of wrack in bags degredation bags over the course of two degredation trials, a) April, b) July, 2009.

Table 7.3 Rates of wrack degradation in different habitats and after different amounts of time. * is the mean daily rate of degradation divided by total initial wrack biomass. Un-veg = unvegetated offshore habitat; veg = vegetated offshore habitat (seagrass meadow).

TIME (WKS)	RATE OF DEGRADATION (g DW kg^{-1} d^{-1})							
	MAY - JUNE				JULY - SEPTEMBER			
	Beach	Surf	Un-veg	Veg	Beach	Surf	Un-veg	Veg
2	5.1 + 1.1	5.8 + 1.5	6.6 + 0.6	8.7 + 1.8	2.1 + 1.1	7.1 + 3.1	14.8 + 1.5	12.8 + 2.6
4	4.3 + 0.9	4.8 + 0.3	3.8 + 0.2	6.6 + 1.2	3.5 + 0.7		13.6 + 1.3	13.4 + 1.1
8	5.5 + 0.4				2.8 + 0.3		12.8 + 1.2	11.9 + 1.7
12					2.0 + 0.2		11.3 + 0.2	12.2 + 0.2
Days to loss*	201.5	189.3	194.2	130.4	380.2	140.5	76.2	79.5

7.2.4 Significance of results

Wrack degradation rates varied between times and location. The highest degradation rates occurred in the vegetated and un-vegetated zones, and these rates were greater in the July period than in the May period. It is probable that the more frequent storm activity in the July period increased mechanical breakdown of the wrack at this time.

The breakdown of wrack on the beach occurred at much slower rates compared to other zones, especially in July-September. This zone lacks wave energy and the associated mechanical breakdown of the other zones. It also has fewer invertebrate fauna, which can contribute to mechanical breakdown of wrack.

The relative time taken for wrack to breakdown in each zone can be factored into the wrack transport model, allowing differential break-down rates to be determined depending upon whether particles reside in the water column or on the beach.

Wrack degradation rates and time taken for wrack to completely break-down help to account for declines in biomass when calculating whole bay estimates for wrack mass balance (Section 6.1). Results here suggest that approximately 11 000 t of wrack that are unaccounted for on either the beach, un-vegetated habitat or in the meadow in July are likely broken down into fine particulate matter through biological and mechanical degradation.

7.3 Nutrient content, bacterial abundance and DOC leaching from wrack

7.3.1 Objective

To determine the biogeochemical characteristics of wrack accumulations in Geographe Bay, including the nutrients and gases released during decomposition, the sources of carbon that fuels microbial decomposition and the source of sulphur contributing to H_2S production.

7.3.2 Methods

The biogeochemistry of wrack was determined using three approaches:

- the nutrient content of wrack accumulations of different ages and sizes was measured in-situ and the effect of aging on nutrient content determined experimentally;
- the amount and types of organic carbon leaching from wrack, and its bio-availability to heterotrophic bacteria, was determined in laboratory experiments; and,
- the production of H_2S gas, and factors influencing the rate of production, were studied through a combination of field measurements and laboratory experiments.

7.3.2.1 Nutrient content of wrack particles

Fresh *P. sinuosa* leaves, *A. antarctica* stems and leaves, and red epiphytic algae (*Laurencia*) were collected from seagrass meadows in Geographe Bay and from beach wrack. Additionally, *P. sinuosa* leaves and *A. antarctica* stem and leaves that had passed through the pump in wrack by-pass operations at Port Geographe were also collected. All treatments had five replicates.

Two types of aging were assessed: 'in air' (the material was exposed to air on moist sediment) and 'buried' (2 cm below moist sediment and not exposed to air). Samples were retrieved for nutrient analysis after 0, 2, 4 and 8 weeks for 'in air' samples (between 15th August and 6th October 2008) and after 0 and 4 weeks for buried samples. Samples were dried and ground to a fine powder using a ball mill. Total nitrogen and total carbon content was determined using a continuous flow isotope ratio mass spectrophotometer (20-20 IRMS, Europa, Crewe, United Kingdom).

7.3.2.2 Nutrient content of wrack

Three sites with large wrack accumulations of different age and size were sampled to provide insight into the biogeochemistry of large wrack accumulations. The accumulations were categorized as: Big (> 1 m deep) or Small (< 0.5 m deep); and Old (having been on the beach for at least 12 weeks) or New (having been on the beach for less than 6 weeks). Big Old (Siesta Park), Big New (Guerin St) and Small New (Abbey) accumulations were sampled.

At each site four replicate wrack piles were sampled in four zones, Surface (10 cm under the surface of the wrack pile), Mid (half-way between the surface and the saturated zone), Saturated (where the wrack was in water) and Sediment (the sediment below the wrack) (see Figure 6.14). Wrack was sampled from each zone for bacterial counts and nutrient analysis (carbon, nitrogen). From the saturated zone water samples were taken for total dissolved organic carbon (TDOC), total nitrogen (TN), total phosphorus (TP), ammonia (NH_4-N), nitrate+nitrite (NOx-N) and filterable reactive phosphorus (FRP-P or PO_4-P). Sediment samples were taken for total carbon, total nitrogen, total phosphorus and total organic carbon determinations.

Heterotrophic bacteria counts were performed on wrack and sediment following Duhamel and Jacquet [2006]. Triplicate samples for heterotrophic bacterial counts were taken from each zone of the wrack. Surface, mid and saturated samples were collected with tweezers and placed into a volume of 1 mL, whereas sediment samples were collected undisturbed. Filtered (0.2µm) seawater (2.88 mL) was added and then this was fixed (with 120 µL of 25 % Glutaraldehyde to get a final concentration of 1 %) and samples stored on ice in the dark. That day, 1 mL of 0.04 M sodium pyrophosphate was added to get a final concentration of 0.01 M. The sample was then sonicated three times for 1 minute in a water bath, shaken manually after every minute then left to settle for 30 seconds and a 1 mL sub-sample taken and stored on liquid nitrogen.

Cell counts were determined in a FACS Canto II flow cytometer. Samples were quick thawed in a 37 ºC water bath, 1mL was transferred into a 1mL Eppendorf and then centrifuged at 1000 rpm for 60 seconds. These were diluted 1 in 20 with 50 µL of supernatant mixed with 950 µL of prefiltered (0.2 µm) TE buffer. Samples were further diluted 1 in 10 into a U-bottom plate with TE buffer and 5 µL of SYBRgreen. Plates were wrapped in alfoil and agitated for 30 seconds on a shaker, and then incubated for 15 min on a 80ºC heater block. Then 10 µL of standard bead stock made from 100 µL bead stock (2.5 µL of 1690 fluorescent beads + 9 mL filtered (0.2 µL sheath fluid) and 900 µL of prefiltered Sheath Fluid Samples was added prior to running samples. Blanks were also run consisting of TE buffer, SYBRgreen and bead

stock solution. The sample flow parameters were flow rate: 1 µL s^{-1}; sample volume: 120 µL; mixing volume: 50 µL; mixing speed: 200 µL s^{-1}, 2 mixes; and wash volume: 200 µL. Data were stored as FCS 2.0 files and cell counts (cells mL^{-1}) were calculated using CYTOWIN 4.3 following [*UWA*, 2008]. Triplicates were averaged per zone.

TDOC samples were filtered through a 0.45 µm cellulose acetate filter and was analysed on a Shimadzu TOC-V CSH organic carbon analyser. Water samples for total nutrients and dissolved nutrients (passed through a 0.45 µm cellulose acetate filter) were analysed on a Skalar autoanalyser SAN System. Wrack and sediment C & N were dried and ground into a fine powder and then run in a continuous flow isotope ratio mass spectrophotometer (20-20 IRMS, Europa, Crewe, United Kingdom). Sediment organic carbon was analysed by a Shimadzu Corporation Solid Sample Module SSM-5000A using manual combustion-NDIR method and total phosphorus by acid digest and then orthophosphate measured in a Lachat Automated Flow Injection Analyser.

7.3.2.3 Amount and timing of dissolved organic carbon leachate from P. sinuosa wrack

To assess the DOC release from *P. sinuosa* wrack, an incubation experiment was run over 14 days. Three replicates of unscraped and scraped, fresh *P. sinuosa* leaves were incubated by placing 180 g wet weight in 1.4 L of artificial seawater in acid washed 2 L glass beakers. Scraping leaves to remove epiphytes prior to incubation was designed to test the effect of surface abrasion on DOC leaching, as may occur during the transport of detached wrack. A blank of artificial seawater was incubated at the same time. Samples for DOC and nutrient analysis (ammonia (NH_4-N µg N L^{-1}), nitrate+nitrite (NOx-N, µg N L^{-1}) and orthophosphate (PO_4-P, µg P L^{-1}) were collected after 1, 3, 5, 7, 10, 14 days of incubation, and the whole artificial seawater replaced each time. The leachate was filtered through a series of Whatman glass fibre filter papers and then a 0.45 µm, hydrophilic polypropylene membrane filter and analyzed for total dissolved organic carbon with a Shimadzu Total Organic Analyzer 9000.

7.3.2.4 Characterisation of dissolved organic carbon composition of wrack of different types and ages

Two experiments were conducted to determine the amount and composition of DOC released from wrack and how this changes with increased degradation. The first experiment examined the effect of wrack type (*P. sinuosa* leaves, *A. antarctica* leaves, *A. antarctica* stems, *Laurencia* sp., fine fraction (>0.1 - <1 mm) from natural beach wrack that had been on the beach for at least two months) on the amount and composition of DOC leachate. The second experiment examined the effect of aging on DOC release from one wrack type (*P. sinuosa* leaves) after 1, 2, and 4 weeks of aging on the beach.

Fresh samples (3 kg) of seagrass (*P. sinuosa*, *A. antarctica*) and epiphytic algae (*Laurencia* sp.) were collected in 0.5 m depth at Luscombe Bay, Garden Island, Western Australia (S 32° 13.477', E 115° 41.872') on 23/10/08. Fresh material was returned to the laboratory and stored in a cool room at 4 ºC for a maximum of two weeks until leachate experiments were initiated. Natural wrack accumulations were collected on 13/08/08 on Busselton Beach, Geographe Bay, Western Australia (S 33º 39.317', E 115º 16.812') and then sieved to separate the fine fraction. Samples were stored at 4 ºC for a maximum of four months until leachate was collected.

For the second experiment fresh samples (5 kg) of seagrass *P. sinuosa* was collected in 0.5 m depth at Colpoys Point, Garden Island, Western Australia (S 32° 13.477', E 115° 40.365') on 30/03/09. For 'aged' material, approximately 500 g of fresh *P. sinuosa* was placed in nylon mesh litter bags (mesh size < 5 mm), and attached to pickets on the shoreline, within wrack accumulations for 1, 2, and 4 weeks with three replicates for each time period. Once again fresh material was transported immediately to the laboratory and stored in a cool room at 4 ºC for a maximum of two days until leachate was collected. After each aging period the material was collected and returned to the laboratory for leachate experiments.

DOC leachate extraction

Each wrack type and age was incubated to extract DOC, however, for *A. antarctica* seagrass the plants were separated into stems and leaves. All leaves of both seagrass species were scraped lightly with a razor blade to remove algal epiphytes. Due to time constraints only one wrack type could be incubated at a time. For each incubation, four replicate samples of the wrack type and one blank were incubated. Between 100 - 150 g wet weight of plant material was placed in 0.5 L artificial seawater (Red Sea Salt, alkalinity: 2.2 - 2.5 milliequ L^{-1}) in acid washed 2 L glass beakers that were sealed and incubated for 16 hours at 18 °C. The blank was prepared as described above but with no wrack.

After the 16 hours, the leachate was filtered through a series of Whatman glass fibre filter papers and then a 0.45 µm, hydrophilic polypropylene membrane filter (Pall Life Sciences).

In a further experiment the effect of scraping prior to incubation on the amount of DOC released from leaves of fresh *P. sinuosa* was examined, to allow comparisons between naturally generated wrack which is unlikely to have the leaf surface abraded as much as would occur from scraping with a razor blade. Three replicates of unscraped and scraped leaves were incubated by placing 180 g wet weight in 1.4 L of artificial seawater in acid washed 2 L glass beakers. A blank of artificial seawater was incubated at the same time. Samples for DOC leachate were collected after 1, 3, 5, 7, 10, 14 days of incubation, and the whole artificial seawater replaced each time. The leachate was filtered as described above and analyzed for total dissolved organic carbon with a Shimadzu Total Organic Analyzer 9000.

Characterization of DOC

DOC composition was characterized by fractionation using open column chromatography following modified methods of Chow *et al.* [2004] and Cleveland *et al.* [2004]. The leachate was fractionated into hydrophobic DOC (fulvic and humic acids; [*Hughes*, 2007]) and hereafter referred to as 'humic fraction' by retaining on the DAX-8 resin, transphilic DOC ('slightly humic fraction') by retaining on the XAD-4 resin and hydrophilic DOC ('non-humic fraction'), the eluent passing through the DAX-8 and XAD-4 column [*Thurman and Malcolm*, 1981]. The non-humic fraction is composed predominantly of low molecular weight compounds, including carbohydrates and amino acids [*Cleveland et al.*, 2004].

DAX-8 Superlite (Sigma-Aldrich) and XAD-4 Amberlite (Sigma Aldrich) resin columns were prepared in a similar manner. The resin was mixed with water (milli Q) to form a slurry, which was then poured into a glass column (30 x 1.5 cm) that was fitted with a tap. The bed volume for the resin was approximately 20 mL. The column was conditioned by passing Milli-Q water (200 mL) though the column dropwise followed by six alternating washes of 0.1 M NaOH (40 mL) and 0.1 M HCl (40 mL), again applied dropwise. The final wash was with 0.1 M HCl so as to leave the column in an acidic condition.

The DOC leachate (200 mL) was acidified with 35% HCl to pH 2 and then passed through the DAX-8 resin (dropwise or with a flow rate not exceeding 3 mL min^{-1}). The first 10 mL of the eluent was discarded (as it was just the displaced acid). When most of the leachate had been applied to the column, 0.1 M HCl (2 bed volumes or 40 mL) was applied to the top of the column. It is imperative that the resin bed is not left without liquid. The acid was passed down through the column dropwise to elute all but the fulvic and humic acids. The eluent (leachate and acid) was then passed through the XAD-4 column in a similar manner. However, in this instance the acid was added to elute all but the "slightly humic" fraction. The eluent from this second column is the nonhumic or hydrophilic fraction.

The humic and slightly humic fractions were removed from the DAX-8 and XAD-4 resins respectively by passing 0.1 M NaOH down the resins dropwise. The volume of base added was typically 5 bed volumes (100 mL) or until the absorbance of the eluent at 254 nm was similar to the blank (the eluent from a resin which had seawater and not leachate as the sample).

The total volume of each fraction was recorded. All prefiltered leachate samples and fractionated samples were acidified with 35% HCl to pH 2 and analyzed for total dissolved organic carbon with a Shimadzu Total Organic Analyzer 9000. The UV absorbance for each of the acidified samples was also recorded at 254 nm. The absorbance values were recorded using a Shimadzu UV-1601 spectrophotometer.

Bioavailability of DOC

The bioavailability of the filtered DOC leachate was tested on treatments in the first experiment based on Cleveland *et al.* [2004]: the short-term response of a bacterial inoculum to the different DOC leachates was observed as growth rate over a 24-hour period.

Filtered DOC leachate (200 mL) was combined with a bacterial inoculum (2 mL) in acid-washed glass flasks, wrapped and capped in aluminium foil. The bacterial inoculum was created by combining 100g of moist beach sediment with 100 g of moist wrack with 800 mL artificial seawater in an acid washed glass beaker wrapped in aluminum foil to promote heterotrophic bacterial growth. This was left for 24 hours at 18°C and then filtered through a Whatman 3 filter paper with the filtrate used as the bacterial inoculum. For each DOC leachate type four replicates and four blanks (200 mL artificial seawater + 2 mL bacterial inoculum) were incubated at 25°C. Triplicate sub-samples (1 mL) were taken

at 0, 3, 18 and 24 hours of incubation and fixed with glutaraldehyde (0.5% final concentration) for 15 min in the dark (Marie et al., 1999) then stored in liquid nitrogen until further processing. Heterotrophic bacterial cell counts were determined using flow cytometric analysis following Seymour et al. (2005) on a FACS Canto II flow cytometer. Samples were diluted with TE buffer (1:50 dilution) and stained with SYBR Green I for 15 min. at 80°C. Acquisition was run for 2 min at a speed of 1 µl s^{-1}. Data were stored as FCS 2.0 files and cell counts (cells mL^{-1}) were calculated using the CYTOWIN 4.3 software.

Once the bioassay was completed sub-samples were collected for bacterial cell size estimation using epifluorescence microscopy adapted from the methods of Servais *et al.* [1999] and Porter and Feig [1980]. Samples were stained with 4',6-diamidino-2-phenylindole dihydrocholride (DAPI; 5 µg mL^{-1}) and 3,6-acridinediamine, monohydrochloride (Proflavin, 5 µg mL^{-1}) then filtered through black polycarbonate membrane filters (0.2 µm pore size, 25 mm, Nuclepore), placed on glass slides and stored at -80°C until further processing. Bacterial cell sizes were estimated from images of DAPI stained cells using a Leica DMLB compound microscope with fluoresence (UV filter) attachment and a 35 mm DSLR camera (Nikon D40X - 10 Mp). The length (L) and width (W) of randomly chosen cells were determined using the software ImageJ 1.41o. and the biovolume (V) calculated as [*Bratbak*, 1985; *Felip et al.*, 2007]:

$$V = \frac{\pi}{4} \cdot W^2 \left(L - \frac{W}{3} \right) \qquad \textbf{Eq. 7-1}$$

Bacterial biovolumes were converted to carbon content per cell (fg C $cell^{-1}$) using the following relationship [*Felip et al.*, 2007]:

$$C = 120 \cdot V^{0.72} \qquad \textbf{Eq. 7-2}$$

Statistical Analysis

Analyses of variance (ANOVA) were used to test for difference in the amount and composition of DOC released.

A one-way ANOVA was used to test for differences between the total DOC released in Experiment 1 with Wrack type as fixed factor. A two-way ANOVA was then used to test for differences between proportions of functional DOC fractions with Wrack type and DOC fraction as fixed factors. A one-way ANOVA was used to test for differences between the total DOC released in Experiment 2 with Age a fixed factor. A two-way ANOVA was then used to test for differences between functional proportions of functional DOC with Age and DOC fraction as fixed factors. A one-way ANOVA was used to test for differences between the total DOC released in Experiment 3 with Scraping as fixed factor. A two-way ANOVA was then used to test for differences between the estimated daily DOC releases with Scraping and Incubation time as fixed factors.

The assumption of homogeneity of variances was tested using Cochran's test. When significant the data were natural log-transformed or arcsin-transformed for proportions and percentage values. When transformation did not remove heterogeneity the analysis was continued with original data (Exp.1, two-way ANOVA; Exp. 3, one-way ANOVA).

7.3.3 Results

7.3.3.1 Nutrient content of wrack

The nutrient content of wrack varied among wrack types (Table 7.4). *A. antarctica* stems had the highest carbon content (~ 40% DW), followed by *P. sinuosa* leaves (~ 34% DW), then *A. antarctica* leaves (~30% DW) and algae was variable, ~25-34% DW. Leaves of *A. antarctica* and *P. sinuosa* that had been by-passed had on average higher proportion of carbon than fresh leaves or leaves on the beach.

The nitrogen content in fresh material was greatest in *P. sinuosa* leaves (~1.4% DW), followed by *A. antarctica* leaves and algae (~0.9% DW) while *A. antarctica* stems had the lowest nitrogen content (0.5% DW, Table 7.4). The nitrogen content of *P. sinuosa* leaves was lower in wrack on the beach, and lower again in wrack that had been by-passed (accounting for the higher proportion of carbon in these leaves). There were no significant differences in nitrogen content between wrack type for the other species and source of wrack.

The effect of aging on nutrient content of wrack varied among wrack types (Figure 7.7). For *P. sinuosa* leaf material, there was no clear trend in %C with age but %N declined with time in buried samples; there was no clear trend in the %N of sampled exposed to air. In *A. antarctica* stems, carbon and nitrogen content increased with age in both 'in air' and 'buried' samples after 2 - 4 weeks, though 'in air' samples decreased further by eight weeks. In *A. antarctica* leaves nitrogen content increased after eight weeks of aging 'in air. Carbon-content of *Laurencia* decreased with aging 'in air' (Figure 7.7).

Table 7.4 Nutrient content of different wrack types collected fresh from seagrass meadows, from wrack piles on beaches or after passing through the Port Geographe bypassing pump. All values are means ± stdev.

	TISSUE NUTRIENT CONTENT (% OF DW)			
NUTRIENT	WRACK SOURCE	WRACK TYPE		
		FRESH	BEACH	OUT OF PUMP
Carbon	*P. sinuosa*	33.70 ± 1.71	34.96 ± 2.12	38.80 ± 0.70
	A. antarctica stem - new	41.55 ± 2.33	41.55 ± 3.38	42.94 ± 1.59
	A. antarctica stem - old	-	41.78 ±2.41	-
	A. antarctica leaf - new	29.30 ± 2.10	31.39 ± 2.73	33.05 ± 3.45
	A. antarctica leaf - old	-	33.38 ±2.12	-
	Algae	25.60 ± 1.0	33.67 ± 4.47	-
Nitrogen	*P. sinuosa*	1.39 ± 0.13	0.87 ± 0.27	0.64 ± 0.05
	A. antarctica stem - new	0.53 ± 0.07	0.65 ± 0.19	0.85 ±0.26
	A. antarctica stem - old	-	0.55 ± 0.22	-
	A. antarctica leaf - new	0.97 ± 0.11	1.20 ± 0.16	1.22 ± 0.12
	A. antarctica leaf - old	-	1.11 ± 0.11	-
	Algae	0.93 ± 0.04	1.06 ± 0.18	-

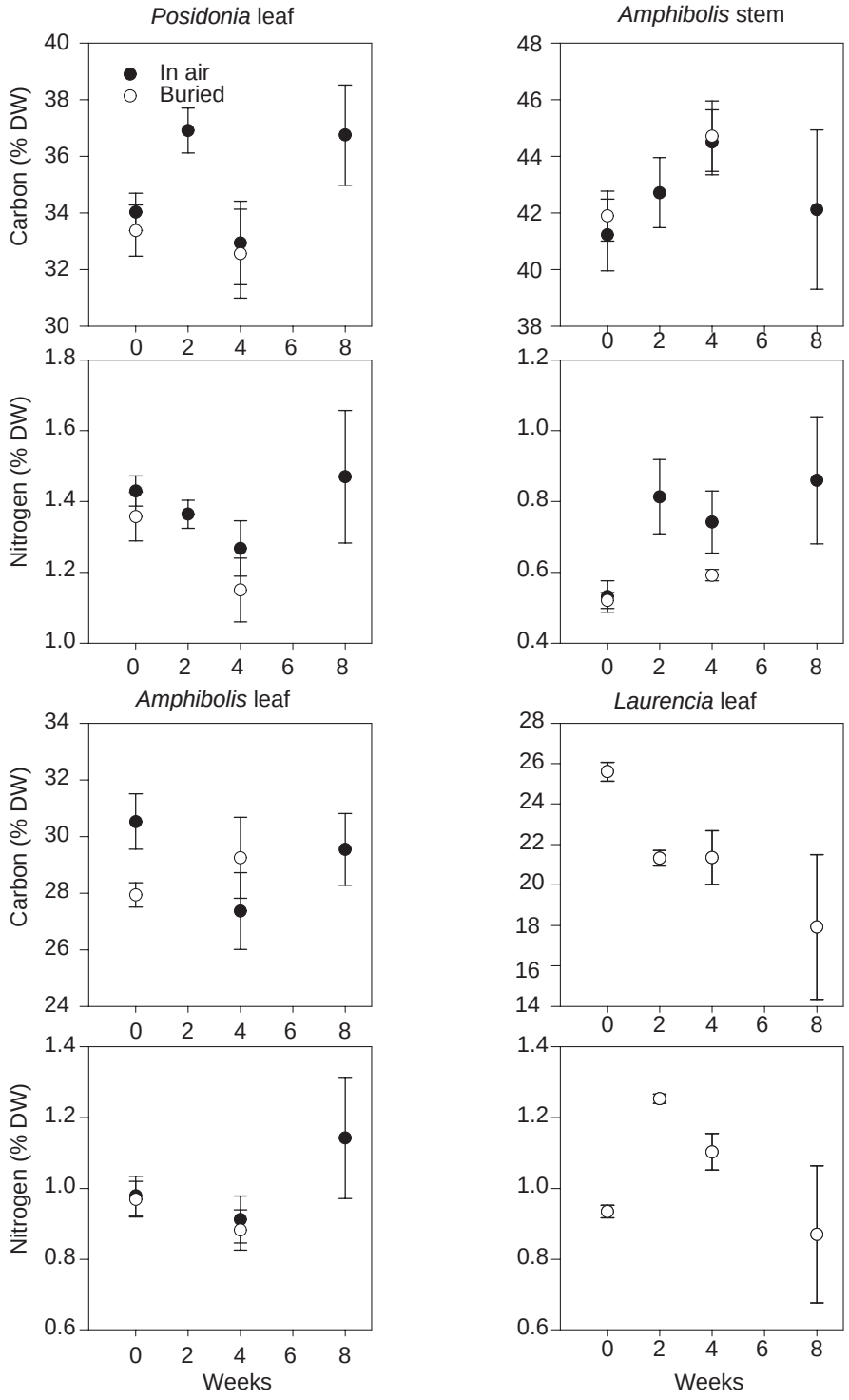

Figure 7.7 Nutrient content of wrack after 2, 4, 6, 8 weeks in air or buried in the sediment.

7.3.3.2 Heterotrophic bacteria

Average cell counts per site and zone ranged from 0.19 - 5.33 x 10^8 cells mL^{-1} (Figure 7.8). Across all sites, there were less heterotrophic bacteria in sediments (average all sites 0.76 x 10^8 cells mL^{-1}) than other wrack zones (average all sites 1.66 - 2.13 x 10^8 cells mL^{-1}), with no clear difference between the surface, mid and saturated zones. The larger older wrack piles had more bacteria (averaged over all zones: 2.59 x 10^8 cells mL^{-1}) than both the large new (1.18 x 10^8 cells mL^{-1}) and small new (1.00 x 10^8 cells mL^{-1}) accumulations.

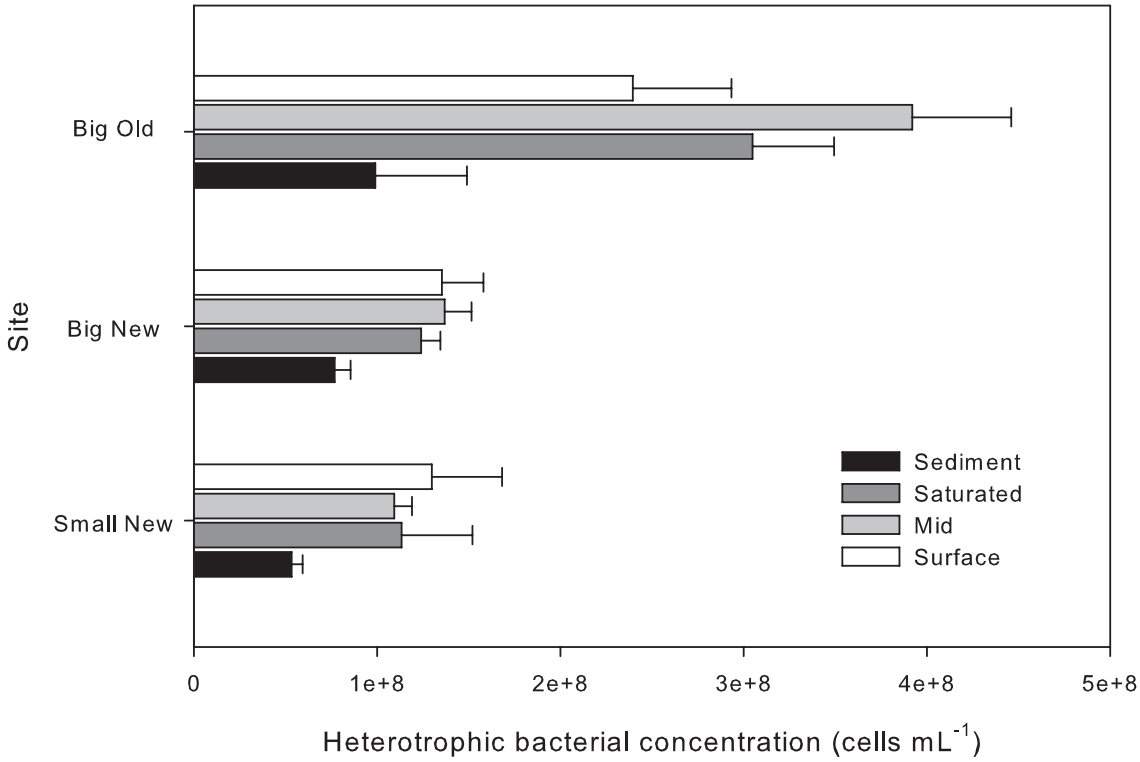

Figure 7.8 Heterotrophic bacterial concentrations (cells mL^{-1}) in the different zones of large wrack accumulations of different size and age.

7.3.3.3 Wrack nutrients

In large wrack accumulations there were similar amounts of nitrogen in wrack from the surface, mid and saturated zones (averaging 0.52-0.62% DW) but lower values in the sediment (averaging 0.39-0.52% DW across all sites) (Figure 7.9). There were no consistent patterns among wrack piles of different size and age. There were no obvious differences in wrack carbon content between sites, but there was more carbon in the surface wrack (34.0% DW) compared to wrack in the sediment (31.0% DW).

The $\delta^{15}N$ value of wrack was highly variable, ranging from 0.89 – 2.5‰ (avg: 1.69‰) and with no consistent patterns among zones in the wrack or different sizes and ages of wrack (Figure 7.10). The $\delta^{13}C$ was also highly variable, ranging from –14.74 to – 8.69 ‰ (Avg: -10.04‰), with no consistent patterns among wrack of different size and age, but with values for wrack in the sediment lower than in other zones (zone avg: -9.35 vs. -10.51 to -10.05‰).

7.3.3.4 Saturated zone nutrients

The concentration of dissolved organic carbon (DOC) in the saturated zone ranged from 10-68 mg L^{-1} (avg: 33 mg L^{-1}) (Table 7.5). On average the Big accumulations of wrack had higher DOC concentrations than Small (avg: 12.9 mg L^{-1}) and, within the Big piles, New accumulations (avg: 50.7 mg L^{-1}) had higher concentrations than Old (34.3 mg L^{-1}). Similar patterns among different sizes and ages of wrack accumulations were also observed for total nitrogen, ammonium, total phosphorus and orthophosphate (Table 7.5). The concentration of ammonium showed slightly different patterns. The highest average concentration was observed in the Big New piles, then the medium concentration in the Small New piles, and the lowest in the Old Big piles, however there was great variation in the concentrations observed.

7.3.3.5 Sediment nutrients

TOC in the sediment porewater was greatest in the Big Old accumulations (avg: 1.10 % DW), followed by Big New (avg: 0.85 % DW) and least in the Small New piles (0.40 % DW) (Table 7.5). A similar pattern was observed among sites with total carbon except that there was no difference between the Big New and Small New piles. Total phosphorus in the sediments ranged from 0.28-0.59 mg P g^{-1} sediment (avg: 0.42). The greatest amount of phosphorus in sediments was observed in Small New piles (0.49 mg P g^{-1} sediment), followed by Big Old piles (0.42 mg P g^{-1} sediment), and the least in Big New piles (0.33 mg P g^{-1} sediment).

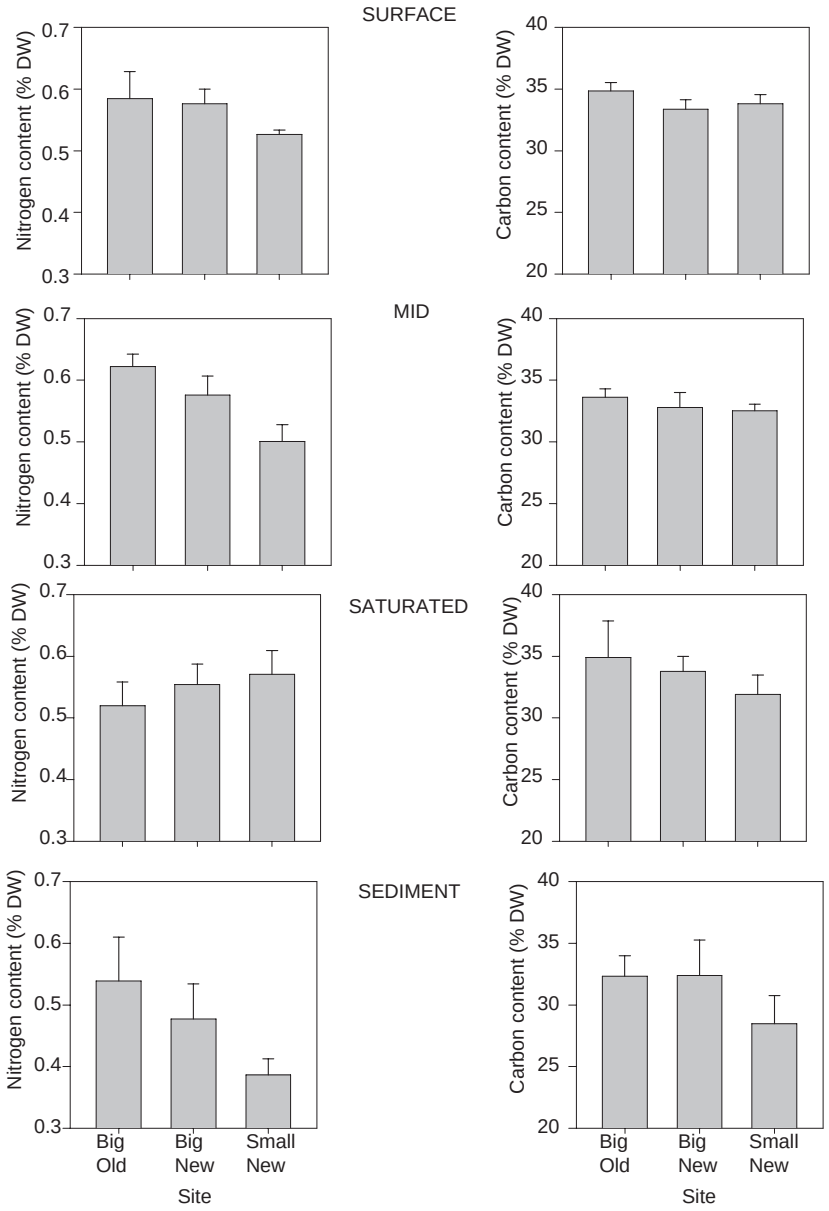

Figure 7.9 Nitrogen and carbon content of wrack from different depths (Surface, Mid, Saturated, Sediment) in three different types of large wrack accumulations (Big = > 1m high; Small = 0.5-1 m high; Old = present on beach for at least 12 weeks; new = present on beach for 6 weeks or less). All data are means ± std error.

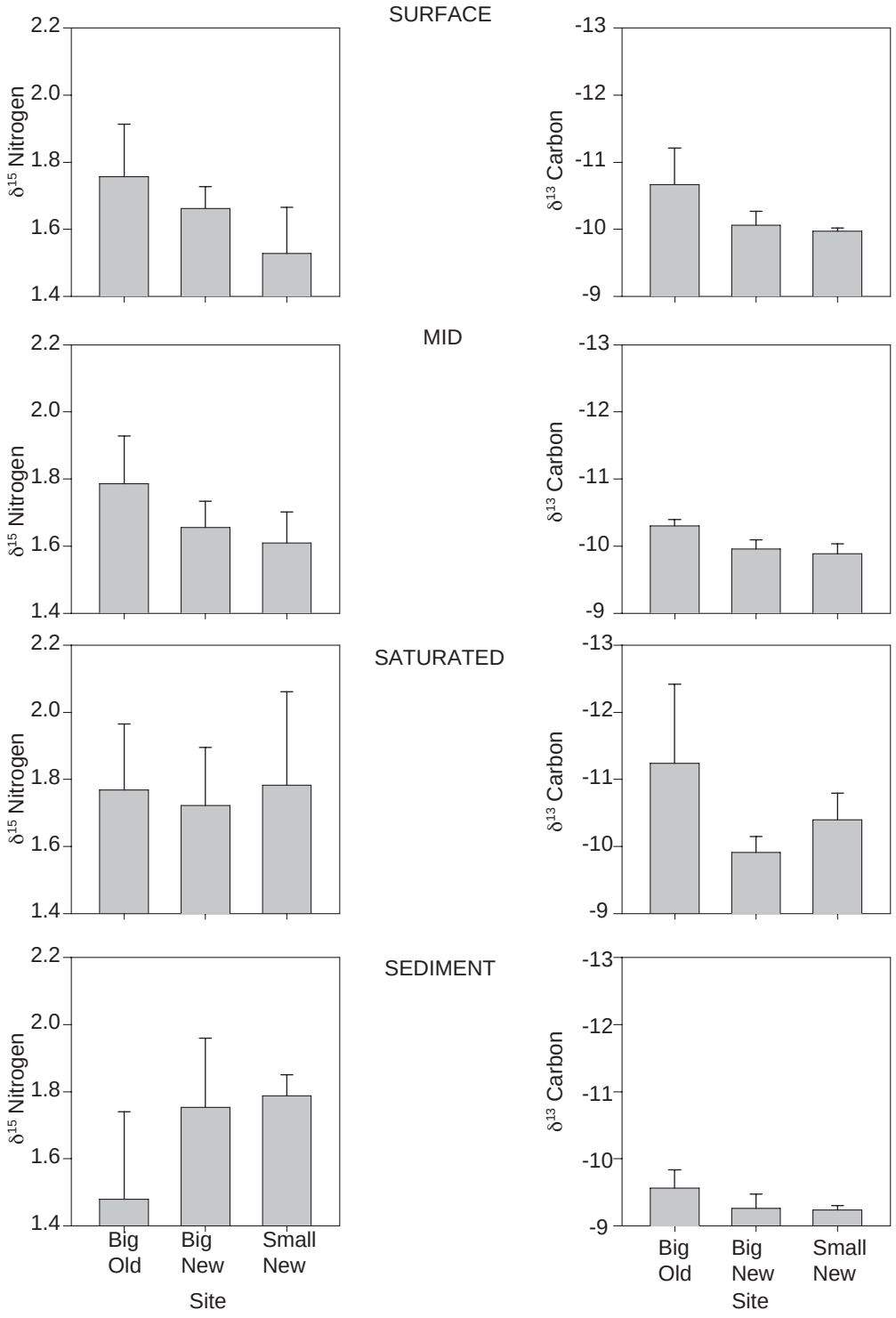

Figure 7.10 $\delta^{15}N$ (left) and $\delta^{13}C$ (right) values (‰) of wrack from different zones (Surface, Mid, Saturated, Sediment) in three different types of large wrack accumulations (Big = > 1m high; Small = 0.5 - 1 m high; Old = present on beach for at least 12 weeks; New = present on beach for 6 weeks or less). All data are means ± std error.

Table 7.5 Chemical constituents of the water in the saturated zone of large wrack accumulations and the underlying sediment porewaters. (Big = > 1 m high; Small = 0.5-1 m high Old = present on beach for at least 12 weeks, new = present on beach for 6 weeks or less).

	WRACK TYPE		
NUTRIENT	BIG OLD	BIG NEW	SMALL NEW
SATURATED ZONE WATER			
Dissolved inorganic carbon (mg L^{-1})	206.5 ± 40.4	247.3 ± 21.2	93.2 ± 2.6
Dissolved organic carbon (mg L^{-1})	34.3 ± 4.3	50.7 ± 9.2	12.9 ± 1.1
Total nitrogen (µg N L^{-1})	5 517 ± 1719	10 500 ± 2048	2 299 ± 234
NO_x (µg N L^{-1})	67.5 ± 24.6	92.7 ± 21.3	39.7 ± 9.1
NH_4 (µg N L^{-1})	1 392 ± 749	2 065 ± 631	1 968 ± 180
Total phosphorus (µg P L^{-1})	902.5 ± 267.1	1 696 ± 411	275.7 ± 12.0
PO_4 (µg P L^{-1})	259.6 ± 113.5	413.1 ± 138.9	95.1 ± 12.6
SEDIMENT POREWATER			
Total organic carbon (% DW)	1.10 ± 0.52	0.85 ± 0.10	0.40 ± 0.12
Total carbon (% DW)	9.78 ± 0.45	8.02 ± 0.31	8.06 ± 0.16
Total phosphorus (mg P g^{-1})	0.42 ± 0.02	0.33 ± 0.02	0.49 ± 0.04

7.3.3.6 DOC leachate from wrack

Significantly different amounts of total DOC were leached by different wrack types (Table 7.6). Fresh algae (*Laurencia* sp.) leached about four times the amount of DOC released by fresh *P. sinuosa* leaves, six times that released by *A. antarctica* leaves, more than 11 times that released by *A. antarctica* stems and more than 90 times that released by the fine fraction of natural wrack accumulations.

The recovery of DOC after fractionation into humic, slightly humic and non-humic fractions was good, between 78 and 94% (Table 7.6). Non-humic material was dominant in all wrack types (37 – 68%) and was overwhelmingly comprised of glucose. The humic fraction contributed between 17 – 31% to the total DOC and the lowest contributing organic carbon component was the slightly humic fraction (4 – 11%). The proportion of each fraction significantly varied with wrack type, but this was dependent on the type of DOC (Table 7.6). The amounts of humics in *A. antarctica* leaves and Laurencia sp. were similar to those of *P. sinuosa* as well as those of *A. antarctica* stems and the fine fraction, whereas the latter two had a higher proportion of humics than *P. sinuosa*. No significant differences were found for the slightly humic fraction between the wrack types. For the non-humic fraction the proportions of *P. sinuosa* were the highest, followed by those of *A. antarctica* materials and *Laurencia* sp and the fine fraction had the lowest proportions.

Table 7.6 Dissolved organic carbon leached from different source materials determined through resin separation. Shared subscript letters indicate no significant difference in the amount leached by different wrack types.

	DISSOLVED ORGANIC CARBON RELEASED OVER 16 HR (mg kg^{-1} PLANT MATERIAL) (%)				DOC RECOVERY BY RESINS
	TOTAL	HUMICS	SLIGHTLY HUMICS	NON-HUMICS	
Fresh *Posidonia* leaves	1 724 ± 76 $_a$	298 ± 14	138 ± 6	1173 ± 58	93%
		17% $_a$	8% $_a$	68% $_a$	
Fresh *Amphibolis* leaves	1 102 ± 24 b	284 ± 26	48 ± 4	676 ± 21	91%
		26% $_{ab}$	4% $_a$	61% $_b$	
Fresh *Amphibolis* stems	588 ± 31 $_c$	180 ± 13	58 ± 4	312 ± 29	94%
		31% $_b$	10% $_a$	53% $_b$	
Fresh *Laurencia* algae	6 749 ± 278 $_d$	1 998 ± 64	675 ± 95	3 554 ± 213	93%
		30% $_{ab}$	10% $_a$	53% $_b$	
Fine fraction of natural wrack accumulation	74 ± 1 $_e$	22 ± 3	8 ± 5	27 ± 1	78%
		30 % $_b$	11 % $_a$	37% $_c$	

There was no significant reduction in the amount of DOC leached from *P. sinuosa* leaves after one week of degradation (Table 7.7). With two weeks aging on the beach the amount of DOC leached by *P. sinuosa* was significantly reduced, to 9% of that leached from fresh material, and by four weeks aging the amount again was significantly reduced, to only 5%. The non-humic fraction was the most dominant in all ages (48 – 67%). The humic fraction contributed between 16 – 27% to the total DOC and the lowest contributing organic carbon component was the slightly humic fraction (11 – 17 %). Differences in the proportions of the DOC fractions with aging were dependent on the type of DOC fraction (Table 7.7). In the humic fraction the proportion of oen week aged *P. sinuosa* was not significantly different from the two weeks and four weeks aged *P. sinousa*, whereas the latter had a lower humic proportion than the 2 weeks old. Fresh *P. sinuosa* had the lowest proportion of humics. No significant differences were found in the proportions of the slightly humic fraction for the different ages. For fresh and four weeks old *P. sinuosa* the proportions of non-humics were significantly higher than those of the one and two weeks old.

Table 7.7 Dissolved organic carbon composition of *Posidonia sinuosa* of different ages determined through resin separation.

	DISSOLVED ORGANIC CARBON RELEASE OVER 16 HR (mg kg^{-1} PLANT MATERIAL) (%)				DOC RECOVERY BY RESINS
	TOTAL	HUMICS	SLIGHTLY HUMICS	NON-HUMICS	
Fresh *Posidonia* leaves	1 419 ± 93 $_{a}$	223 ± 18	181 ± 17	855 ± 45	89%
		16% $_{a}$	13% $_{a}$	60% $_{a}$	
1 week old *Posidonia* leaves	1 627 ± 192 $_{a}$	417 ± 13	277 ± 32	783 ± 120	91%
		26% $_{bc}$	17% $_{a}$	48% $_{b}$	
2 weeks old *Posidonia* leaves	133 ± 17 $_{b}$	36 ± 4	19 ± 4	67 ± 7	91%
		27% $_{b}$	14% $_{a}$	50% $_{b}$	
4 weeks old *Posidonia* leaves	67 ± 2 $_{c}$	12 ± 1	7.2 ± 0.2	67 ± 1	96%
		18% $_{c}$	11% $_{a}$	67% $_{a}$	

There was no significant effect of scraping leaves prior to incubation on the total amount of DOC leached from *P. sinuosa* after 14 days (scraped: 1830 ± 12 mg kg^{-1}, unscraped: 1938 ± 206 mg kg^{-1}, Table 7.8). However, there were significant differences in daily leachate amount over the time course, but only at a number of time periods (Figure 7.11, Table 7.8). After 1 d incubation the amount of DOC leached from scraped *P. sinuosa* was significantly higher (3x) than unscraped leaves, and at 4 - 5 days incubation the amount of DOC leached from unscraped leaves was two times higher than scraped leaves. For both treatments 93 – 95% of the total DOC was released after the seven-day incubation

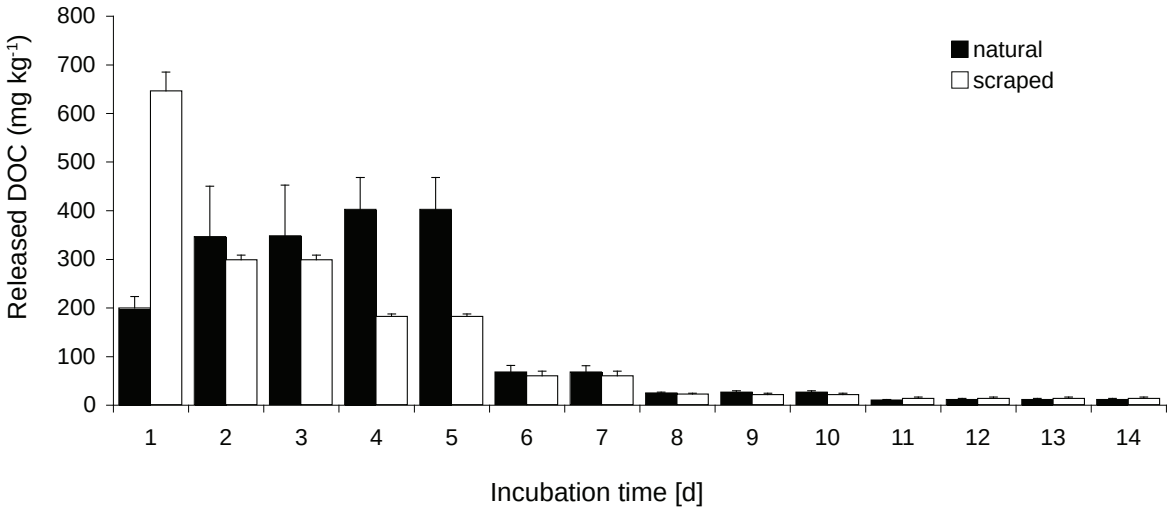

Figure 7.11 Average daily DOC release from *P. sinuosa* leaves during the 14-day incubation.

Table 7.8 Results of ANOVA tests for significant differences in total DOC leachate concentrations among different wrack material, different ages of *P. sinuosa* leaf and between scaped and unscraped leaf.

	DF	F	P		DF	F	P
EXPERIMENT 1, WRACK TYPE				EXPERIMENT 1, WRACK TYPE X DOC FRACTION			
wrack type	4	1909.16	<0.001	wrack type	4	1.38	0.255
residuals	15			fraction	2	253.7	<0.001
total	19			wrack type x fraction	8	6.36	<0.001
				residuals	45		
				total	59		
EXPERIMENT 2, AGE				EXPERIMENT 2, AGE X DOC FRACTION			
age	3	290.19	<0.001	age	3	0.43	0.731
residuals	8			fraction	2	328.43	<0.001
total	11			age x fraction	6	9.26	<0.001
				residuals	24		
				total	35		
EXPERIMENT 3, SCRAPING				EXPERIMENT 3, SCRAPING X TIME			
scraping	1	0.17	0.701	scraping	1	0.23	0.636
residuals	4			time	13	130.21	<0.001
total	5			scraping x time	13	3.63	<0.001
				residuals	56		
				total	83		

7.3.3.7 Bioavailability of organic carbon leachate from wrack for heterotrophic bacteria

The bioavailability of *Laurencia* sp. and fresh *P. sinuosa* leachates were tested with the same bacterial inoculum and an average of 1.03×10^7 cells were added to each flask (Table 7.9). For leachates of both *A. antarctica* material a different bacterial inoculum was used but approximately the same number of cells (1.12×10^7) were added at the beginning. The leachate of the fine fraction was incubated with a third inoculum and here only 4.90×10^6 cells were added.

The bacterial abundance over a 24 hr period in all leachates of the different wrack types is plotted in Figure 7.12 together with that in the water blanks that were incubated at the same time. To calculate the growth rate, linear equations were fitted on the data with an R^2 ranging between 0.47 and 0.99 (Table 7.9). After 18 hr incubation the cell concentration for the fine fraction declined therefore only data till 18 hr were used for the linear regression. For those treatments with a significant linear regression the proportion of the bacterial growth due to the DOC leachate ranged from 93 to 100% (Table 7.9).

The leachates of *Laurencia* sp. had the highest DOC concentration at the beginning of the incubation (7585 ± 1066 mg L^{-1}), followed by the fresh *P. sinuosa* leachates (1983 ± 46 mg L^{-1}) (Table 7.8). The DOC concentration in the leachates of *A. antarctica* leaves and stems was about 100 times lower (67 ± 8 mg L^{-1} and 94 ± 14 mg L^{-1}). The leachates of the fine fraction had the lowest DOC concentration (10 ± 2 mg L^{-1}).

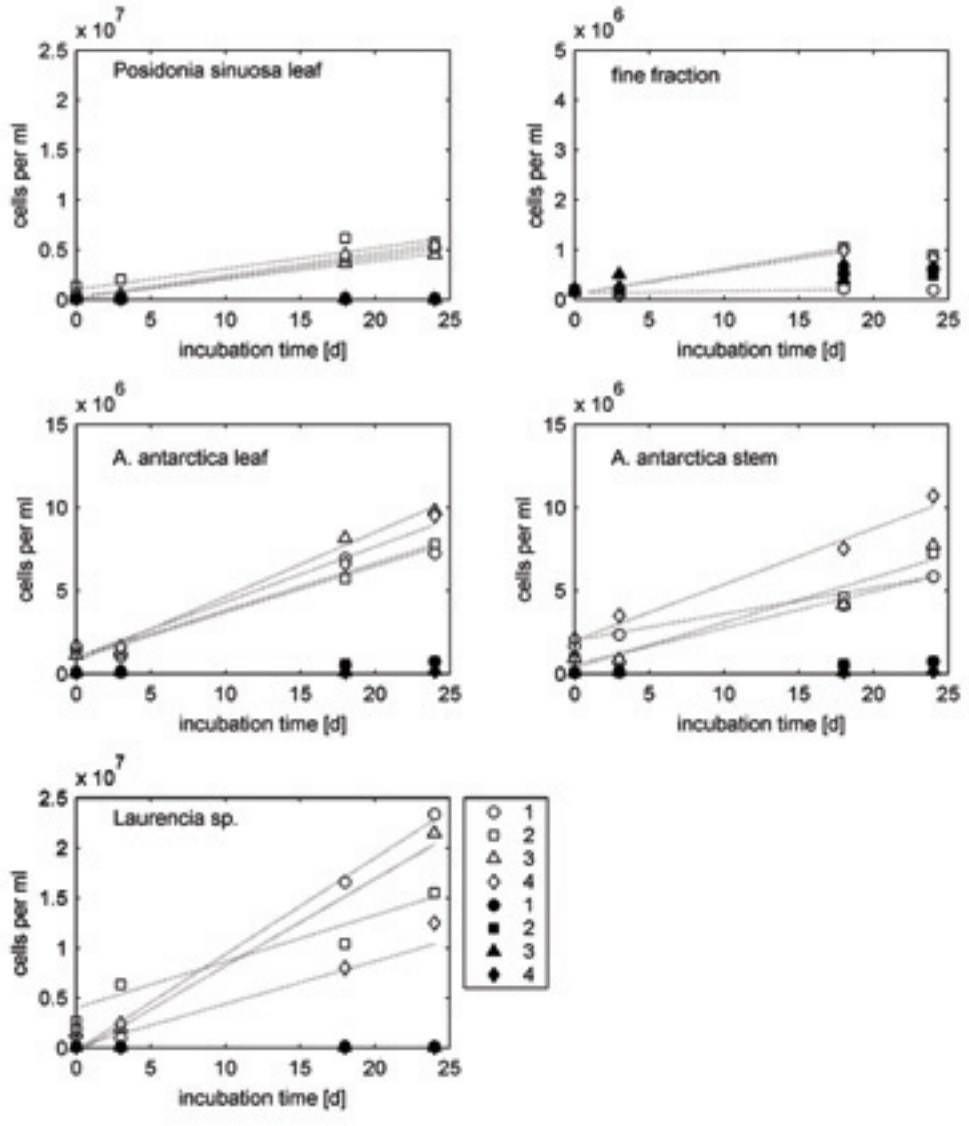

Figure 7.12 Abundance of heterotrophic bacteria in DOC leachates of the different wrack types. Filled symbols = leachate, open symbols - DI water.

Table 7.9 Linear equation fitted to changes in bacterial abundance over time in leachates from different wrack types.

ADDED	BLANK	FITTED LINEAR	R^2	p	FLASK	DOC START	FITTED LINEAR	R^2	p
BACTERIA		EQUATION				[mg L^{-1}]	EQUATION		
1.03E+07	water 1	-1367x + 106674	0.834	0.087	Algae 1	9207	964360x -295786	0.99	0.007
	water 2	-497x + 90031	0.686	0.172	Algae 2	5482	463226x + 4000000	0.94	0.031
	water 3	-1154x + 97426	0.994	0.003	Algae 3	9622	869871x - 503825	0.99	0.015
	water 4	-759x + 90195	0.776	0.119	Algae 4	6027	427770x + 100000	0.97	0.060
					Pos 1	2072	209009x + 83276	0.99	0.006
					Pos 2	1977	208012x + 1000000	0.92	0.038
					Pos 3	2027	179456x + 282367	0.99	0.007
					Pos 4	1857	220620x + 218153	0.98	0.011
1.12E+07	water 1	27657x + 50467	0.995	0.003	A. stem 1	84	283253x + 985061	0.95	0.027
	water 2	28626x + 40834	0.995	0.002	A. stem 2	46	278306x + 908091	0.98	0.010
	water 3	3173x + 78919	0.688	0.038	A. stem 3	75	388081x + 747539	0.99	0.005
	water 4	1783x + 85430	0.534	0.269	A. stem 4	63	331568x + 1000000	0.97	0.011
					A. leaf 1	135	159094x + 2000000	0.97	0.015
					A. leaf 2	87	219803x + 547505	0.96	0.018
					A. leaf 3	83	270690x + 367933	0.93	0.038
					A. leaf 4	72	336357x + 2000000	0.98	0.009

4.90E+06	water 1	19249x + 156820	0.996	0.002	Fine 1	11	4535x + 122026	0.46	0.526
	water 2	17031x + 172537	0.806	0.102	Fine 2	8	50795x + 112243	0.97	0.116
	water 3	88219x + 300487	0.325	0.430					
	water 4	22223x + 185847	0.927	0.037	Fine 4	6	47117x + 113238	0.94	0.156

For the bioavailability test on fresh *P. sinuosa* leachates, an average of 1.03 x 10^7 cells were added to each flask and about 4.90 x 10^6 cells of a different bacterial inoculum were added to the one-month old *P. sinuosa* (Table 7.10).

The bacterial growth over a 24 hr period for both ages is plotted in Figure 7.13 together with the bacterial growth in the water blanks that were incubated at the same time. To calculate the growth rate linear equations were fitted on the data with an R^2 ranging between 0.19 and 0.99 (Table 7.10). After 18 hr incubation the cell concentration for the 1-month old *P. sinuosa* declined, therefore only data up to 18 hr were used for the linear regression. For those treatments with a significant linear regression, the proportion of the bacterial growth due to the DOC leachate is listed in Table 7.11.

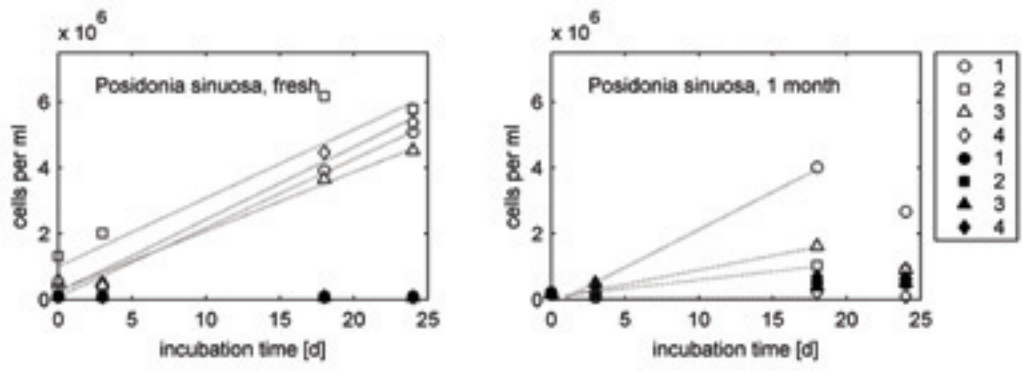

Figure 7.13 Growth of heterotrophic bacteria added to DOC leachates of different aged *P. sinuosa*. Filled symbols = leachate, open symbols - DI water.

Table 7.10 Linear equation fitted to changes in bacterial abundance over time in leachates from *P. sinuosa* wrack of different ages.

ADDED	BLANK	FITTED LINEAR	R^2	p	FLASK	DOC START	FITTED LINEAR	R^2	p
BACTERIA		EQUATION				[mg L^{-1}]	EQUATION		
1.03E+07	water 1	-1367x + 106674	0.834	0.087	Pos 1	2072	209009x + 83276	0.99	0.006
	water 2	-497x + 90031	0.686	0.172	Pos 2	1977	208012x + 1000000	0.92	0.038

	water 3	-1154x + 97426	0.994	0.003	Pos 3	2027	179456x + 282367	0.99	0.007
	water 4	-759x + 90195	0.776	0.119	Pos 4	1857	220620x + 218153	0.98	0.011
4.90E+06	water 1	19249x + 156820	0.996	0.002	P. old 1	12	228772x -167965	0.97	0.118
	water 2	17031x + 172537	0.806	0.102	P. old 2	8	51389x + 78937	0.93	0.167
	water 3	88219x + 300487	0.325	0.430	P. old 3	11	86769x + 28663	0.96	0.133
	water 4	22223x + 185847	0.927	0.037	P. old 4	16	2823x + 14901	0.19	0.712

Table 7.11 Percentage of bacterial growth based on DOC leachate for treatments with a significant linear relationship between incubation time and bacterial abundance.

TREATMENT	CELL ABUNDANCE AFTER 24 H	% OF GROWTH DUE TO LEACHATE
Algae 1	2.28E+07	100
Algae 2	1.51E+07	100
Algae 3	2.04E+07	100
Algae 4	linear regression not significant	
Posidonia leaf 1	5.10E+06	100
Posidonia leaf 2	5.99E+06	100
Posidonia leaf 3	4.59E+06	100.0
Posidonia leaf 4	5.51E+06	100
Amphibolis stem 1	7.78E+06	93
Amphibolis stem 2	7.59E+06	93
Amphibolis stem 3	1.01E+07	95
Amphibolis stem 4	8.96E+06	94
Amphibolis leaf 1	5.82E+06	91
Amphibolis leaf 2	5.82E+06	91
Amphibolis leaf 3	6.86E+06	92
Amphibolis leaf 4	1.01E+07	95
Fine particulates 1	linear regression not significant	
Fine particulates 2	linear regression not significant	
Fine particulates 3	linear regression not significant	
Fine particulates 4	linear regression not significant	

Posidonia leaf old 1	linear regression not significant	
Posidonia leaf old 2	linear regression not significant	
Posidonia leaf old 3	linear regression not significant	
Posidonia leaf old 4	linear regression not significant	

The mean cell biovolume ranged from 0.118 to 0.216 µm³ for the different source materials, with an average of 0.16 µm³ (Table 7.12). Borsheim et al. (1990) found a mean biovolume of 0.127µm³ for bacteria derived from naturally seawater samples after 24 hours incubation. The average carbon content per cell varied between 25 and 39 fg for the different source materials with an average of 31 fg carbon cell^{-1} (Table 7.12). The bacterial carbon production over the 24 hours incubation is plotted for four different wrack types (Figure 7.14).

Table 7.12 Biovolume and carbon content per cell of bacterial assemblages grown on the leachates of different wrack types after 24 hr incubation.

	SOURCE MATERIALS				
	P.sinuosa leaves	*Laurencia sp*	*A. antarctica* stems	*A. antarctica* leaves	Mean of all sources
biovolume [µm³]	0.118 ± 0.010	0.127 ± 0.010	0.216 ± 0.016	0.184 ± 0.011	0.161 ± 0.007
Carbon content [fg C cell-1]	25 ± 2	27 ± 1	39 ± 2	35 ± 2	31 ± 2

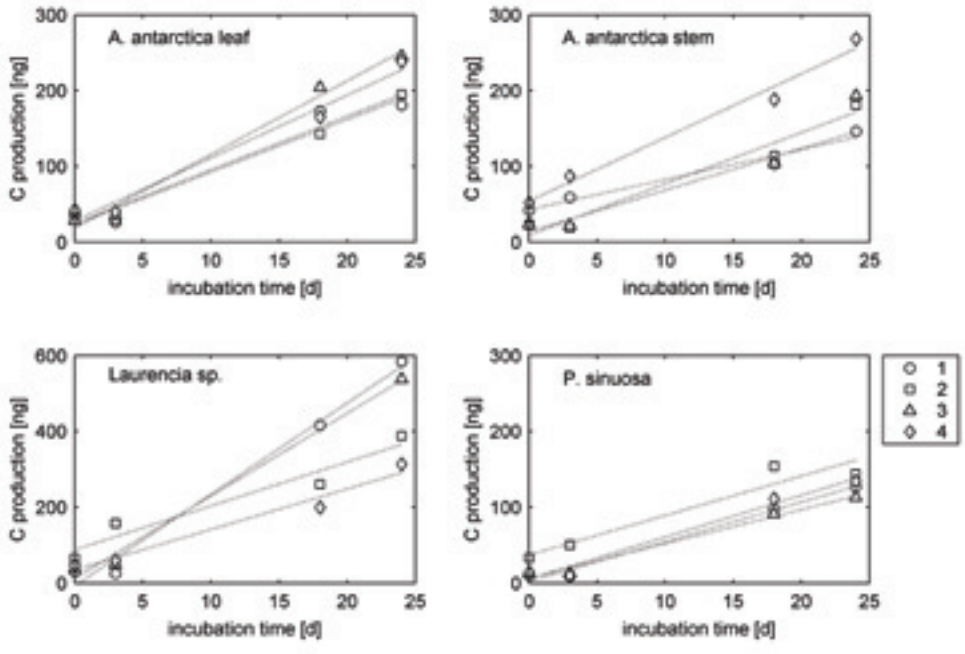

Figure 7.14 Bacterial carbon production during 24 h incubation in leachate from different types of wrack. Symbols indicate replicate samples.

7.3.4 Significance of results

Heterotrophic bacteria, the organisms that generate H_2S, were present throughout the large wrack accumulations and underlying sediments. Assuming those bacteria had sufficient carbon and the environmental conditions (i.e. redox potential) were appropriate, then H_2S production could occur throughout the accumulations.

With respect to redox potential, information presented in Section 7.1 indicated that the saturated and sediment zones of large wrack accumulations were typically anoxic, and it is these zones where H_2S production will occur. In oxygenated zones of the large wrack accumulations, such as the surface and mid zone, aerobic decomposition would occur with CO_2 produced as the by-product. However, H_2S may accumulate throughout the wrack accumulations if sufficient production from the saturated zone can diffuse upwards.

With respect to carbon supply, there were high amounts of dissolved organic carbon (up to 50 mg L^{-1}) in the saturated zone that could fuel bacterial activity. The leaching experiments showed that high amounts of organic carbon do leach out of fresh wrack material, with >60% a highly labile fraction which is bio-available to heterotrophic bacteria. With aging for one month, the amount that leaches out of *P. sinuosa* reduced dramatically, down to 51 mg kg^{-1}. It is unlikely that carbon is limiting bacterial activity in wrack accumulations. Thus, freshly deposited wrack is likely a major contributor to the abundant DOC available within the saturated zone, though aged wrack can still contribute DOC, albeit at a much lower rate.

The leaching of organic carbon and physical breakdown of wrack also influences the sediment. In large accumulations, larger and older piles had more elevated, possibly resulting in H_2S formation. H_2S production is likely to be greatest in banks with fresh wrack and deep enough to contain a saturated layer of wrack.

In addition to the implications for H_2S production, the leaching experiments indicate that wrack can supply large amounts of DOC to beaches, which can drive food webs. Taking into account the amount of DOC leached from the different types of wrack, from 0.8 – 2.8 kg of DOC m^{-2} is likely to be released, though the extreme estimate is as high as 8.2 kg m^{-2}. These estimates are for small accumulations, typical of natural beaches and demonstrate the importance of wrack for beach ecology.

7.4 Gas production in beach wrack

7.4.1 Objectives

The investigations summarized in Sections 7.1 to 7.3 indicate that the conditions required for both aerobic and anaerobic decomposition of wrack occur in wrack accumulations on Geographe Bay beaches. Furthermore, the conditions required for the production of H_2S commonly occur in larger wrack accumulations with saturated zones. However, some key aspects of the H_2S production cycle remain unclear for Geographe Bay beaches, including:

- the rates of H_2S production in typical wrack accumulations;
- the relationships between wrack accumulation characteristics and gas production;
- whether the H_2S produced from wrack is dependent on the presence of the wrack as a carbon supply and/or as barrier to oxygen diffusion. It is possible that even in the absence of wrack, sufficient carbon has been accumulated in the beach sand to drive H_2S production.

Management of H_2S requires an understanding of what types of accumulations are likely to be most important in generating the gas and whether management of H_2S requires management of the accumulations alone or also the underlying sediments.

The objectives of the gas production study were to:

- quantify the flux of hydrogen sulfide (H_2S) and carbon dioxide (CO_2) from wrack into the atmosphere;
- determine the relationship between flux rates, wrack height and wrack age;
- determine the spatial variability of the gas fluxes; and,
- through laboratory experiments, investigate the key processors driving H_2S and CO_2 production in wrack accumulations.

7.4.2 Materials and methods

Two approaches were used to address the four aims. Aims (a)-(c) were addressed through field measurements of gas fluxes from a range of wrack accumulations on Geographe Bay beaches. Aim (d) was addressed through a controlled laboratory experiment.

7.4.2.1 Field measurements of gas production

The fluxes of H_2S and CO_2 were measured during two field visits on 23rd - 26th July 2008 (Trip 1) and 16th September 2008 (Trip 2). On Trip 1, gas fluxes were measured at three sites with large wrack accumulations of different size and age (Big Old: Siesta Park; Big New: Guerin St; Small New: Abbey Beach). At each site four replicate measures were taken at the surface of each wrack pile. These were in the same locations as the replicates where wrack composition (Section 6.4), physical characteristics (Section 7.1) and biogeochemistry (Section 7.3) were taken. On Trip 2, gas fluxes were measured at 10 locations at Siesta Park (Big Old) beach. No additional measures were taken during Trip 2.

Hydrogen sulfide gas flux measurements were made using a custom acrylic gas flux chamber that encloses a wrack area of 0.0269 m^2 (Figure 7.15). The flux chamber was inserted into the wrack leaving a 1.5 L headspace for gas accumulation. Initial concentrations of H_2S were purged and then the gas was allowed to accumulate in the headspace for 30 – 60 minutes (soak time). The accumulated gas was recirculated through a 25 mL midget impinger tube filled with zinc acetate trapping solution [*Balasubramanian and Kumar*, 1990] until > 99% of the sulfide was precipitated. The trapped sulfide was then analyzed using the methylene blue method [*Lodge*, 1989]. Fluxes were calculated as:

$$F_{H_2S} = \frac{C_S V}{AMt} \qquad \textbf{Eq. 7-3}$$

where F_{H2S} is the flux of H_2S gas (mmol m^{-2} min^{-1}), C_s is the measured concentration of sulfide trapped in the impinger tube (mg L^{-1}), V is the volume of the impinger tube (0.025 L), A is the surface area of wrack enclosed by the flux chamber (0.0269 m^2), M is the atomic mass of sulfur (32.06 g) and t is the soak time (min). During the sampling periods, occasional field blanks and control samples (from a certified 10 ppm H_2S gas cylinder) were collected for quality control and sulfide trapping efficiency checks. The minimum detection limit for the method was C_s = 46.2 mg L^{-1}, which equates to 4.46 x 10^{-2} mmol H_2S m^{-2} min^{-1} for a 30 minute soak time and 8.92 mmol H_2S m^{-2} min^{-1} for a soak time of 60 minutes.

The flux of CO_2 gas was measured using a LiCor® Li-6400XT portable photosynthesis system with a 6400-09 soil CO_2 flux chamber (Figure 7.15). Briefly, the instrument works by first scrubbing the flux chamber of CO_2 by recirculating the volume through a soda lime column. The accumulation rate of the CO_2 in the chamber is measured by an integral Infrared Gas Analyzer. The flux of CO_2 is then calculated from the accumulation rate and the area of the soil flux chamber (71.6 cm^2). The measurements with the LiCor instrument are rapid and allowed for multiple readings at each measurement location. In general, the number of measurements taken at any particular site depended on the variability in the flux. In contrast, only one H_2S flux measure was performed at each site due to the long soak times required to achieve detectable levels of sulfide in the impinger tubes.

Figure 7.15 H_2S flux chamber (right) and LiCor soil CO_2 flux chamber (left).

During Trip 1, the depth profiles of internal H_2S gas concentration were obtained by inserting a plastic tube into the wrack and pumping 1.5 L of pore space gases through the midget impinger tubes. Absolute concentrations from these measurements could not be determined because 1) the air pressure and temperature within the pore spaces was not measured and 2) the trapping capacity of the zinc acetate solution was exceeded when concentration was >10 ppm. However, the results provided qualitative measures that aided in understanding the gas production and flux processes.

On Trip 2, profiles of gases at the flux locations were obtained using a Geotech GA2000 portable gas analyzer. The gas analyzer measures CO_2 and methane (CH_4) using an infrared detector and oxygen using an internal electrochemical cell. The analyzer was equipped with a hydrogen sulfide sensor that malfunctioned during the trip. Therefore, no H_2S profile data were available from Trip 2.

7.4.2.2 Laboratory experiment

To investigate the underlying processes driving H_2S generation, a laboratory experiment was conducted testing the hypothesis that organic carbon supply and the barrier to diffusion that wrack accumulations provide do not effect H_2S fluxes from saturated beach sediments. A closed mesocosm experiment was established with four treatments: Control (beach sediment only); + Barrier (beach sediment plus plastic wrack which mimicked the physical barrier that wrack would represent to gas diffusion without offering a source of DOC); + DOC (beach sediments plus dissolved organic carbon in the form of treacle, to test whether the sediments require carbon loading to produce H_2S); and, + Barrier + DOC (beach sediment plus seagrass, which includes both the carbon loading and diffusive barrier effects of seagrass wrack), with five replicates of each treatment. The experiment ran for 11 days.

Sediments were collected from Port Geographe beach on 4 September, 2009 (one day prior to putting into the experimental array). Sediment cores were taken to 10 cm depth and sieved through an 8.0 mm sieve to remove large shells and other debris. These were then homogenized in the laboratory. Fresh *P. sinuosa* seagrass was collected from Port Geographe location also on 4 September, then stored at 4°C, until placed into the experimental array.

Clear plastic Perspex cylinders, sealed at both ends, were used for the mesocosms (Figure 7.16). Mesocosms were filled with sediment to 15 cm, then approximately 2.4 L artificial seawater added, leaving 0.0017m^3 headspace. In '+ barrier' treatments, 62 leaves of plastic wrack were added (equal in biomass to seagrass in '+ barrier + DOC treatments'). In '+ DOC' treatments 0.49, 0.07, 0.043 and 0.023 g of treacle were added on days 3, 6, 8 and 11 respectively. Treacle additions matched amounts of DOC leaching from equivalent biomass of seagrass (see Figure 7.11). In '+ barrier + DOC' 180 g of fresh *P. sinousa* leaves were added. Pure (99.9 %) nitrogen bag reservoirs with valves were attached to the mesocosms. These were opened when gas samples were extracted to replace air removed from the headspace.

Water samples were collected at the start and end of the experiment for the determination of dissolved oxygen (D.O.) and redox conditions, at the water surface and sediment-water interface. The redox condition was recorded with a TPS 90-FLMV probe and dissolved oxygen (% saturation) with a OxyGuard Polaris Dissolved Oxygen meter. Once an anoxic layer had formed on the sediment surface (this occurred on day 5), a syringe was inserted into the headspace through a rubber stopper, and 80 mL of air were collected for H_2S determination. The syringe was connected to a Jerome® 631-X™ Hydrogen Sulfide Analyzer, allowing immediate analysis of H_2S.

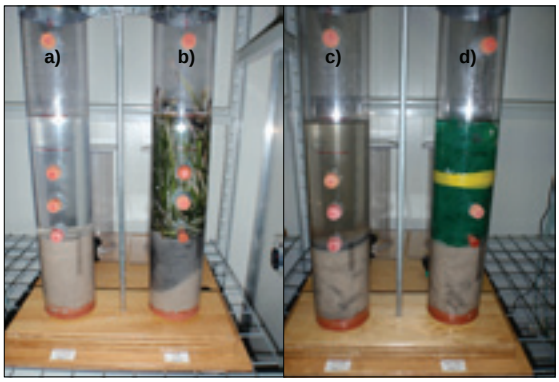

Figure 7.16 Treatments used in the laboratory mesocosm experiment to test the whether the DOC supply and the diffusive barrier created by wrack, significantly affect H_2S production. From left to right: Control; + barrier + DOC; + DOC; + barrier.

7.4.3 Results

7.4.3.1 Field measurements of gas fluxes

Only two measured fluxes of H_2S gas on Trip 1 were above the detection limit, both at Abbey Beach, in the Small New wrack accumulations (Figure 7.17 and Table 7.13). The mean measured fluxes of CO_2 on Trip 1 ranged from a high of 31.8 µmol m^{-2} s^{-1} at Big New (Guerin St, replicate 4) to a low of 1.52 µmol m^{-2} s^{-1} at Big Old (Siesta Park, replicate 4, Figure 7.17). In general, the highest fluxes were measured at Big New (Guerin St) and the lowest fluxes were measured at Big Old (Siesta Park) accumulations.

CO_2 fluxes were spatially variable across all sites and beaches (Figure 7.18), and also temporally variable at some individual sites. For example, both Small New (Abbey Beach, replicate 2) and Big New (Guerin St, replicate 4) demonstrated high variability, and thus a wide range of measured values. In both cases, the variability was related to systematic changes in the flux over time rather than stochastic variability (Figure 7.19).

The mean CO_2 fluxes at Old Big accumulations at Siesta Park (SP) in Trip 2 ranged from 0.490 µmol m^{-2} s^{-1} (SP4) to 27.3 µmol m^{-2} s^{-1} at SP6a (Figure 7.19). At replicates, SP6, SP7 and SP8, additional flux measures were made after moving the soil CO_2 flux chamber approximately 10 cm over from the original location. These measures were designated SP6a, SP7a and SP8a respectively. The difference between the measured fluxes at SP6/SP6a and SP8/SP8a indicated that the spatial heterogeneity of the beach wrack system is very high (Figure 7.19).

Table 7.13 Depth of the wrack pile and the H_2S flux at the Siesta Park (SP), Abbey Beach (AB) and Guerin St (GB) sites measured on Trip 1 (24^{th} -26^{th} July 2008). Fluxes below the detection limit are designated bdl.

SITE & REPLICATE	WRACK DEPTH SURFACE TO BOTTOM OF SATURATED ZONE (M)	H_2S FLUX µmole m^{-2} min^{-1}
Big Old 1	1.0	bdl
Big Old 2	1.0	bdl
Big Old 3	1.0	bdl
Big Old 4	1.7	bdl
Big New 1	1.25	bdl
Big New 2	1.5	bdl
Big New 3	1.0	bdl
Big New 4	1.25	bdl
Small New 1	0.5	0.036
Small New 2	0.6	0.392
Small New 3	0.5	bdl
Small New 4	0.5	bdl

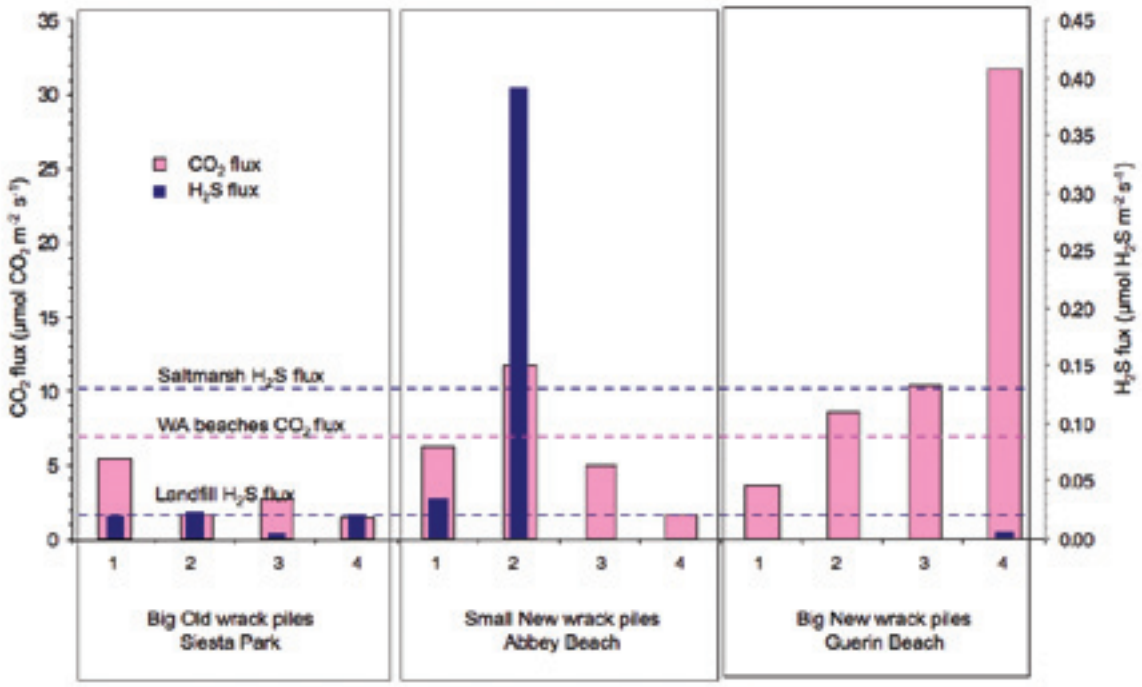

Figure 7.17 Fluxes of H_2S (blue, right scale) and CO_2 (pink bars, left scale) from the wrack at four replicates on three beaches. The upper and lower horizontal dashed lines indicate the mean values for fluxes of H_2S measured at a salt marsh [*Steudler and Peterson*, 1984] and a construction debris landfill [*Eun et al.,* 2007] respectively. The horizontal solid grey line indicates the mean flux of CO_2 measured at Western Australia beaches [*Coupland et al.*, 2007].

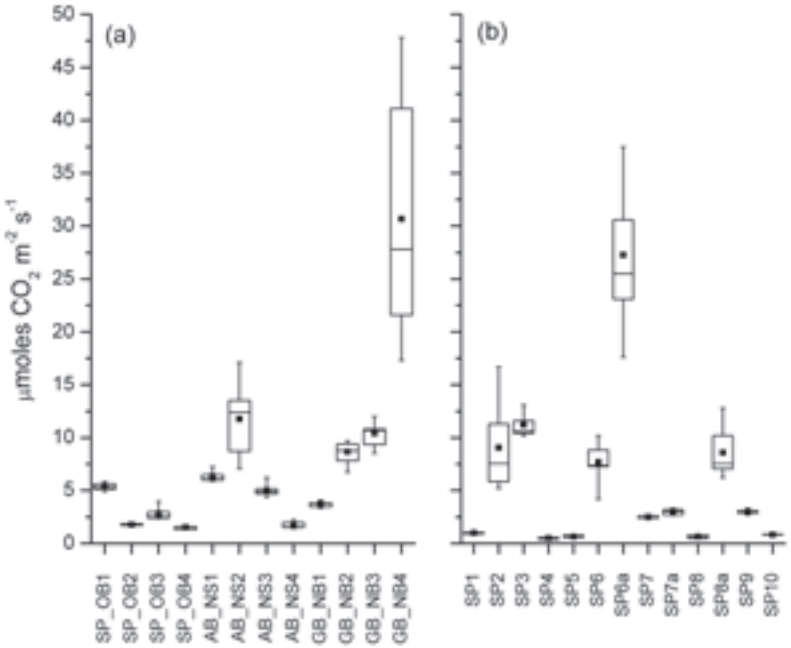

Figure 7.18 Box and whisker plots of the repeated CO_2 flux measures at each site for a) Siesta Park (SP), Abbey Beach (AB) and Guerin St (GB) during Trip 1 on 23rd – 26th July 2008 and b) for 10 sites at Siesta Park on 16th September 2008. The CO_2 fluxes exhibit both high spatial variability across all replicates, and high temporal variability at some replicates (e.g. AB_NS2, GB_NB4, SP2 and SP6a).

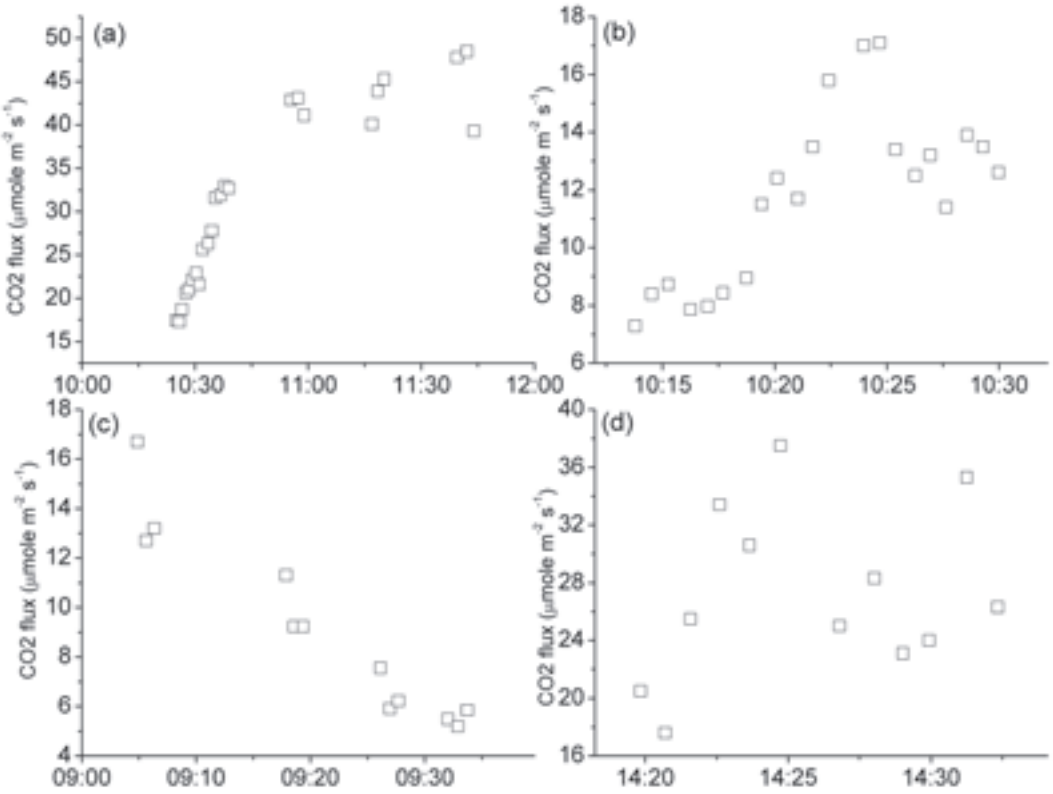

Figure 7.19 Time series of CO_2 flux measurements during Trip 1 at (a) Guerin St replicate 4, (b) Abbey Beach replicate 2, and during Trip 2 (c) Siesta Park replicate 2 and (d) Siesta Park replicate 6a. These four replicates exhibited temporal variability in measured flux that was not observed at most of the other sites. In (a), (b) and (c), the variability appears to be due transients in the flux, while in (c), the variability appears to be stochastic.

The profiles of H_2S concentration at the Big Old accumulations on Trip 1 yielded measurable concentrations at replicates 1, 2 and 3 (Figure 7.20). In all three cases, the H_2S concentration increased sharply just above the saturation zone (waterlogged wrack). The reported concentrations of 10 ppm are minimal because the trapping capacity of the zinc acetate solution in the impingers was exceeded at 10 ppm. There is an unusually high reading (>10 ppm) near the surface at replicate 3 of the Big Old site. This reading may be due to a hotspot of organic matter degradation and localized H_2S production within the wrack. Alternatively, the high reading may be due to tapping into a preferential transport pathway towards the surface of the wrack for H_2S produced in the saturated zone. All readings from replicate 4 at the Big Old site were below the detection limit. At the New Big site, the concentration near the saturated zone at replicate 1 was 1.5 ppm. All other concentrations at Big New and Small New sites were below the detection limit.

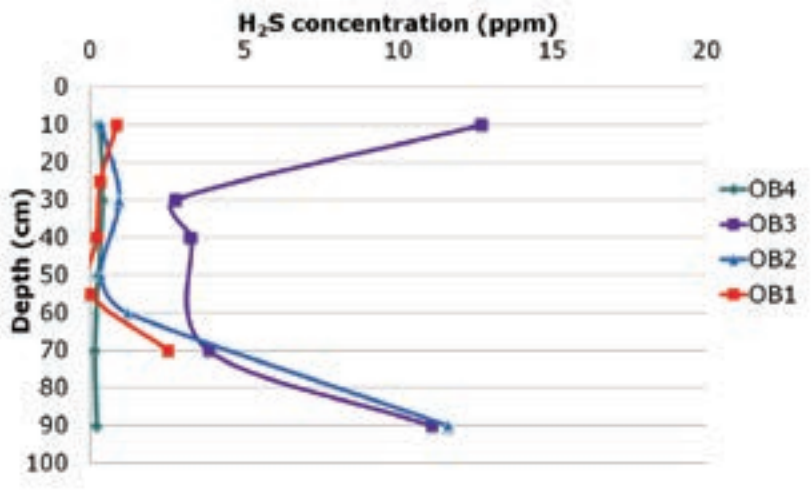

Figure 7.20 Pore space H_2S concentration profiles at Siesta Park on Trip 1 (24th July 2008). Replicates OB1, OB2 and OB3 all demonstrate sharp increases in concentration just above the saturation zone. Values >10 ppm are minima since the trapping capacity of the zinc acetate solution in the impingers was exceeded. The high reading near the surface at replicate OB3 is anomalous and may reflect an internal hotspot of biogeochemical activity in the seagrass wrack pile, or the presence of a preferential H_2S transport pathway through the wrack pile from the saturated zone (i.e. a sulfide chimney).

At replicate SP3, O_2 was less than 10% at 0.1 m below the wrack surface and was negligible by 0.4 m below the surface. Concentrations of CO_2 and CH_4 were extremely high at 0.1 m below the surface and reached 42.9% and 39.9% of the gas volume respectively at 1.0 m below the wrack surface. At SP8, the decrease in O_2 was more gradual as concentration fell from 19.9% at 0.1 m to 1.9% at 0.85 m below the surface. Meanwhile, CO_2 increased from 2.9% to 20.3% and CH_4 increased from below detection limit to 7.5%. There was a sharp decrease in O_2 and a sharp increase in CO_2 and CH_4 between 0.7 - 0.8 m. The replicates SP3 and SP8 were the only two measured on Trip 2 that had wrack piles greater then 1 m deep. High concentrations of CO_2 were found in the wrack and O_2 was depleted with respect to the atmosphere. However, the CO_2 increases and O_2 decreases were not as large as at SP3 and SP8. Methane was not detectable in the wrack at the other replicates.

7.4.3.2 Laboratory tests of H_2S production

Dissolved Oxygen and Redox

All treatments showed a significant decline in the saturation of dissolved oxygen at the water column surface and at the sediment-water interface by the end of the 11-day experimental period (Figure 7.21) (Two-way ANOVA, $p < 0.05$). The '+ DOC' and '+ Barrier + DOC' treatments had lower D.O. saturation than the other treatments.

Redox potential at the water column surface (Figure 7.21) declined between the start and the end of the experiment for all treatments (Two-way ANOVA, $p < 0.05$). Post-hoc testing indicated that '+ DOC' and '+ Barrier + DOC' treatments were significantly lower than the other treatments. Trends and levels in Redox at the sediment/water interface were similar to those at the water surface, except that Redox levels in the Control were higher compared to the + Barrier treatments.

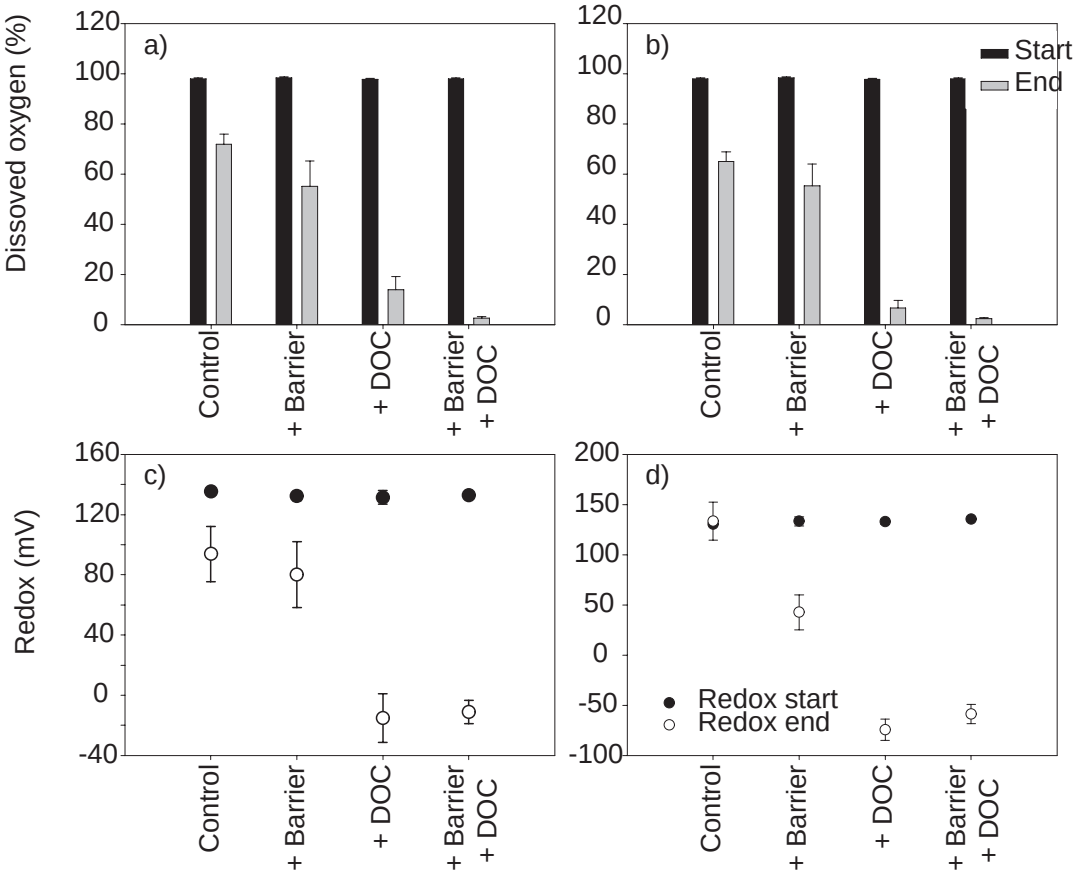

Figure 7.21 The effect of different wrack and carbon loading treatments on dissolved oxygen saturation and redox potential at the surface of the water column and at the sediment water interface in experimental mesocosms.

Carbon dioxide concentrations (% by volume) were greatest in the treatment with a layer of real seagrass over sediment ('+ Barrier + DOC'), and increased with duration, from 0.062 ± 0.005 % at commencement of the experiment to 3.69 ± 1.3% over 11 days (Figure 7.22). Samples collected from all other treatments (Control, + Barrier, + DOC) varied over the experimental period. Carbon dioxide flux rates (nmol m^{-2} min^{-1}) were nearly ten times greater in the '+ Barrier + DOC' treatment than all other treatments and ranged from 0.009 ± 0.004 to 0.015 ± 0.006 nmol m^{-2} min^{-1} with no obvious trend over the experimental period (Figure 7.22). As with CO_2, there was little difference in flux between all other treatments.

Trends in H_2S concentration were consistent with CO_2 (Figure 7.22); concentrations were higher in the '+ Barrier + DOC' treatment than all other treatments by as much as 12,000 times (after 11 days), as well as increasing with duration from 0.0004 ± 0.0001 ppm on the 5th October (experiment start) to 24.7 ± 14.3 ppm on the 16th October. Samples collected from all other treatments (Control, + Barrier, + DOC) varied little between treatments or with duration, ranging between 0.002 ± .002 on the 5th October to 0.04 ± 0.03 ppm in the + Barrier and + DOC treatments respectively.

H_2S flux rates (nmol m^{-2} min^{-1}) were also approximately 3 orders of magnitude greater in the '+ Barrier + DOC' treatment than all other treatments (Figure 7.22), ranging from 0.0005 ± 0.003 to 0.0006 ± 0.0003 nmol m^{-2} min^{-1}. There was also a high degree of variability within this treatment, as demonstrated by the high standard errors. There was little difference in flux between all other treatments, ranging from $6.12 \times 10^{-6} \pm 4.16 \times 10^{-6}$ to $1.37 \times 10^{-3} \pm 1.22 \times 10^{-4}$ nmol m^{-2} min^{-1}.

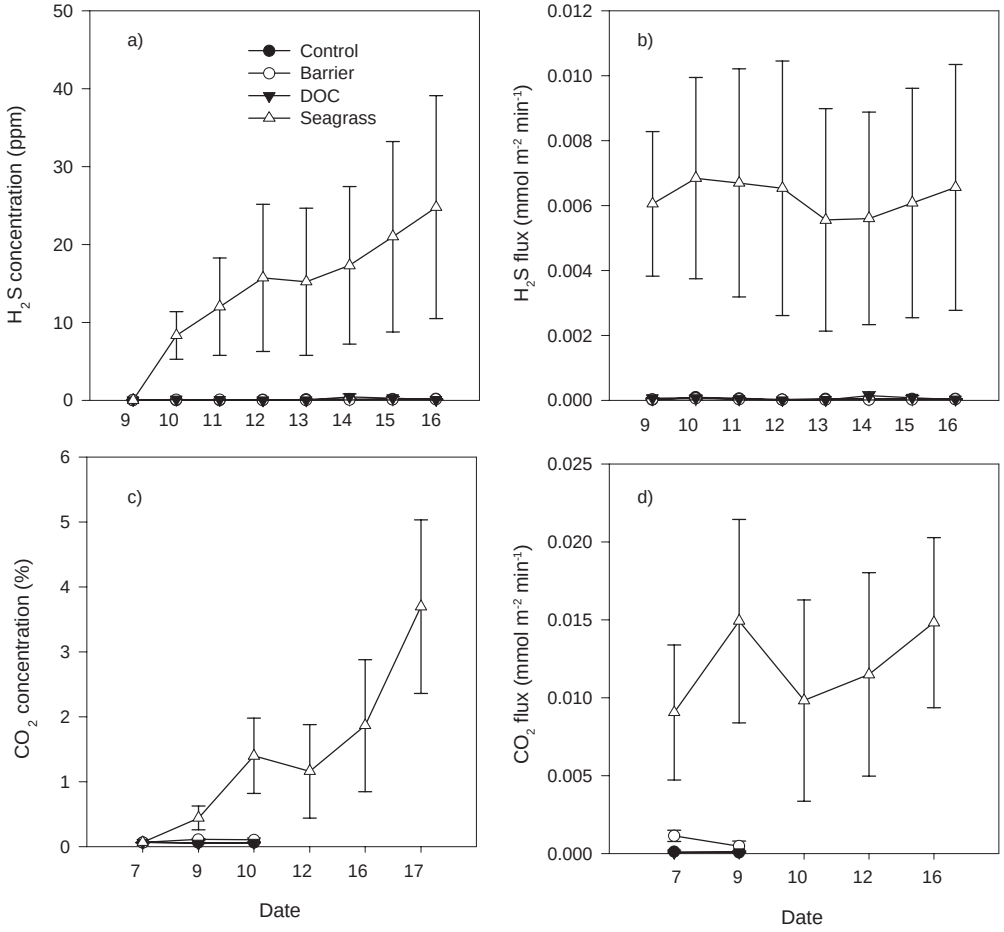

Figure 7.22 Concentrations and fluxes of CO_2 and H_2S in the headspace of mesocosm cores containing seagrass wrack and carbon loading treatments. a) H_2S concentration, b) H_2S flux, c) CO_2 concentration, d) CO_2 flux.

7.4.4 Significance of results

Few data on surface fluxes of H_2S are available in the primary literature, and none were found for beach wrack. However, wrack fluxes can be compared with the few data available from other environments known to be hotspots for H_2S production through sulfate reduction. One flux, measured at Abbey Beach in replicate 2, was greater than the saltmarsh value of 1.25 x 10^{-1} µmol m^{-2} min^{-1} reported by Steudler and Peterson [1984], shown as the upper dashed line in Figure 7.17, and one (replicate 1) was below. Eun *et al* [2007] reported a mean value of 2.38 x 10^{-2} µmol m^{-2} min^{-1} (shown as the lower dashed line in) and high spatial variability at a construction debris landfill (Figure 7.17). Many of their measured fluxes were below their detection limit. Finally, Bodenbender *et al.* [1999] found mean H_2S fluxes between 3.6 x 10^{-5} µmol m^{-2} min^{-1} and 5.1 x 10^{-3} µmol m^{-2} min^{-1} at an intertidal flat in northern Europe. The measured fluxes from the beach wrack at Geographe Bay were not unusually high in comparison with other environments known for high rates of hydrogen sulfide production.

The flux of CO_2 gas from the wrack to the atmosphere on both sampling trips is consistent with the mean value of 6.62 *µmole* CO_2 m^{-2} s^{-1} found by Coupland *et al.* [2007] on other wrack-covered beaches in Western Australia. These results from beaches in Geographe Bay support the conclusion that wrack deposits on beaches are hotspots of CO_2 production from the degradation of organic carbon, with rates that exceed those found in all major terrestrial biomes [*Coupland et al.*, 2007].

On Trip 1, Guerin St (Big New) and Siesta Park (Big Old) had similar depths of seagrass wrack on the beach, but the CO_2 flux at Guerin St was higher than at Siesta Park. This pattern might be explained by the age of the wrack deposits on the beach. The wrack on Guerin St was newer and, based on the leachate experiments, would therefore be expected to have a higher loading of labile organic carbon the older piles in Siesta Park. This is supported by the significantly higher concentrations of TDOC found in the saturated zone at the bottom of the wrack piles (Table 7.5), and from the higher leachate measured in fresh vs. aged wrack (see Section 7.3). Thus, Guerin St was supporting higher rates of organic carbon degradation driven by the high concentration of labile carbon. In comparison, rates in Siesta Park were lower because the labile carbon fraction was more depleted leaving a more refractory organic carbon source.

The H_2S profiles through the wrack piles on Trip 1 lend some insight into the location of sulfate reduction and the factors affecting the accumulation of gases in the pore spaces of the wrack. The sharp increases in concentration at the Siesta Park sites just above the saturation zone suggest that H_2S production through sulfate reduction is occurring in the saturated zone of the wrack piles. Sulfate reduction requires the absence of oxygen, low redox potential, a source of sulfate and a source of organic carbon. All of these requirements are met in the saturated zone where seawater supplies the sulfate and acts as a barrier to oxygen diffusion. Within the unsaturated wrack, oxygen was still present throughout the profiles at all beaches and there is no substantial supply of sulfate. These findings are reinforced by the observation that the characteristic rotten egg smell of H_2S gas was strongest when the excavation of wrack reached the saturated zone at all of the sites.

The presence of H_2S in the pore spaces at Siesta Park on Trip 1 when H_2S was generally below detection limit in the pore spaces at Guerin St and Abbey Beach may indicate a fundamental difference in the transport of gases through the wrack rather than a difference in H_2S production rates. The older wrack at Siesta Park was more consolidated (higher bulk density) than the newer wrack at Guerin St and Abbey Beach due to the mechanical (greater proportion of fines) and biogeochemical breakdown of the seagrass. These characteristics would slow the transport of H_2S gas from the saturated zone to the surface and allow the accumulation of gas in the pore spaces. The newer piles at Guerin St and Abbey Beach would allow for faster diffusion of gas through the pore spaces thus preventing the build up of gases within the wrack piles. This could explain why some replicates at Abbey Beach had a significant surface flux of H_2S with no detectable H_2S concentration in the wrack interior.

The absence of detectable fluxes at Siesta Park (Big Old) during Trips 1 and 2 was unexpected. However, as mentioned previously, the wrack piles there were noticeably more consolidated than at sites with new wrack. It could be that permeability of the wrack was quite low with respect to the diffusion of gases. In other words, the old wrack had become a barrier to the diffusion of H_2S from the saturated zone. The extremely high CO_2 and CH_4 concentrations found within the pore spaces at SP3 and SP8 during Trip 2 indicate very high rates of organic carbon degradation within the wrack pile and retention of these gases due to low permeability.

The following conclusions can be drawn from the work presented in this section:

- wrack piles are hotspots for organic carbon degradation with the subsequent production of CO_2 gas as a by-product. Wrack piles can also become significant producers of CH_4;
- the fluxes of H_2S from undisturbed wrack piles are significant, though no larger than those found from intertidal mudflats and less than what has been measured in saltmarshes;
- the production of H_2S occurs in the saturated zone underneath wrack piles. Disturbance of the saturated zone can cause release of the dissolved gases when exposed to the atmosphere; and
- gas fluxes from natural wrack piles are highly variable in time and space, making it difficult to calculate production rates of gases. This variability appears to be related to the age and size of the wrack accumulations, which may affect the supply of DOC to sustain bacterial decomposition, and the porosity of the accumulations, which affects the diffusion of oxygen into, and H_2S out of, the accumulations.

The mesocosm experiments provide valuable insights in the mechanism behind H_2S generation in wrack accumulations. Seagrass wrack accumulations can present both a barrier to oxygen diffusion and a source of DOC. Together, these effects would potentially lead to enhanced bacterial consumption of oxygen and reduced replenishment of oxygen through diffusion from the overlying water, resulting in hypoxic or anoxic conditions and reduced redox potential in the accumulations, conditions favourable to the production of H_2S. The presence of artificial seagrass (plastic) failed to

generate hypoxia or sufficiently low redox potentials in the accumulations to allow H_2S production. Thus, the effect of wrack on diffusion is, by itself, insufficient to generate redox potentials favourable to H_2S production. The treatments which had treacle (a source of DOC) added to them did generate hypoxia and low redox potentials comparable to those of the seagrass treatments, indicating that the DOC loading may the primary mechanism though which wrack accumulations drive the production of H_2S.

Paradoxically, only seagrass treatments produced significant concentrations and fluxes of H_2S, despite the DOC loading (treacle) treatments generating similar redox potential conditions. A plausible explanation for this is that the treacle treatments lacked a necessary element for the production of H_2S, and most plausibly this was sulphur. Holmer and Neilsen [2007] and Holmer *et al.* [2009] have demonstrated that seagrasses can accumulate significant amount of elemental sulphur in their tissues as a means of dealing with the intrusion of sulfides from sediments. It is plausible that the H_2S being generated in the seagrass treatments is formed from sulphur within the seagrass wrack rather than sulfates in the seawater. If the seawater sulfates are contributing to H_2S formation, then it must be at an undetectable level or the treacle treatment would have shown similar levels of H_2S production. This is a significant finding as it indicates the wrack itself is the source of H_2S production and that management should focus on the wrack and need not address the underlying sediments, which appear to be incapable of supporting significant H_2S generation even under ideal redox conditions. Maintaining oxic conditions in the saturated zone of the wrack should be sufficient to significantly reduce H_2S generation.

These results confirm field observations that closely tie the production of these gases to the presence of seagrass wrack in the saturated anoxic zone of wrack piles. The high variability of gas production within seagrass treatments is also consistent with field observations, which noted high spatial variability. The findings of the field observations and laboratory experiments are also consistent with those of The Odour Unit (2008), who found the highest concentrations of H_2S were above wrack in pooled water (ranging 41 to 96 ppm). These concentrations were consistent with submerged seagrass treatment in the mesocosms experiment (25 ± 14 ppm) and also field observations in the present investigation (Figure 7.20). These findings confirm our understanding that the presence of water is required in the production of H_2S. They also suggest that part of the management response to reduce odour issues associated with wrack accumulation should focus on minimising the water in the vicinity of wrack piles.

8 HYDRODYNAMICS AND PARTICLE TRANSPORT MODELS

The hydrodynamic conditions or processes in coastal environments are determined by local topography/bathymetry and forcing functions and will result in transport and accumulation of material (e.g. seagrass wrack). Thus the transport of materials in coastal environments is strongly determined by circulation patterns, the combination of wave heights and directions, as well as tides and storm surges, whilst the beach slope and the near shore bathymetry control the rate of accumulation. The material transport and accumulation in near shore environments can be investigated by coupling hydrodynamic/wave models with appropriate material (particle) transport models.

8.1 Objectives

The numerical models for Geographe Bay was used to simulate:

(1) the hydrodynamics under the action of the main forcing mechanisms of water levels, wind and surface waves; and,

(2) the transport of the seagrass wrack particles under the prevailing hydrodynamic conditions.

Two distinct models, as described below, were developed and coupled.

8.2 Hydrodynamic model setup

The DHI MIKE model system was used to simulate the hydrodynamics and wave climate within Geographe Bay. The DHI Mike model system is one of the most well known, user-friendly tools for the study of many aspects of hydrodynamics in the marine environment. The model system has a wide range of engineering and environmental application in coastal hydraulics, oceanography, wave dynamics, harbours, rivers, environmental hydraulics, and sediment processes. This software has been extensively used in the simulation of hydrodynamics, wave dynamics, water quality, and all related processes in estuaries, bays and coastal areas. In this project we used the Mike21 depth-averaged flow model coupled with the spectral wave module to simulate hydrodynamics and wave climate in Geographe Bay and the Port Geographe Marina.

Given the relatively shallow and unstratified nature of Geographe Bay, it was decided that a depth-averaged two dimensional hydrodynamic model was most appropriate. The main forcing input data to the model are bathymetry, water levels, surface winds and wave climate (see details below). The model validation/calibration parameters are the bottom friction coefficient and eddy viscosity. For this work, we used a constant bed stress and eddy viscosity. The model allowed flooding and drying over the computational grid during the simulation.

Wave-current interaction was simulated by iteratively coupling the depth-averaged hydrodynamic model to the spectral wave (SW) model. The SW model simulated the growth, decay and transformation of wind-generated waves and swells in offshore and coastal areas.

The main features and effects included in the hydrodynamic and spectral wave model were:

- 2D primitive equations for elevation, currents, and waves,
- eddy viscosity assumption,
- drying and flooding,
- unstructured grid (flexible mesh),
- momentum dispersion,
- bottom shear stress,

- coriolis force,
- wind shear stress,
- wave radiation stresses, and
- wave growth within the model domain due to local winds.

8.3 Model bathymetry and mesh grid

The model domain was selected to ensure that it covered the locations where data were available to force the model: the Bunbury tide station data for water level data, Cape Naturaliste wave buoy records for wave data, wind speed and direction data from Bunbury, Busselton and Cape Naturaliste. The model domain also covered the locations where data were available for validation: water level data and wave data from offshore Busselton and Port Geographe.

The model domain extended 85 km (east-west) and 60 km (north-south) (Figure 8.1), The coordinates (GDA94 MGA zone 50) of the model grid corners were:

South-west corner	292558 Easting	6258210 Northing
North-east corner	377280 Easting	6317546 Northing

Three ocean boundaries (northern, western and southern) were included. The western boundary (46 km in length) was placed to approximately follow the 50 m contour, the northern boundary (86 km in length) was angled to the north-west to be incident to storm wind and waves. The coastline boundary extended from Cowaramup Bay in the south, and to Bunbury in the north.

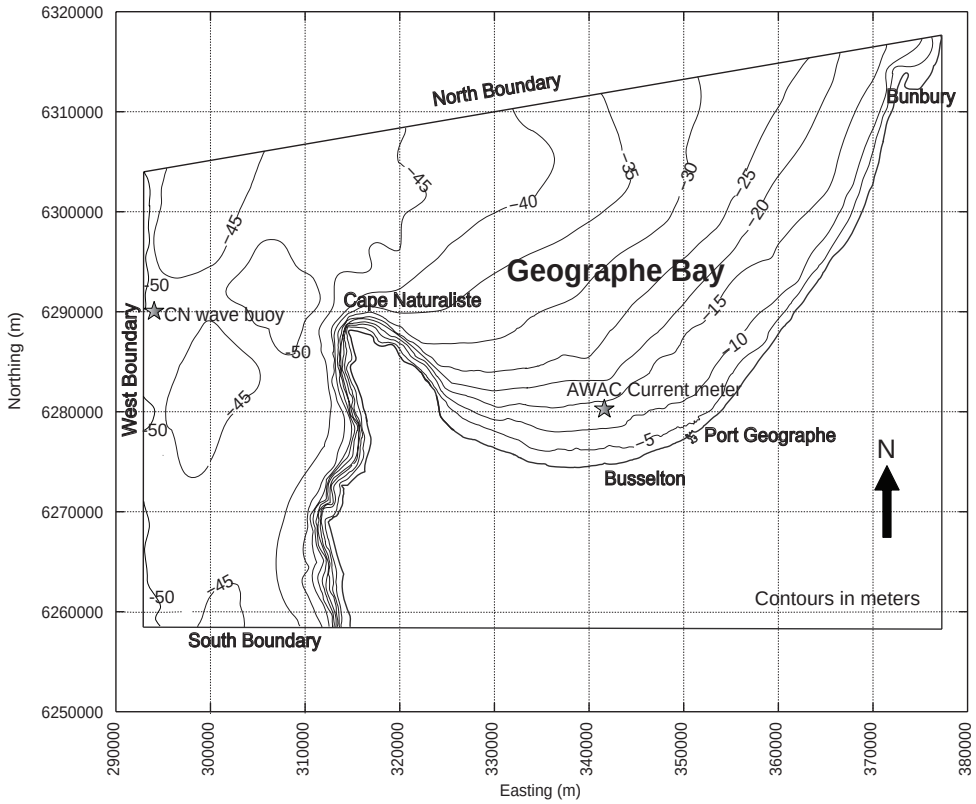

Figure 8.1 Map of Geographe Bay showing the model boundaries, general bathmetry and the locations of model forcing data.

The mesh grids were set-up for both the wave and hydrodynamic modelling (Figure 8.2). Using a fine resolution grid over the large spatial extent of the model domain resulted in very long runtimes. The stability constraints on the model limit the maximum time-step used. These constraints are in turn dependent on the water depth and the grid size. Therefore the Geographe Bay model area was divided into five sub-regions, each with a different mesh size; the outer, relatively deeper sub-regions had larger meshes and the areas of interest, i.e. Port Geographe and Busselton region, had finer meshes (Figure 8.2). The meshes in this sub-region were sufficiently dense near structures and near the vicinity of the Port Geographe to model the flow field in detail. The total mesh consisted of 14,378 surface nodes in 28,693 elements.

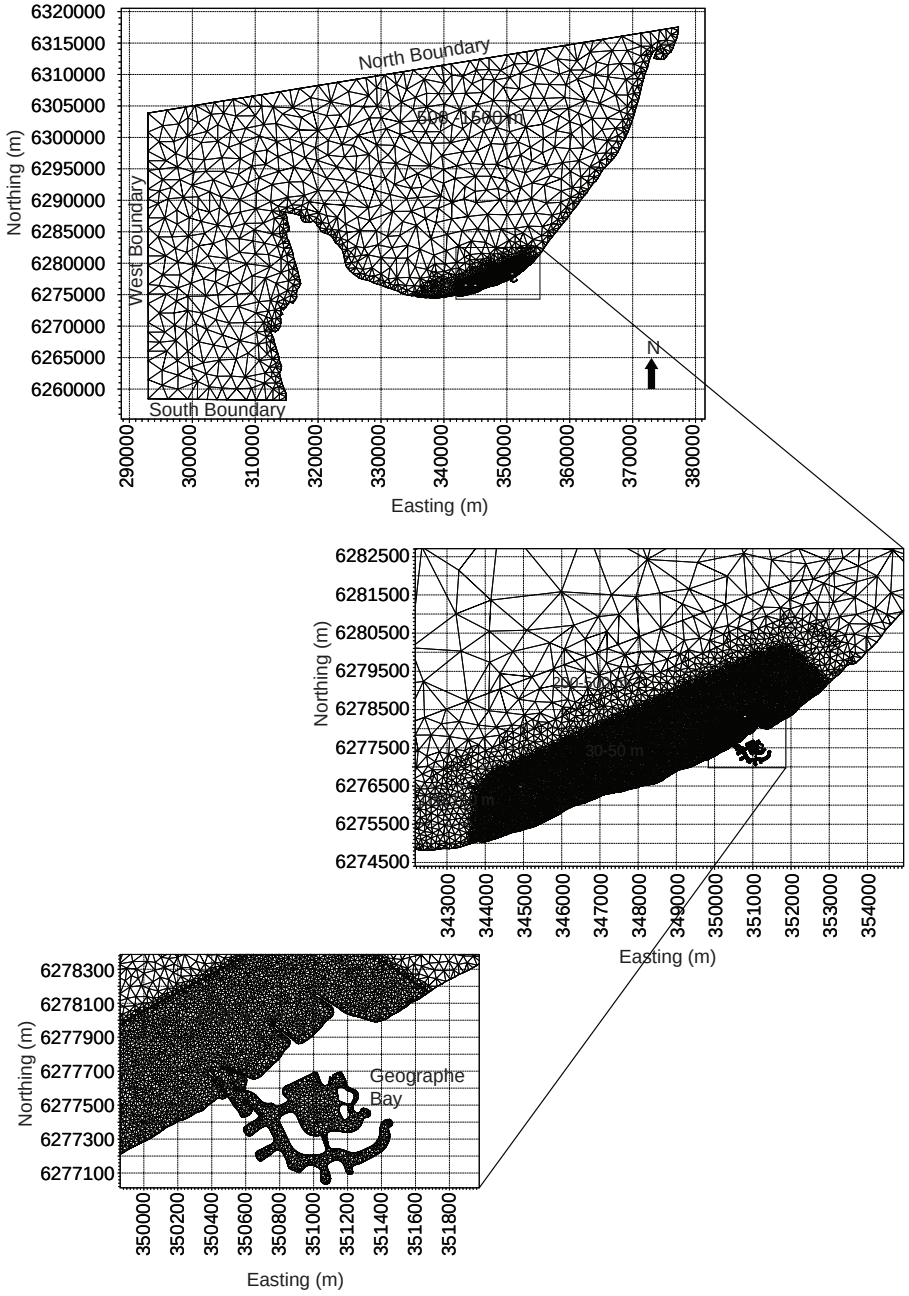

Figure 8.2 Model grids of the Geographe Bay showing different scales used for the model domain. The fine grids are in the Port Geographe and near shore region of Busselton.

One of the most important aspects in any hydrodynamic model setup is to obtain a bathymetry of high accuracy. For this project we gathered data from various sources to construct the model bathymetric grids. Bathymetry data were available at 250 m horizontal resolution from Geoscience Australia's Australia-wide database. For the near shore areas from Quindalup to Wonerup, DPI surveys provided high (> 10 m horizontal) spatial resolution data and detailed survey data around Port Geographe.

The high-resolution data were nested within the low-resolution data to create a model domain with resolution varying from 1000 m offshore to 10 -15 m in the near shore areas surrounding Port Geographe and Busselton (Figure 8.2). Ten to fifteen metre resolution was found to sufficiently resolve near-shore flow features (Figure 8.3), while minimising model runtimes and maximising model stability. All depth data were standardized to the Australian Height Datum (AHD). All spatial coordinates were re-projected into Australian Geographic Datum (AGD94) Map Grid of Australia zone 50 (MGA50) coordinates. Shoreline vector data were also from Geoscience Australia. In addition, beach profiles obtained by Department of Transport in October 2009 were incorporated to generate shoreline bathymetry for selected model runs (e.g. model runs with extended beach, see Section 10).

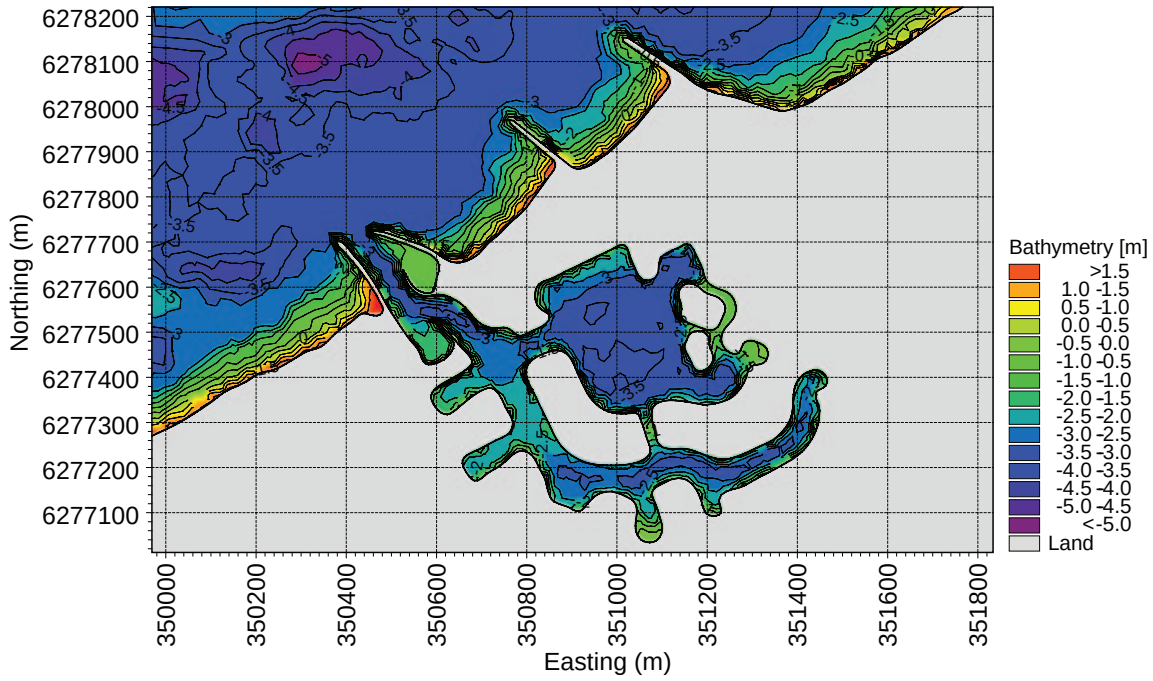

Figure 8.3 Model bathymetry of the Port Geograpе and Busselton area in the current configuration.

8.3.1 Hydrodynamic model forcing

The model was forced with water levels, waves along the open boundaries and winds on the surface. The sea surface pressure variation over the domain was also included. Water levels and velocities within the domain were set to zero as model initial conditions. No fluxes through closed boundaries were specified. We assumed there were no morphological (bathymetric) changes within the domain while the model was running; we excluded the sand transport module in the MIKE model selection.

8.3.2 Open boundary conditions

The open boundaries were located along the three offshore (southern, western and northern) edges of the model domain (Figure 8.1, Figure 8.2). The open boundary condition was specified as the monitored water level and wave time series. The forcing of water levels (tides) at the three open boundaries (southern, western and northern) was determined using a combination of field data, knowledge of tidal propagation in the region and experience gained from previous

numerical modelling of the region (Fahrner & Pattiaratchi, 1994). Monitored water levels for Bunbury (Figure 8.4, DPI) were filtered and applied directly to the northern boundary. Previous studies showed that cross-shore changes in amplitude and phase were negligible [*Eliot and Pattiaratchi*, submitted] therefore no cross-shore variation was prescribed. An appropriate correction factor (obtained from the Australian National Tide Tables) was applied to the tidal predictions for the southern boundary, near Cowaramup Bay. For the western boundary, the tidal conditions at the southern and northern boundaries were linearly interpolated. Both the tidal and low frequency (storm surge) components of water levels were included in the model forcing.

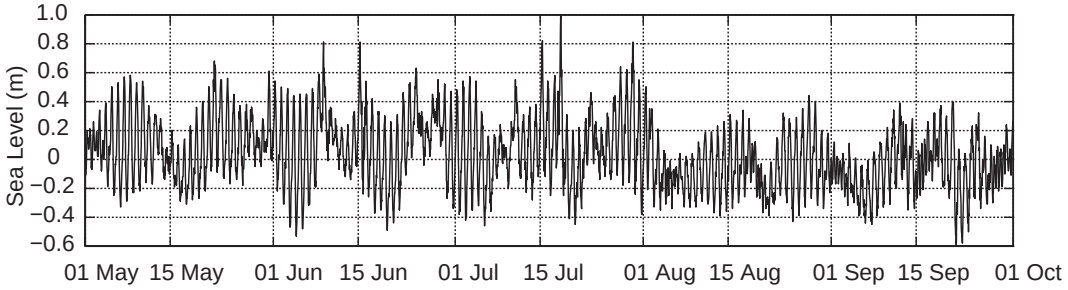

Figure 8.4 Open boundary water level forcing data, from the Bunbury tide gauge (data provided by the Department of Transport).

Swells in the near-shore region are critical for deposition of seagrass wrack onto the beach, erosion from the beach, and movement of the wrack along the shoreline. The MIKE21 spectral wave (SW) model simulates the growth, decay and transformation of wind-generated waves and swells. In this model, we introduced a time series of measured wave data at the boundaries. The SW model then calculated the movement and transformation of these waves across the model domain, including the effects of the action of the specified winds on these waves. Data were available from the Cape Naturaliste Wave Buoy (location: 33.52 °S, 114.78 °E), operated by Department of Transport for the model time period, with a few data gaps when the buoy was not operational. These gaps were filled by linear interpolation between data points (Figure 8.5). The wave buoy provided hourly measurements of wave height and period, but did not record direction. In order to incorporate swell direction into the model, directional data was extracted for the nearest grid point from the Global Wavewatch III wave model and interpolated to an hourly time scale. This method was used by Hemer *et al*. (2007) to analyse the wave climate of the south-west of Western Australia.

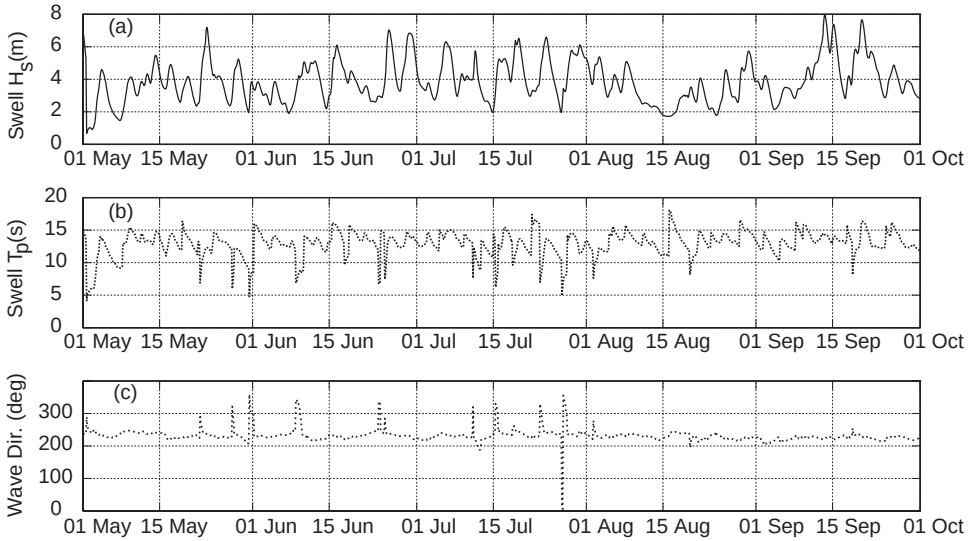

Figure 8.5 Open boundary wave climate forcing data, obtained from the Cape Naturaliste Wave Buoy and the Global Wave-watch III wave model: (a) significant wave height, (b) mean wave period and (c) mean wave direction.

8.3.3 Surface wind stress

The action of wind along the sea surface results in a stress that forces surface water in the wind direction; it is an important forcing mechanism of the currents. It also directly and indirectly affects the movement of wrack suspended in the water column and floating on the water surface. The wind forcing was included and applied over the complete domain (time and space) in both hydrodynamic (HD) and spectral wave (SW) modules.

Wind speed and direction data were obtained from the Bureau of Meteorology at the locations depicted in Figure 8.1. The wind speeds and directions at the Cape Naturaliste, Busselton and Bunbury meteorological stations are shown in Figure 8.6, Figure 8.7 and Figure 8.8 respectively. Ten-minute wind speed and direction data at these stations were used to construct temporally and spatially varying wind-fields over the model domain, based on a moving average interpolation. As an example, a snapshot of the wind vectors across the model domain, over a single time step, is shown in Figure 8.9. Wind data in the east-west (Figure 8.10) and north-south (Figure 8.11) directions were input to the model. The sea surface pressure variations over the temporal and spatial domain were also constructed based on a moving average interpolation.

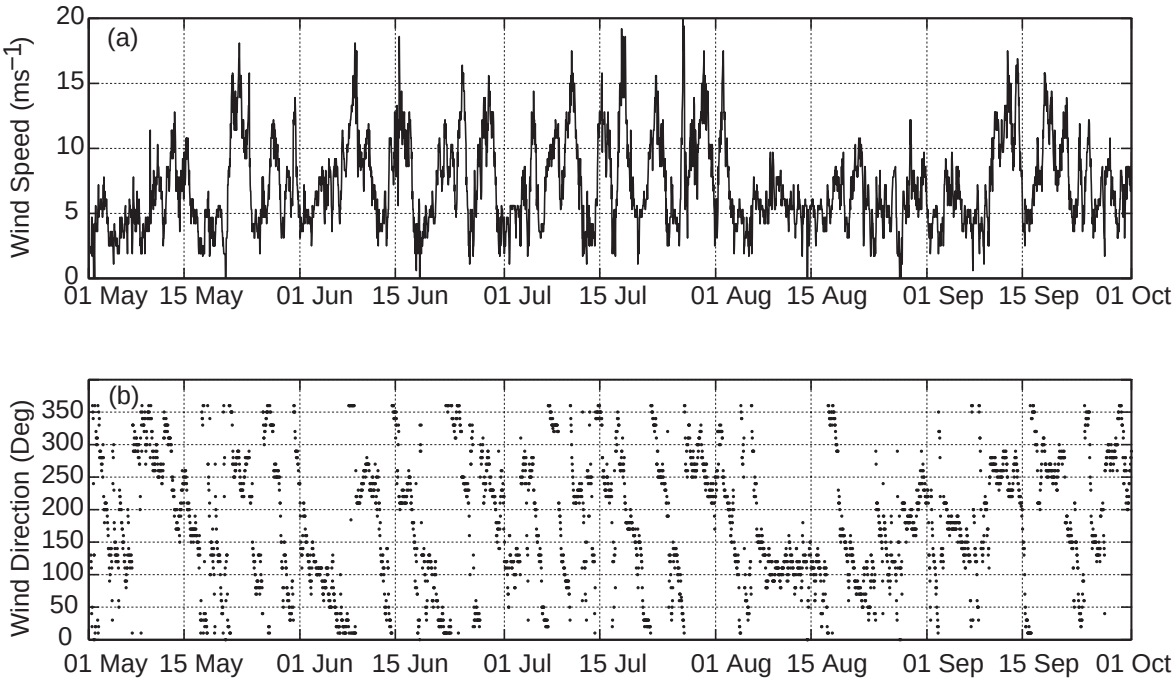

Figure 8.6 Wind speed (a) and direction (b) data from Cape Naturaliste meteorological station.

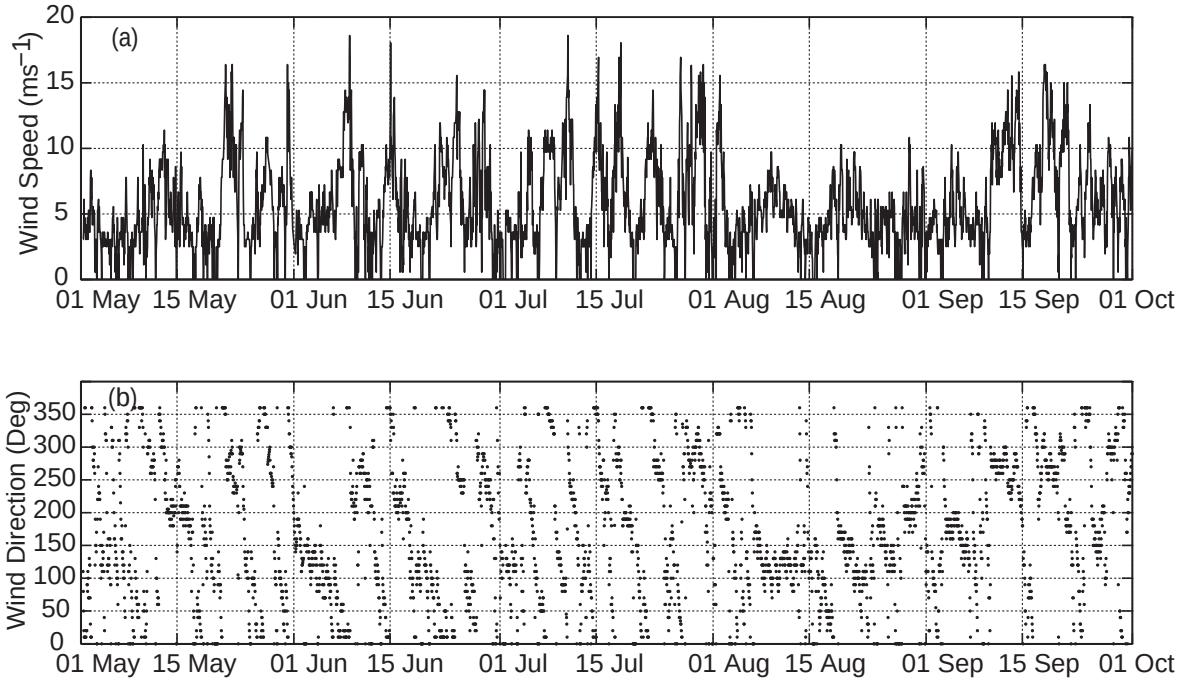

Figure 8.7 Wind speed (a) and direction (b) data from Busselton meteorological station.

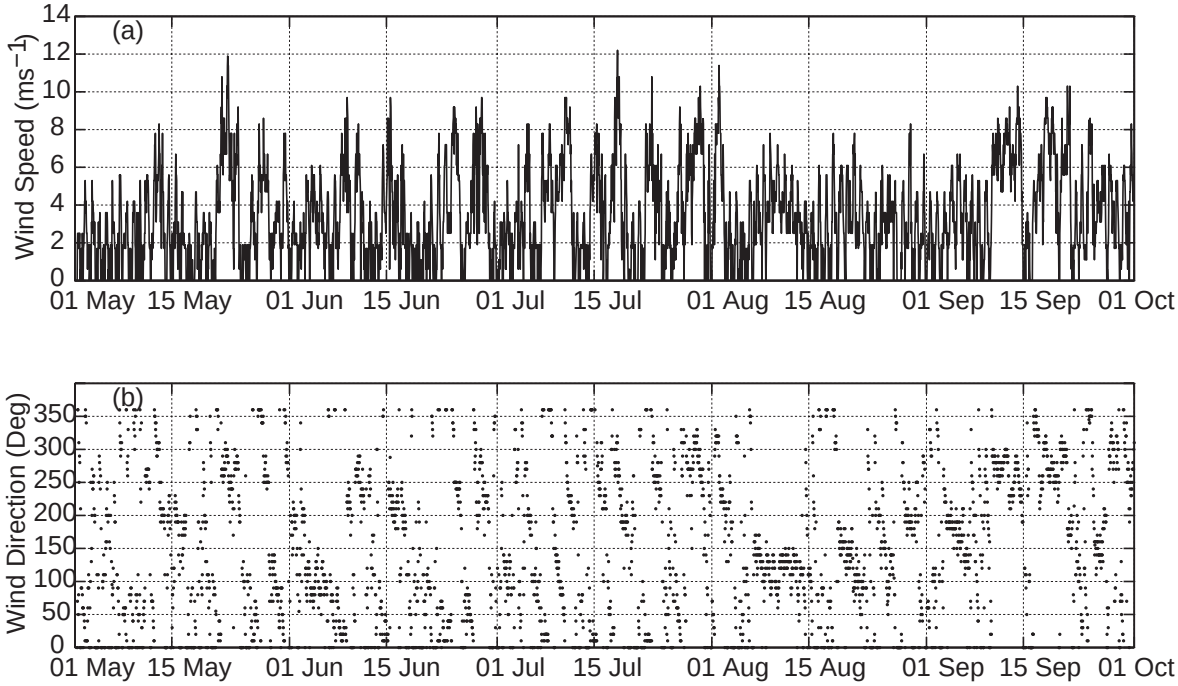

Figure 8.8 Wind speed (a) and direction (b) data from Bunbury meteorological station.

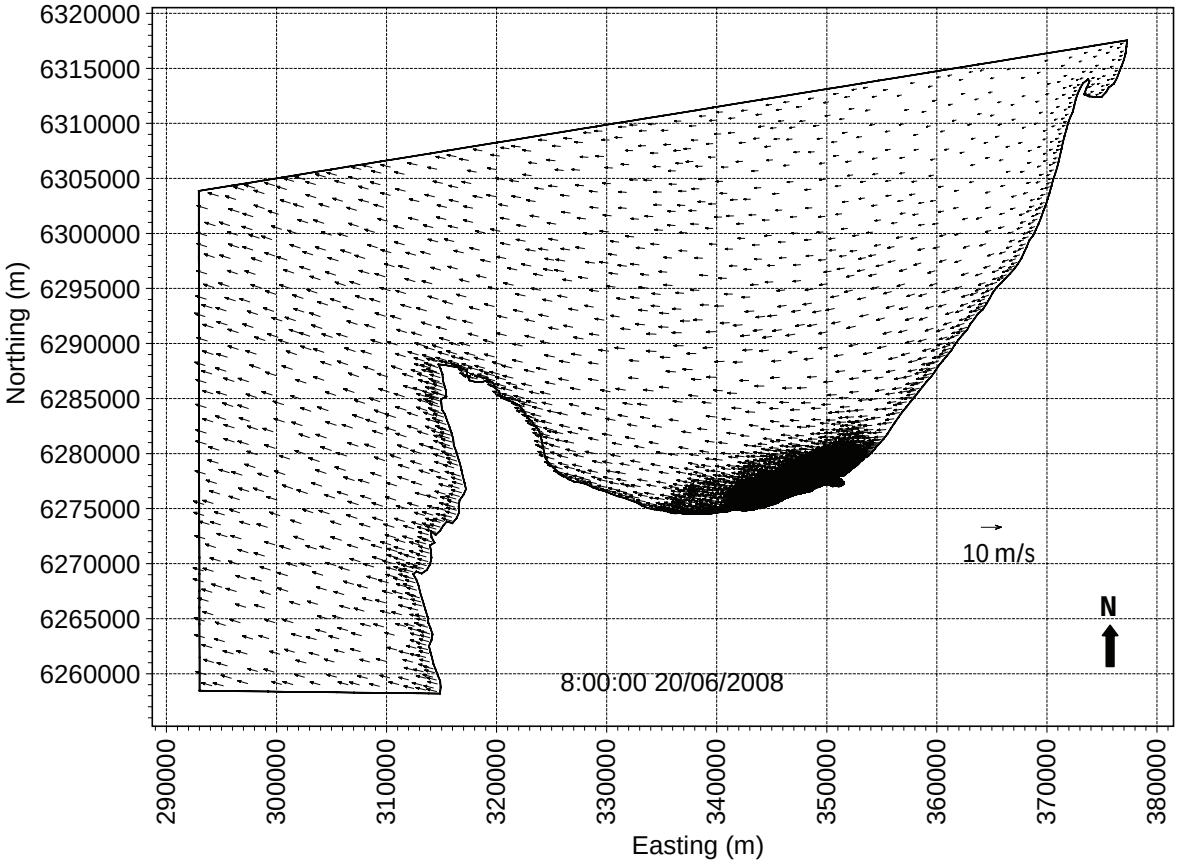

Figure 8.9 A snapshot of interpolated winds vectors over the model domain (easterly wind).

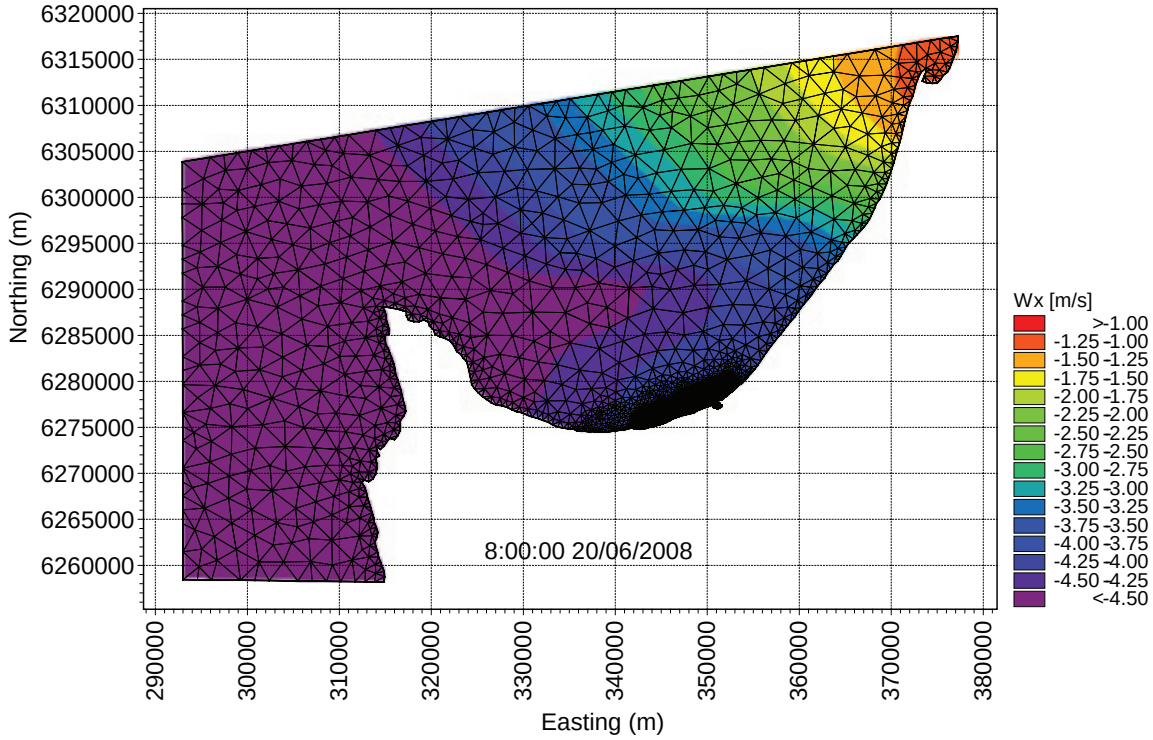

Figure 8.10 A snapshot of interpolated east-west wind speeds over the model domain.

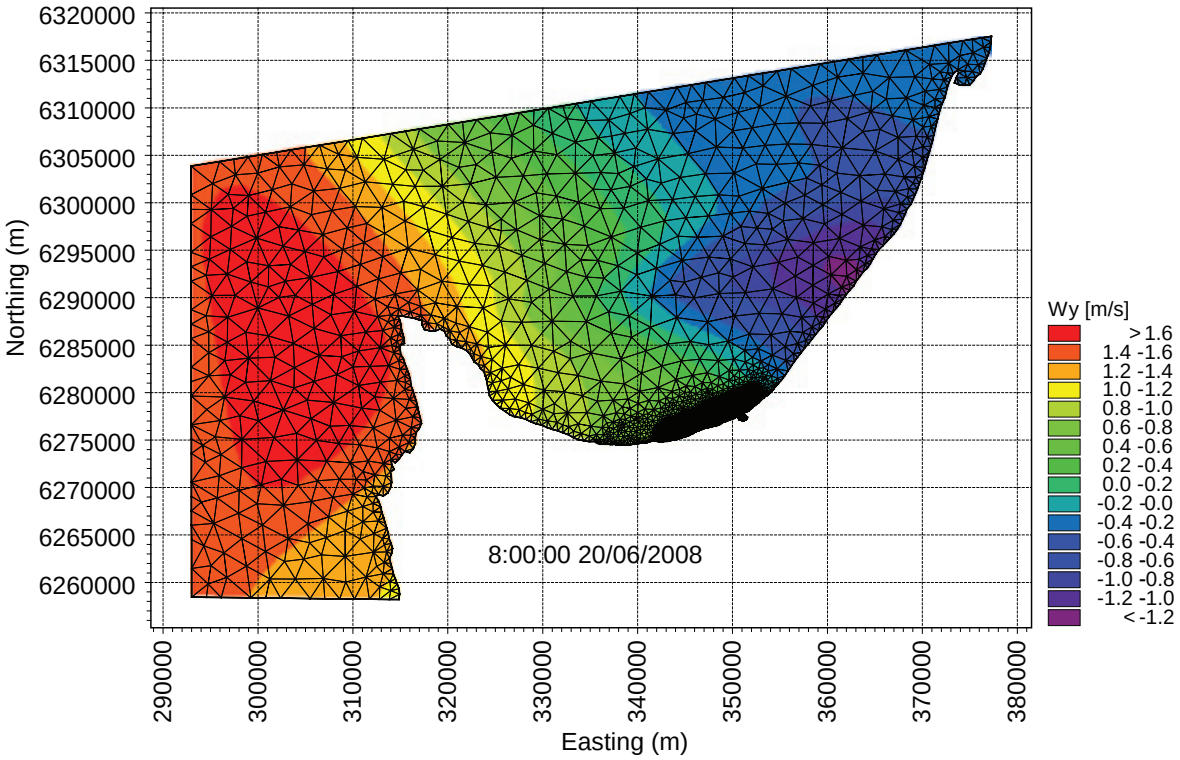

Figure 8.11 A snapshot of interpolated north-south wind speeds over the model domain.

8.3.4 Initial conditions

All the model runs were initiated from a 'cold' start; all velocities and water levels within the model domain were set to zero. The model was then run for one day as a 'warm-up' period over which the forcing parameters were increased from zero. After this warm-up period, the model ran with true forcing data for the four to five month period.

8.4 Particle transport model setup

A Lagrangian based particle-tracking model was developed to investigate seagrass wrack transport in the Geographe Bay. Hydrodynamic and spectral wave model outputs of the velocity field, water levels and wave climate data were used to force the particle transport model. The particle transport model was run for the same period as the hydrodynamic model, i.e. from May to August, 2008. However, the first three days of hydrodynamic model *'warm up'* were not included in the particle transport model run period.

At model startup, particles were randomly seeded in the region inside the bay between the 3.5 m and 12 m depth contours; initial results suggested this was likely the wrack catchment area for Geographe Bay.

8.4.1 Seagrass wrack transport formulations

In the particle transport model, three states of wrack behaviour were considered:

- particle settling on the seabed,
- particle transport in the water column and
- particle settling on the beach.

Each of these states were described by a set of equations for re-suspension, transport and dry re-suspension respectively.

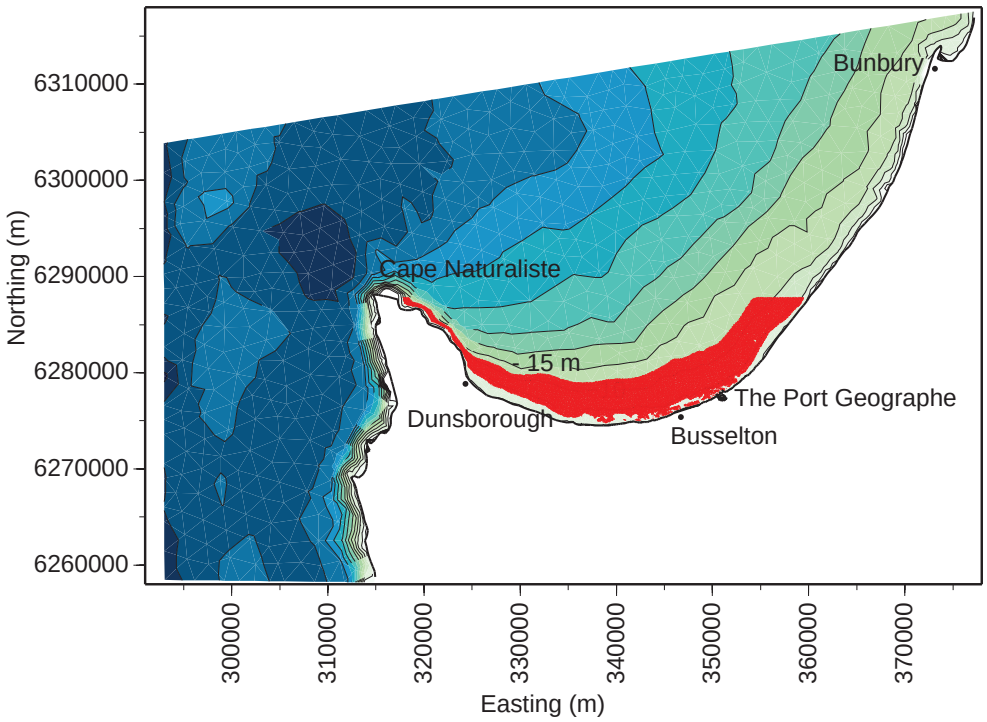

Figure 8.12 Initial position of wrack (red dots) in dispersal model.

8.4.1.1 Re-suspension

Re-suspension occurs when the currents induce a bottom stress sufficient to lift a seagrass particle off the seabed up to a calculated height in the water column.

The elevation above the bottom is calculated using a random walk given as:

$$\delta z = a\sqrt{6E_v dt} \qquad \textbf{Eq. 8-1}$$

where δz is the variation of elevation in one model time step, a Is a normally distributed random number [0-1]; and E_v the calibrated vertical eddy diffusivity [0.002 $m^2\ s^{-1}$], and dt is the model time step.

The bottom stress induced by the current is calculated using the shear stress equation (Eq. 8-2).

$$\tau = \frac{\left(u^2 + v^2\right)\kappa^2}{\ln^2\left(\frac{0.37h}{z_0}\right)} \qquad \textbf{Eq. 8-2}$$

where τ is the shear stress, u and v are the depth-averaged horizontal velocities (east and north respectively), κ is the Von Korman constant (0.41), h is the water depth and Z_0 is the roughness length (roughness of the sea floor). When this shear stress exceeds a critical value resuspension occurs. The critical value was measured for *Posidonia* and *Amphibolis* in a laboratory experiment, as described in Section 5.3. From the experiments, the critical shear stresses were estimated to be 8 x 10^{-5} N m^{-2} for *Posidonia* leaves and 5 x 10^{-5} N m^{-2} for *Amphibolis* leaves.

Although waves can be responsible for the resuspension of wrack, this feature is not included in the model. Wave resuspension has been studied for sediment and sand but the lack of experimental data for wrack resuspension by

waves prevents its implementation in the model. Large waves in the bay occur concurrently with strong wind-driven currents. Therefore we assumed that only currents are responsible for wrack particle resuspension in Geographe Bay.

8.4.1.2 Transport

Once resuspended, the wrack particles are displaced by currents and turbulence in all three dimensions. The hydrodynamic model simulates a 2-dimensional current field; it does not simulate vertical currents nor small scale turbulence. To simulate the dispersive effect of random turbulence on wrack particles, a random walk model was again used. The horizontal transport is given as:

$$dx = u_z dt + \bar{u}_s dt + a\sqrt{E_h dt} \qquad \textbf{Eq. 8-3}$$

where dx is the horizontal displacement over time step dt, u_z is the horizontal current velocity at the depth of the wrack, $\bar{u}_s$ is the Stokes drift, a is a normal random number [-1 1], E_h is the horizontal eddy diffusivity [0.002 m^2 s^{-1}].

The vertical transport is given as:

$$dz = w_s dt + a\sqrt{E_v dt} \qquad \textbf{Eq. 8-4}$$

where dz is the vertical displacement over time step dt, W_s is the fall velocity [m s^{-1}] and E_v is the vertical eddy diffusivity [0.002 m^2 s^{-1}].

The fall velocities (W_s) of the seagrass wrack particles were measured in the laboratory as described in Section 5.3.

The horizontal current velocity at the depth of the wrack (U_z) was calculated by assuming a logarithmic profile of velocity through the water column. The profile was calculated using the depth-averaged velocity simulated by the hydrodynamic model as:

$$u_z = u_0 \frac{\ln\left(\frac{z}{z_0}\right)}{\ln\left(\frac{0.37h}{z_0}\right)} \qquad \textbf{Eq. 8-5}$$

where U_0 is the depth average velocity, z is the depth of the wrack, z_0 is the seabed roughness length scale and h is the total water depth.

Stokes drift is caused when wave-induced horizontal orbital velocities decrease closer to the seabed (van Rijn 1989); $\bar{u}_s$ is a second-order mean Lagrangian velocity in the direction of wave propagation. In the offshore environment, Stokes drift velocities become insignificant, however closer to shore they can be significant. Stokes drift can be calculated from linear wave theory as:

$$\bar{u}_s = \frac{1}{8}\varpi k H^2 \frac{\cosh(-2kz)}{\sinh^2(kh)} \qquad \textbf{Eq. 8-6}$$

where ϖ is angular frequency (radians s^{-1}), k is wavenumber (radians m^{-1}) and H is the wave height (m).

8.4.1.3 Beach re-suspension

When wrack gets deposited on the beach it dries in the sun. Experimental work (See Section 5.3) indicated that after less than 24 hr of drying, the wrack particles floated when transported back to the water, i.e. their settling velocities were zero. After about two hours in the water, the particles sank as previously described. To account for this behaviour in the model, when a wrack particle reached the beach its fall velocity was reset to zero. When subsequent resuspension occurred, over the first two hours of being transported in the water column, the fall velocity gradually returned to its original value.

Large accumulations of wrack on the beach become compacted and trapped sand. This leads to a modification of the beach profile, sometimes creating a large wrack step, often visible on the west side of Port Geographe during winter. The complexity and the general lack of understanding of this process and the larger-scale nature of this study precluded the implementation of this wrack dynamic in the model.

The parameters used for the particle transport model are given in Table 8.1.

Table 8.1 Particle transport model parameters.

PARAMETER DESCRIPTION	VALUE	UNIT	ORIGIN
Number of particle to release	53760	-	-
Dispersal model time step, dt	50	s	Calculated
Horizontal eddy diffusivity, Eh	0.002	$m^2\ s^{-1}$	Estimated
Vertical eddy diffusivity, Ev	0.002	$m^2\ s^{-1}$	Estimated
Settling velocity, ω_s	-0.018	$M\ s^{-1}$	Experimental
Roughness length, z_0	0.01	m	Estimated
Critical shear stress, τ_c	8×10^{-5}	$N\ m^{-2}$	Experimental
Time to recover settling velocity after being dried	7200	s	Experimental

9 MODEL VALIDATION

9.1 Hydrodynamic model validation

Field measurements of currents from the Department of Transport instrument (Acoustic Wave and Current Profiler, AWAC) deployed offshore of Busselton Jetty and the time series from the Busselton tide gauge at Port Geographe, allowed for calibration and validation of the hydrodynamic model. Validation of results was performed both qualitatively and quantitatively.

The agreement between the predicted and measured currents and water levels was quantified by estimating the model skill, which produces 0 in cases of no agreement and 1 for perfect agreement [*Willmott*, 1984].

$$\text{Model skill} = 1 - \frac{\sum \left| X_{\text{model}} - X_{\text{obs}} \right|^2}{\sum \left(\left| X_{\text{model}} - \overline{X}_{\text{obs}} \right| + \left| X_{\text{obs}} - \overline{X}_{\text{obs}} \right| \right)^2} \qquad \textbf{Eq. 9-1}$$

The MIKE21 hydrodynamic model has two key calibration parameters: the bed resistance coefficient and the horizontal eddy viscosity. Calibration of the model can be achieved easily by adjustment of these factors. We have chosen Chezy-type bed resistance with an estimated coefficient value of 32 $m^{1/2} s^{-1}$; this coefficient was kept constant over the model domain.

The horizontal eddy viscosity was based on the Smagorinsky formulation [*Smagorinsky*, 1963] with a range of 1.8 x 10^6 – 10^7 $m^2 s^{-1}$. The Smagorinsky method provides time-dependent adjustments of eddy viscosity based on simulated velocities. We have also varied the Coriolis parameter over the domain. The model validation was undertaken for both the hydrodynamic and spectral wave models by comparing predictions with time series data of water levels, current speeds, current direction and wave statistics, collected from two stations inside Geographe Bay (Figure 8.1).

9.1.1 Water levels

The 4-month model runs started from 1 May 2008. The first three days of model spin up were not included in the model validation. Figure 9.1 depicts time series of water levels at AWAC 1 and Busselton from 8 May - 31 August 2008. The predicted tide and other high frequency oscillations (seiches) are in good agreement with observed data (correlation coefficient of 0.95). The model also predicted all peak surges.

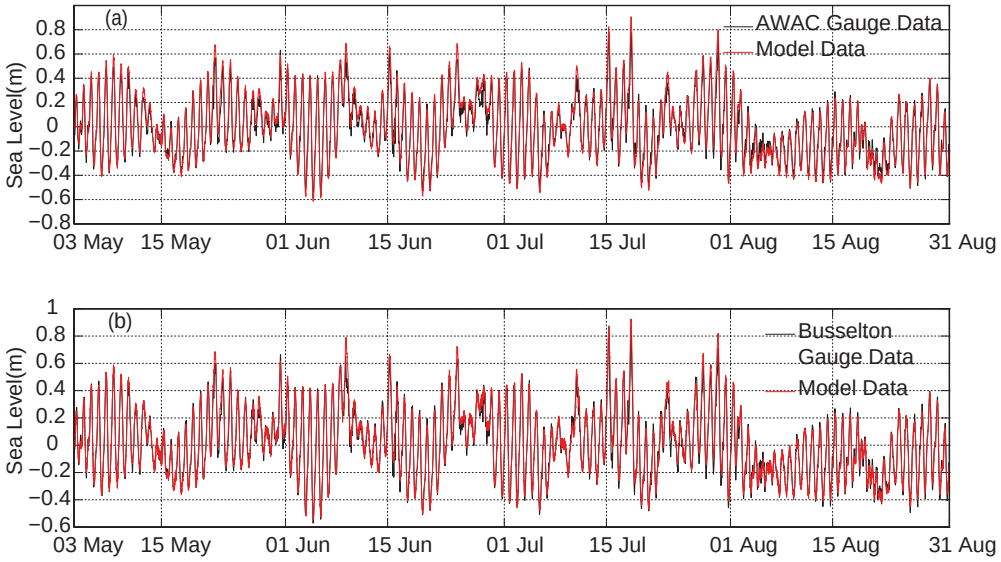

Figure 9.1 Measured and predicted water levels at the a) AWAC and b) Busselton sites from 8 May – 31 Aug 2008. Black lines denote observed data and red lines denote model output.

9.1.2 Velocities

A time-series of Acoustic Wave and Current Profiler (AWAC) data, collected offshore from Busselton (33° 35.854 S; 115° 17.805 W) in 15 metres of water depth, was used to validate the predicted velocities. When the measured velocities were averaged over the flow depth, they compared well with the predicted depth-averaged velocities (Figure 9.2).

The predicted low-frequency currents in the east-west direction compared well with the observations, (skill > 0.85); the model captured the trends observed. However, the predicted north-south current speeds did not compare well with the observations, (skill < 0.68). During periods of light wind and currents, the model tended to under-predict water velocities. This can be explained by the presence of other forcing mechanisms that were not included in the model (e.g. density-driven currents and the influence of the Leeuwin Current). It should be noted that these low energy periods were not considered the focus of this project and therefore the lack of such process description on the model was considered acceptable.

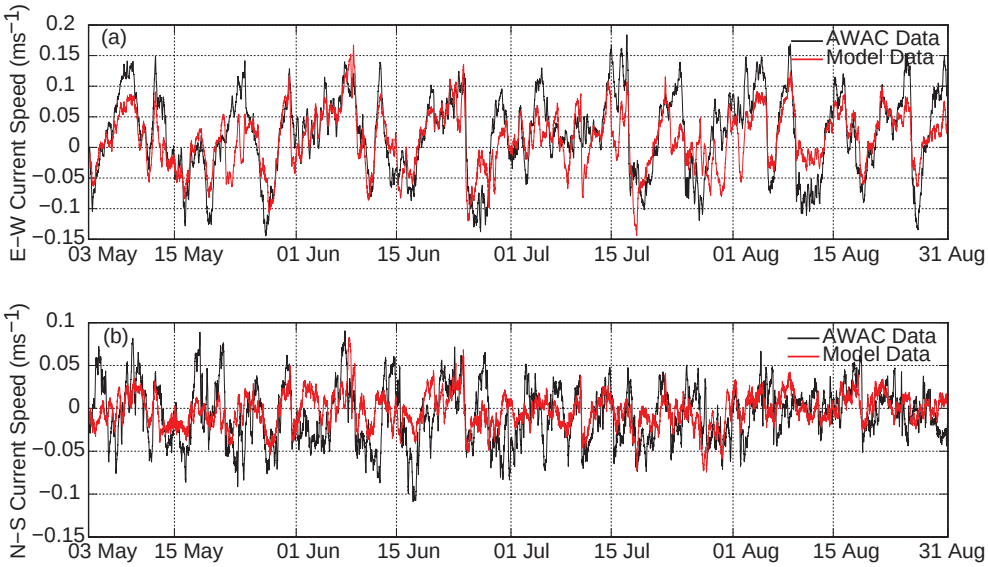

Figure 9.2 Measured and predicted a) east-west and b) north-south current speeds. Measured data was collected at the AWAC site from 8 May – 31 Aug 2008. Black lines denote observed data and red lines denote model output.

9.1.3 Wave climate

There was good agreement between the predicted significant wave height, peak wave period and wave direction, and those measured by the AWAC mooring (Figure 9.3). The model slightly underestimated peak wave periods, but the trend was well correlated with measured values. The measured and predicted peak wave directions were also in good agreement in general, however some sudden changes of wave direction were not predicted by the model; this was attributed to the resolution of the wind data input to the model.

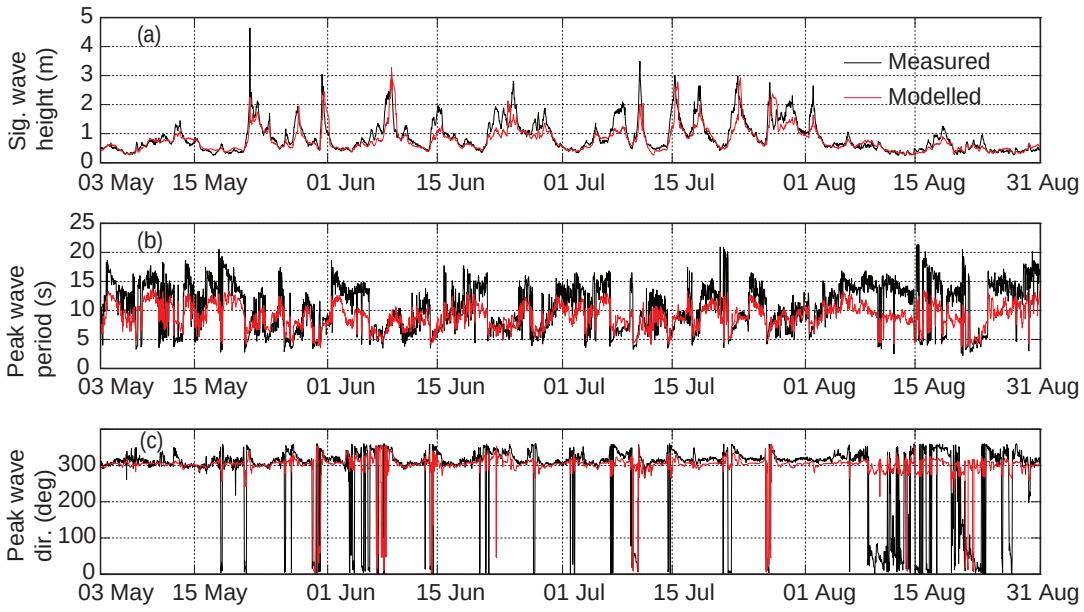

Figure 9.3 Measured and predicted wave statistics: a) significant wave height, b) peak wave period and c) peak wave direction. Measured data was collected at the AWAC site from 8 May – 31 Aug 2008. Black lines denote observed data and red lines denote model output.

9.2 Seagrass particle transport model validation

9.2.1 Linking wrack accumulation with hydrodynamic conditions

The accumulation and disappearance of wrack along Geographe Bay's beaches is affected by weather and ocean conditions. Therefore an attempt was made to determine the meteorological and ocean conditions that resulted in wrack movement onshore and offshore from the beaches. Data on the weather conditions (wind speed and direction), water levels and incident waves were available for the experimental time period (July to August 2008). Here the 'wrack indices', determined from analysis of photographs (obtained from volunteers) were compared with corresponding environmental data (as described in Section 6.2) to determine the conditions that caused the deposition/erosion of wrack on the beach. Due to the limited spatial and temporal availability of photographs, several sites were selected as most representative of the movement of wrack onto/off the beach. Here, we focus on site 998E (998 Port Geographe Road), a site which saw above-average accumulations (compared to other sites) in 2008 as well as noticeable changes in wrack mass on the beach throughout the winter.

Wrack movement for this site was quantified by creating a plot of the difference (next day – current day) in the wrack abundance (see Table 6.4). Using this approach, an event which deposited wrack onto the beach, was represented by a positive number and erosion of wrack was negative. Because of the limited (1 day) temporal resolution of the wrack, abundance data, events were to be interpreted as occurring near this date (+/- 1 day).

For site 998E, most movement onto and off the beach occurred in the beginning of June and the second half of July, with most extreme events happening in the last two weeks of July. Almost no movement occurred during the month of August (Figure 9.4 and Figure 9.5).

Four factors were used to investigate which conditions were likely causing wrack to move on and off the beach, with a focus on the first three:

- wind speed
- wind direction
- water levels
- wave height

In winter these factors followed a predictable pattern, as cold fronts passed through the region. Analysis for 2008 showed that stronger winds generally came from the west or south-west during which times water levels and wave heights also reached a maximum. For this reason we proposed that a simple indicator of the passage of a storm event could be provided by an analysis of storm surge peaks (Figure 9.6). Wrack movement was plotted against winds and water levels for May - September 2008 (Figure 9.4) and July - August 2008 (Figure 9.5). Highest winds, water levels, and wave heights occurred during July, whilst August was unusually calm, with most winds coming from the south at speeds of less than 15 knots. Storm events occurred in May and June but they were less frequent than in July. The storm surge plot shows seven events occurring in July and none in August (Figure 9.5).

At site 998E movement of wrack occurred during each of the seven storm events shown in the storm surge plot (Figure 9.6). These events corresponded to winds from the north-west, west or south-west, large waves, and high water levels. Extreme events (such as the storm on July 17-19, or July 27-29, Figure 9.5) corresponded to large changes in the wrack abundance. Because there was only one photo per day, it was not possible to determine which phase of the storm cycle caused deposition and which caused erosion of the wrack. Small changes in wrack abundance (< 2) were not considered to be reliable due to the qualitative nature of the analysis. Taking this into account, we detected three major wrack deposition/erosion events at site 998E during July 2008 (Figure 9.5). In particular, the wrack deposition was observed during high water levels whist erosion occurred during lower water levels (Figure 9.6).

This correlation between storm surge events and wrack movement is consistently observed across other sites but with varying degrees of clarity and confidence. For this reason analysis was undertaken on the numerical model results for extreme events, in order to increase reliability of the conclusions.

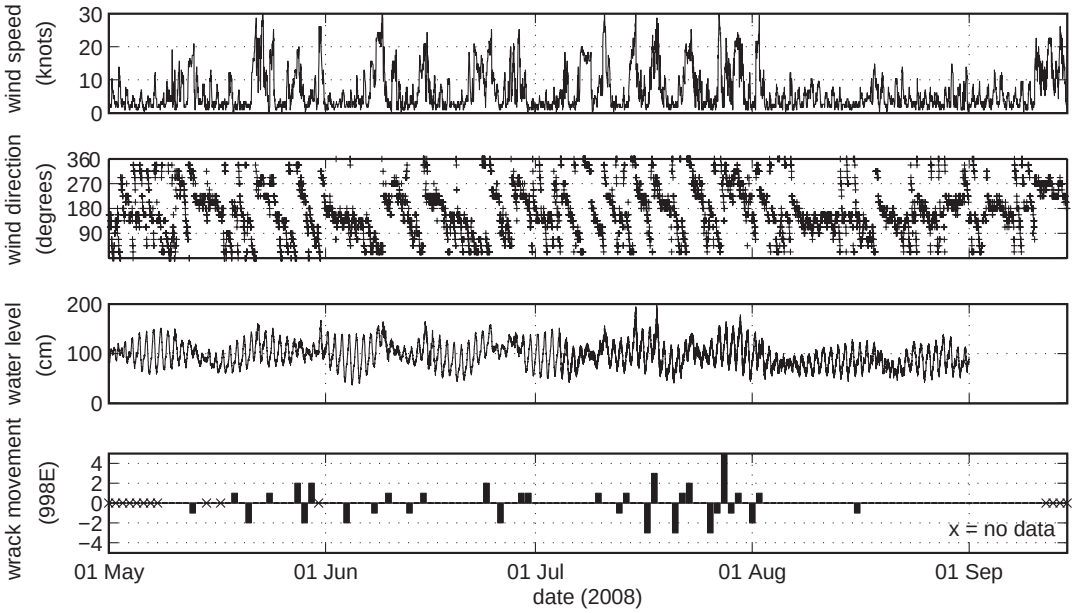

Figure 9.4 Time series of a) wind speed, b) wind direction, c) water level and d) wrack movement (ie difference in wrack index on a daily basis) for the period 1 May to 15 September 2008.

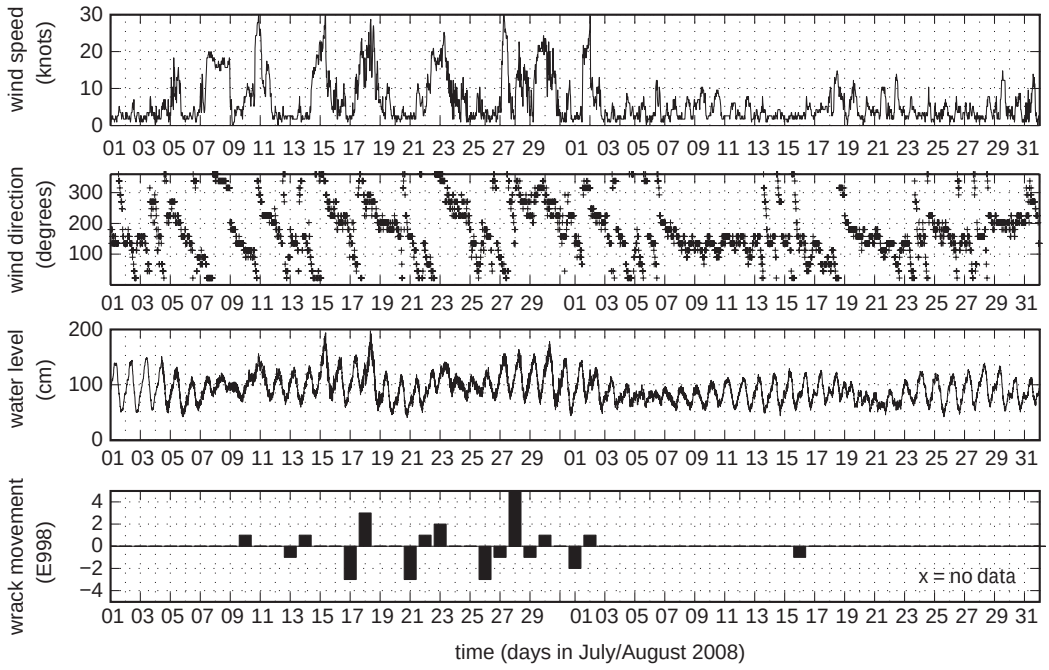

Figure 9.5 Time series of a) wind speed, b) wind direction, c) water level and d) wrack movement (ie difference in wrack index on a daily basis) for the period 1 July to 31 August 2008.

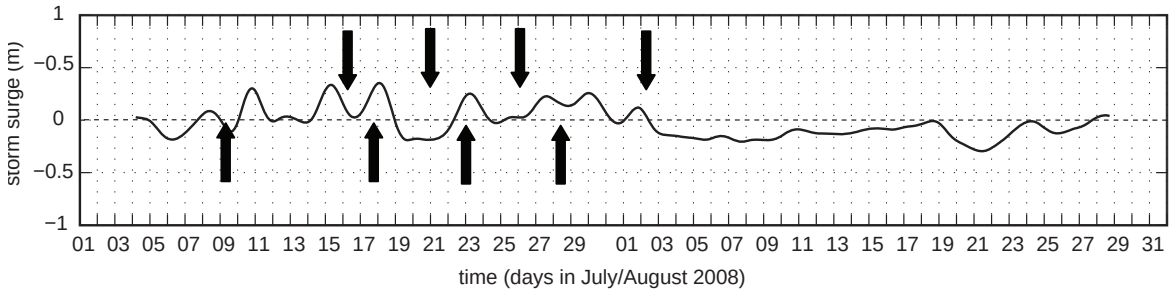

Figure 9.6 Time series of storm surges (ie the water level record with the tidal component removed for the period 1 July to 31 August 2008. Arrows indicate erosion (downward arrow) and deposition events (upward arrow) identified from the wrack movement.

9.2.2 Simulated seagrass wrack movement

Fifty particles representing seagrass wrack were introduced 200 metres offshore and 500 metres to the west of the Port Geographe groyne. Bathymetry was very detailed in this area and confidence was high in the reliability of the model to predict currents in this region. Other release points were examined, and the number of released particles was varied, but the presented simulations were ideal for allowing particles to reach the beach and also be transported offshore. Computational limitations prevented release of many more particles throughout the area. As the aim was to investigate the ability of the model to transport the 'wrack' onto and off of the beach and see how it was affected by varying conditions, it was determined (through sensitivity analysis) that 500 particles released at this location was sufficient to investigate transport processes.

Model predictions of particle movement under a single storm event are shown in Figure 9.7 and illustrate the process of wrack deposition. At the beginning of the storm, the water level was low and no particles were present on the beach

(Figure 9.7a). As the storm progressed the mean water level increased as a result of the storm surge transporting the particles onshore (Figure 9.7b).

After the peak of the storm, the water level decreased but the particles were then deposited on the beach. This process of wrack deposition during higher water levels, was observed through the analysis of photographs (see Section 9.2.1). Thus the model prediction of wrack deposition is in agreement with the observations.

Wrack deposition and erosion during the 2-month period of model predictions were examined. The distribution of particles, over 10-day intervals, is shown in Figure 9.8. At the beginning (1 July, Figure 9.7a), the particles were just released but 10 days later a considerable number were located in the nearshore region, due to the storm event. Subsequent to the next storm event on 17 - 18 July (Figure 9.5), a considerable number of particles had been deposited on the beaches (Figure 9.8c). Ten days later, on 1 August, some of the wrack still remained on the beach and remained there until the end of August, as there were no major storm events in August. These predictions are in agreement with the field observations.

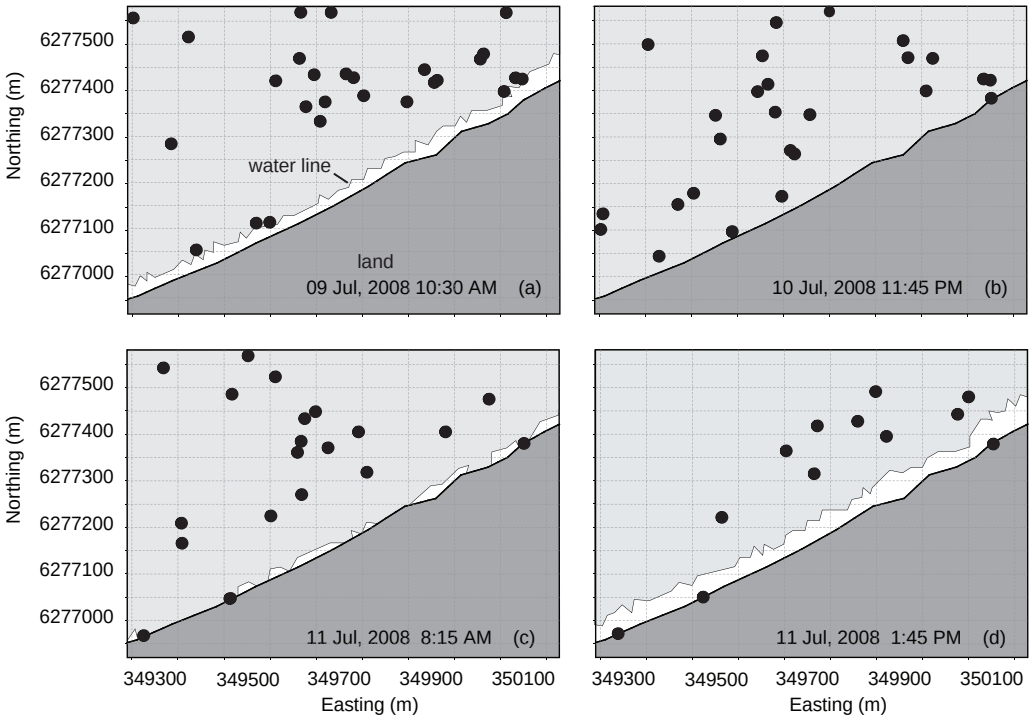

Figure 9.7 Predicted distribution of seagrass wrack particles over a storm event.

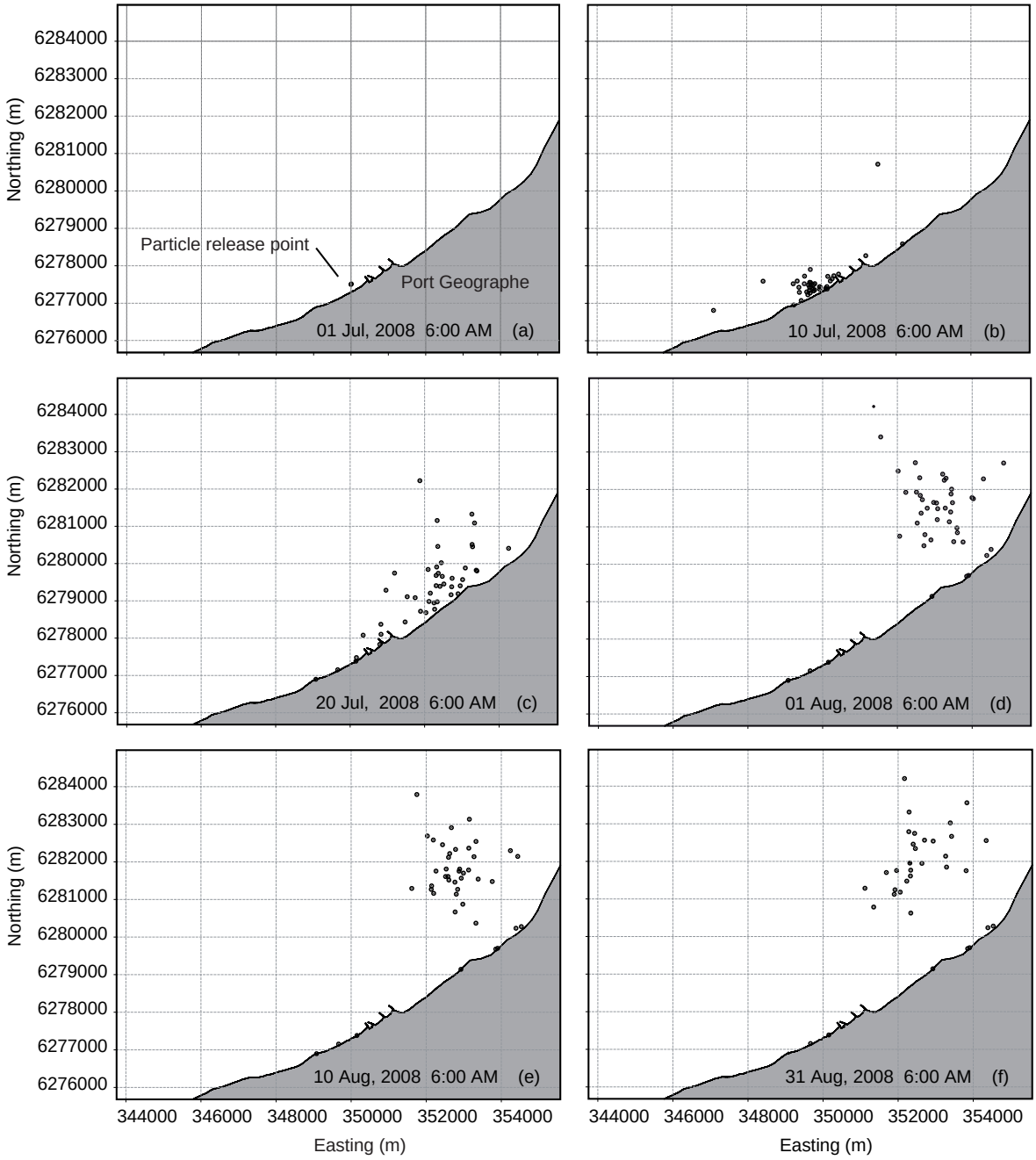

Figure 9.8 Predicted distribution of seagrass wrack particles over 10-day intervals from 1 July to 31 August.

9.2.3 Simulations of wrack accumulation at Port Geographe

The seagrass transport model validations were undertaken by comparing predictions with field observations of seagrass wrack distribution on the beaches, across different months. The model clearly showed that the seagrass wrack transport took place from the end of May to the end of July, particularly associated with storm events. The simulated seagrass wrack distribution at the end of August is shown in Figure 9.9. The model simulations revealed that the strongest accumulation of wrack occurred on the beach west of the marina, consistent with observations. It can also be seen that some wrack accumulated within the pocket beach groynes, particularly at the western inner corners.

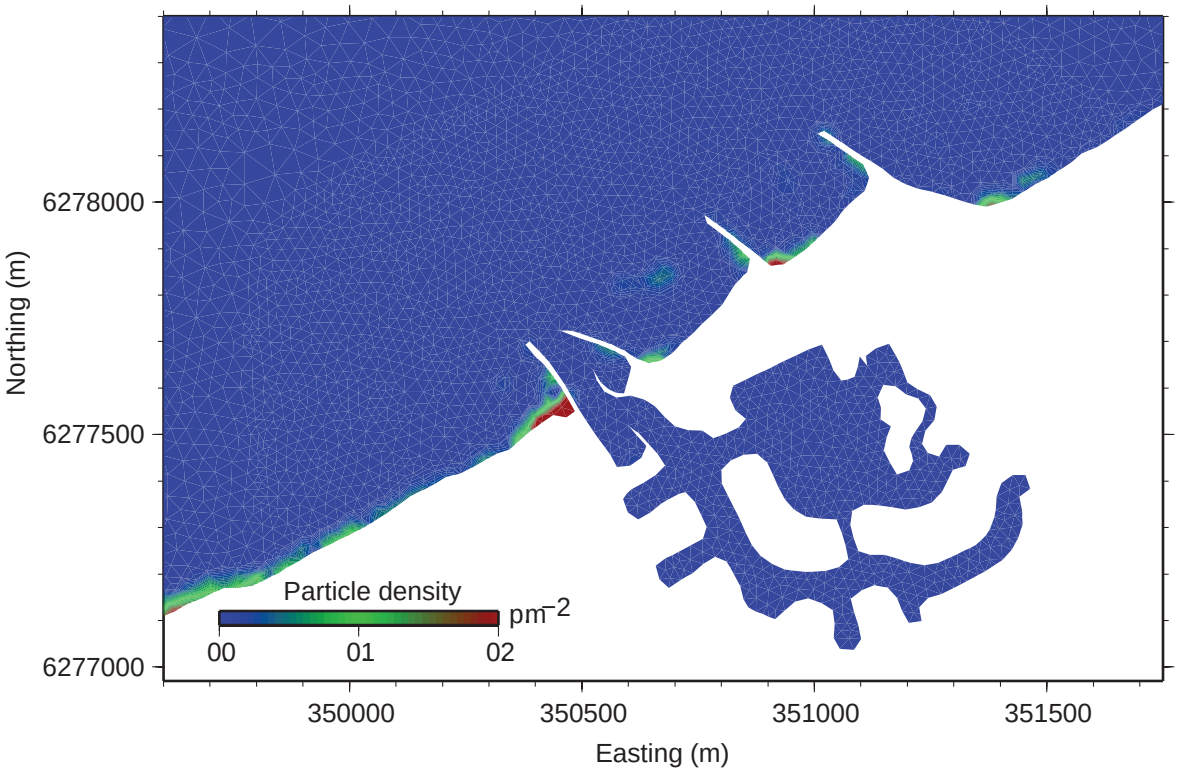

Figure 9.9 Locations of predicted seagrass wrack accumulations on the beach in the vicinity of Port Geographe at the end of August 2008.

10 SCENARIOS

To evaluate the transport and accumulation of seagrass wrack under the prevailing conditions four-month simulations were completed, starting from 1 May 2008. This period was selected based on past records of seagrass wrack transport and accumulation on the beach in the vicinity of Port Geographe. Typically, the major storm events occur from May to August. In addition, mean water levels are also typically high during the winter period and are thus able to deposit wrack further up the beach.

10.1 Hydrodynamic and particle transport simulations – existing conditions

The hydrodynamic model setup with the existing configuration was described in Section 8. Comparison of hydrodynamic and spectral wave model predictions of Geographe Bay, with measured sea levels, velocities and wave statistics were presented in Section 9. The mesh grid, interpolated bathymetry and forcing wind field for the Port Geographe area are shown in Figure 10.1 and Figure 10.2 respectively.

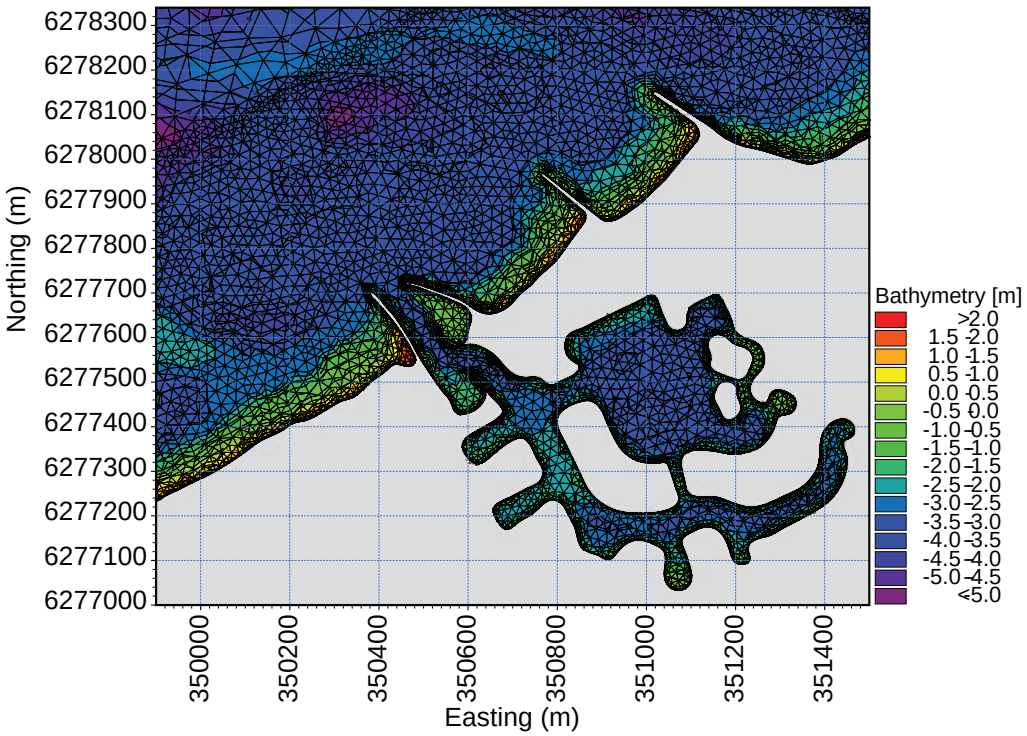

Figure 10.1 Fine mesh grid and interpolated bathymetry onto meshes for the existing groyne configuration, in the vicinity of Port Geographe.

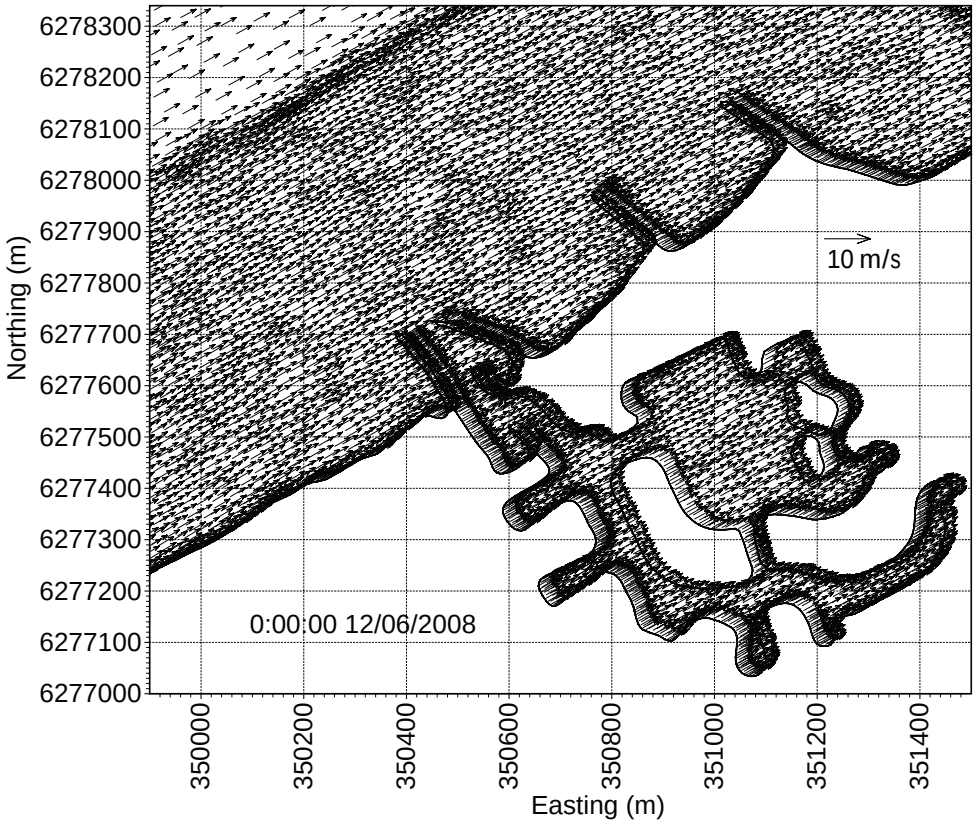

Figure 10.2 A snapshot of the interpolated wind field onto the mesh grid for the existing groyne configuration, in the vicinity of Port Geographe.

A comparison of predicted sea levels inside and outside Port Geographe (AWAC site) is shown in Figure 10.3. The sea level oscillations inside the port are almost the same as predicted outside the port. Tide, seiche oscillations and trends are nearly the same order of magnitude and there is no significant phase delay in water levels inside the marina and offshore. These results indicate that there is no damping or choking of sea levels through the existing entrance channel.

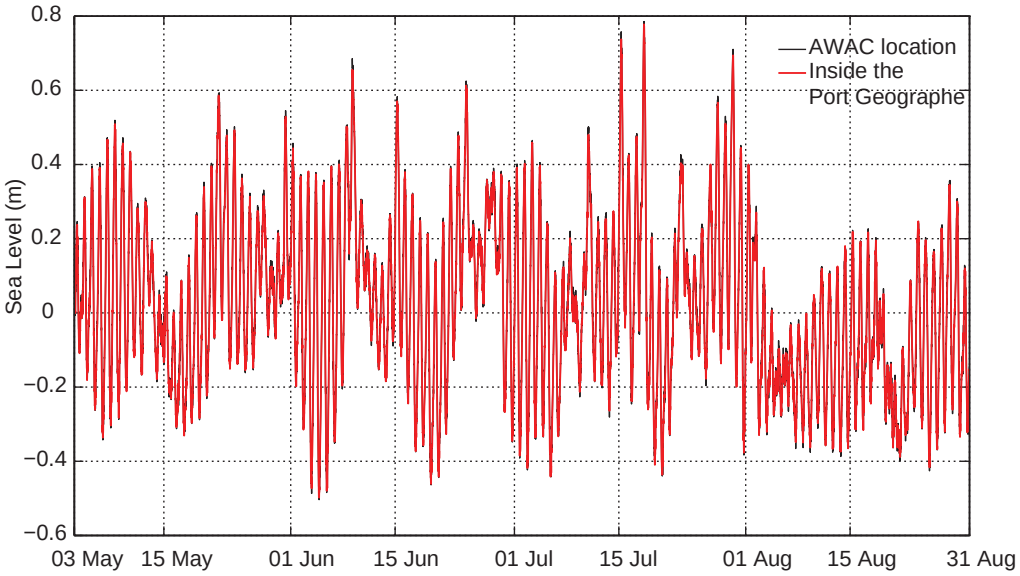

Figure 10.3 The predicted sea levels at the AWAC site (black line) and inside Port Geographe (red line), for the existing groyne configuration.

The predicted mean current speeds through the port entrance channel are shown in Figure 10.4. Flows through the entrance are directly forced by water level fluctuations, whereas tide- and seiche-induced currents dominate the entrance channel. Seiche-induced currents are present at all times with mean amplitudes of 0.1 ms^{-1} and a maximum amplitude of 0.25 ms^{-1}. Flows are strong during storm events, particularly during June and July 2008.

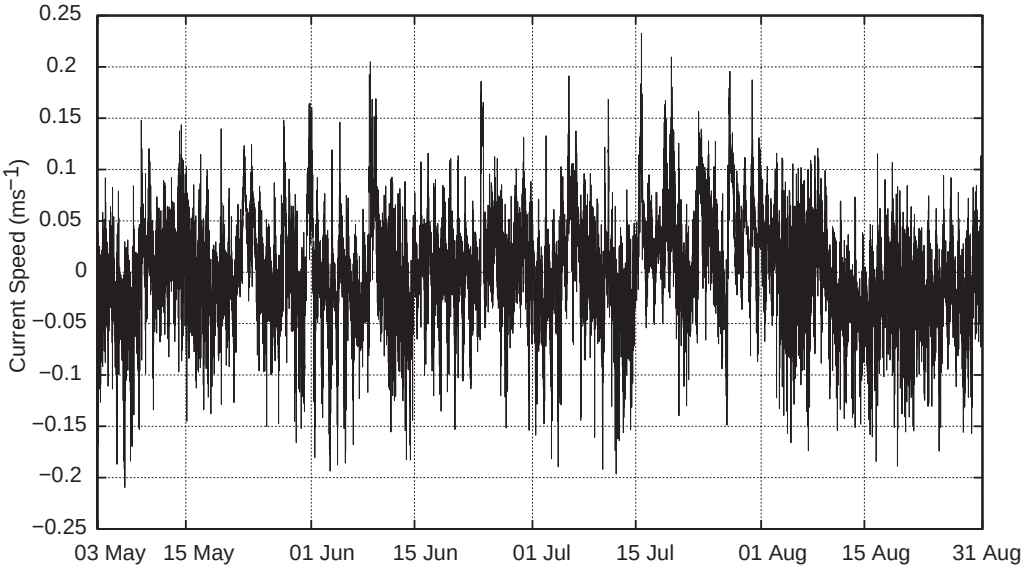

Figure 10.4 The predicted mean current speeds through the Port Geographe entrance channel, for the existing groyne configuration.

Inspection of vector plots of velocities illustrates that the currents in Geographe Bay are strongly influenced by wind, bottom topography and shoreline orientation. The contribution from tidal and other water level fluctuations to the forcing of barotropic currents within Geographe Bay, were relatively small. Current speeds generally increased when the wind direction was parallel to the coast.

Figure 10.5 and Figure 10.6 show the predicted depth-averaged currents in the vicinity of Port Geographe, during north-easterly and south-westerly winds, respectively. Currents predicted during transitional (weak) winds are also shown (Figure 10.7).

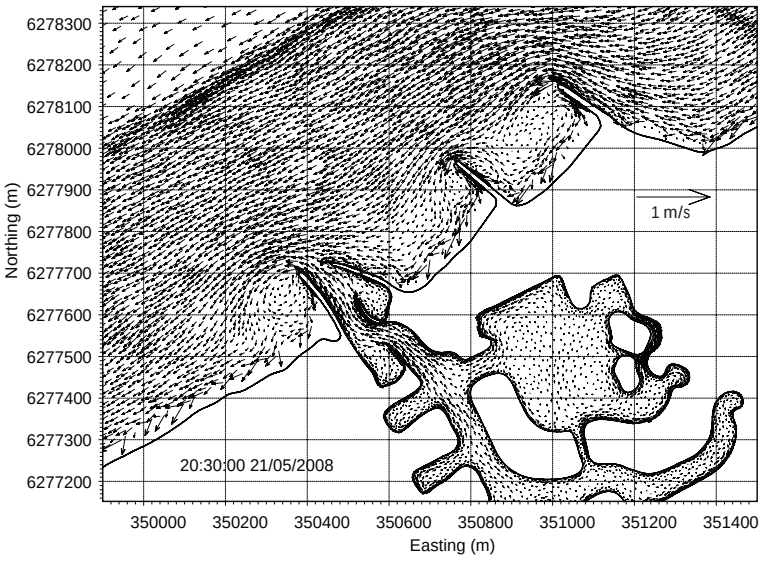

Figure 10.5 Snapshot of predicted current pattern during north-easterly winds in the vicinity of Port Geographe, for the existing groyne configuration.

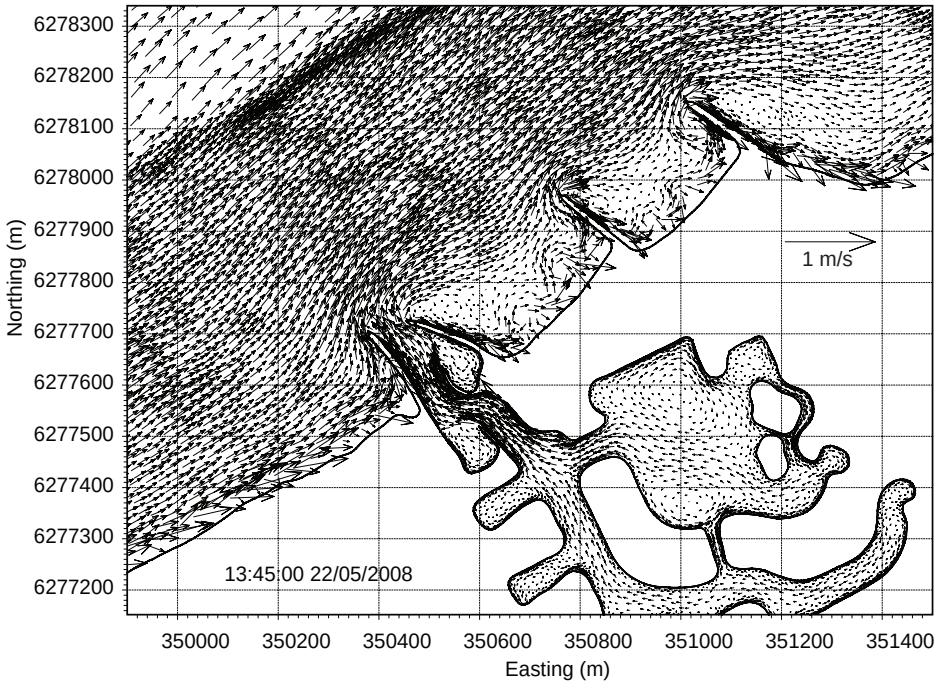

Figure 10.6 Snapshot of predicted current pattern during south-westerly winds in the vicinity of Port Geographe, for the existing groyne configuration.

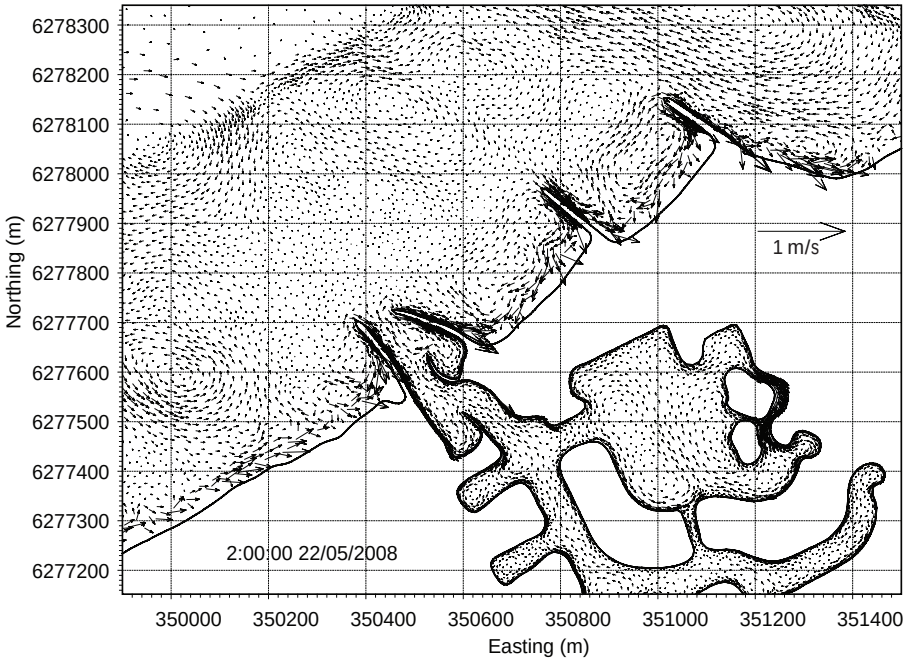

Figure 10.7 Snapshot of predicted current pattern during weak winds in the vicinity of Port Geographe, for the existing groyne configuration.

The velocity field during north-easterly winds highlights the anti-clockwise eddy circulation (Figure 10.5) in the lee of the groynes; clockwise eddy circulation occurs during south-westerly winds (Figure 10.6). During the period of wind direction transition and weak winds, low current speed eddies were generated in the off-shore sand bar areas (Figure 10.7).

Representative circulation patterns for a region west of the Port Geographe are best shown using the vector plots which correspond to the passage of a winter cold front between July 17 and 18 2008 (Figure 10.8 - Figure 10.12). Winds started from the south-east (Figure 10.8), then with the passage of the front rotated to east-north-easterlies (Figure 10.9), north-easterlies (Figure 10.10), westerlies (Figure 10.11), and finally southerlies (Figure 10.12) in a counter-clockwise manner, over a period of two days. Depth-averaged circulation patterns are shown for the corresponding wind conditions. This time period was chosen for simulation as it corresponds to an event in which wrack moved onto and off the beaches at nearby sites (Figure 9.4).

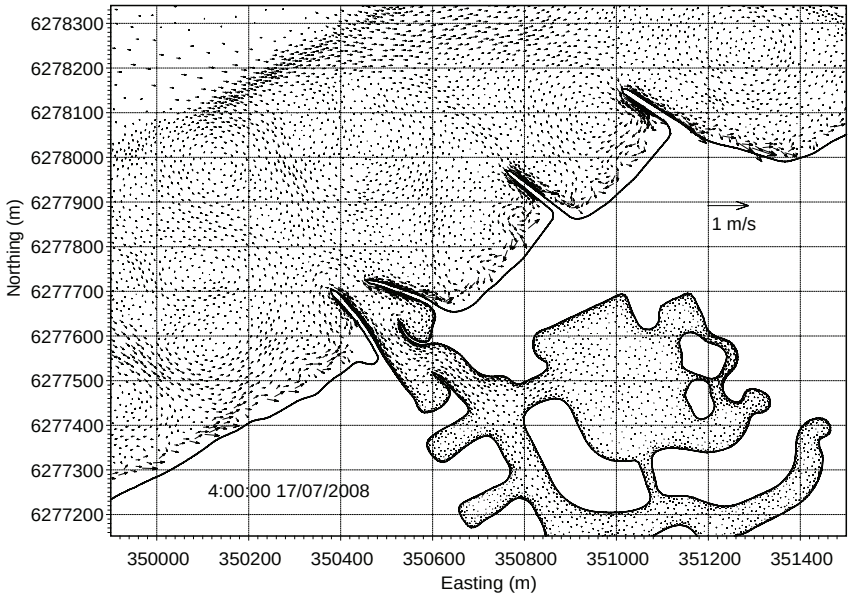

Figure 10.8 Predicted current pattern in the Port Geographe area at 4 am July 17 under south-easterly winds, for the existing groyne configuration.

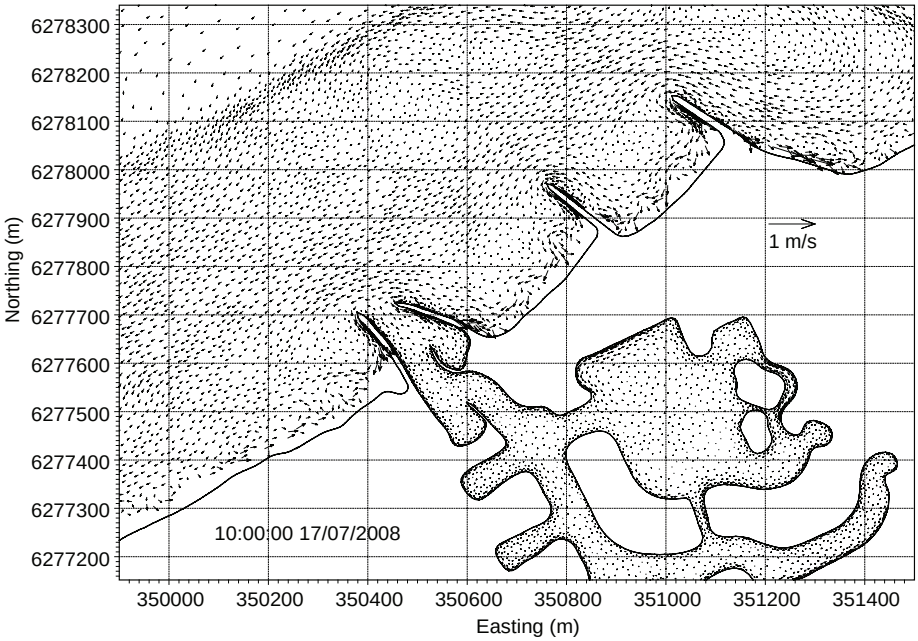

Figure 10.9 Predicted current pattern in the Port Geographe area at 10 am July 17 under east-north-easterly winds, for the existing groyne configuration.

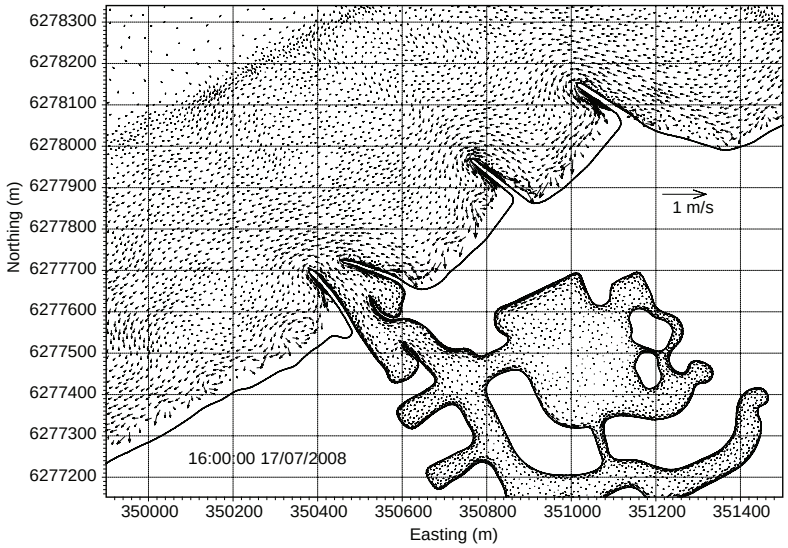

Figure 10.10 Predicted current pattern in the Port Geographe area at 4 pm July 17 under north-easterly winds, for the existing groyne configuration.

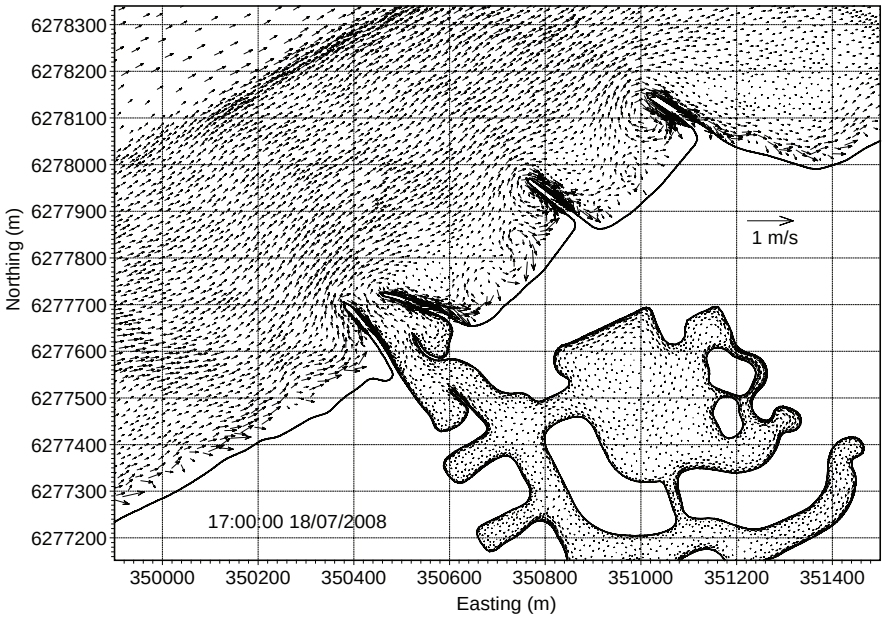

Figure 10.11 Predicted current pattern in the Port Geographe area at 9 pm July 18 under westerly winds, for the existing groyne configuration.

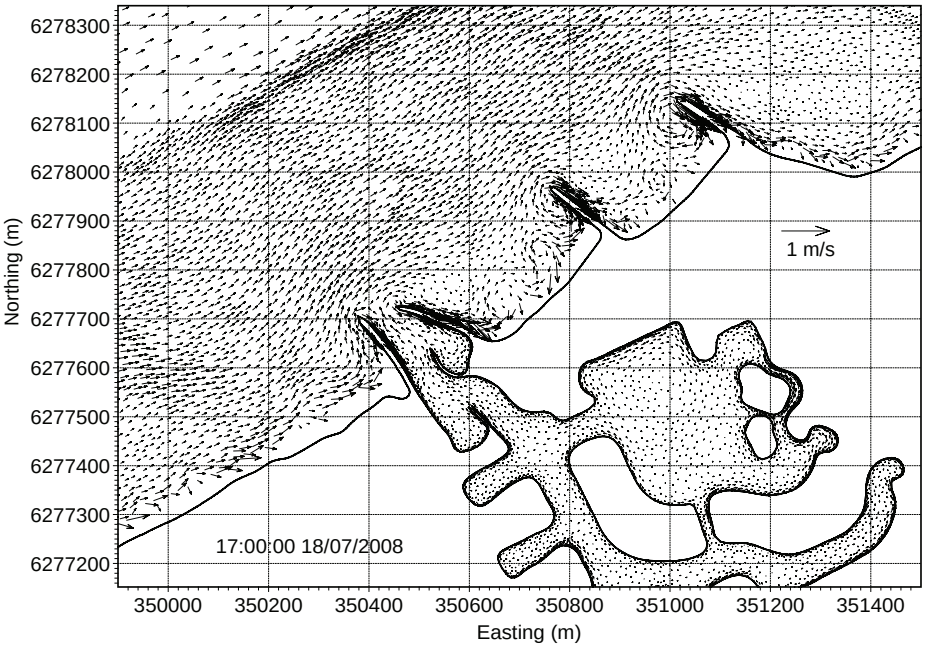

Figure 10.12 Predicted current pattern in the Port Geographe Area at 5 pm July 18 under southerly winds, for the existing groyne configuration.

Winds were < 5 m s^{-1} from the south-east as a high pressure system moved to the south of the state. Currents were uniformly weak and moving alongshore towards the north-east. Current velocities were generally less than 0.10 m s^{-1}, though slightly higher near the shoreline. Eddies were present around the offshore sand bars and current speeds were negligible in the deeper areas.

The high-pressure system moved further east and the winds remained relatively light. The circulation patterns appear similar to Figure 10.10 but with the circulation reversed, with along-shore currents now flowing from east to west (Figure 10.11). The approaching storm front caused the winds to shift from the north and to increase to about 7 m s^{-1}. Current speeds were still quite low but circulation ceased to be dominated by the along-shore component and flow patterns were highly variable. Bottom topography seemed to have a large influence on flows which locally intensified around eddies and near shore regions. Waves were entering the area from the northwest and may explain some of the variation in currents near shore. The full force of the storm was affecting all of Geographe Bay. Winds were from the west with speeds > 13 m s^{-1}. Circulation again changed direction and strong currents (0.30- 0.50 m s^{-1}) were uniformly flowing along-shore, from west to east. Current speeds were higher along-shore, but were also relatively strong offshore. Eddies caused by the bathymetric gradient (sand bar) were absent. However clockwise eddies appeared at the tip of groynes. Current speeds were much smaller and variable in direction between the eastern groyne fields.

Another high-pressure system moved into the area and the winds shifted to the south but were still blowing at 8 m s^{-1}. Current speeds dropped to less than 0.10 m s^{-1} for the majority of the region but locally were still up to 0.25 m s^{-1} (Figure 10.12). The flow direction was along-shore towards the northeast but more variable in direction and speed. Eddies were again visible surrounding offshore sand bars.

The predicted flow patterns at the peak of storm events on 18 July and 30 July 2008 are shown in Figure 10.13 and Figure 10.14 respectively. The flows were strong at the western part of the marina and offshore region of the groynes. Strong currents (0.30- 0.50 m s^{-1}) were uniformly flowing along-shore from west to east. Jet-like flow nearly reached the tip of the groynes and their side walls, while flow speeds between the groyne fields were small and variable in direction.

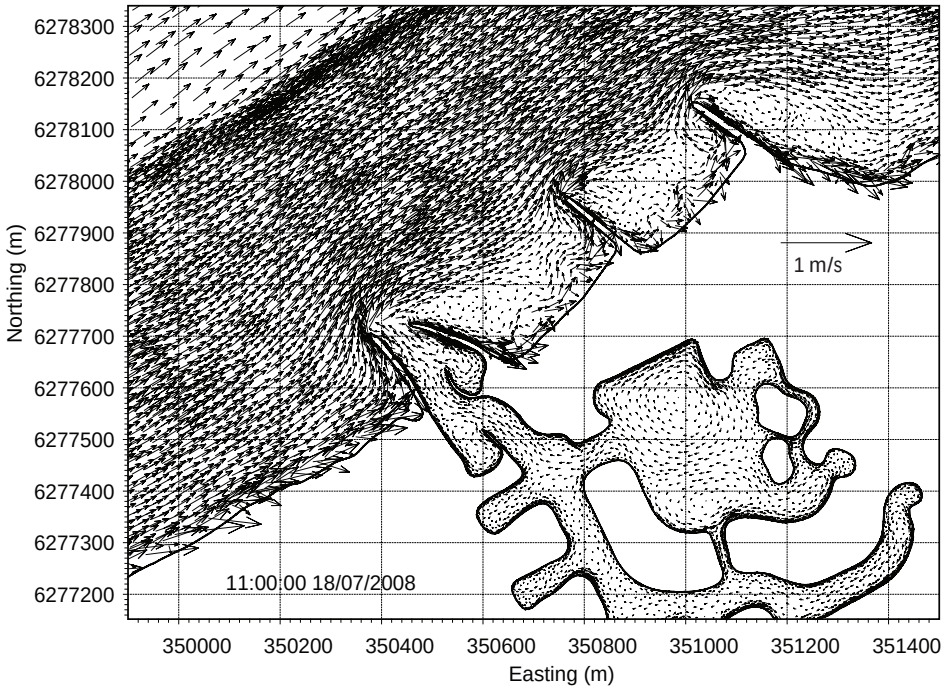

Figure 10.13 Predicted current pattern in the Port Geographe area at the peak of storm on July 18 for the existing groyne configuration.

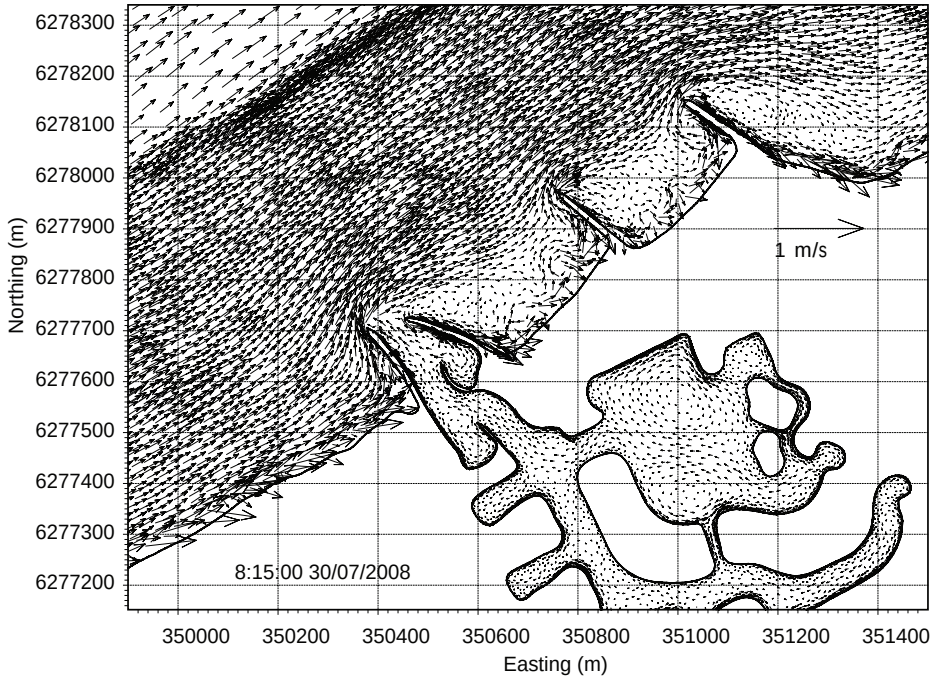

Figure 10.14 Predicted current pattern in the Port Geographe area at the peak of storm on July 30 for the existing groyne configuration.

The predicted seagrass accumulation on the beach and near-shore areas is shown in Figure 10.15. At the end of August, most of the seagrass wrack was accumulated on the western shoreline of the marina. As expected, seagrass wrack was also accumulated within the pocket beach groynes. Some seagrass wrack was deposited in the nearshore regions, most likely due to flow modification by bathymetric irregularities.

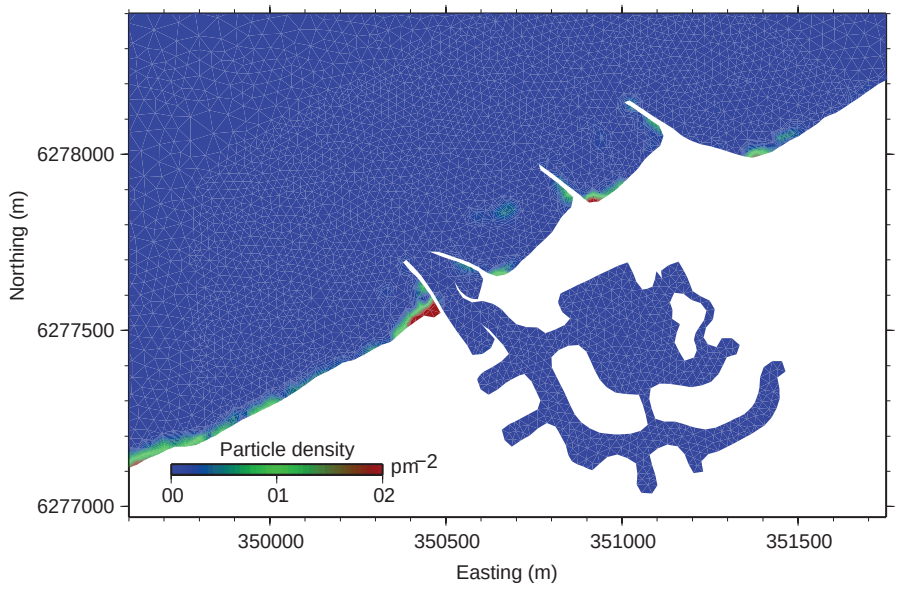

Figure 10.15 Locations of predicted seagrass wrack accumulation on the beach in the vicinity of Port Geographe, at the end of August 2008, for the existing groyne configuration.

10.2 Hydrodynamic and particle transport simulations – the scenarios

The Port Geographe groynes are the primary structural cause of the wrack accumulations west of the development and in the pocket beaches (Moonlight Bay). Removing the structural cause of the problem will achieve a reduction in wrack accumulation, maintain amenity in the areas currently affected by accumulations and ensure a close to natural supply of seagrass wrack to beaches east of the development. It should be noted that the structures are in place to maintain sufficient depth through the marina entrance channel, to ensure safe navigation; the depth of the marina entrance channel is mainly governed by sand transport.

Current speed and direction, water levels, wave climate (wave heights, direction etc.) will be changed as a result of the groyne modifications and other morphological changes in the Port Geographe area, thus changes in the seagrass transport would be expected. In addition, knowledge of the flow patterns can help to understand the possible location of sand and seagrass accumulation.

The validated model was used to assess the impact on the hydrodynamics and wave climate, of such measures as:

- changing the dimensions of the Port Geographe groynes,
- the orientation and shape of the groynes,
- narrowing the entrance channel,
- mechanically pumping water out through the canal system during tide transitions from high to low,
- shoreline changes (with and without the western beach, vertical groynes etc).

MJ Paul and Associates [2005] proposed six possible groyne re-configurations (Figure 10.16). Four key design features were contained within the MJ Paul configurations:

1. variable length of the western training wall,
2. addition of a groyne on the eastern side of the marina entrance channel,

3. addition of a spur groyne to the east of the development, and

4. extension of the pocket beaches to the east of the marine entrance channel.

Three additional design features were also considered for testing as part of the present study:

1. varying the orientation of the western beach,

2. varying the width of the marina entrance channel, and

3. pumping of water into the canals to enhance ebb velocities through the marina entrance channel.

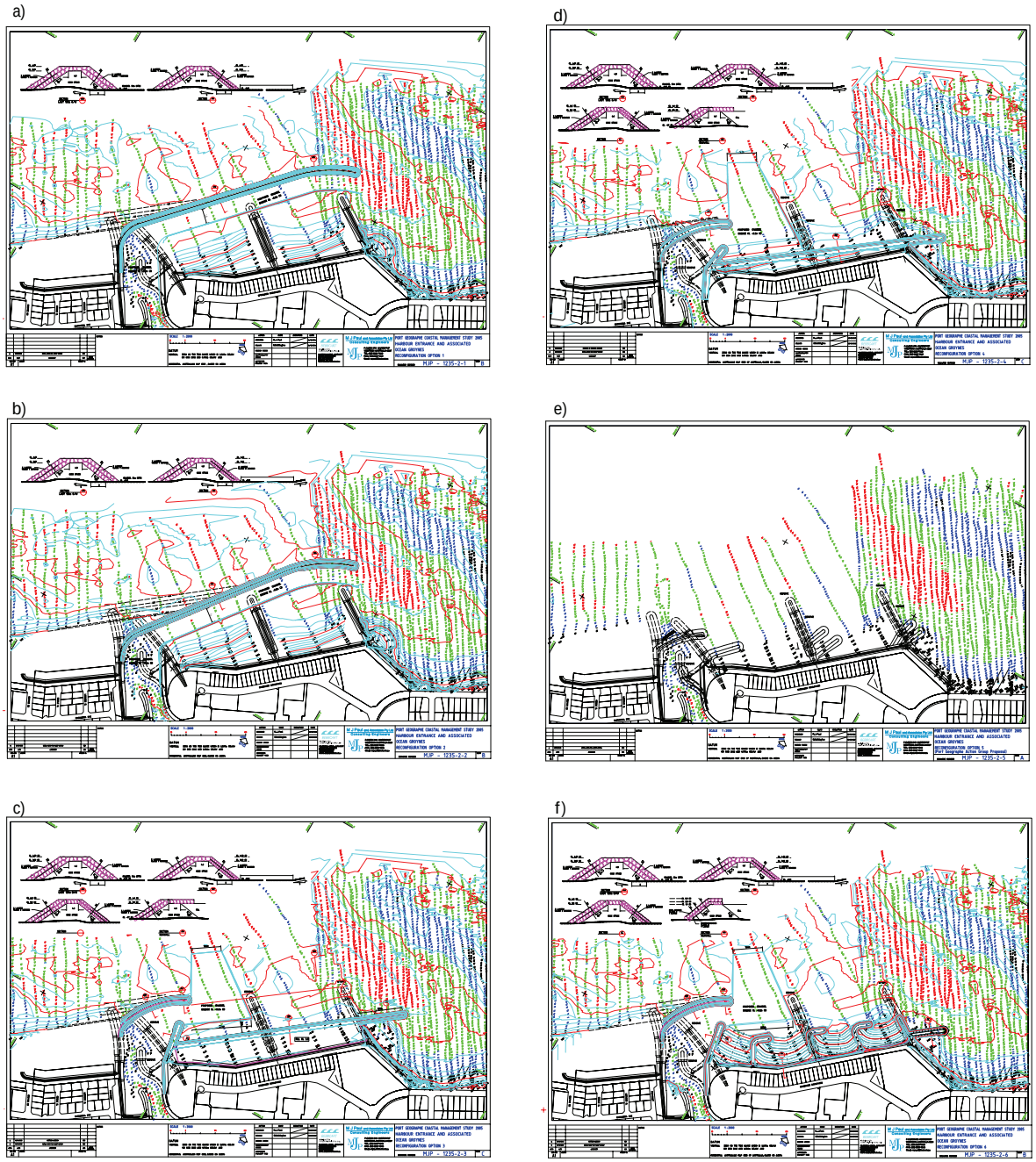

Figure 10.16 The six groyne configurations originally proposed by MJ Paul and Associates Pty Ltd [2005]. a) MJP Option 1; b) MJP Option 2; c) MJP Option 3; d) MJP Option 4; e) MJP Option 5; f) MJP Option 6.

Options 3 and 6 (Figure 10.16c and Figure 10.16f) were considered representative of the key design elements within the MJ Paul configurations and were therefore selected for modelling. The additional design features were included in a further five configurations as summarised in Table 10.1 and described in more detail in the following sections. A total of seven scenarios were modelled, plus the current groyne configuration. The mesh grids were reconstructed for each of the proposed groyne re-configurations.

Table 10.1 Summary of main features of the re-configuration of the Port Geographe coastal structures for each of the modelled scenarios.

SCENARIO (FIGURE)	ORIGIN	WESTERN BEACH ADDED	WESTERN TRAINING WALL	ENTRANCE CHANNEL	EASTERN GROYNES	EASTERN SPUR GROYNE	PUMPING	CANAL DEVELOPMENT STAGES
0	Current configuration							
1	MJ Paul Option 3	No	Curved to the east	Wide	No	Yes	No	Stage 1
2	MJ Paul Option 6	No	Curved to the east	Wide	Yes	Yes	No	Stage 1
3	Steering Committee Option 1	Yes	Curved to the east	Narrow, eastern side concave	No	No	No	Stage 2
4	Steering Committee Option 2	Yes	Curved to the east	Narrow, eastern side concave	No	No	Yes, from high to low tide	Stage 2
5	Steering Committee Option 3	Yes, with further smoothing	Curved to the east	Narrow, eastern side convex	No	No	No	Stage 2
6	Steering Committee Option 4	No	Oblique, easterly orientation	Narrow, eastern side convex	Yes, but shortened	No	No	Stage 2
7	Steering Committee Option 5	Yes, with additional extension	Current configuration	Current configuration	Yes	No	No	Stage 1

Initially, the hydrodynamic model was run with the model forced by wind, wave and water levels. Then the particle transport model was run simulating seagrass wrack transport under the proposed configurations. In order to compare the different scenario predictions, all model runs were carried out using data from 1 May 2008 to Sep 2008. The same control parameters (friction coefficient, eddy viscosity etc.) were used for all model scenarios.

10.2.1 Scenario 1

The fine mesh grid, with element lengths of 10 - 20 m, for Scenario 1 is shown in Figure 10.17. The bathymetry was interpolated and smoothed onto the mesh grids. The wind field interpolated onto the mesh grids for the Scenario 1 configuration are shown in Figure 10.18.

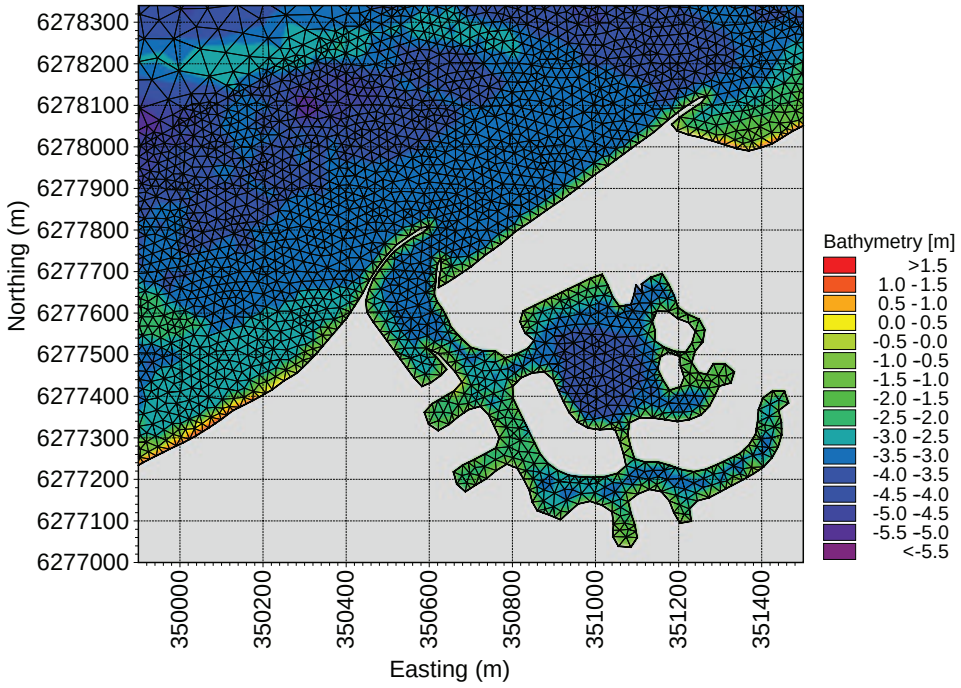

Figure 10.17 Scenario 1: the fine mesh grid and interpolated bathymetry.

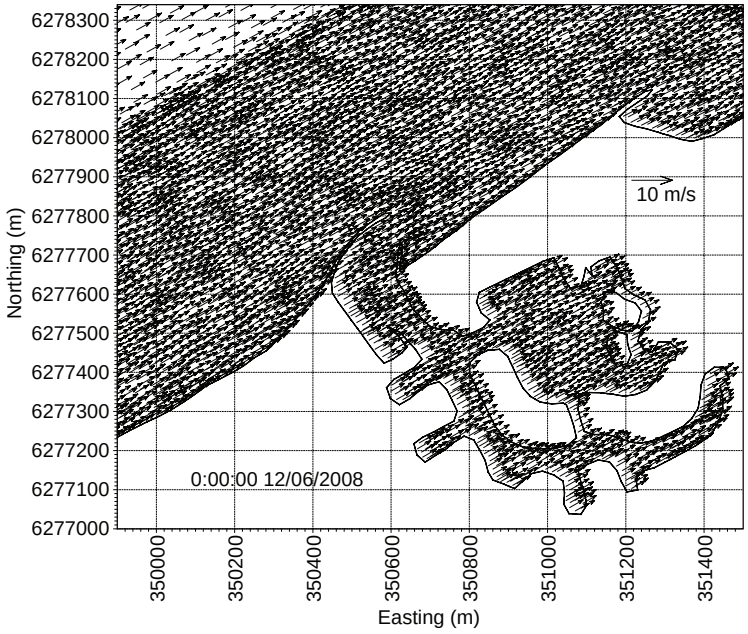

Figure 10.18 Scenario 1: a snapshot of the wind field interpolated onto the mesh grid.

A change in current speeds near Port Geographe was to be expected, although water levels were not much affected. A comparison of predicted sea level inside and outside Port Geographe (AWAC site) are shown in Figure 10.19. As Scenario 1 was similar to the existing configuration, there was no significant damping or choking of sea levels through the entrance channel. The seiche-induced currents were superimposed over the tidal currents and dominated the entrance channel (Figure 10.20).

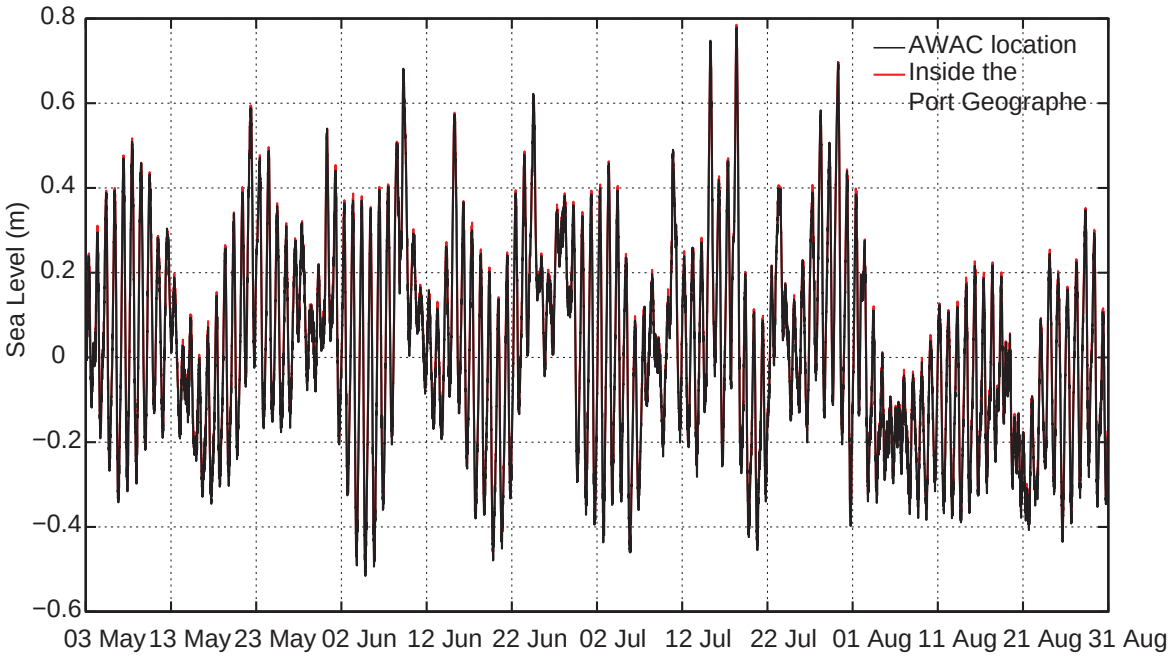

Figure 10.19 Scenario 1: the predicted sea level at the AWAC site (red line) and inside the Port Geographe (black line).

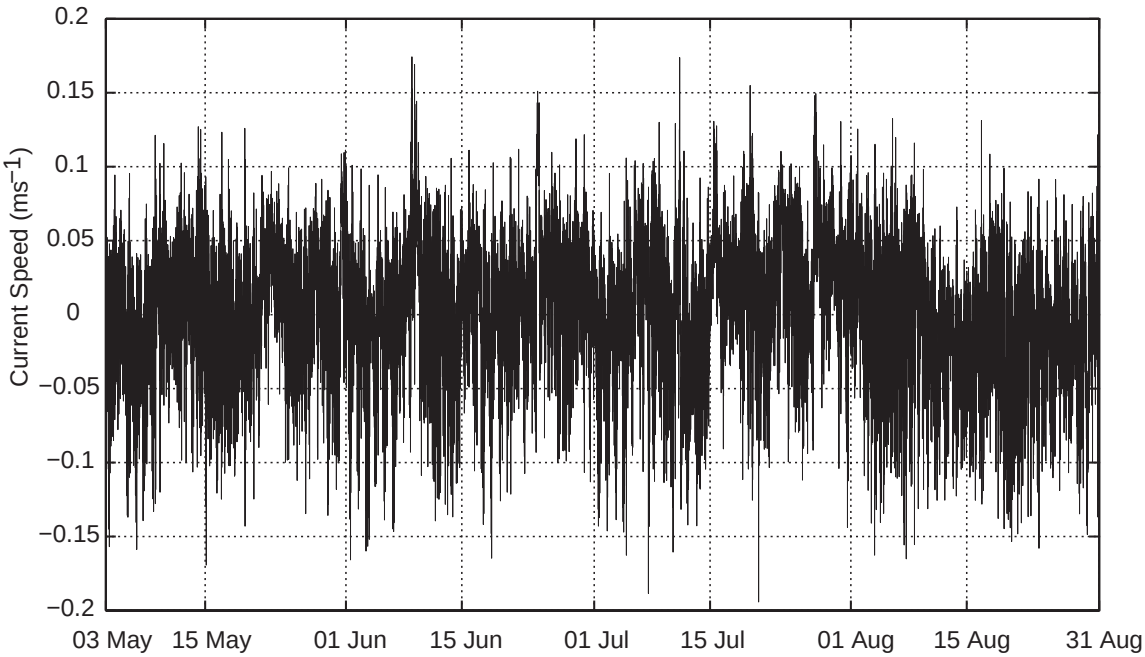

Figure 10.20 Scenario 1: the predicted mean current speeds (average speeds perpendicular to the channel) through the Port Geographe entrance channel.

The vector plots of velocity fields under different conditions (easterly winds, westerly winds, weak winds, peak of storm events etc.) are shown in Figure 10.21 – Figure 10.25. Inspection of these figures clearly shows that Scenario 1 significantly altered the flow pattern in the vicinity of the Port Geographe. During easterly and westerly winds, eddies were not visible on the western shoreline; flows were smooth and parallel to the coast. It appears that this scenario would easily allow seagrass wrack to be transported from the western side of the marina entrance channel to the eastern side. However, during westerly winds clockwise eddies were formed at the tip of the groynes, which could cause accumulation of seagrass wrack on the eastern side of the channel; from there, the wrack could enter the entrance channel during flood currents. There was also a clockwise eddy circulation at the eastern end of the spur groyne during westerly winds.

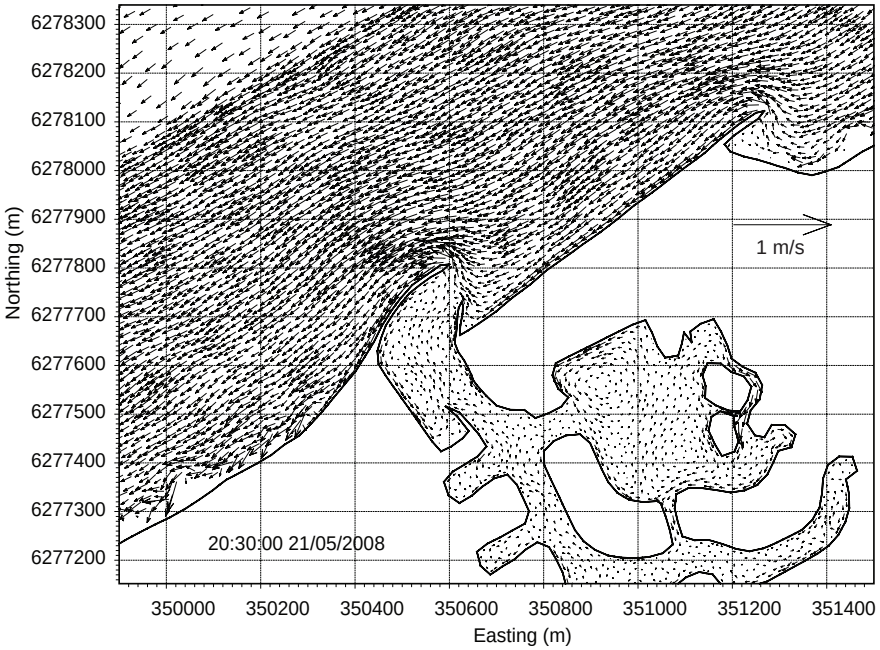

Figure 10.21 Scenario 1: a snapshot of predicted currents during easterly winds, in the vicinity of Port Geographe.

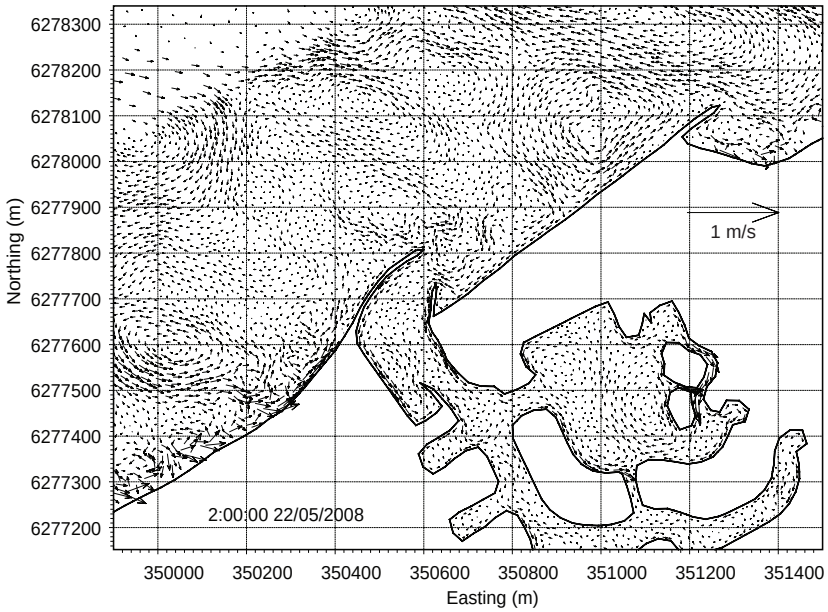

Figure 10.22 Scenario 1: a snapshot of predicted currents during weak winds (a period of wind direction transition), in the vicinity of Port Geographe.

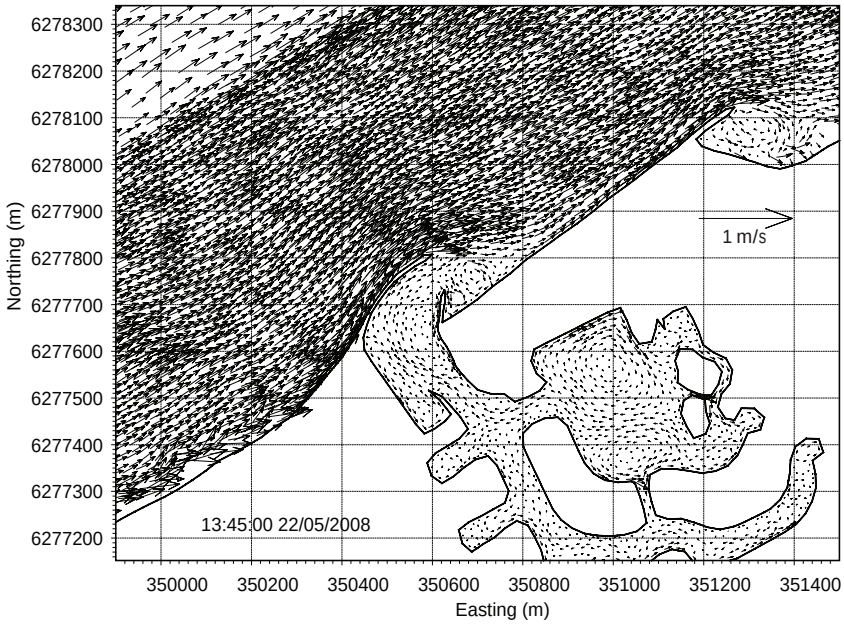

Figure 10.23 Scenario 1: a snapshot of predicted currents during westerly winds, in the vicinity of Port Geographe.

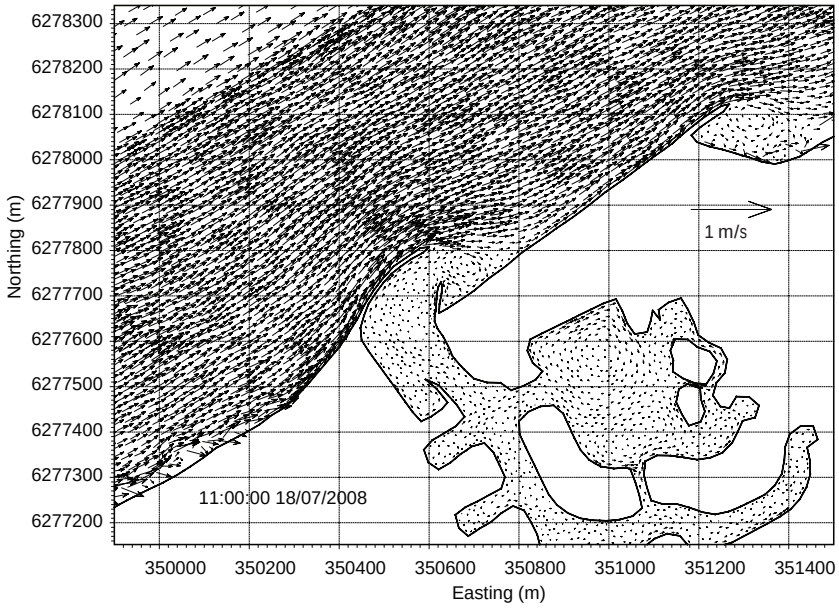

Figure 10.24 Scenario 1: predicted currents in Port Geographe area, at the peak of a storm on July 18.

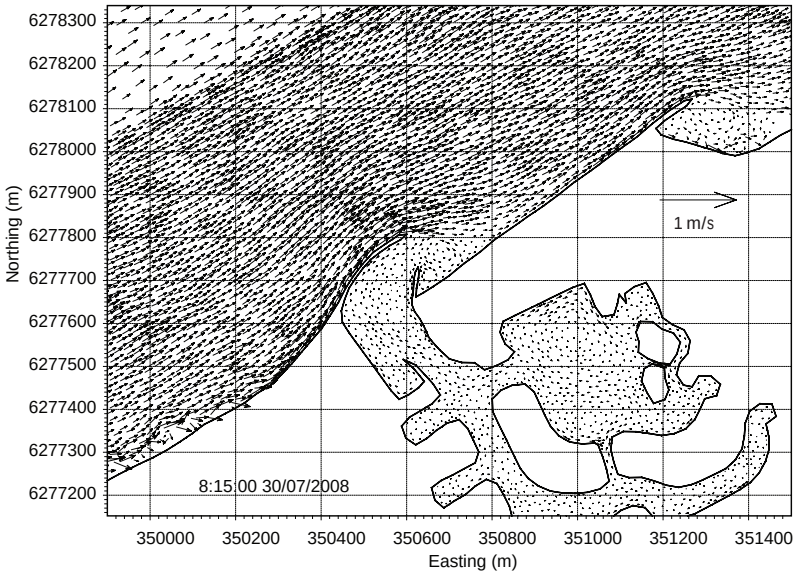

Figure 10.25 Scenario 1: predicted currents in Port Geographe area, at the peak of a storm on July 30.

Predictions of seagrass wrack accumulations for Scenario 1 indicated that it is possible to alter the orientation of the western training wall such that will seagrass wrack will not accumulate on the western beach. However, there were large accumulations within the marina entrance (Figure 10.26).

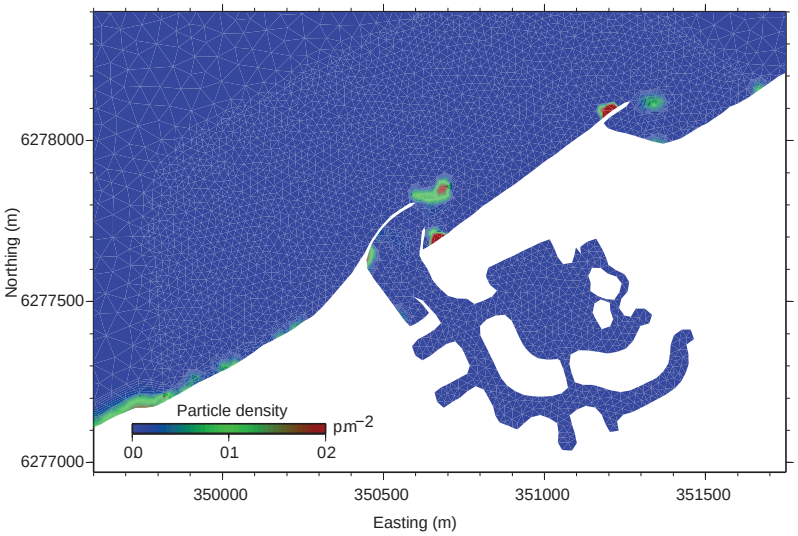

Figure 10.26 Scenario 1: Locations of predicted seagrass wrack on the beach in the vicinity of Port Geographe, at the end of August 2008.

10.2.2 Scenario 2

In Scenario 2, the western training wall configuration was similar to Scenario 1, however additional groynes were added at the eastern side of the marina entrance. The mesh grid and interpolated bathymetry onto the meshes are shown in Figure 10.27. The wind field interpolated onto the mesh is shown in Figure 10.28.

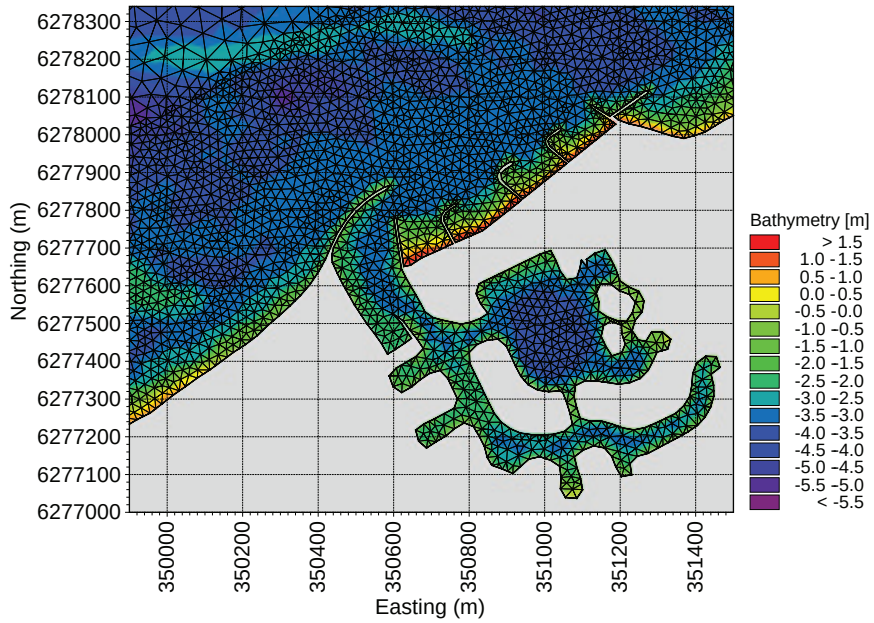

Figure 10.27 Scenario 2: the fine mesh grid and bathymetry interpolated onto the mesh.

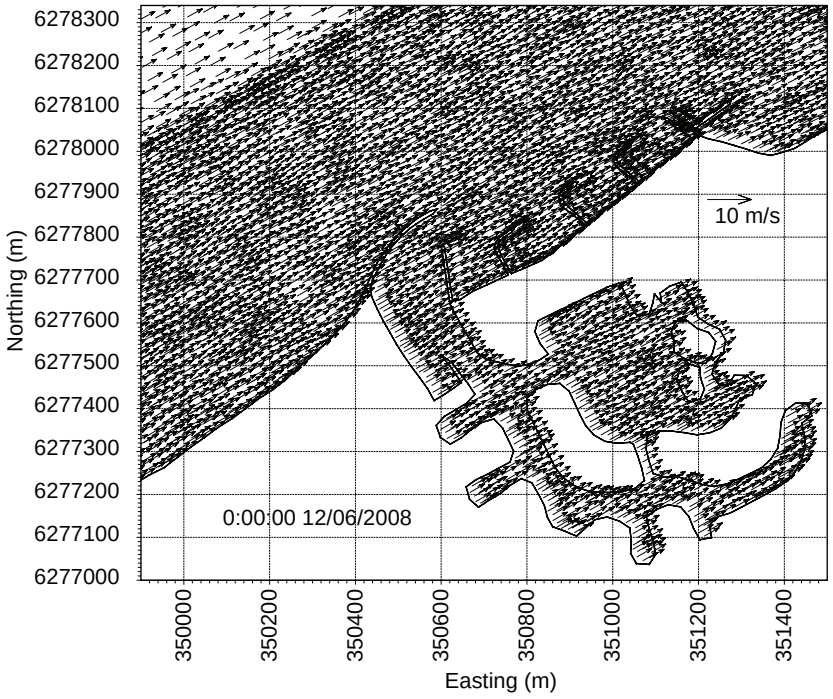

Figure 10.28 Scenario 2: a snapshot of the wind field interpolated onto the mesh.

A comparison of predicted water levels inside and outside Port Geographe (AWAC site) are shown in Figure 10.29. The water level fluctuations inside and outside are almost the same with no frictional or hydraulic damping through the entrance channel. As with the existing configuration and Scenario 1, flows through the entrance channel were driven by the water level fluctuations. However, the predicted maximum current speeds through the entrance channel were slightly smaller than those predicted for the existing conditions and for Scenario 1 (Figure 10.30).

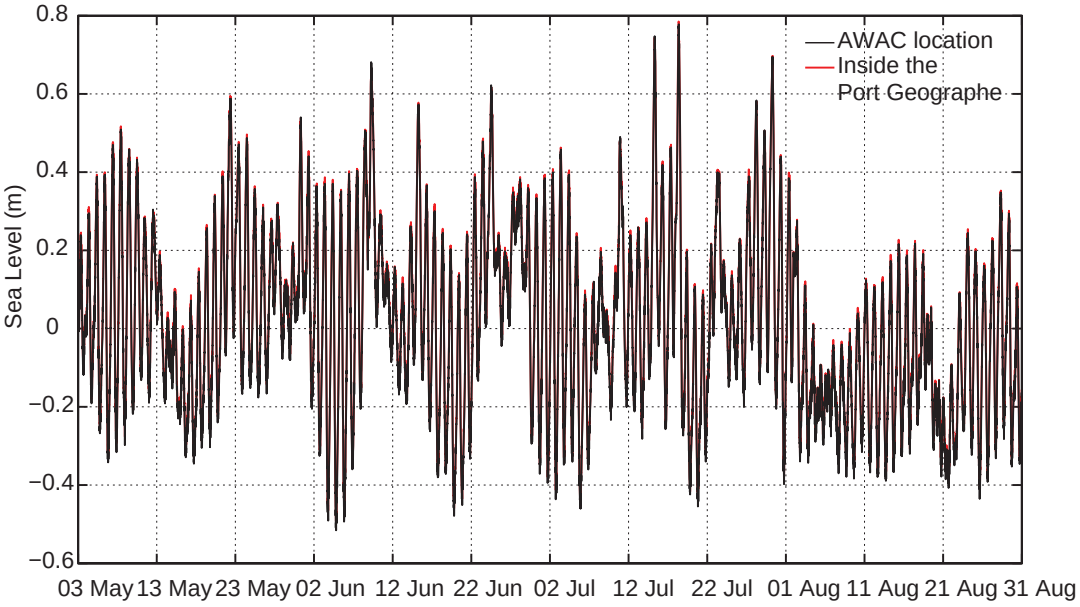

Figure 10.29 Scenario 2: the predicted sea level at the AWAC site (black line) and inside Port Geographe (red line).

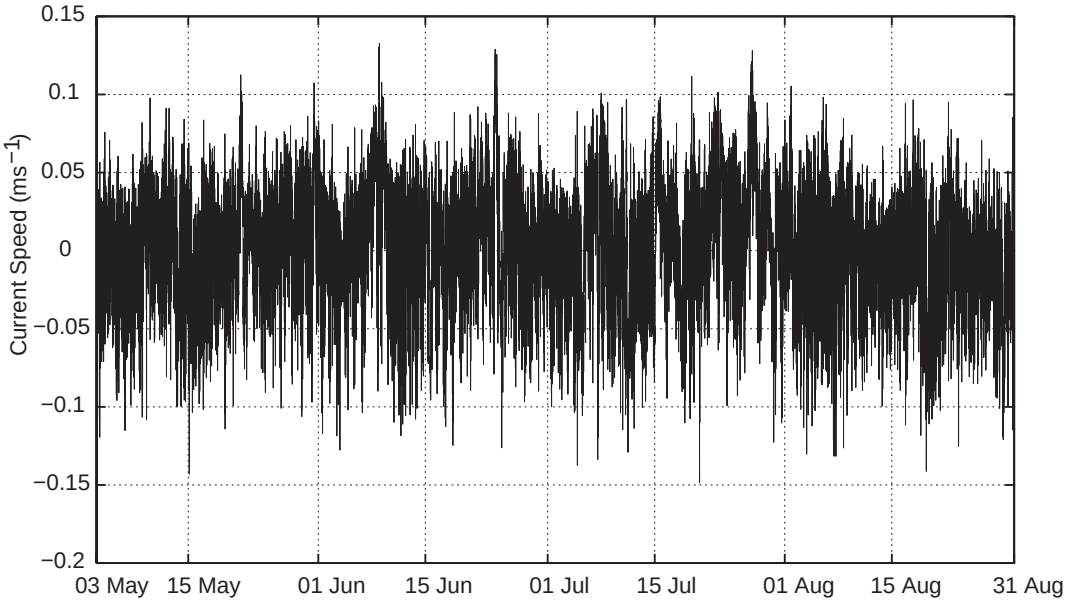

Figure 10.30 Scenario 2: the predicted mean current speeds through the Port Geographe entrance channel.

The predicted current patterns at the vicinity of Port Geographe during north-easterly and south-westerly winds are shown in Figure 10.31 and Figure 10.32 respectively. Clockwise eddies are formed inside the Moonlight Bay groynes and in the marina entrance channel during both north-easterly and south-westerly winds. Eddies with reduced velocities close to the groynes may result in rapid sand deposition and seagrass accumulation. Comparison of the predicted flows for Scenario 1 and Scenario 2 showed that the curved western training wall enhanced current speeds along the western shoreline. During weak winds, low current clockwise and counter-clockwise eddies were generated at the offshore sand bar area, as well as in the nearshore areas (Figure 10.33).

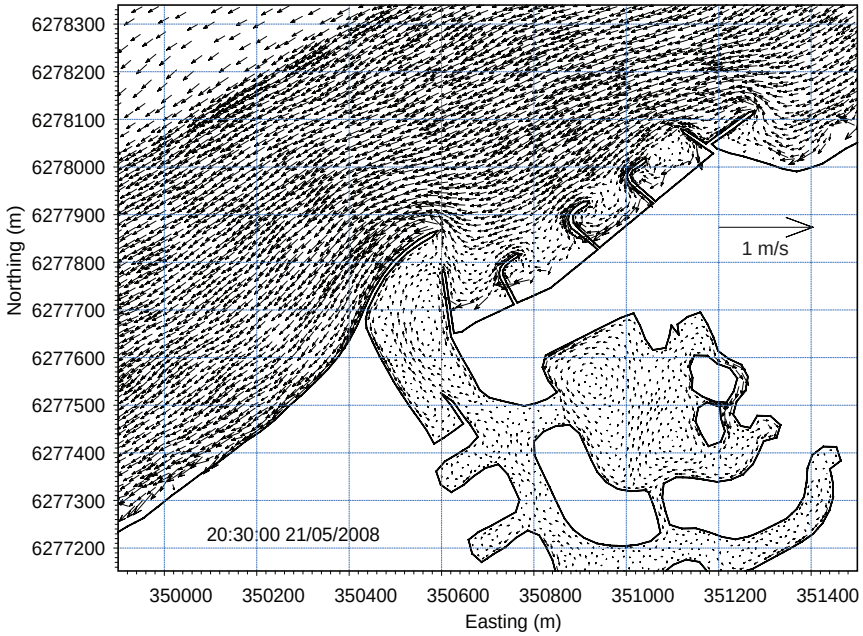

Figure 10.31 Scenario 2: a snapshot of predicted currents in the vicinity of Port Geographe, during north-easterly winds.

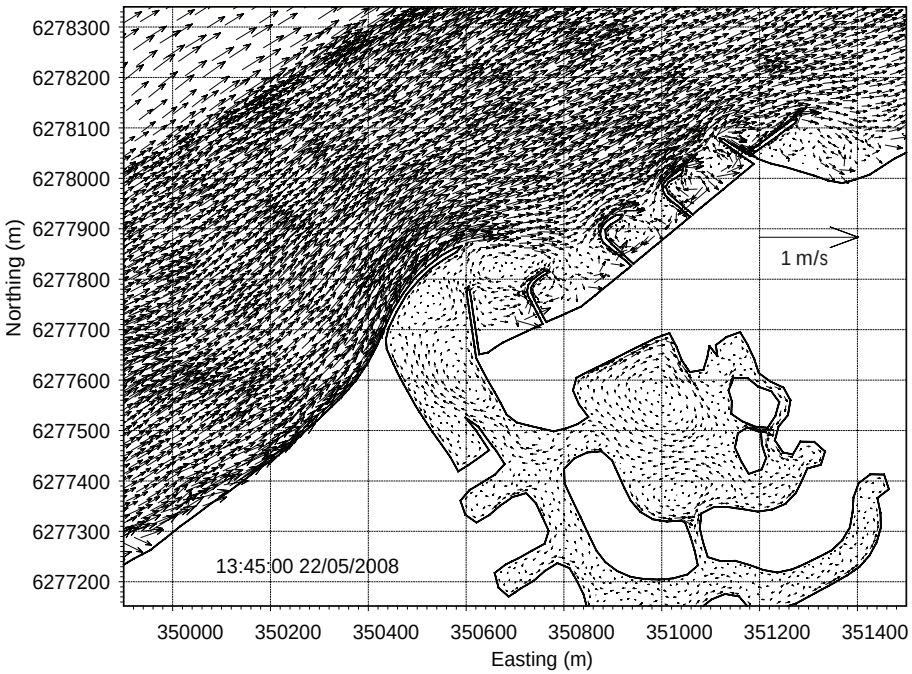

Figure 10.32 Scenario 2: a snapshot of predicted currents in the vicinity of Port Geographe, during south-westerly winds.

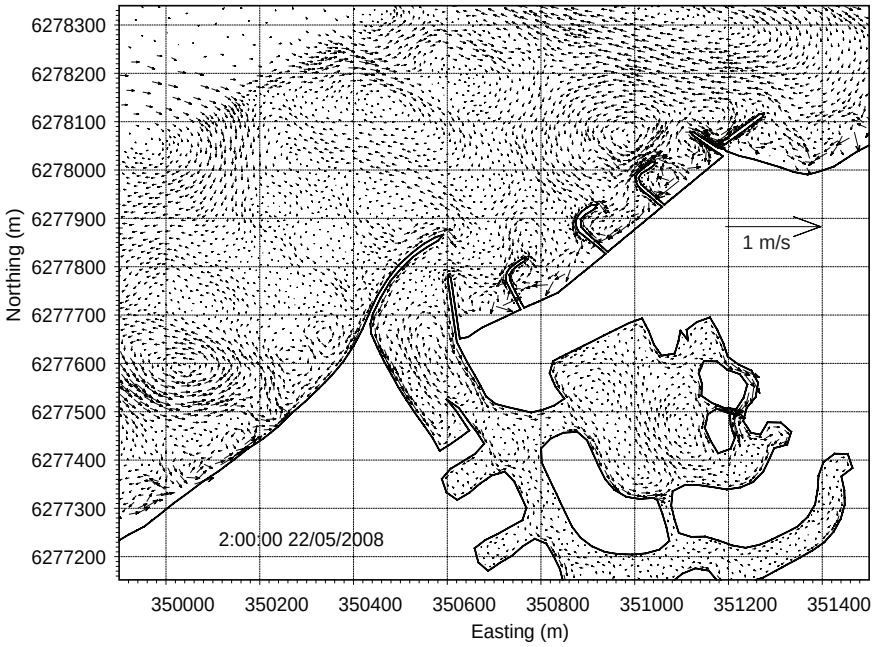

Figure 10.33 Scenario 2: a snapshot of predicted currents in the vicinity of Port Geographe, during a period of weak winds.

The predicted currents at the peak of the storms on 18 July and 30 July are shown in Figure 10.34 and Figure 10.35 respectively. Current speeds were strong at the western shoreline and immediately offshore of the groynes. Flows were smooth and parallel to the shoreline west of the entrance channel. However, at the tip of the groynes, clockwise eddies formed and low current speed eddies were visible between the eastern side of the groynes.

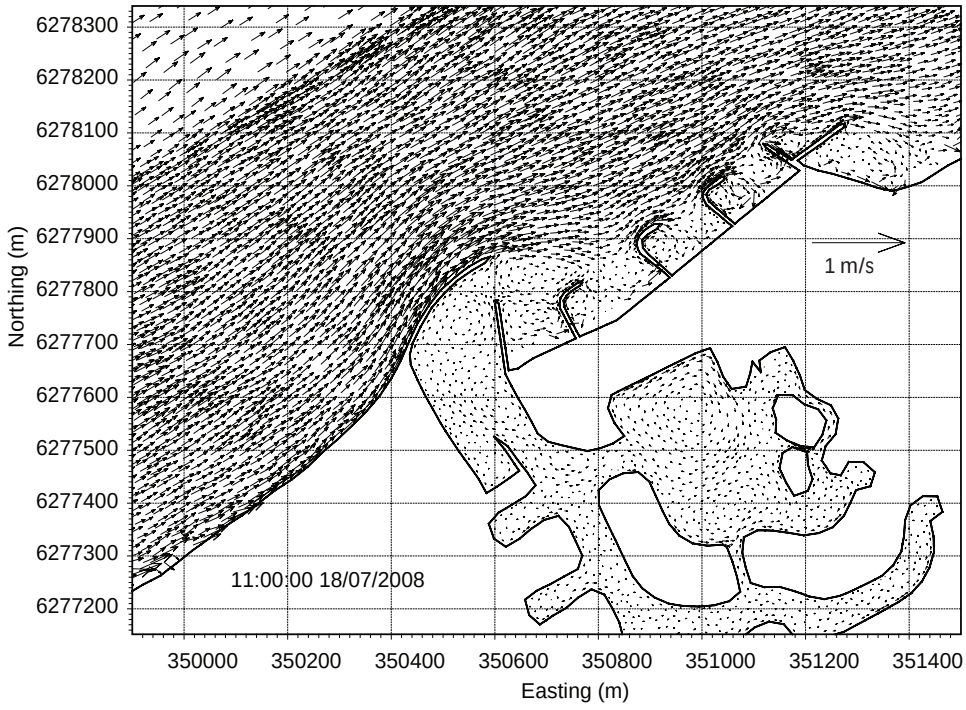

Figure 10.34 Scenario 2: predicted currents in the Port Geographe area, at the peak of the storm on July 18.

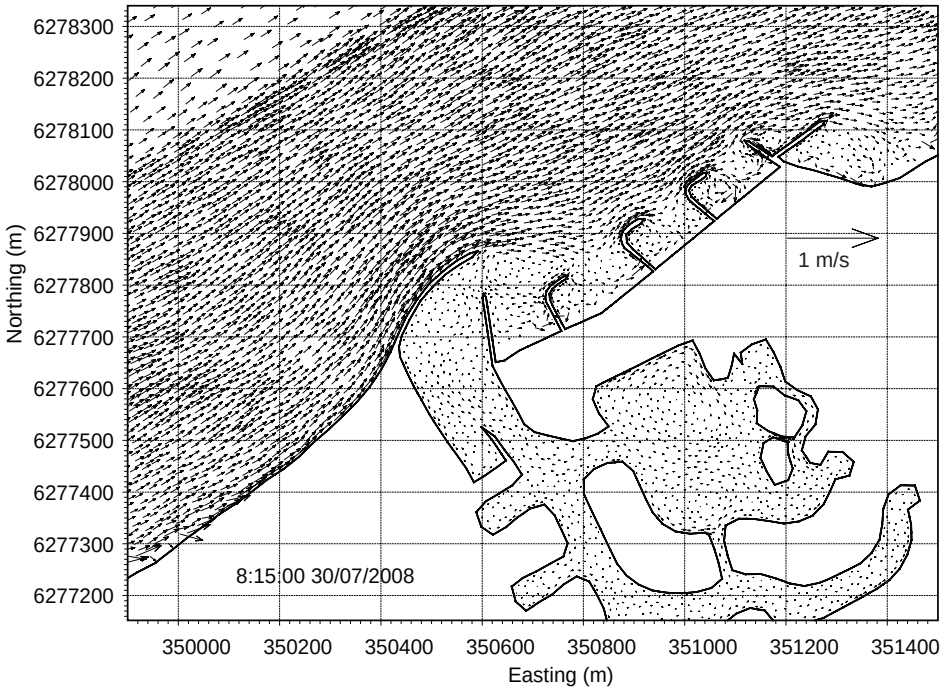

Figure 10.35 Scenario 2: predicted currents in the Port Geographe area, at the peak of storm on July 30.

Scenario 2 trapped sea grass wrack within the proposed groynes on the eastern side of the marina entrance (Moonlight Bay) and in the entrance channel (Figure 10.36). Therefore it was decided not to undertake any further investigation of Scenario 2.

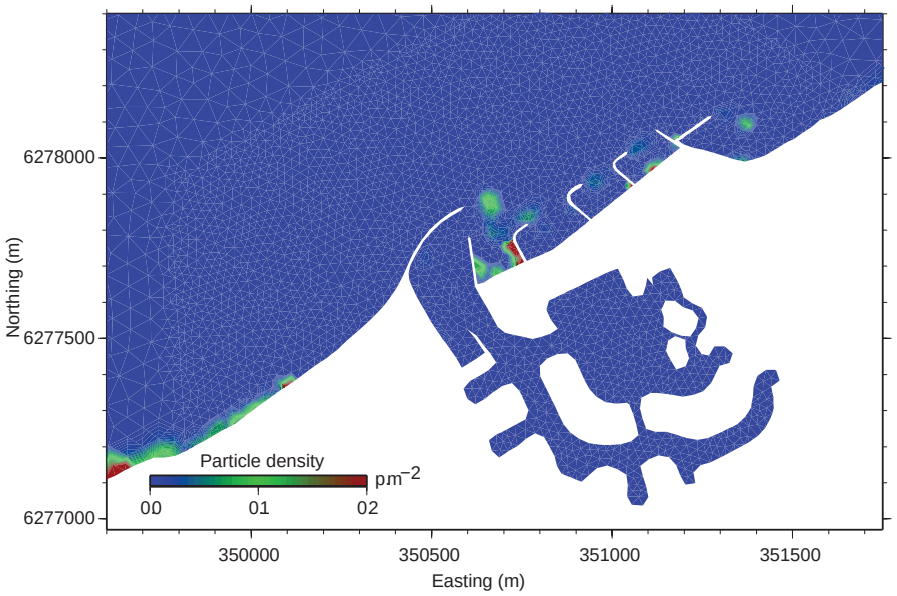

Figure 10.36 Scenario 2: locations of predicted seagrass wrack accumulation in the vicinity of Port Geographe, at the end of August 2008.

10.2.3 Scenario 3

Based on the simulated flow patterns, eddy formation, entrance current speeds, flow patterns at the breakwaters and seagrass accumulation, for the existing groyne configuration and Scenario 1 and 2, several additional groyne configurations were suggested by the Steering Committee for further simulations. The main objectives of these additional scenarios were:

- addition of a beach on the western side of western training wall,
- minimal alterations to the existing groynes,
- modification of the pocket beache groynes (Moonllight Bay),
- narrowing of the marina entrance channel to increase the flow speed through the channel,
- curving the edges of the eastern breakwater,
- changing the orientation and length of the western training wall as included in Scenario 1 and Scenario 2,
- including Stage 2 of the canal development, and
- incorporating pumping in the upper canal during the outgoing tide to increase velocities through the entrance and enhance the flushing of wrack from the marina entrance channel.

Scenario 3 (without pumping) and Scenario 4 (with pumping) used the same configuration; the pocket beach groynes were removed and the eastern breakwater had a concave shape. The mesh grid and interpolated bathymetry for Scenario 3 are shown in Figure 10.37. The wind field interpolated onto the mesh is shown in Figure 10.38.

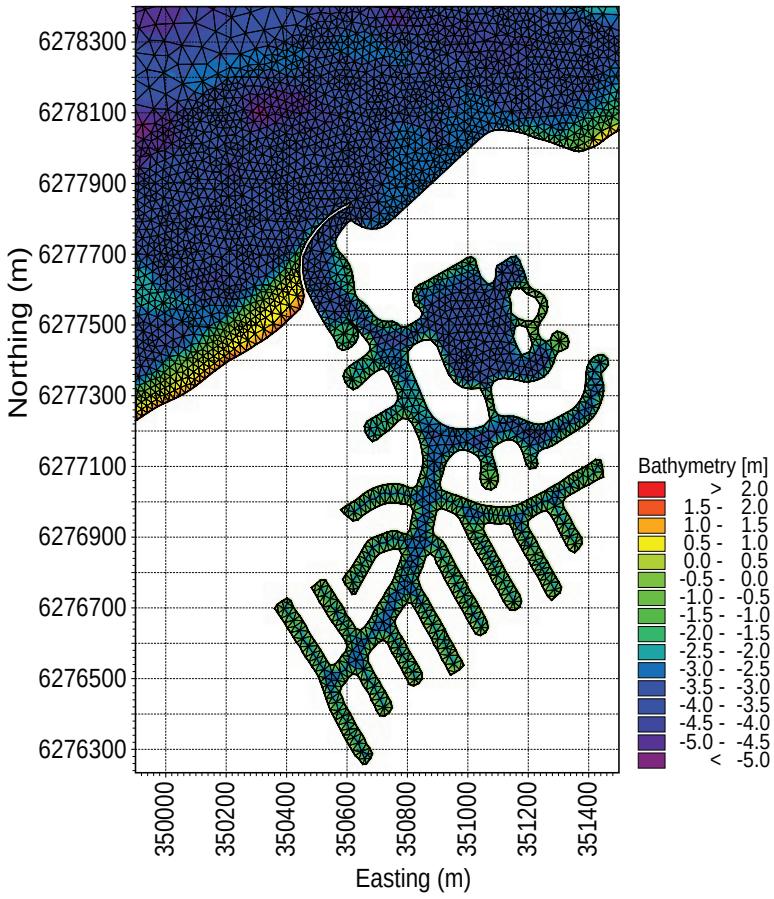

Figure 10.37 Scenario 3: the fine mesh grid and bathymetry interpolated onto the mesh.

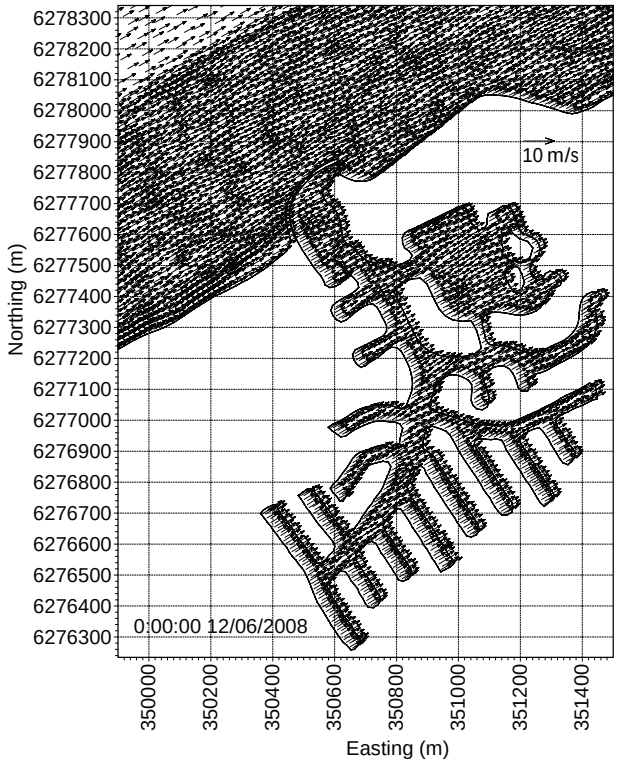

Figure 10.38 Scenario 3: a snapshot of the wind field interpolated onto the mesh grid.

Inspection of the predicted water levels inside and outside Port Geographe shows slight damping through the entrance channel; both tidal and seiche amplitudes are slightly smaller compared to outside the port (Figure 10.39). The mean water levels inside the port were marginally higher than those outside. This may result in slightly higher outflows due to increased pressure gradient through the entrance during ebb tide.

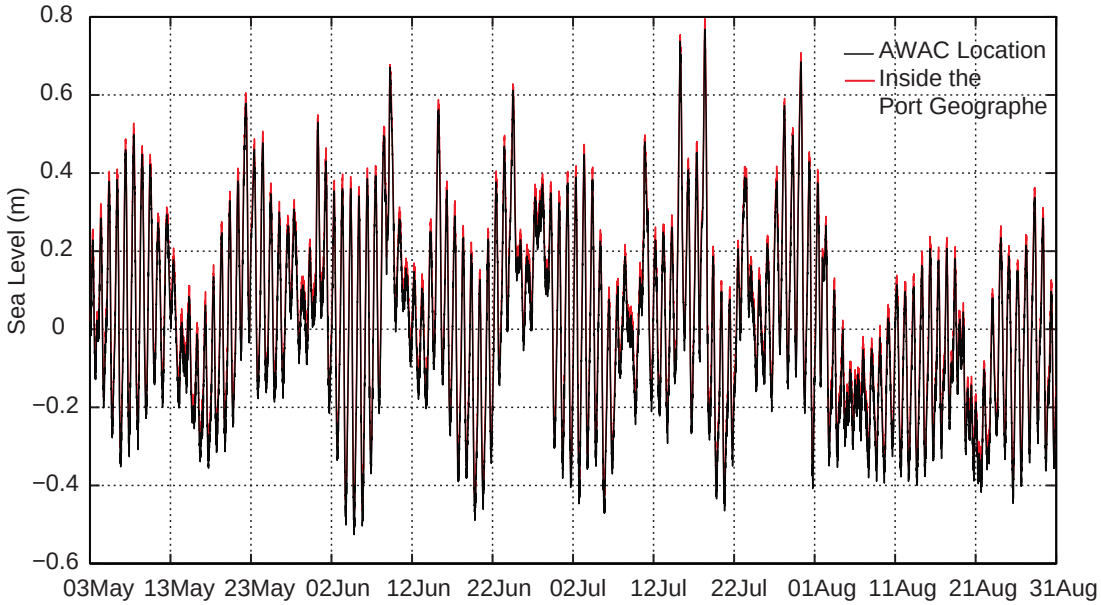

Figure 10.39 Scenario 3: the predicted sea levels at the AWAC site (black line) and inside Port Geographe (red line).

The predicted mean currents through the entrance channel are shown in Figure 10.40. It can be clearly seen that narrowing the entrance channel significantly increased both ebb and flood current speeds. The predicted currents speeds through the entrance channel were nearly three times larger than simulated for the existing condition and both tide- and seiche-induced currents dominated the entrance.

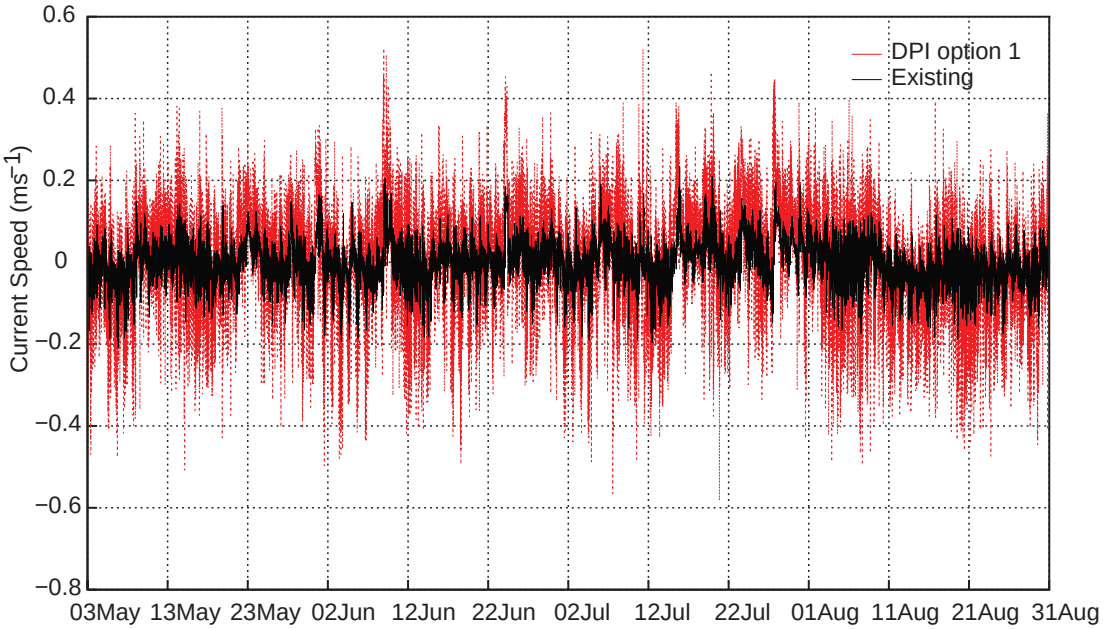

Figure 10.40 The predicted mean current speeds through the entrance channel (black: existing condition, red: Scenario 3).

The predicted current patterns during easterly, westerly, and weak winds are shown in Figure 10.41, Figure 10.42 and Figure 10.43 respectively. Flows were smooth and parallel to the coastline, however some eddies were generated at the entrance channel during both easterly and westerly winds. Jet-like outflows at the entrance channel were induced. During westerly winds and flood flows, eddy circulation at tip of the western training wall was clockwise and eddy-generated currents entered the entrance channel (Figure 10.44). However, no eddy-generated currents entered during ebb tide, due to strong outflows.

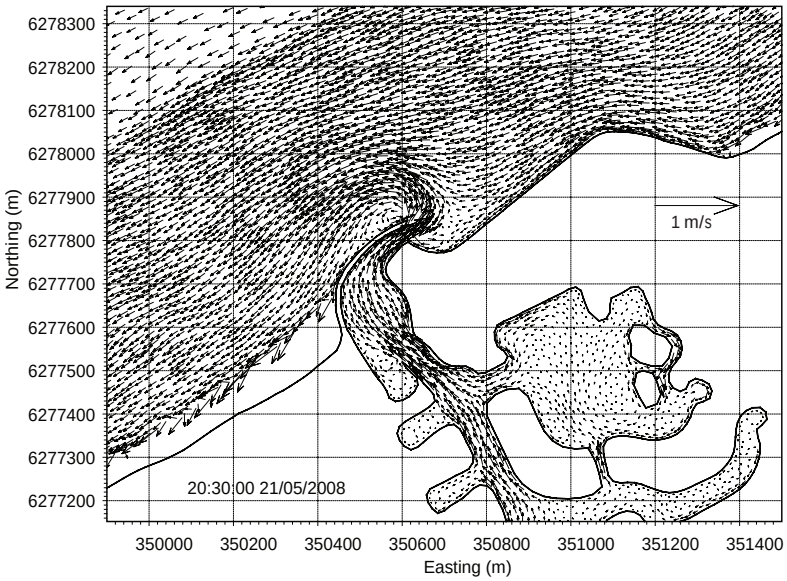

Figure 10.41 Scenario 3: a snapshot of predicted currents during easterly winds.

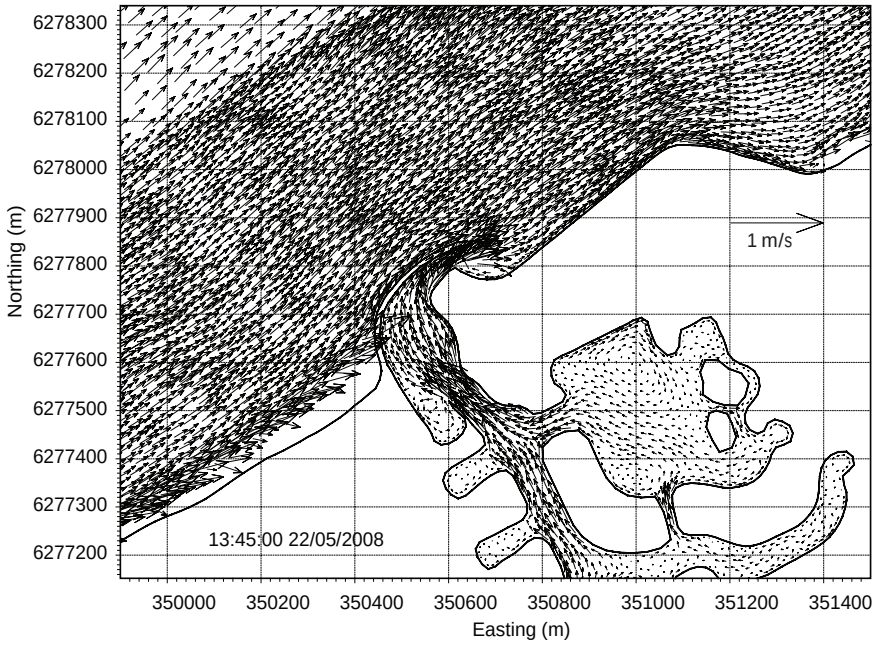

Figure 10.42 Scenario 3: a snapshot of predicted currents during westerly winds.

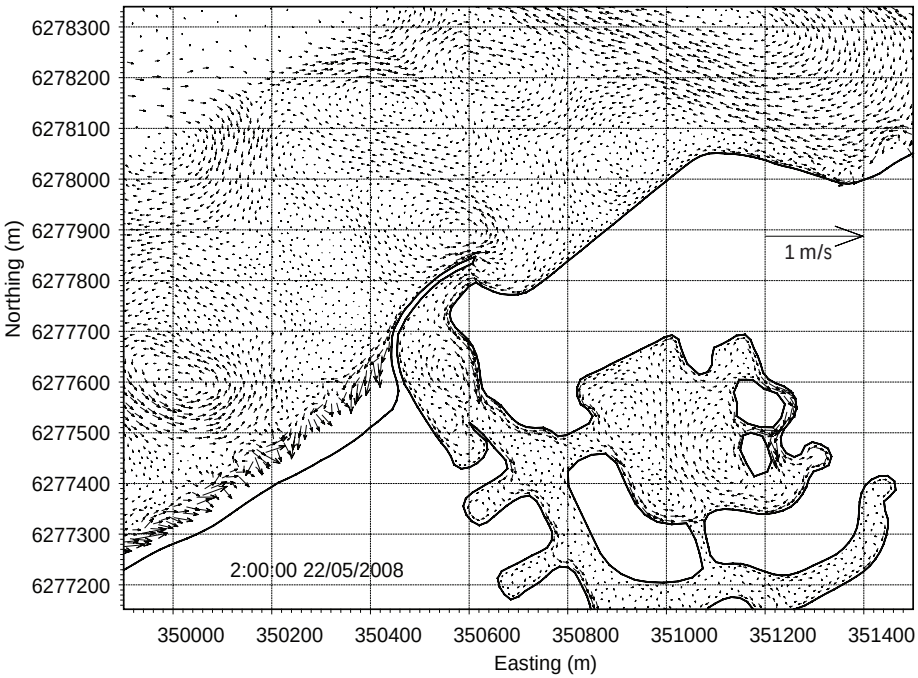

Figure 10.43 Scenario 3: a snapshot of predicted currents during weak winds.

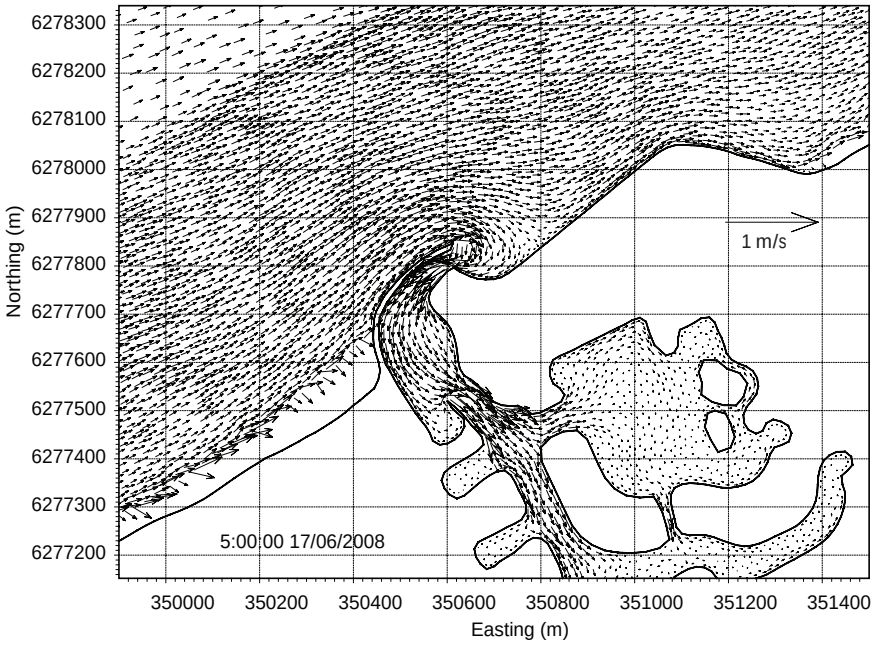

Figure 10.44 Scenario 3: a snapshot of predicted currents during westerly winds and flood flows through the entrance channel.

The predicted velocity vector plots at the peak of storms (18 and 30 July) are shown in Figure 10.45 and Figure 10.46. Flows were strong along the coast as well as in near shore areas, and flowed from west to east. The jet-like outflow from the entrance channel exceeded 0.6 m s^{-1}.

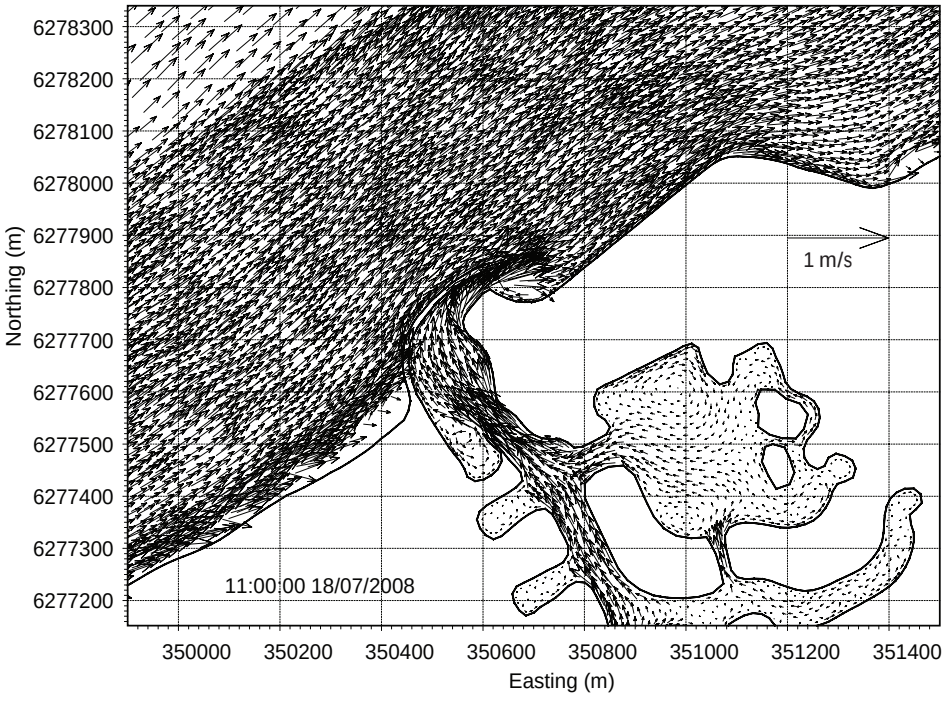

Figure 10.45: Scenario 3: predicted currents at the peak of storm on July 18.

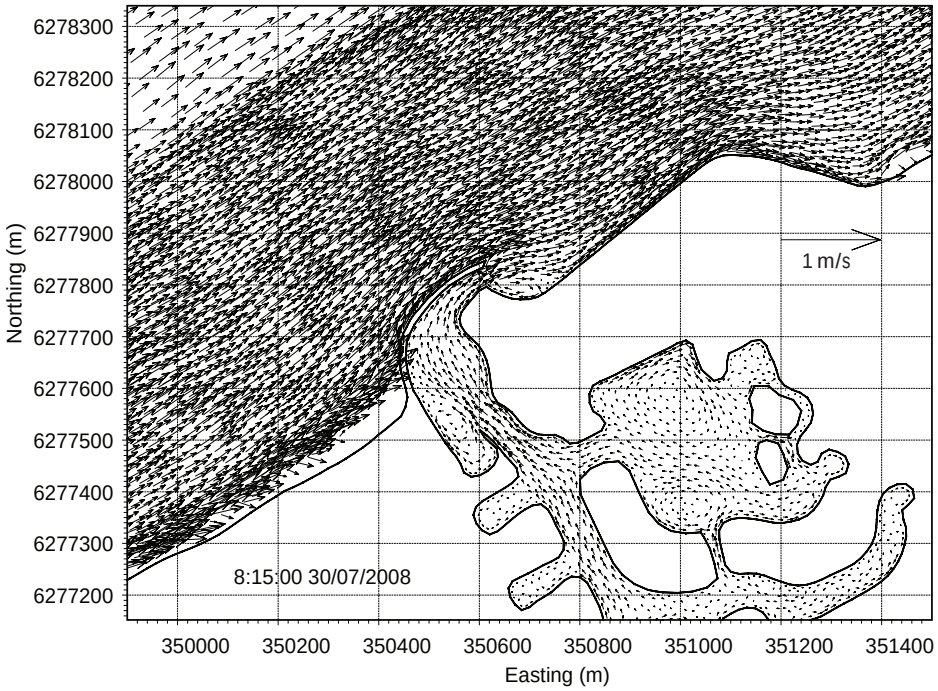

Figure 10.46 Scenario 3: predicted currents at the peak of storm on July 30.

The simulations indicated that significant amounts of seagrass wrack accumulated on the western side of the marina entrance channel by the end of August (Figure 10.47). Some seagrass wrack also accumulated inside the entrance channel.

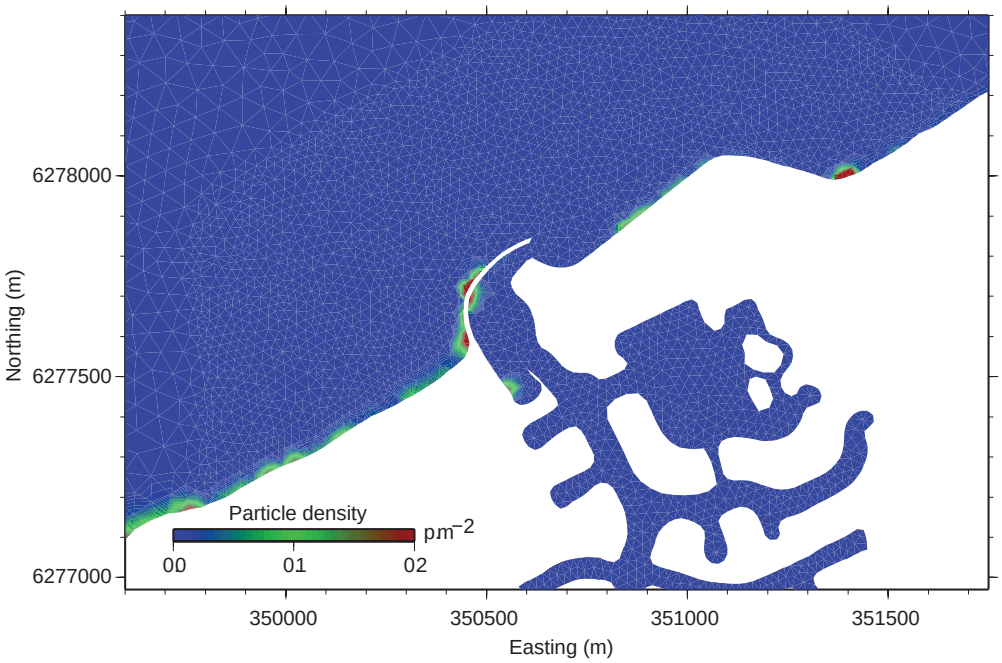

Figure 10.47 Scenario 3: locations of predicted seagrass wrack accumulation at the end of August 2008.

10.2.4 Scenario 4

In this scenario, the model domain, bathymetry, mesh grid, canal segments were all similar to Scenario 3. However during ebb tide, water pumping in the upper canal was included. The water pumping location is shown in Figure 10.48 and the time series of discharge is shown in Figure 10.49. As expected under this scenario, during ebb tide the flow through the entrance channel increased slightly. A comparison of cumulative fluxes through the entrance channel, with and without pumping, is shown in Figure 10.50. No significant changes in flow pattern or speeds could be attributed to the pumping; most simulations results were similar to Scenario 3 results (i.e. without pumping).

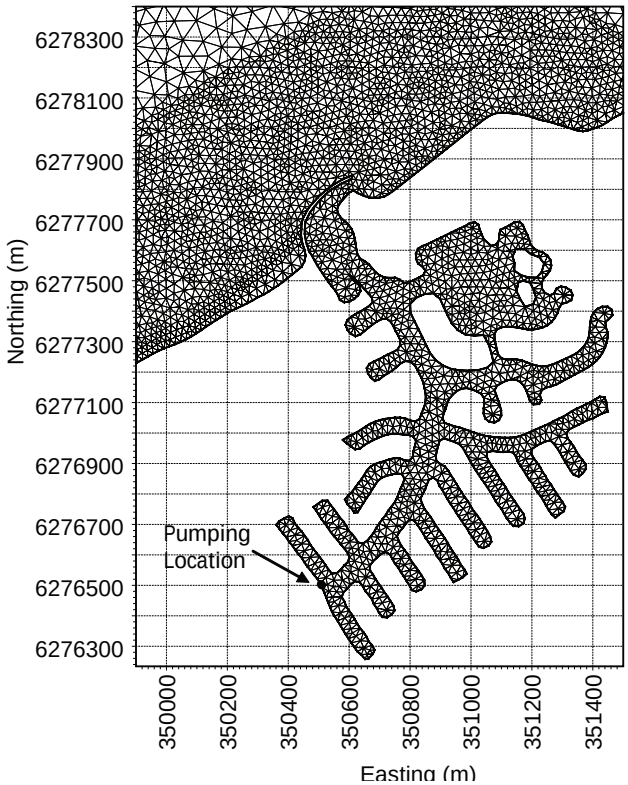

Figure 10.48 Scenario 4: the pumping location in the upper canal segment.

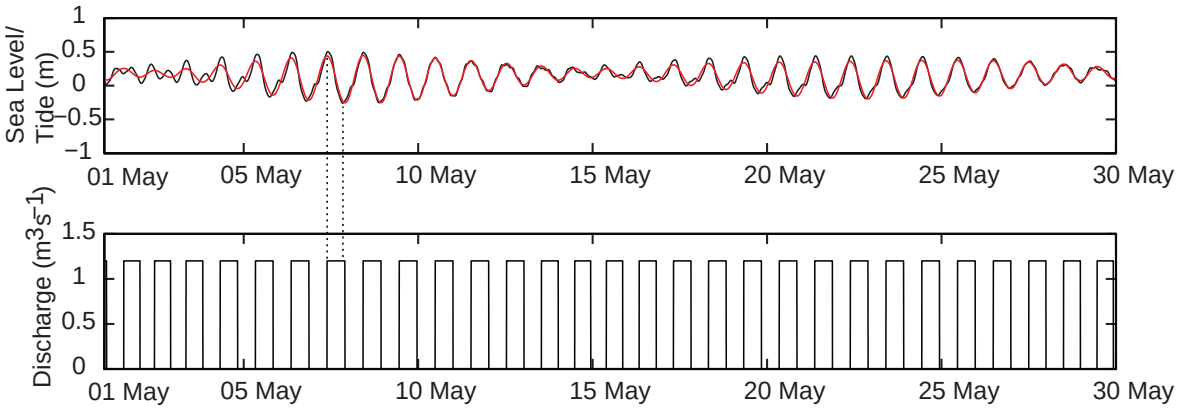

Figure 10.49 Scenario 4: the sea level in the entrance channel and the discharge in the upper segment of the canal during low tide.

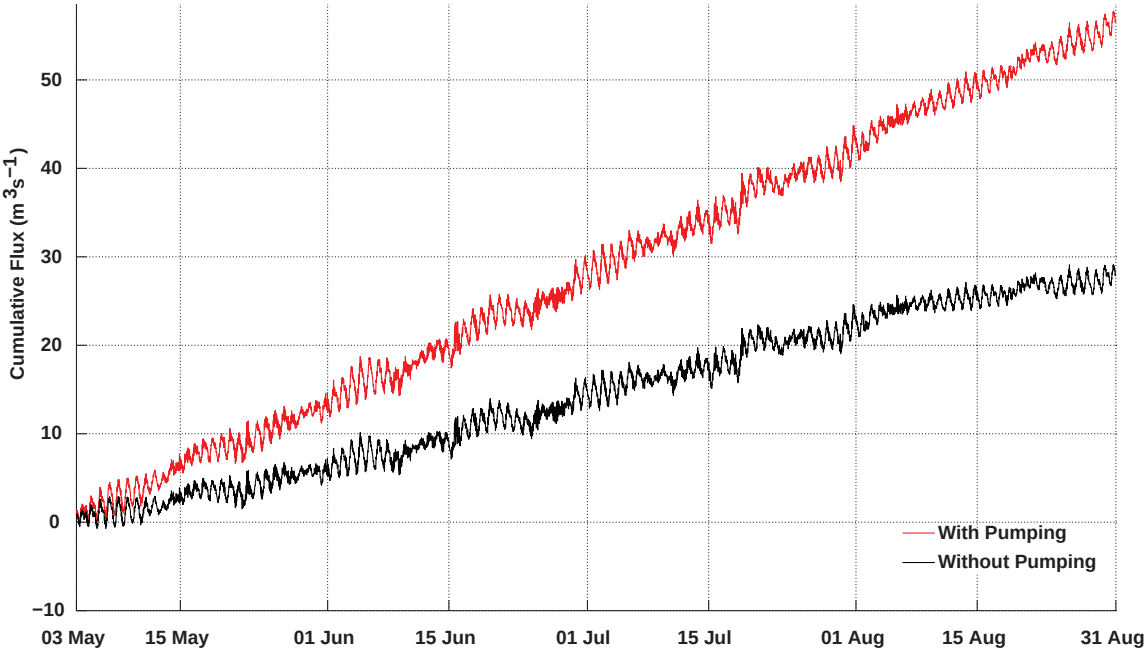

Figure 10.50 Scenario 4: a comparison of the cumulative flux through the entrance channel, with and without pumping.

The simulated seagrass wrack accumulation at the end of August is shown in Figure 10.51. A comparison with the predicted seagrass wrack accumulation in Scenarios 3 and 4, highlighted that less seagrass wrack accumulated inside the entrance channel with pumping, i.e. Scenario 4. However the effect was not considered to be significant and this scenario was not investigated further.

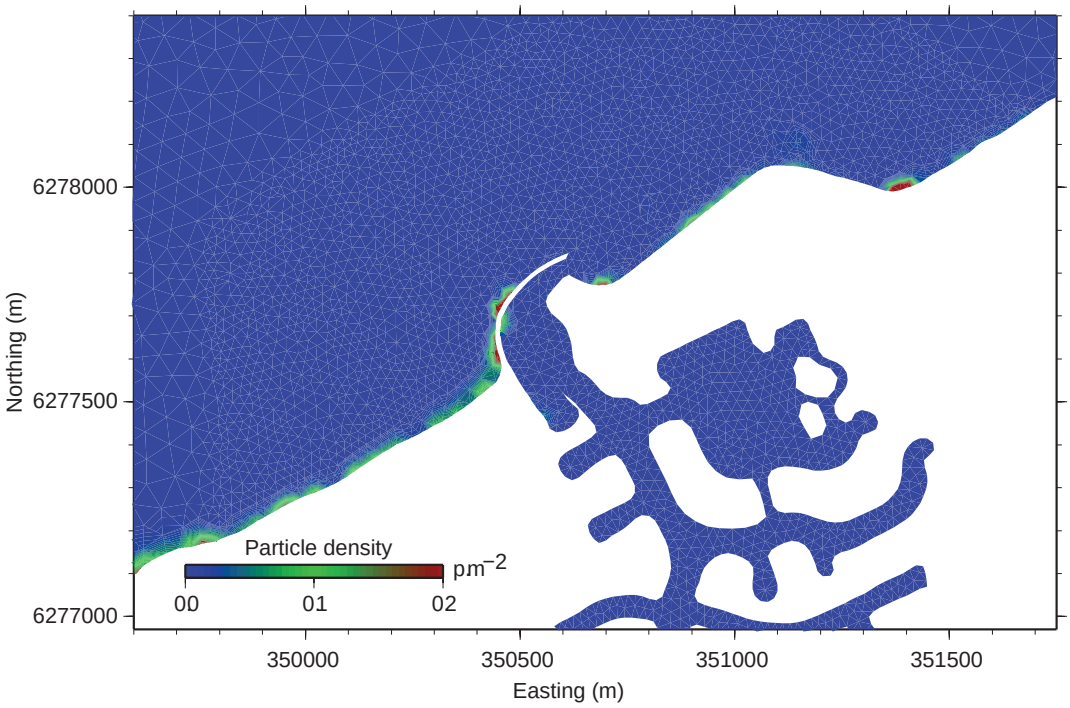

Figure 10.51 Scenario 4: locations of predicted seagrass wrack accumulation at the end of August 2008.

10.2.5 Scenario 5

Based on the hydrodynamic and transport model simulations for Scenario 3 and Scenario 4, in Scenario 5, the eastern breakwater on the eastern side of the marina entrance channel was changed from convex to concave. In addition, the beach on the western side of the marina was further smoothed. The fine mesh grids with bathymetry and wind fields interpolated onto the mesh, in the vicinity of Port Geographe, are shown in Figure 10.52 and Figure 10.53 respectively.

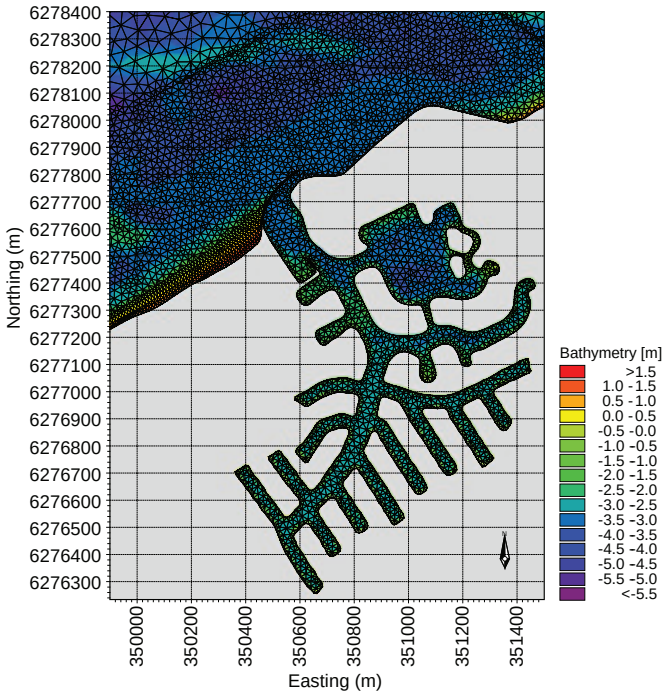

Figure 10.52 Scenario 5: the fine mesh grid and bathymetry interpolated onto the mesh of the Port Geographe area.

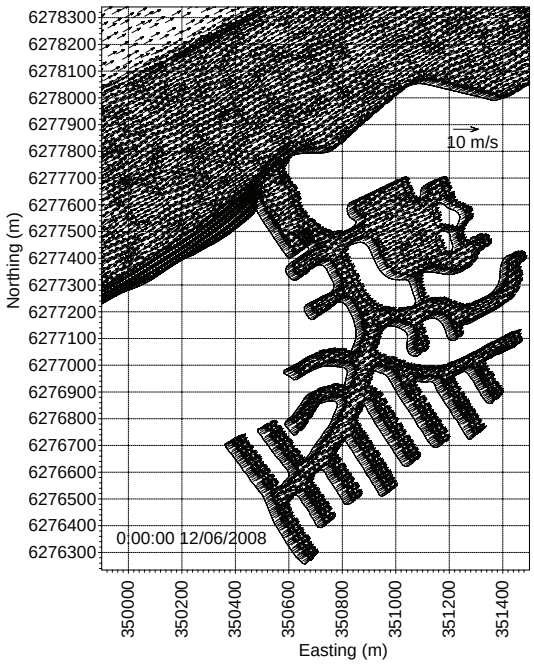

Figure 10.53 Scenario 5: a snapshot of the wind fields interpolated onto the mesh grid of the Port Geographe area.

As found in Scenario 3 and 4, the predicted water levels inside and outside Port Geographe showed slight damping through the entrance channel. The mean water level inside the port was marginally higher than outside (Figure 10.54).

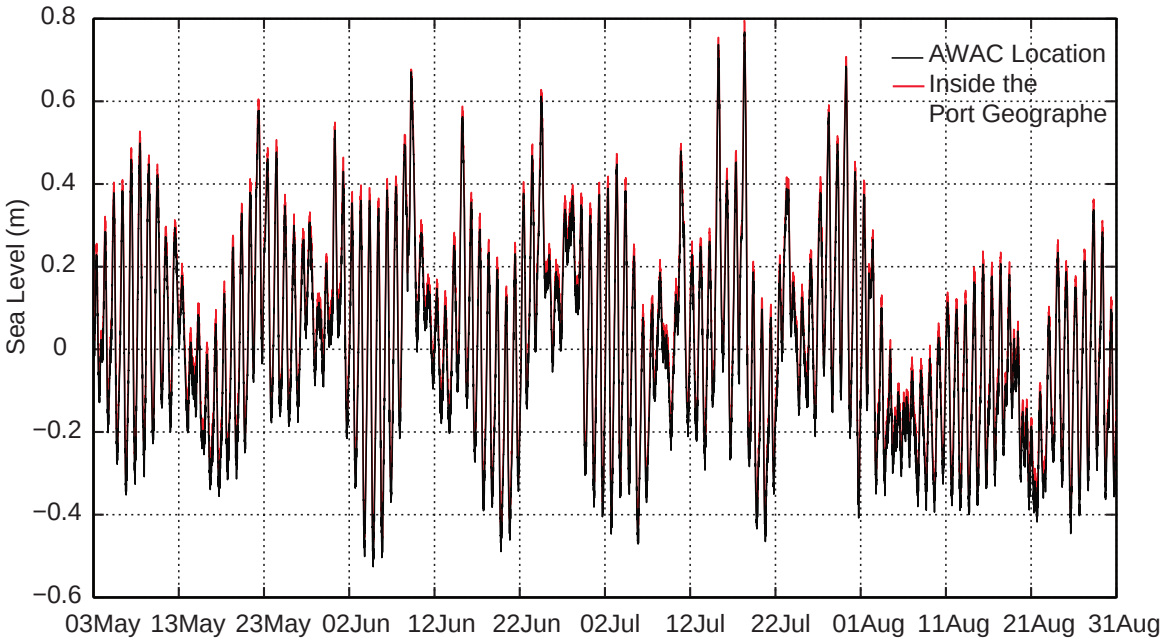

Figure 10.54 Scenario 5: the predicted sea levels at the AWAC site (black line) and inside Port Geographe (red line).

Current patterns during easterly and westerly winds around Port Geographe are shown in Figure 10.55 and Figure 10.56 respectively. No eddies formed at the tip of groyne during westerly winds. Flows were parallel to the shoreline throughout the domain. However, anti-clockwise eddies formed at the tip of the groyne during easterly winds. During westerly winds and flood flows a jet-like flow was created in the entrance channel (Figure 10.57).

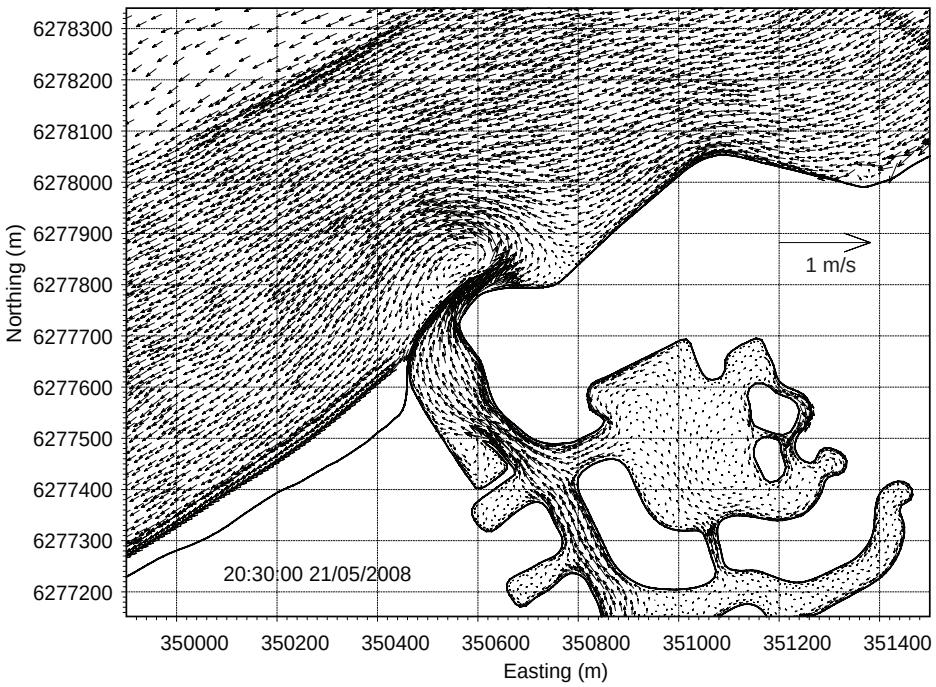

Figure 10.55 Scenario 5: a snapshot of predicted currents in the vicinity Port Geographe, during easterly winds.

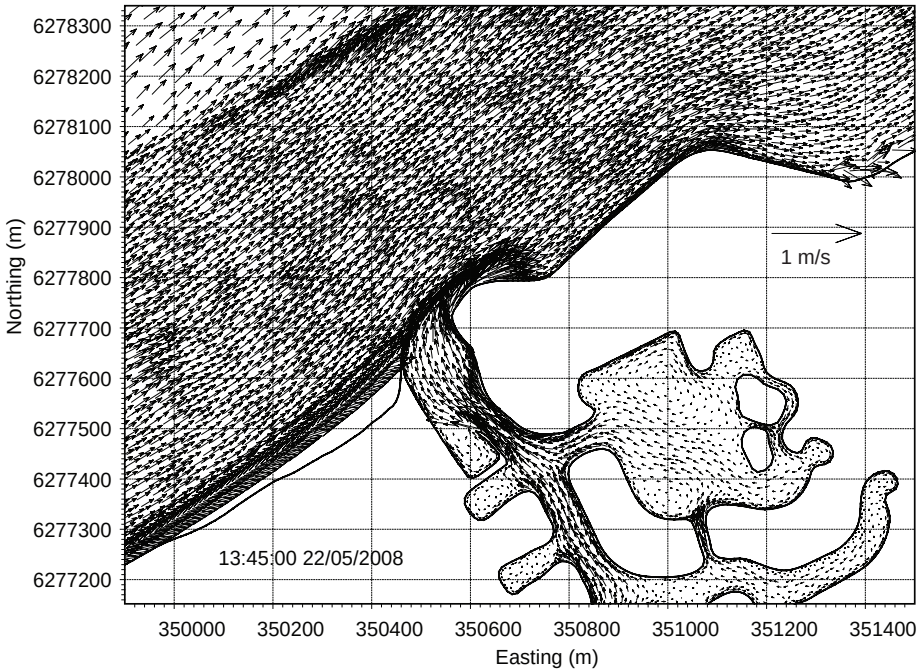

Figure 10.56 Scenario 5: a snapshot of predicted currents in the vicinity of Port Geographe, during westerly winds.

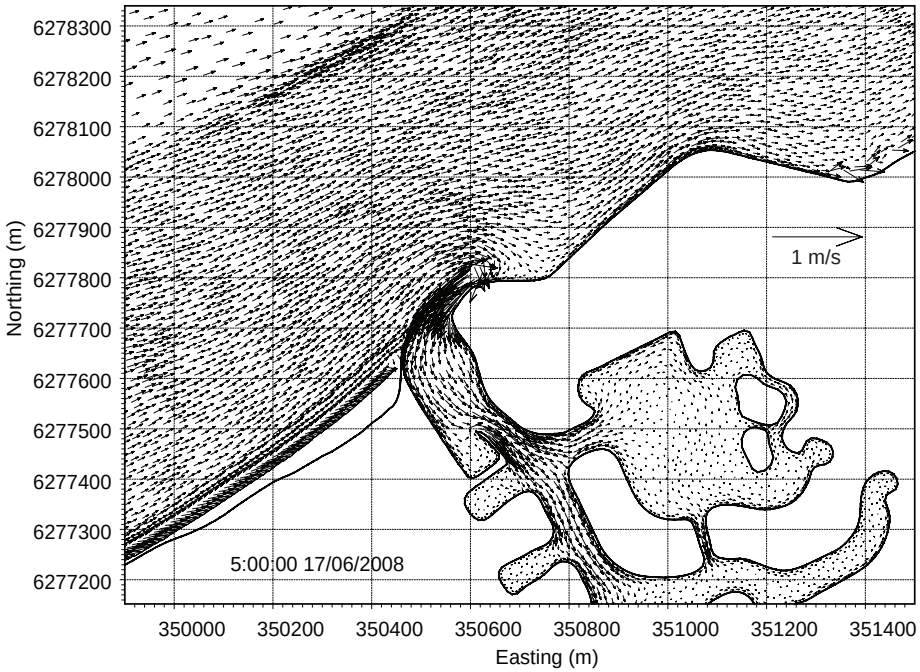

Figure 10.57 Scenario 5: a snapshot of predicted currents in the vicinity of Port Geographe during westerly winds and flood flows through the entrance channel.

The predicted velocity vector plots at the peak of storms (18 and 30 July) are shown in Figure 10.58 and Figure 10.59. As found in Scenario 3 and 4, flows were strong along the coast as well as in nearshore areas and flowed from west to east. The jet-like outflow at the entrance channel exceeded 0.6 ms^{-1}.

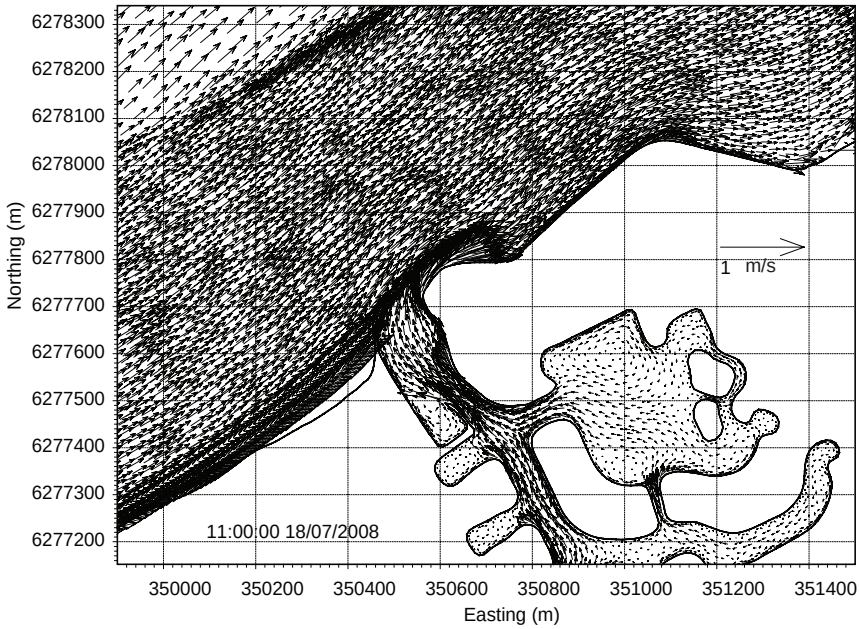

Figure 10.58 Scenario 5: predicted currents in the Port Geographe area, at the peak of the storm on July 18.

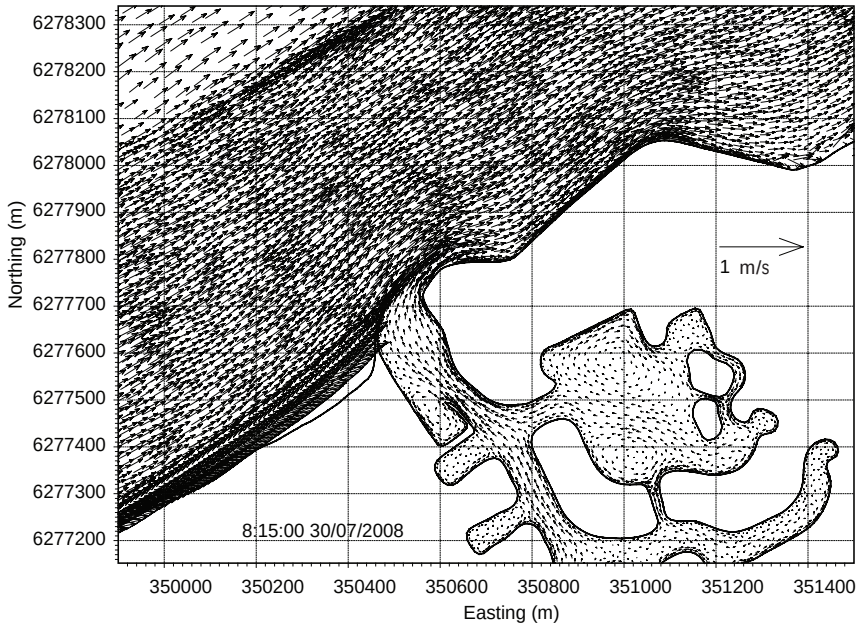

Figure 10.59 Scenario 5: predicted currents in the Port Geographe area, at the peak of storm on July 18.

The predicted seagrass wrack accumulation at the end of August is shown in Figure 10.60 and indicates that some accumulation of wrack on the western side of the marina entrance channel would occur but these accumulations are in water below mean sea level as the beach has been extended offshore. Thus the accumulations as shown are indicated to be sitting offshore.

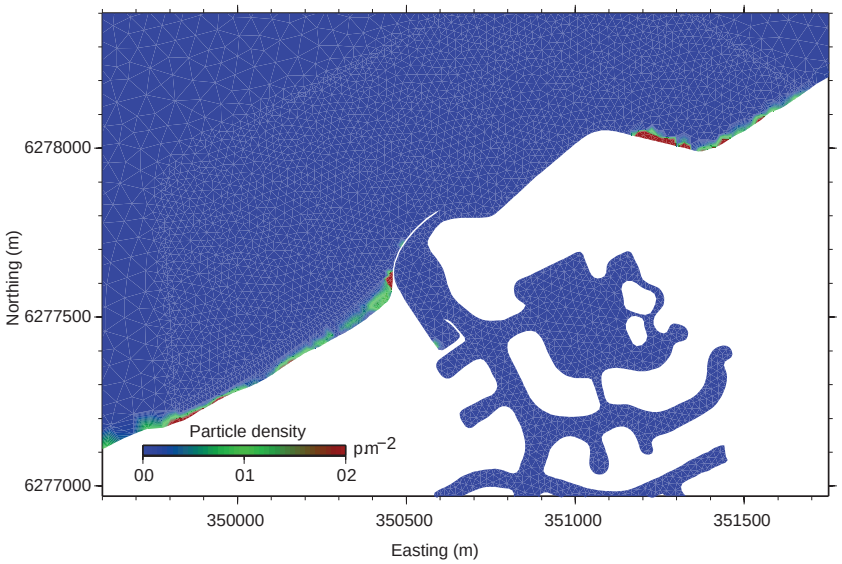

Figure 10.60 Scenario 5: locations of predicted seagrass wrack accumulation in the vicinity of Port Geographe, at the end of August 2008.

10.2.6 Scenario 6

This Scenario contained a slight modification of the existing groyne configuration; the pocket beach groynes were shortened to about half their current length. The marina entrance channel groynes were configured to run easterly oblique to the shoreline. In order to maintain high flows through the entrance channel, the channel entrance was narrowed. Stage 2 of the canal development was also included in this Scenario. The mesh grid with bathymetry and wind fields interpolated onto the mesh are shown in Figure 10.61 and Figure 10.62, respectively.

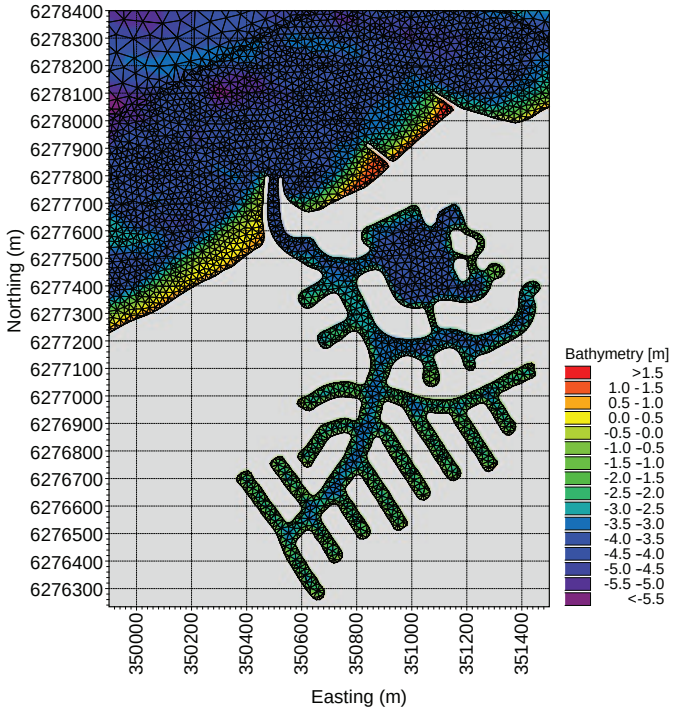

Figure 10.61 Scenario 6: the fine mesh grid and bathymetry interpolated onto the mesh of the Port Geographe area.

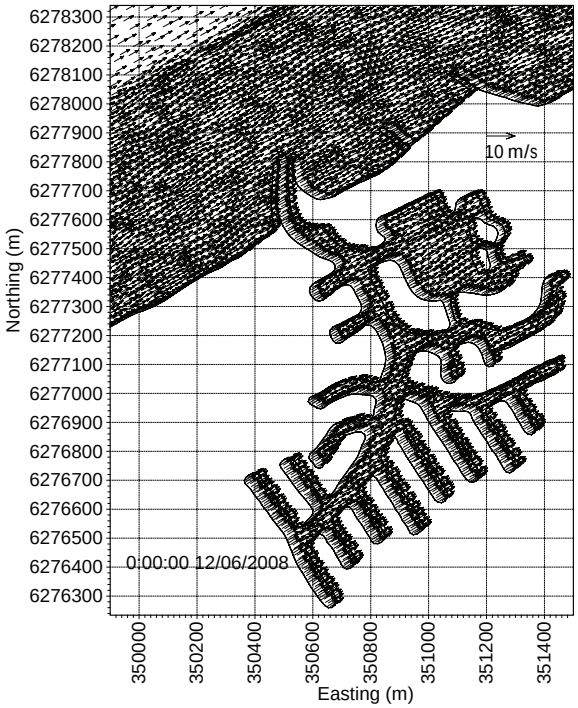

Figure 10.62 Scenario 6: a snapshot of the wind field interpolated onto the mesh of the Port Geographe area.

The predicted sea levels inside Port Geographe and outside (AWAC site) are shown in Figure 10.63. Significant damping can be seen through the entrance channel. The mean water levels inside the port were somewhat higher than outside. The predicted flow patterns during both easterly and westerly winds show eddies circulating at the tip of the groynes (Figure 10.64 and Figure 10.65 respectively).

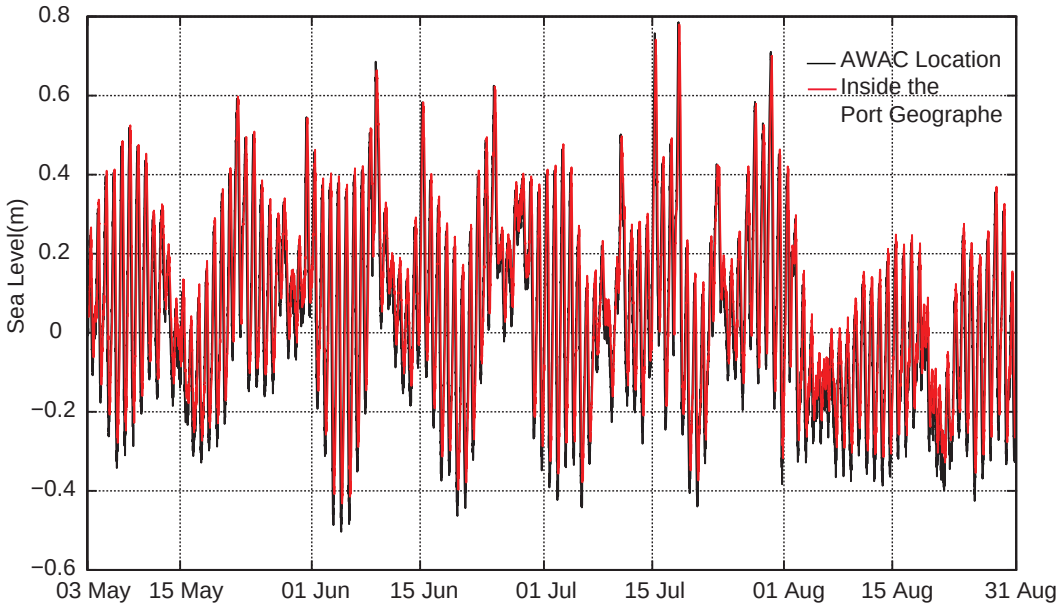

Figure 10.63 Scenario 6: the predicted sea levels at the AWAC site (black line) and inside Port Geographe (red line).

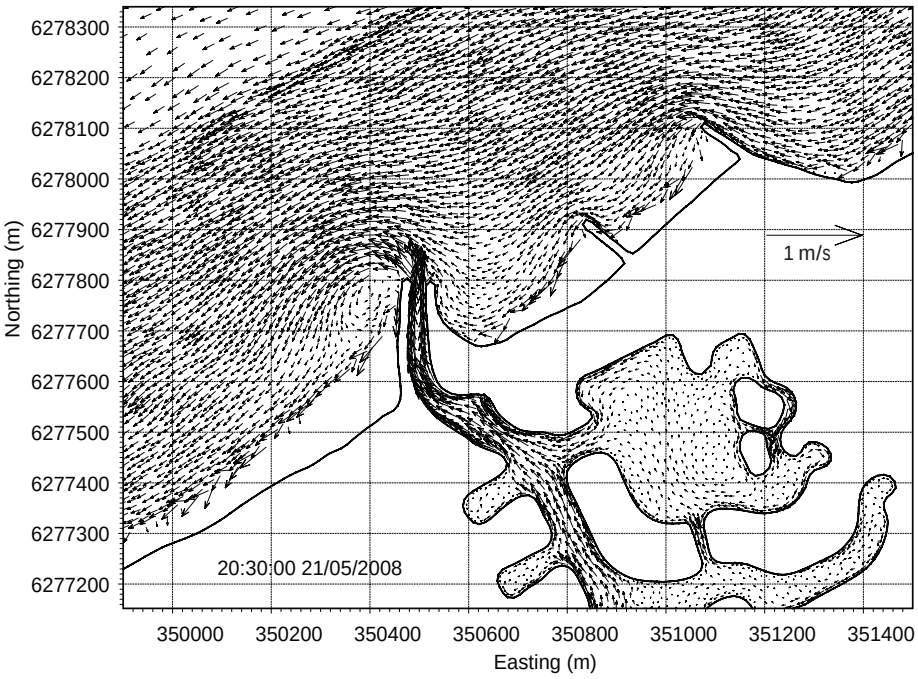

Figure 10.64 Scenario 6: a snapshot of predicted currents in the vicinity of the Port Geographe, during easterly winds.

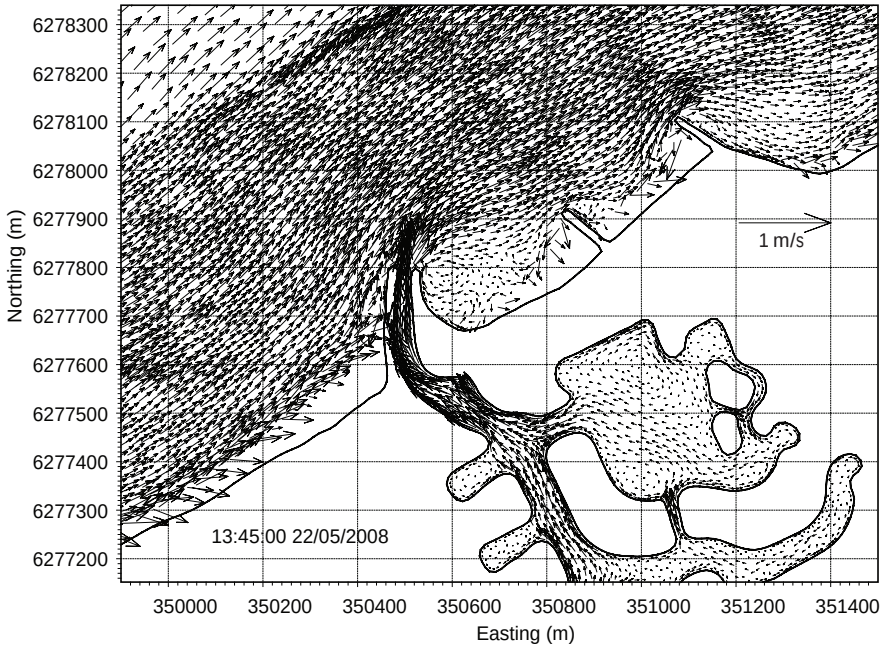

Figure 10.65 Scenario 6: a snapshot of predicted currents in the vicinity of the Port Geographe, during westerly winds.

The predicted flow pattern at the peak of the storms on 17 and 30 July are shown in Figure 10.66 and Figure 10.67, respectively. Flows through the entrance were strong and outflows were jet-like. Given the predicted clockwise eddy circulation and decreasing flow speeds at the eastern side of the entrance groynes, accumulation of wrack can be expected within the pocket beach groynes.

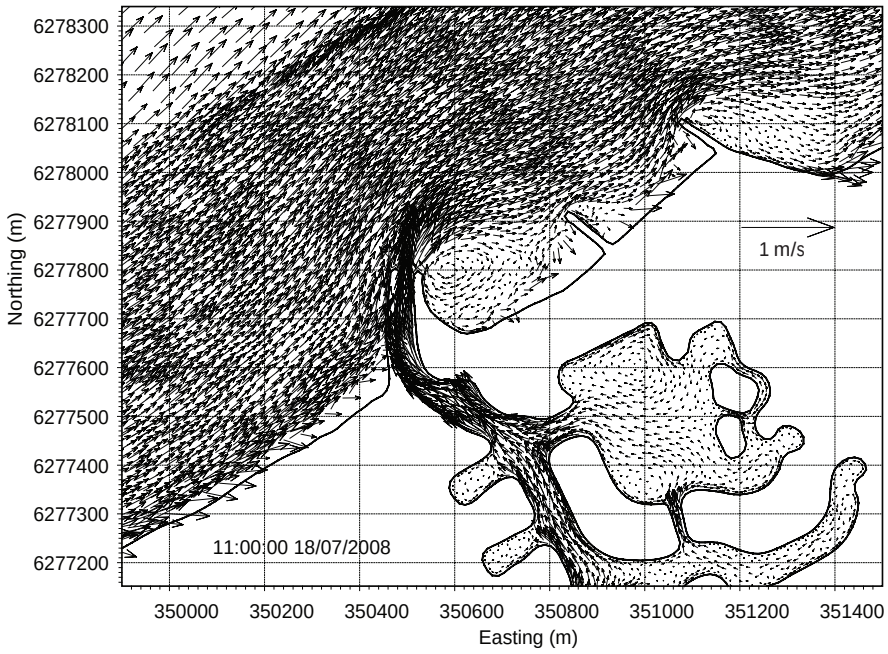

Figure 10.66 Scenario 6: predicted currents in the Port Geographe area, at the peak of storm on July 18.

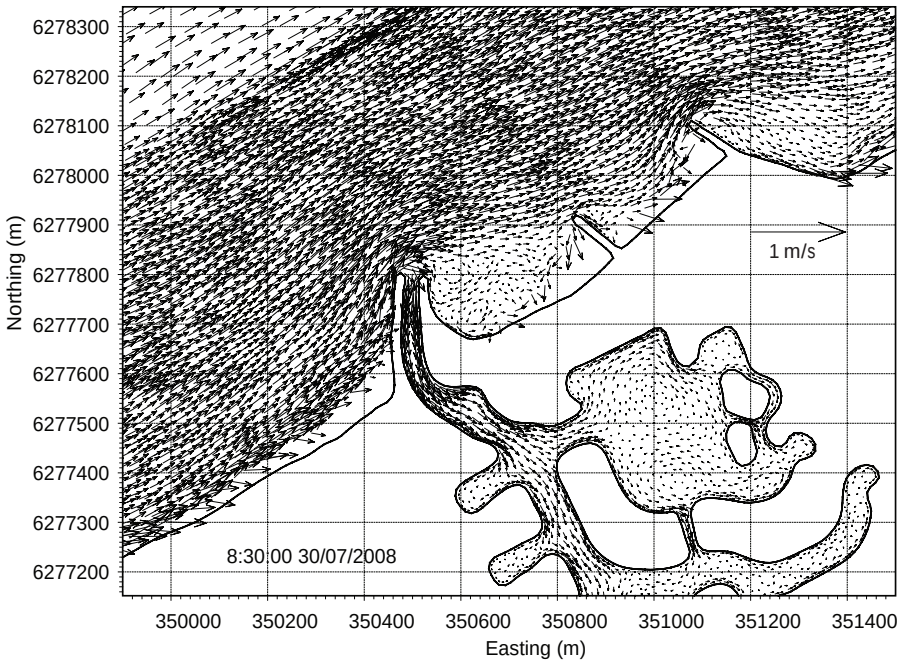

Figure 10.67 Scenario 6: predicted currents in the Port Geographe area, at the peak of storm on July 30th.

The predicted seagrass wrack accumulation at the end of August is shown in Figure 10.68 indicating accumulation on the western side of the western groyne as well as on the eastern side in between the pocket beach groynes. Thus this scenario was not considered further.

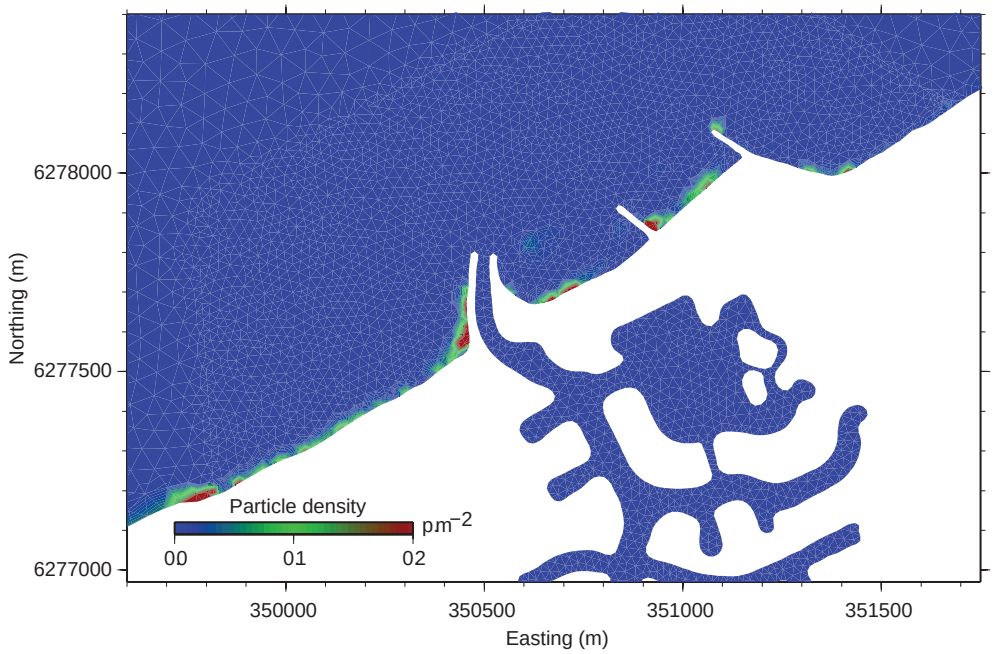

Figure 10.68 Scenario 6: locations of predicted seagrass wrack accumulation in the vicinity of Port Geographe, at the end of August 2008.

10.2.7 Scenario 7

This Scenario was based on the existing configuation but with the beach on the western side of the western training wall reflecting the conditions recorded in October 2009. Note that due to the nature of the model, which currently does not have the ability to dynamically alter the shoreline, the same beach configuration was used from May to August, which is not realistic (the beach would progressively accrete over time). The aim of this situation was to examine whether there could be natural by-passing of wrack when the western beach was saturated (i.e. the beach extended to the seaward end of the western training wall).

The mesh grid with bathymetry and wind fields interpolated onto the mesh are shown in Figure 10.69 and Figure 10.70, respectively.

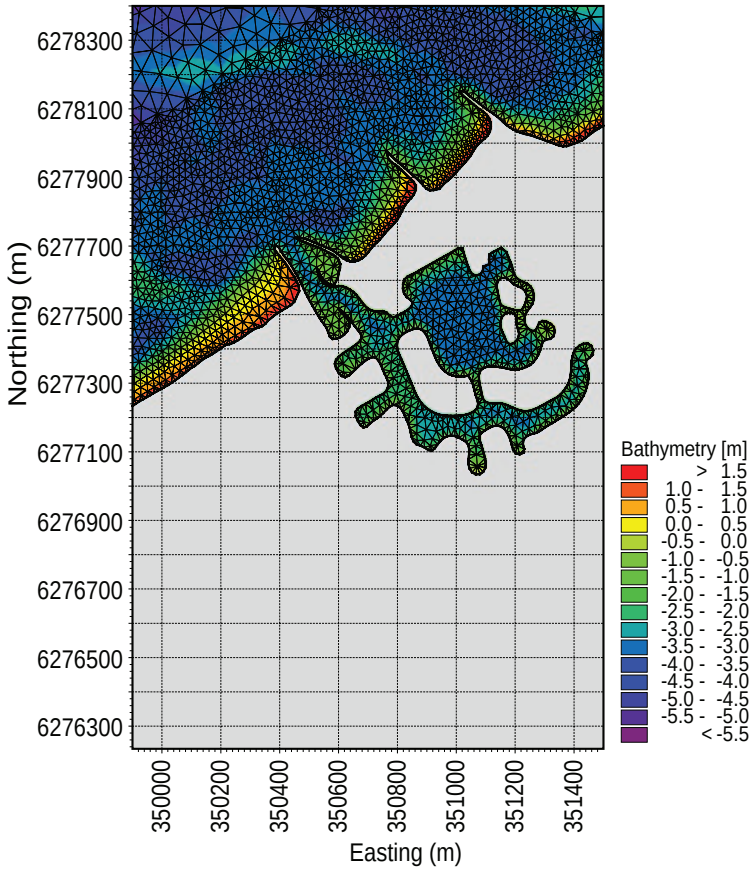

Figure 10.69 Scenario 7: the fine mesh grid and bathymetry interpolated onto the mesh of the Port Geographe area.

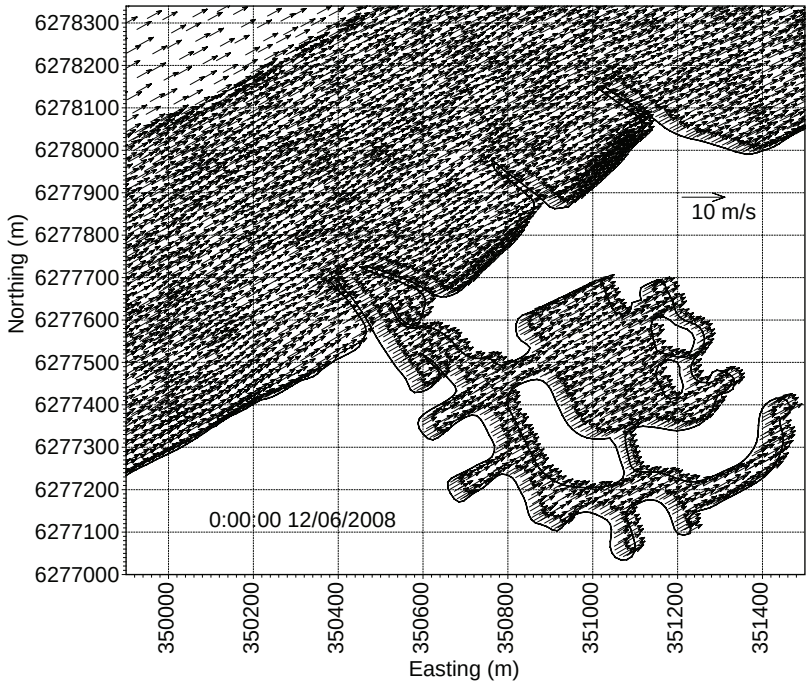

Figure 10.70 Scenario 7: a snapshot of the wind field interpolated onto the mesh grid of the Port Geographe area.

The simulated flow patterns during easterly and westerly winds, and at the peak of the storms (18 and 30 July) are shown in Figure 10.71, Figure 10.72, Figure 10.73 and Figure 10.74 respectively. As found under the existing conditions, eddies were generated at the tips of the groynes and in between the pocket beach groynes.

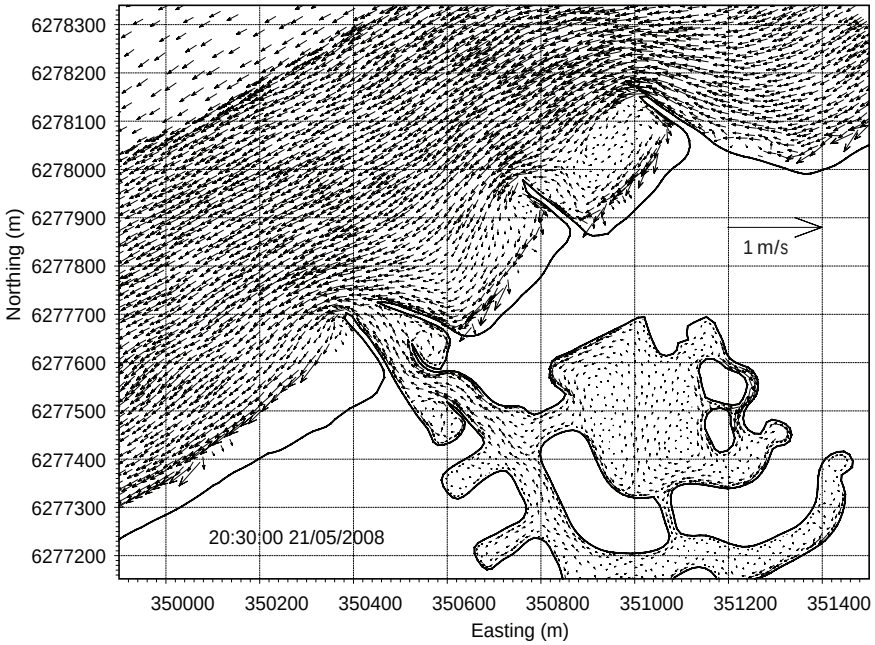

Figure 10.71 Scenario 7: a snapshot of predicted currents in the vicinity of the Port Geographe, during easterly winds.

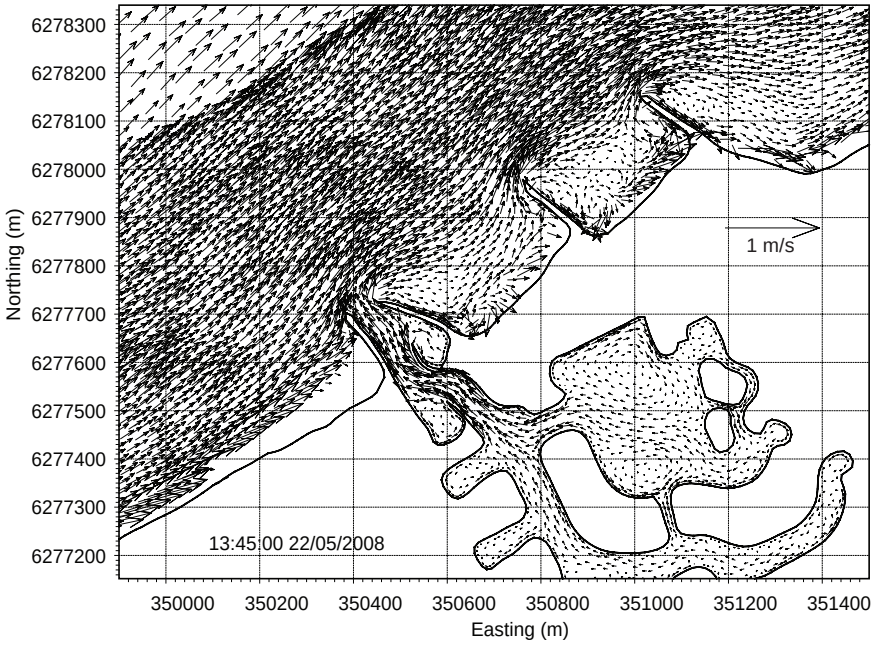

Figure 10.72 Scenario 7: a snapshot of predicted currents in the vicinity Port of Geographe, during westerly winds.

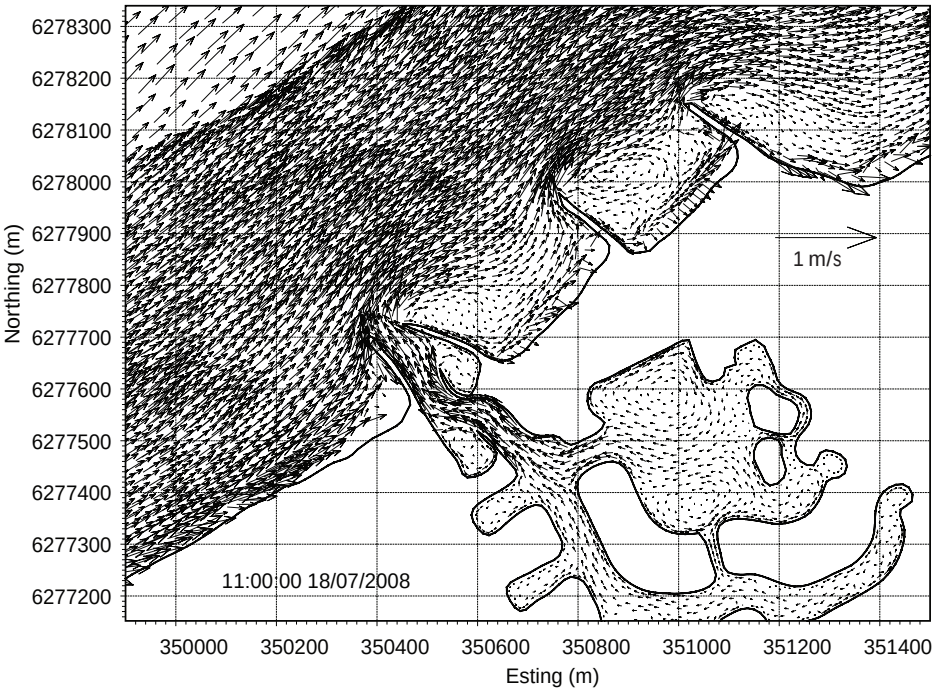

Figure 10.73 Scenario 7: predicted currents in the Port Geographe area, at the peak of the storm on July 18.

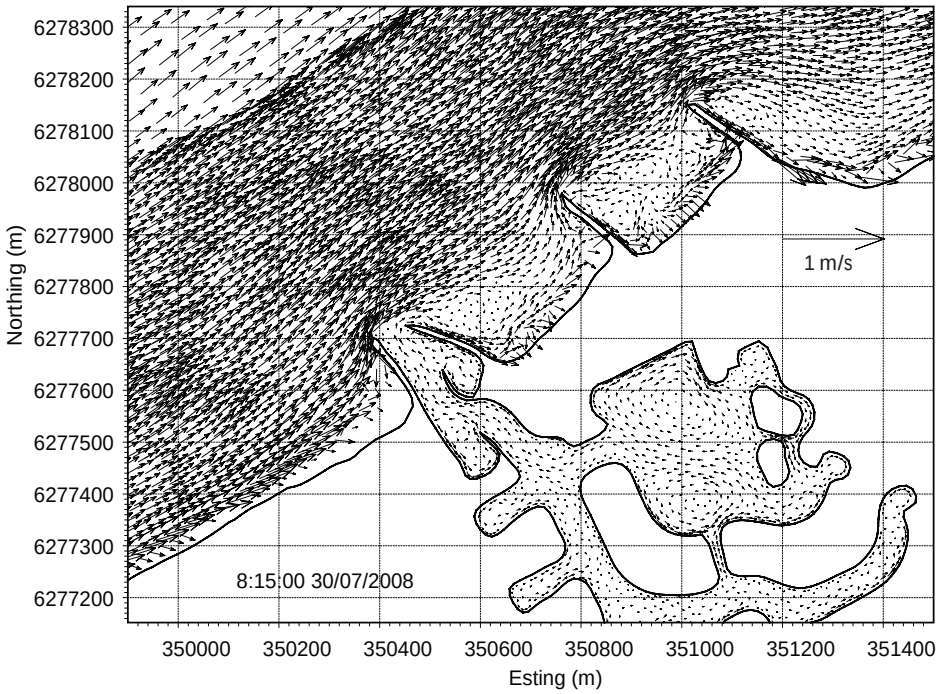

Figure 10.74 Scenario 7: predicted currents in the Port Geographe area, at the peak of the storm on July 30.

The simulation of seagrass wrack accumulation at end of the August, indicates that significant wrack was transported from the western to the eastern side of the marina (Figure 10.75). As expected, some wrack became trapped between the pocket beach groynes.

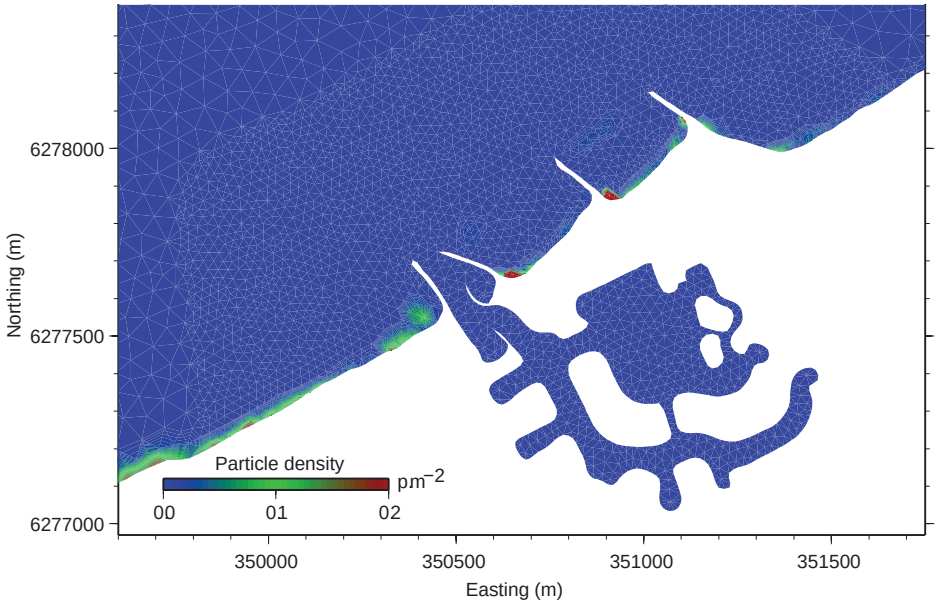

Figure 10.75 Scenario 7: locations of predicted seagrass wrack accumulation in the vicinity of Port Geographe, at the end of August 2008.

10.3 Summary

In comparing the different configurations, it can be seen that the general hydrodynamic features of Geographe Bay are unchanged. Most of the hydrodynamic changes are localised and appear in the vicinity of Port Geographe. The model simulations revealed that the winds play a more dominant role than the tides, in the generation of barotropic currents in Geographe Bay. However, tidal and other low frequency oscillation currents (induced by seiches etc) dominate the Port Geographe entrance channel and canal segments. Depth-averaged currents throughout the model domain followed a distinct pattern that was repeated with each passing weather system. Extreme water levels on the coast were generated by a combination of high tides, storm surges and high winds.

Strong currents (sometimes exceeding 50 cm s^{-1}) were clearly visible along the coast while current speeds were much lower in the offshore regions. Current velocities were higher and much more variable during May-July, compared to August-September. Over the simulation period, the east-west component of the water velocities was generally stronger than the north-south component (i.e. water velocities tended to be higher in the alongshore direction compared to the offshore-onshore direction). This was attributed to the orientation of the coast and bathymetry. The movement of wrack generally occurred during periods of high winds; under these conditions the predicted current speeds and directions closely matched observed data. This provides confidence in the model's ability to simulate current patterns during times of seagrass wrack transport.

The interaction between wind stress and large bathymetric gradients (e.g. groynes, sand bars) generated eddies within the Port Geographe area and also in the shallow parts of the bay. In the near-shore sand bar regions, eddies were generated during the changes in the wind direction and generally persisted during low current conditions. When the winds were strong, the eddies disappeared and currents were nearly in the same direction as wind. Small eddy structures also appeared inside Port Geographe. The presence of these eddies may enhance the flushing of inner port waters.

Hydrodynamic and transport model simulations showed that circulation, flow speeds and wave climate were changing in the vicinity of Port Geographe due to groyne modifications and thus affecting seagrass wrack transport and accumulation on the beaches.

The hydrodynamic and particle transport modelling showed that Scenario 5 (Figure 10.52) was the optimal groyne configuration for improved management of seagrass wrack around Port Geographe. The Scenario 5 configuration should now be used for simulation of sand transport in the Port Geographe area. Continued evolution of the groyne configuration is expected as results from the sand modelling are investigated. Ultimately, the hydrodynamic, particle (seagrass wrack) transport and sand models must be used together to identify the optimal groyne configuration for improved management of both seagrass wrack and sand around Port Geographe.

11 SYNOPTIC OVERVIEW & MANAGEMENT IMPLICATIONS

This study set out to provide a better understanding of the wrack properties and the mechanisms for natural deposition and removal of wrack from the western beach at Port Geographe. Over two years, the study team undertook a two-pronged approach to improve this understanding and develop recommendations for the management of wrack at Port Geographe:

1. extensive field and laboratory studies, which have improved our understanding of wrack dynamics in Geographe Bay and the physical properties of wrack relevant to its transport. This improved understanding was an essential pre-requisite for the second approach;
2. the incorporation of that new knowledge into a numerical model. Numerical models are simply sets of mathematic equations that allow predictions to be made about the behaviour of complex systems. In this case, a hydrodynamic model initially predicts the movement of water under different weather conditions in Geographe Bay. A linked particle transport model then tracks the movement of wrack particles under those hydrodynamic conditions. In particular, the model allowed the study team to examine the movement of wrack particles in the vicinity of Port Geographe and assess the usefulness of various alternative groyne configurations for allowing the natural bypassing of wrack.

The first significant outcome of the study, therefore, is an improved understanding encapsulated in a model. This has made it possible to look at management options in a consistent way across a range of potential scenarios and put forward a set of preferred options for further consideration. In that sense, the study outcome is not an end point but a significant step in identifying an appropriate management solution to the issues at Port Geographe.

Specifically the study was asked to:

1. Review M J Paul and Associates Pty Ltd [2005], and make comment on the alternatives for :

- changes to the groyne and entrance structures, and
- bypassing processes in the light of the further knowledge gained from this study on the behaviour of seagrass and seagrass wrack.

2. Recommend alternative techniques for managing the wrack. Particular questions that need to be addressed were:

- does the mechanical pushing of wrack from the beach back into the water provide an advantage? And if so, when should this be done?
- where does wrack pushed or naturally removed from the shore west of Port Geographe eventually end up?
- review the orientation of beaches to determine whether there is a controlling point at which wrack stranded on the beach will no longer be removed by ocean forces.
- recommend any further work that is needed to improve the understanding of seagrass wrack movement in order for decisions to be made at Port Geographe.

In addressing these requirements it is useful to synthesise our current understanding of wrack dynamics and the processes contributing to the accumulations at Port Geographe.

11.1 What we now know

The lifecycle of wrack in Geographe Bay has been clarified through the two-year study, with the key components conceptualized in Figure 11.1. The key components of the lifecycle are:

- the generation of wrack (1 in Figure 11.1),

- its transport away from meadows and to adjacent habitats, including the beaches of Geographe Bay (2);
- its movement onto and off beaches due to natural processes (3);
- its movement in longshore currents when it is suspended in nearshore waters , including its accumulation at Port Geographe (4); and
- its degradation and biogeochemical transformations while on the beaches and in nearshore waters, including the release of H_2S.

The improved conceptual understanding of wrack dynamics in Geographe Bay is summarized in the following six sections.

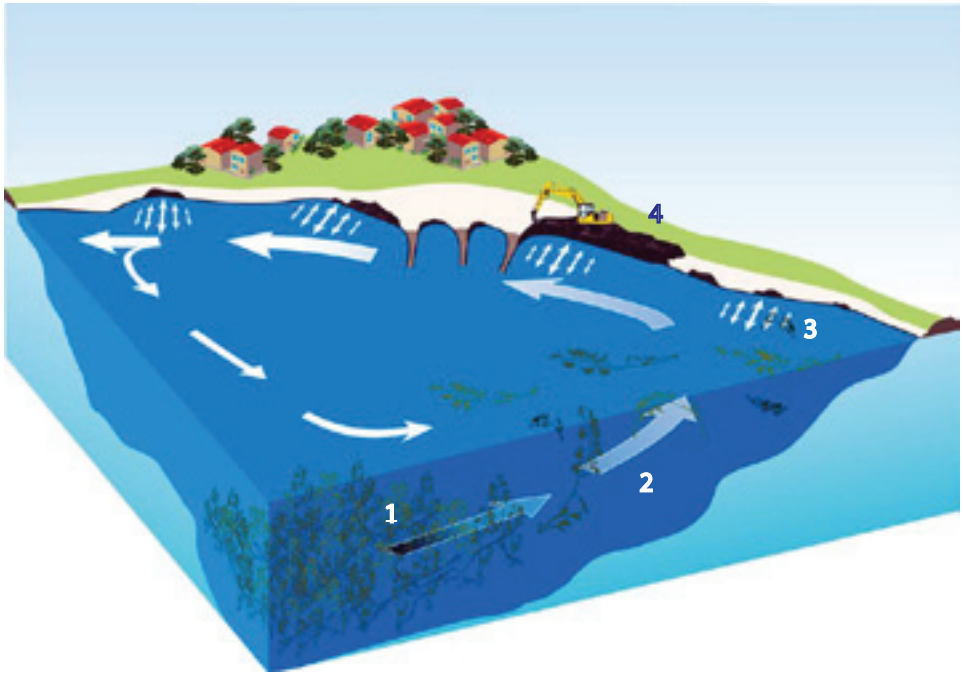

Figure 11.1 The lifecycle of seagrass wrack in Geographe Bay. Wrack is generated in offshore seagrass meadows and accumulates in the meadows and unvegetated zones until autumn (1). The first significant storms suspend wrack in the water column and transport it to adjacent habitats, including the beaches of Geographe Bay (2). The wrack moves on and off the beaches depending on local hydrodynamic and meteorological conditions (3). When transported off the beaches and while suspended in the near shore water column, longshore currents move the wrack towards Port Geographe (4). While the wrack is being transported in the water and when it is accumulated on beaches, it undergoes natural degradation and transformation, including the release of H_2S.

11.1.1 Defining a Baseline: the existing wrack dynamics on the beaches of Geographe Bay and how Port Geographe fits into this context

Geographe Bay contains extensive offshore seagrass meadows that are a valuable natural asset. A feature of seagrass growth is the continuous shedding of leaves and/or stems (wrack) that are subsequently transported to the beaches. The wrack typically accumulates on beaches following the first major storms of autumn. The beaches of Geographe Bay are characterised by highly transient wrack accumulations, indicating complex processes that account for the continual deposition and removal of wrack from late autumn to early spring. Despite the highly variable nature of wrack accumulations, beaches generally had more wrack on them during mid-winter (July – August).

The accumulations can vary from relatively thin sheets of wrack, only a few leaves deep, through to extensive piles more

than 1 m deep. Wrack biomass on the surface of the beach ranged from 0.001 – 3.64 kg m^{-2}, averaging 0.37 kg m^{-2}. At some beaches and times, wrack may also be buried as deep as 45 cm below the sediment surface, highlighting the potential for loss of wrack from the system through burial, but also the potential for wrack to subsequently be released during beach erosion events.

The accumulation of wrack on the beaches was not strongly correlated with beach profile. It is possible that offshore features, such as sandbars, play a role in the accumulation of wrack on beaches. However, the most significant factors appear to be storms and high water events that drive wrack onto beaches and subsequently assist in its removal.

Port Geographe is highly unusual in the context of Geographe Bay beaches, in two ways.

1. The accumulations are significantly greater at Port Geographe than anywhere else. While the accumulations on other beaches are typically in the order of 0.67 m^3 m^{-2}, those recorded at Port Geographe, have been estimated to in the order of 3.75 m^3 m^{-2} over a 2 km stretch [*DPI*, 2007]. At the end of winter 2009, an estimated 97% of all the wrack present on beaches from Dunsborough to Forrest Beach, was found at Port Geographe.
2. The accumulations at Port Geographe are persistent, unlike the transient accumulations typical of most other beaches. This reflects the engineering design of Port Geographe that was intended to create a sediment trap to the west of the development. The structure is also highly efficient at trapping wrack and preventing the normal processes that cause wrack to be removed from beaches and transported along the shoreline.

Further evidence of Port Geographe acting as a structural trap for wrack, is the distribution of wrack accumulations across the beaches in Geographe Bay. Sites close to the Port Geographe western training wall had the most wrack, followed by Quindalup and Abbey Beach. Sites north east of the Port Geographe groyne had the least wrack. These findings are consistent with groynes interfering with the natural processes responsible for removal of wrack from beaches and along the shore.

11.1.2 Generation of wrack – what species and from where

Geographe Bay contains extensive meadows of seagrass, overwhelmingly dominated by two species: *Posidonia sinuosa* (ribbon weed) and *Amphibolis antarctica* (wire weed). *P. sinuosa* accounts for about 70 % of all the mapped seagrass coverage in the bay, while *A. antarctica* and its close relative *A. griffithii* account for about 20 %. *P. sinuosa* and *A. antarctica* are the main seagrass species contributing to the supply of beach wrack. *P. sinuosa* provides large amounts of leaf material and accounted for up to 90 % of the beach wrack leading up to winter. *A. antarctica* contributes both tough wiry stems and leaves to the beach wrack, with the greatest contribution during winter, when storms are severe enough to remove whole stems and clumps of the seagrass. During winter, *A. antarctica* accounted for as much as 30% of beach wrack at some sites.

The meadows throughout Geaographe Bay will provide wrack to the beaches (process 1 in Figure 11.1). However, modelling results suggested that the majority of wrack accumulating at Port Geographe orginates in the nearshore meadows that are in less than 10 m water depth, and predominantly to the west of Port Geographe.

Wrack is produced throughout the year in the seagrass meadows. *P. sinuosa* shoots produce 2-3 leaves per year, with the maximum biomass and leaf density in summer. At the end of summer the oldest leaf is shed from the plant, though some shedding will occur at other times of year. In addition, the older tips of the leaves become necrotic with age and can often simply fall off the plant under sufficiently high-energy conditions. These leaves tend to accumulate in the meadow and in the nearby, unvegetated sediments, particularly in areas of slight depression in the seabed. *A. antarctica* has a vertical stem from which clusters of leaves arise. A new leaf is produced from a cluster about every 14 days and these stay on the plants for about three months before falling off, providing a more regular supply of wrack compared to the leaves of *P. sinuosa*. However, the stems of *A. antarctica* live for about 2 years and generally only break off from the below ground parts of the plant in winter, when the wave energy is higher. By the end of summer, a large store of wrack is found in the offshore seagrass meadows and unvegetated sediments and is available for transport to the beaches under appropriate hydrodynamic conditions.

11.1.3 The physical properties of wrack and their implications for transport

The physical properties of wrack change dramatically during its life, with important implications for both its transport throughout Geographe Bay and the way it decomposes at sea and on the beaches. A range of physical properties of

wrack have been documented during the study, but those proving most relevant to transport and handling of wrack are the specific gravity, bulk density and tensile strength of wrack.

Fresh wrack is negatively buoyant and thus sinks in seawater, with leaves sinking more slowly than stems. Within the first few hours of detaching from the plant, the specific gravity of wrack increases, presumably as airspaces within the tissue become saturated. Thereafter, it remains relatively constant. The decomposition of wrack is a slow process and it is mainly the physical fragmentation through wave action that changes the dimensions of the particles. The most dramatic changes to the particles occur once they accumulate on beaches. Individual particles of *P. sinuosa* leaf and *A. antarctica* stems increase in density as they are exposed to air and age on the beach. Additionally, the accumulations themselves gradually compact under the action of wave energy and the weight of newly added wrack, causing an increase in the bulk density of the accumulations.

Small, thin piles of wrack have the greatest bulk density due to the greater proportion of sand worked into the accumulations. Excluding the contribution of sand, large wrack accumulations have a greater bulk density than small, thin piles, reflecting some compaction of the wrack and drying. As the bulk density increases, more energy is required to transport wrack accumulations off the beach, and this is considered further in Section 11.1.5, processes moving wrack on to and off beaches.

The tensile strength of wrack is relevant to the bypassing of wrack material through mechanical pumps. The maximum tensile strength observed was 33 mPa, for *A. antarctica* and 25 mPa for *P. sinuosa* leaves, and was higher for dry material found on the beach than for either fresh wrack or aged material that was wet. The greater tensile strength of dried material and of *Amphibolis* stems may need to be considered when conducting bypass pumping.

11.1.4 The lifecycle of wrack following its production in seagrass meadows

Annually, about 32,000 – 35,000 tonnes of wrack is produced from those nearshore seagrass meadows that are most likely to produce wrack that accumulates at Port Geographe. In this study, by the end of May, about 22,000 tonnes of this wrack had been produced, more than 98% of it located in the offshore habitats and 1.3% on the beaches. The wrack is negatively buoyant and sits on the seabed. Hydrodynamic tests showed that it requires water velocities in excess of 0.15 m s^{-1} to suspend fresh wrack into the water column, where it can subsequently be transported towards the beaches.

The first few storms of autumn and winter resulted in a large proportion of the wrack being removed from the offshore habitats and transported shoreward (process 2, Figure 11.1). A significant finding of the study is that the wrack does not roll along the seabed as large aggregations, but is largely transported as individual particles suspended in the water column. These suspended particles periodically settle causing the wrack to be distributed as fine sheets over the unvegetated sands between the offshore meadows and the beach, as they gradually move shorewards.

By July, there was a 150-fold increase in the amount of wrack accumulated on beaches compared to May, and an 80% decrease in the amount found in the offshore habitats. As winter progressed, the wrack increasingly accumulated on the beaches and in the surf-zone. Natural processes (see next section) periodically moved the wrack between the beach and the surf zone. While it was in the surf zone, longshore currents moved a large amount of the wrack to the east until it accumulated at Port Geographe and by late July about 97% of all the wrack on beaches in Geographe Bay study area was found at Port Geographe. About 46% of the wrack that was present offshore at the end of May could not be accounted for and was presumably transported out of the bay, either to the north-east or to deeper water, or was degraded through fragmentation and microbial decomposition over the autumn and winter.

11.1.5 The natural mechanisms that cause wrack to be deposited on and removed from beaches

Wrack was deposited onto beaches largely during storm events, when high water levels allowed the wrack to be lifted onto the beach where it was retained as water levels receded. As described earlier, the bulk density of this wrack subsequently increased, largely due to compaction and the incorporation of sand into the accumulations. The individual particles also dried during this period, unless they were within the saturated zone of wrack accumulations. At most beaches, these accumulations were temporary and the wrack was moved back offshore within a matter of days to weeks (process 3, Figure 11.1).

The process by which wrack is removed from beaches is complex, and the improved understanding of this process is a

significant outcome of this study that has allowed wrack movement to be modelled. Smaller, thin aggregations of wrack have a relatively lower bulk density and are likely to be transported off beaches when the water level reaches above the aggregations. Any sand trapped in the accumulation will be washed out, leaving a mass of leaf and stem particles. Experiments indicated that leaves that have dried on the beach, have a greater probability of floating on re-wetting, further contributing to their movement off-shore on inundation. Larger accumulations of wrack require more energy to be removed from the beach because of their high bulk density. Analysis of beach profiles showed that the high water mark regularly reached above the height where small, thin piles of wrack occur. However, with larger aggregations (> 1 m high) the water level was unlikely to move above the height of the aggregations, so a combination of water level increases and wave energy would be required to disrupt these large aggregations and remove the wrack from the beach. This typically occurs during storms or very windy conditions that coincide with spring tides. Analysis of beach accumulations, local meteorological and water level data has confirmed that the majority of wrack movements onto and off beaches occurred during storm and high water periods. Again, once particles are initially removed from the beach and into the water, a large proportion of them will float for up to 18 hours, facilitating their transport away from the beach.

11.1.6 The production of hydrogen sulfide on beaches

During the course of this study, it became apparent that the issue of hydrogen sulfide (H_2S) generation was a significant management issue associated with Port Geographe. Addressing the causes and possible management of this issue was not part of the original objectives of the study. However, at the request of the study's Steering Committee, the study objectives were revised to include this component.

The bacterial decomposition of seagrass wrack results in the release of gases as a by-product (process 4, Figure 11.1). Under conditions where oxygen is present (oxic) conditions, the main by-product is carbon dioxide, an odourless gas. When oxygen is not present (anoxic conditions), a range of different gaseous by-products can be produced depending on the precise chemical conditions, including hydrogen sulfide (H_2S; rotten egg gas). H_2S has an offensive odour and, at sufficiently high concentrations, can have significant adverse health effects.

Based on the reduction-oxidation potentials measured in the accumulations on Geographe Bay beaches, H_2S production is likely to be produced in larger wrack accumulations (> 0.5 m high) and when some or all of the wrack is in contact with water (i.e., in the saturated zone). In these accumulations, H_2S could accumulate within the wrack piles and flux out of the wrack through diffusion or when the accumulations are disturbed, as may occur during by-passing operations. Conditions suitable for H_2S production were also recorded around buried bands of wrack, about 15 - 45 cm below the sediment surface and in contact with the saturated zones. The levels of H_2S recorded within seagrass banks were highly variable but frequently very high, particularly in the large accumulations containing fresh wrack. The fluxes of H_2S from these accumulations were comparable to those recorded in other ecosystems, such as salt marshes. Controlling the redox conditions, by preventing the wrack from becoming saturated, may be an effective means of limiting H_2S production.

Experimental and field studies showed that as wrack ages the internal cellular material leaches out, including dissolved organic carbon (DOC). This DOC can support bacterial growth and without it H_2S is not produced. A significant finding of the study was that if an alternative (i.e. not from seagrass) source of carbon is provided, the conditions suitable for H_2S production occur, but the gas is not produced. This suggests that the seagrass itself is the source of the sulphur that is subsequently released as H_2S.

11.2 Management options

The current accumulation of seagrass wrack to the west of Port Geographe and the current management approach creates a number of management issues:

1. the loss of amenity and access to beaches west of the Port during the accumulation period and to the east of the entrance following bypassing operations. This loss of amenity includes visual impact, odours associated with the release of significant amounts of hydrogen sulfide (H_2S), noise and heavy vehicle movements associated with by-passing operations;

2. considerable financial cost of by-passing the wrack each year; and
3. the challenges of ensuring that the Port entrance is navigable at all times.

Fundamentally, these issues all relate to the presence of the large accumulations of wrack and sediment, which is a result of the coastal structures at Port Geographe preventing the normal process of wrack removal. Management should focus on those aspects of the lifecycle of wrack that can reduce the amount of wrack accumulating at Port Geographe (Figure 11.2).

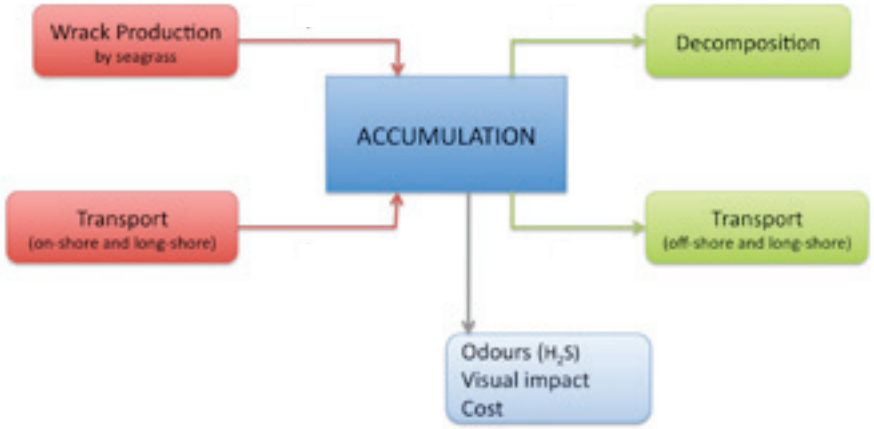

Figure 11.2 Factors influencing the accumulation of wrack at Port Geographe. The red boxes indicate factors leading to an increase in wrack accumulation; the green boxes indicate factors leading to a reduction in wrack accumulation.

Factors that influence the amount of accumulation at Port Geographe are:

1. the production of wrack: Wrack is produced in the offshore seagrass meadows. The constant shedding of mature leaves appears to account for most of the seagrass wrack that ultimately accumulates at Port Geographe. In addition, some leaves and whole clumps of meadow can be ripped out of the sediment during storm events.
2. the transport of wrack from the offshore meadows to Port Geographe: The first major storms of the autumn-winter period transport a large proportion of the off-shore wrack into the surf zone and onto the beaches of Geographe Bay. Beach-cast wrack can subsequently be transported back offshore, into the surf zone, where long-shore transport moves it eastwards until it is obstructed by the Port Geographe breakwater where the wrack accumulates.
3. the transport of wrack offshore and eastwards of the Port: Under high-energy and high water level conditions, wrack may be removed from beaches and transported off-shore. If it moves a sufficient distance offshore, it may be able to bypass Port Geographe.
4. the degradation of wrack: Wrack can be degraded, either through physical fragmentation or decomposition by microbes.

11.2.1 Possible management strategies

Management strategies should focus on the processes with the potential to decrease accumulation of wrack (1 & 2, above) or increase processes leading to the removal of wrack accumulations (3 & 4, above). The majority of effort in the background studies associated with this research has been directed at understanding the lifecycle of wrack so that each of these four components can be addressed. For completeness, this report presents options for addressing each of these components of the wrack life-cycle. In reality, however, there may be significant logistical or philosophical constraints that limit the capacity to manipulate these aspects of the wrack life-cycle, as discussed below. The options and any potential constraints to their implementation are summarised in Table 11.1.

Table 11.1 Summary of management approaches available to address the accumulation of wrack at Port Geographe, and key feasibility issues.

APPROACH	MANAGEMENT OPTION	TECHNIQUE	FEASIBILITY ISSUES
Reduce wrack production	Reduce area of seagrass	Dredging.	Environmentally unacceptable given the significance of the seagrass resource for Geographe Bay and the importance of wrack for natural beach ecosystems.
	Reduce leaf production	Reduce water clarity.	As above; No proven method.
Reduce transport to shore	Interception in offshore traps	Dredge interception trenches adjacent to meadows.	Not useful in winter due to re-suspension of wrack; Requires offshore harvesting & disposal of material, which is unlikely to be environmentally acceptable.
	Retardation of long-shore transport	Construct 'low-crested' groynes to intercept and retard wrack at a number (to be determined) of locations west of Port Geographe. Dispose offshore, higher up the beach profile or off site.	Community response to 'low cresting groynes'; Dispersal of (smaller) accumulations over many areas may be viewed either positively or negatively by local communities; Disposal of wrack: Moving the wrack to a higher location up the beach profile, to decompose, may not be feasible if no beach area is available. Relocation to a point higher on the beach may also reduce the recycling of nutrients back into Geographe Bay while off-site disposal will definitely have this affect.
	Interception of long-shore transport	Nets, regularly dragged and emptied offshore; Pump wrack from surf-zone; Floating harvester.	Logistically difficult with high labour costs; Issues of disposal, as above.
Enhance decomposition	Maintain oxygenated conditions in wrack	Aerate beach accumulations or drain the saturated zone to prevent anoxia (absence of oxygen).	Requires detailed design to determine appropriate aeration or drainage volumes; Protection of infrastructure: It will be necessary to protect the aeration or drainage pipes, pumps and other infrastructure from damage by heavy vehicles, storm action and erosion on the beaches; Amenity issues – the presence of the infrastructure necessary to provide aeration or drainage may limit public access or use of the beach areas.
	Enhance bacterial activity	Addition of nutrients and aerobic bacterial slurries; Aeration to increase oxygen availability.	Untested approach: This would require background research and development to determine the amount of aeration and promotion of bacterial growth that would optimize the rate of decomposition without causing a depletion of oxygen and the subsequent generation of H_2S.
Enhance natural bypassing	Groyne reconfiguration	Re-orient Port Geographe groynes and possibly construction of additional hard walls.	Cost; Community response to change in structural elements; Requires additional studies to analyse the implications for sand movement and water quality.
Reduce H_2S production	Maintain aerobic conditions in wrack	Aerate the saturated zone of wrack accumulations or drain the underlying saturated zone to prevent anoxia.	Requires detailed design to determine appropriate aeration or drainage volumes; Protection of infrastructure: It will be necessary to protect the aeration or drainage pipes, pumps and other infrastructure from damage by heavy vehicles, storm action and erosion on the beaches; Amenity issues: The presence of the infrastructure necessary to provide aeration or drainage may limit public access or use of the beach areas.
	Move wrack to higher part of beach profile	Excavate wrack to higher, dry portion of beach profile. Has similar effect as above.	Availability of sufficient beach area; Costs associated with handling of wrack; Amenity issue: Possible loss of amenity due to accumulations of wrack on higher portions of the beach profile.

11.2.1.1 Reducing wrack production

Options for reducing the production of wrack accumulation include reducing the area of seagrass or reducing the rate at which existing seagrass produces and sheds its leaves. This would have the effect of reducing the supply of wrack available to be deposited on beaches and subsequently be transported to Port Geographe. Reducing the area of seagrass could be achieved through direct removal (e.g. dredging), but would constitute a significant environmental impact likely to be deemed unacceptable. Similarly, while it may be possible to reduce the rate of leaf production, through shading or some other intervention, this too would likely be viewed as environmentally unacceptable. Seagrass production is an important component of healthy marine ecosystems and is of significant environmental value in Geographe Bay. Its importance extends to the beach ecosystems which are dependent on wrack inputs to sustain the biodiversity of beach fauna, and to contribute to the recycling of nutrients in what is naturally a very nutrient-poor ecosystem. In short, there is no means of reducing the production of wrack that is likely to be deemed environmentally acceptable.

11.2.1.2 Reducing the transport of wrack to beaches

Reducing the transport of wrack from offshore meadows and unvegetated areas to the beach and surf zone would decrease the pool of wrack available for subsequent long shore transport to Port Geographe. Two strategies could effect this:

- intercepting wrack as it move shorewards; and
- retardation and subsequent storage or removal of wrack at other beaches west of Port Geographe.

Interception

The most feasible way to intercept wrack as it travels from the offshore meadows to shore is through trench-like depressions that can trap bottom-moving wrack, akin to sediment traps, or some system of netting that could trap suspended material. Seagrass wrack moves along the seabed during calmer periods. The rate of movement appears to be slow and generally results in large accumulations of wrack in the unvegetated areas adjacent to the meadows, or in depressions within meadows. The most significant movement occurs during high-energy periods when the wrack resuspends and travels shoreward throughout the water column. Seabed wrack traps are likely to be unsuccessful during autumn-winter as most wrack will simply travel over the traps. Traps may be more effective during the summer period if they were located close to the meadows. This may allow a portion of the wrack production to be trapped in trenches, from where it could be dredged and disposed of further offshore or east of Port Geographe.

Another possibility is the use of nets to intercept wrack in longshore currents. An interception line of nets placed to the west of Port Geographe could be used to trap incoming wrack, which could then be removed offshore where currents would move the wrack past Port Geographe. This option would require regular servicing (possibly daily) of the nets during the wrack accumulation period. The cost-effectiveness is questionable and it may require significant effort to develop an effective operation.

Retardation and storage

Retarding the eastward movement of wrack towards Port Geographe would increase the time available for natural decomposition of the wrack or allow the wrack to be removed or stored, preventing the large scale accumulations currently occurring at the Port. The results from this study suggest that decomposition rates may be sufficiently high in the surf-zone during winter to produce a significant decrease in wrack volume over several weeks. Wrack could be retarded by the construction of low cresting groynes at points along the westward beaches. A number of beaches already have this type of groyne that, anecdotally, retards wrack without completely preventing the longshore movement of material. Once wrack is trapped or retarded it could subsequently be:

- left in place, allowing decomposition and physical degradation to occur in the surf-zone. Potential difficulties with this include the localised production of H_2S and loss of visual amenity;
- moved higher up the beach, out of the inter-tidal zone, and allowed to decompose, ensuring continued nutrient input to the local beach ecosystem. Potential issues associated with this strategy include the availability of space to deposit the wrack, and the removal of the wrack from the natural cycling processes in Geographe Bay,

potentially resulting in a loss of nutrient input to habitats that would normally receive the wrack;

- removed to landfill or other off-site users, with the same issue as above; or
- by-passed to the east of Port Geographe.

This would result in more dispersed and smaller wrack accumulations, and a smaller accumulation at Port Geographe. Smaller accumulations at westward beaches may be more manageable and the reduction in size and more gradual accumulation of wrack at Port Geographe may aid in implementing some of the H_2S and bypassing management options at the Port (see below). However, a number of potentially significant logistical and environmental issues would need to be considered, together with the potential impacts on amenity over a wider area.

11.2.1.3 Enhancing decomposition

Enhancing decomposition has the advantage that the end products are natural bacteria, nutrients, water and gases. If decomposition is performed under aerobic conditions, then the gases released are not noxious. Aerobic decomposition is also relatively rapid, thereby reducing the size of accumulations, facilitating both the return of amenity and a reduced need to bypass wrack, with associated cost-savings.

The degradation and decomposition of seagrass wrack was shown to be greatest in the offshore areas and slowest on beaches. This probably reflects the less conducive conditions for decomposition on beaches. Firstly, wrack high on the beach can dry out resulting in the death of bacteria. Secondly and more commonly, the wrack becomes compacted preventing the penetration of oxygen and may accumulate in areas with underlying saturated sediments. In these circumstances, relatively rapid aerobic decomposition is replaced by much slower anaerobic decomposition.

Enhancing the rate of decomposition would require managing the environmental condition to promote rapid, aerobic bacterial activity. The study did not specifically examine the conditions required to optimise seagrass decomposition. However, options include:

- aeration of the wrack (this would complement a later recommendation to minimise H_2S production);
- moving the wrack out of the saturated zone (e.g. higher up the beach) but maintaining moisture, possibly through periodic pumping of seawater onto the wrack; and
- manipulation of nutrient and bacterial supply to enhance bacterial activity.

Enhanced decomposition is a potentially useful area to explore for management of wrack accumulations. However, optimising conditions would require additional research. In the short term, it is probably most appropriate to implement other management strategies (see below) in a way that optimises decomposition rates, rather than focusing on decomposition as the principal strategy.

11.2.1.4 Enhancing natural bypassing

The Port Geographe groynes are the primary structural cause of the wrack accumulations west of the development and in the pocket beaches. Removing the structural cause of the problem is an obvious management approach to achieving a reduction in wrack accumulation, maintaining amenity in the areas currently affected by accumulations and ensuring a close to natural supply of seagrass wrack to beaches east of the Port. The principle approach to achieving this is to modify the coastal structures associated with the Port Geographe development so as to optimise the transport of wrack to the east of Port Geographe while maintaining satisfactory transport of sediment past the structure and maintaining acceptable water quality within the Port Geographe canals. The advantage of this management approach is that it may offer a sustainable and cost-effective solution requiring relatively minor on-going management.

This study has examined several re-configuration options for Port Geographe with respect to the passage of seagrass wrack. A series of different re-configuration scenarios were modelled, as described in Section 10. The rationale behind the choice of scenarios modelled is explained in Section 10, but in brief, alternative configurations previously proposed by M J Paul and Associates Pty Ltd [2005] were assessed; Option 3 and 6 from M J Paul and Associates Pty Ltd [2005] were simulated. As results from these simulations were inspected, an additional five refinements to the MJ Paul options were proposed by the Project Steering Committee. In total, simulations on seven separate configurations were run to assess the impact of the different configurations on seagrass wrack transport around Port Geographe. In general terms,

many coastal developments with structures on the beachfront have a high coastal maintenance requirement (including by-passing operation) that is a known and accepted ongoing requirement. The Port Geographe development was always known to have a significant coastal management aspect however the volumes of seagrass wrack now encountered were never anticipated.

The hydrodynamic and particle transport modeling showed that Scenario 5 (SC Option 3; Figure 10.52) was the optimal groyne configuration for improved management of seagrass wrack around Port Geographe. The main features of this option are:

- addition of a beach at the western part of marina, smoothing the transition from the current beach to the end of the breakwater;
- changing the orientation and length of the curved entrance groyne;
- changing the eastern breakwater to provide a convex shape;
- narrowing of the entrance channel width to increase the flow speed through the channel;
- curve the edges of the breakwater; and
- the inclusion of the full canal development.

It is critical to note that the modelling did not consider the implications of groyne re-configurations for the transport of sand past the entrance channel or for water quality within the Port Geographe canals. In that sense, the recommended scenario/configuration should be viewed as one option with the potential to address the wrack problem, but which must be subsequently evaluated in terms of effect on sediment transport and canal water quality. It is further recognised that the erosion and wrack problems occurring on the beaches at Wonnerup are intrinsically linked and affected by any management option proposed and, therefore, must be included in the further sediment modelling work.

11.2.1.5 Reducing H_2S Production

Implementing any re-configuration of the Port Geographe groynes will require a number of additional engineering assessments, design, approval processes and construction. During that time, wrack will continue to accumulate and produce H_2S emissions. It is also likely that a successful re-configuration of the coastal structures at Port Geographe will continue to have an ongoing coastal management requirement, though to a much smaller extent. As such, H_2S emission may continue to be an issue in the area. For these reasons, and in consideration of the public focus and potential health implications of H_2S emissions, improved management of H_2S is critical.

The study showed that H_2S emissions occurred from wrack accumulations that were wholly or partially saturated with water. These accumulations may be wholly or partially submerged, by either marine water or the groundwater table. Under these circumstances, the lower parts of the accumulation become anoxic and anaerobic decomposition of the wrack occurs. Bacteria convert sulphates in the marine water or the seagrass themselves to H_2S, which builds up within the overlying wrack pile and is then released to the atmosphere. Consequently, maintaining aerobic conditions within the wrack accumulations will prevent the formation, accumulation and release of H_2S.

Aerobic conditions can best be maintained in two ways:

- relocation of the wrack out of the saturated beach zone to a point higher up the beach profile; and
- aeration/drainage of the near-shore water and sediment in the area of wrack accumulation to prevent the formation of saturated zones within wrack accumulations.

A combination of both approaches may be required since relocation may be limited by the availability of space and the effectiveness of aeration is likely to increase with shallower accumulation depths. Existing data on the extent and timing of accumulations at Port Geographe should be sufficient to design the layout of an aeration system, though some additional investigations may be required to determine an appropriate pumping rate to achieve sediment and wrack aeration. A significant issue will be physical protection of the aeration system during bypassing operations, when truck and excavator movements could damage pipes.

11.3 Recommendations

Recommendation 1

It is recommended that the Port Geographe groynes be re-configured to ensure the adequate bypassing of wrack arriving at the western training wall.

Having contemplated a number of alternate management options this study considers that non-structural solutions are either unfeasible or impractical. Conversely, numerical modelling of a number of proposed options for structural change has indicated that significant improvements should be achievable.

This study has analysed options for physical changes to the Port Geographe groyne field (see Section 10). Scenario 5 is recommended as the optimum groyne configuration for wrack by-passing. However, the final re-configuration will need to optimise outcomes for wrack by-passing, sediment by-passing and water quality in Port Geographe canals. Consequently, the most promising scenario from a wrack by-passing perspective is recommended as a starting point for detailed design consideration, commencing with detailed sediment modelling. **Ultimately, the hydrodynamic, particle (seagrass wrack) transport and sediment models must be used together to identify the optimal groyne configuration for improved management of both seagrass wrack and sediment around Port Geographe.**

Recommendation 2

Associated with, and as a pre-requisite to any reconfiguration, additional studies should be undertaken to:

- determine the implications of the preferred groyne configurations to manage both sediment and wrack and also having regard to canal water quality; and
- to recommend the optimum re-configuration to achieve acceptable outcomes with respect to wrack and sediment bypassing and water quality in Port Geographe canals.

It is clear from the knowledge gained in this study that wrack particles are not transported in the same manner as sediment particles. Reconfiguration of the Port Geographe groyne to achieve wrack bypassing requires the removal of the large sediment trap that is engineered into the existing groyne structure. This will result in greater movement of sediment past the entrance channel, and it cannot be assumed that the sediment will be transported in the same manner as wrack. There is a possibility of deposition of seagrass wrack in the channel mouth or in areas further east. Similarly, the reconfiguration recommended for optimum wrack bypassing may require changes to the width and orientation of the entrance channel, with possible consequences for water exchange. This in turn may impact on water quality. The final reconfiguration needs to take into account all three of these factors. Otherwise, there is a risk that addressing the wrack problem may simply increase sediment deposition or degrade water quality in the port.

Two additional recommendations are made in recognition of the medium-long term nature of Recommendation 1. Implementing Recommendation 1 may take several years and in the intervening period, wrack will continue to accumulate at Port Geographe and requires management. Therefore, a number of short-term management options should be maintained or considered.

Recommendation 3

It is recommended that management of wrack accumulations to the west of Port Geographe and in the pocket beaches should continue until such time as Recommendation 1 has been implemented and any conditions attached to its implementation have been satisfied.

It is recommended that a number of modifications to the existing management be considered:

a. Consideration should be given to more continual bypassing of wrack during the typical accumulation period. Current practice is to allow deep accumulations to form over winter followed by bypassing in the non-accumulation period. This allows wrack to accumulate in forms optimal for the generation of H_2S. More regular bypassing will reduce the size of accumulations, maintain amenity and a more natural input of wrack to beaches east of Port Geographe;

b. Associated with more regular bypassing, relocation of wrack that is not bypassed, or which is accumulated during bypassing operations, to a position higher up the beach profile where the lower layers will not intersect the saturated zone.

Recommendation 4

It is recommended that short-term management of H_2S be implemented through:

a. Drainage/aeration of the areas in which wrack accumulates to prevent the creation of anoxic, saturated zones within wrack accumulations; or

b. The re-location of wrack to a position on the beach profile where it does not intercept the saturated zone (as per Recommendation 3). Consistent with (a) and (b), management practices which result in the storage of wrack in saturated conditions should be avioded; and

c. The monitoring of H_2S emissions from the wrack both following winter accumulation and during bypass operations should continue and be used to assist in informing wrack management decisions so as to have proper regard for community health concerns.

ACKNOWLEDGEMENTS

This project would not have been possible without the efforts, cooperation and collaboration of a large number of people.

The Study Team itself was large, comprising the team leaders, postdoctoral fellows, research assistants, postgraduate students and honours students: Cyprien Bosserelle (UWA), Brett Branco (UWA), Tony Chiffings (DHI), Adam Gartner (ECU), Stephanie Hancock (UWA), Yasha Hetzel (UWA), Paul Lavery (ECU), Carolyn Oldham (UWA), Kathryn McMahon (ECU), Michelle Newport (ECU), Chari Pattiaratchi (UWA), Morten Rugbjerg (DHI), Julia Weyers (UWA), Sarath Wijeratne (UWA), Candace Willison (ECU).

We also sincerely thank:

The community members who volunteered to take daily photographs of beaches for the qualitative assessment of wrack accumulations: Anna Gerner, Ron Glencross, Mike Godswell, Deirdre Herbert, Kaye Holland, Brian & Anne Kasten, Gilbert Matthews, Margaret Nixon, Naomi Smith, Andrei Souto, and Belinda Wallace. Also, Alan May and Daryl Green and numerous staff from the Busselton Jetty Interpretive Centre.

Geographe Bay Yacht Club and the Busselton Sea Search and Rescue Group who allowed webcams to be installed on their buildings to monitor beach wrack.

Members of the Steering Committee for valuable and constructive input throughout the duration of the study: - Cleve Flottmann, James Holder, Maureen Davin and Laura Dubczuk (Dept of Transport); Oliver Darby, Sharon Woodford-Jones and Andrei Souto (Shire of Busselton); Dale Olsson (Port Geographe Joint Venture); Stuart Barr (Shore Coastal); and Ray Steedman (GHD).

Brian Lucy and volunteers from the Busselton Volunteer Sea Search and Rescue who provided weather data collected from the Volunteer Sea Search and Rescue Building.

Judy Clarke and Peter Maccora from the Port Geographe Consultative Forum, who provided valuable feedback and a historical perspective on the issues at Port Geographe.

The numerous people who volunteered to assist with the extensive field work involved in the study, including: Wesley Alport, Rob Czarnik, Ute Goeft, Michael Herbst, Denise Lawson, Miguel Mateo and Gail McMahon.

The casual research staff who put in long hours on and under the waters of Geographe Bay: Anthony Bostock, Warren Chisolm, Edward Costello, Rob Czarnik, Tibaut de Bettinges, Samuel Dunn, David Holliday, Denise Lawson, Ashley Lemmon, Geoff Purvis, Abanie Raynal, Aldo Turco, Federico Vitteli, Paulo Vota and Candace Willison.

REFERENCES

Australian Hydrographic Office Australian National Tide Tables (Tidal Prediction).

Balasubramanian, N., and B. S. M. Kumar (1990), Extraction - Spectrophotometric Determination of Hydrogen Sulphide, *Analyst*, *115*, 859-863.

Barnes, P., M. Westera, G. A. Kendrick, and M. Cambridge (2008), Establishing benchmarks of seagrass communities and water quality in Geographe Bay, Western Australia, 113 pp, University of Western Australia, Perth.

Bodenbender, J., R. Wassmann, H. Papen, and H. Rennenberg (1999), Temporal and spatial variation of sulfur-gas-transfer between coastal marine sediments and the atmosphere, *Atmospheric Environment 33*, 3487-3502.

Bratbak, G. (1985), Bacterial Biovolume and Biomass Estimation, *Applied and Environmental Microbiology, 49*(6), 1488-1493.

Chow, C. W. K., R. Fabris, and M. Drikas (2004), A rapid fractionation technique to characterise natural organic matter for the optimisation of water treatment process, *Aqua - Journal of Water Supply: Research and Technology*, *53*, 85-92.

Church, J., G. Cresswell, and J. Godfrey (1989), The Leeuwin current, in *Poleward flows along eastern ocean boundaries*, edited by S. Neshyba, et al., pp. 230–254, Springer-Verlag, New York.

Cleveland, C. C., J. C. Neff, A. R. Townsend, and E. Hood (2004), Composition, Dynamics and Fate of Leached Dissolved Organic Matter in Terrestrial Ecosystems: Results from a Decomposition Experiment, *Ecosystems*, *7*, 275-285.

Collier, C. (2006), Characterisation of the seagrass, *Posidonia sinuosa*, responses to light availability, 225 pp, Joondalup.

Costanza, R., R. dArge, R. deGroot, S. Farber, M. Grasso, B. Hannon, K. Limburg, S. Naeem, R. V. Oneill, J. Paruelo, R. G. Raskin, P. Sutton, and M. vandenBelt (1997), The value of the world's ecosystem services and natural capital, *Nature*, *387*(6630), 253-260.

Coupland, G. T., C. M. Duarte, and D. I. Walker (2007), High Metabolic Rates in Beach Cast Communities, *Ecosystems*, *10*(8), 1341-1350.

DPI (2007), Research Tender: Research Study into Seagrass Wrack Movement at Geographe Bay. DPI 1062/07 31 pp.

Dugan, J., D. Hubbard, M. McCrary, and M. Pierson (2003), The response of macrofauna communities and shorebirds to macrophyte wrack subsidies on exposed sandy beaches of southern California. , *Estuarine Coastal & Shelf Science*, *58S*, 25-40.

Duhamel, S., and S. Jacquet (2006), Flow cytometric analysis of bacteria- and virus-like particles in lake sediments, *Journal of Microbiological Methods*, *64*, 316-332.

Eliot, I., and D. Clarke (1986), Minor storm impact on the beachface of a sheltered sandy beach, *Marine Geology*, *73*(1–2), 61–83.

Eliot, M., and C. Pattiaratchi (submitted), Remote forcing of water levels along the coast of southwest Australia by tropical cyclones, *Continental Shelf Research*.

Eun, S., D. R. Reinhart, C. D. Cooper, T. G. Townsend, and A. Faour (2007), Hydrogen sulfide flux measurements from construction and demolition debris (C&D) landfills, *Waste Management*, *27*(2), 220-227.

Fahrner, C. K., and C. B. Pattiaratchi (1994), The Physical Oceanography of Geographe Bay, Western Australia, Centre for Water Research, University of Western Australia.

Fandry, C., L. Leslie, and R. Steedman (1984), Kelvin-type coastal surges generated by tropical cyclones, *Journal of Physical Oceanography*, *14*(3), 582–593.

Felip, M., S. Andreatta, R. Sommaruga, V. Straskrabova, and J. Catalan (2007), Suitability of flow cytometry for estimating bacterial biovolume in natural plankton samples: Comparison with microscopy data, *Applied and Environmental Microbiology*, *73*, 4503-4514.

Gentilli, J. (1971), *Climates of Australia and New Zealand*, Elsevier, Amsterdam.

Gentilli, J. (1972), *Australian climate patterns*, Thomas Nelson, Melbourne.

Gersbach, G. H., C. B. Pattiaratchi, G. N. Ivey, and G. R. Cresswell (1999), Upwelling on the south-west coast of Australia - source of the Capes Current?, *Continental Shelf Research*, *19*(3), 363–400.

Godfrey, J., and K. Ridgway (1985), The large-scale environment of the poleward-flowing Leeuwin current, Western Australia: longshore steric height gradients, wind stresses, and geostrophic flow, *Journal of Physical Oceanography*, *15*(5), 481-495.

Hamon, B. (1966), Continental shelf waves and the effects of atmospheric pressure and wind stress on sea level, *Journal of Geophysical Research*, *71,* 2883–2893.

Hansen, J. (1984), Accumulation of Macrophyte Wrack Along Sandy Beaches in Western Australia: Biomass, Decomposition Rates and Significance in Supporting Nearshore Production, University of Western Australia, Perth.

Hemond, H., and E. Fechner (2000), *Chemical fate and transport in the environment*, Academic Press, San Diego.

Holmer, M., and R. Neilsen (2007), Effects of filamentous algal mats on sulfide invasion in eelgrass (*Zostera marina*) *Journal of Experimental Marine Biology and Ecology*, *353*(2), 245-252.

Holmer, M., O. Pedersen, D. Krause-Jensen, B. Olesen, M. Petersen, S. Schopmeyer, M. Koch, B. Lomstein, and H. Jensen (2009), Sulfide intrusion in the tropical seagrasses *Thalassia testudinum* and *Syringodium filiforme*, *Estuarine, coastal and shelf science*, *85*(2), 319.

Hughes, C. S. (2007), Origin and fate of plant derived dissolved organic matter in a Swan Coastal Plain wetland, 51 pp, University of Western Australia, Perth.

Huyer, A. (1990), Shelf circulation, in *The sea: ocean engineering science*, edited by B. Le Mehaute and D. Hanes, pp. 423–466, Wiley-Interscience, New York.

Ince, R., G. Hyndes, P. Lavery, and M. Vanderklift (2007), Marine macrophytes directly enhance abundances of sandy beach fauna through provision of food and habitat. *Estuarine Coastal & Shelf Science 74*, 77-86.

Kirkman, H., and G. A. Kendrick (1997), Ecological significance and commercial harvesting of drifting and beach-cast macro-algae and seagrasses in Australia: a review, *Journal of Applied Phycology*, *9*(4), 311-326.

Lavery, P., C. Pattiaratchi, C. Oldham, T. Chiffings, K. McMahon, B. Branco, J. Weyer, Y. Hetzel, M. Newport, and S. Hancock (2009), Research study into seagrass wrack movement in Geographe Bay. Report to WA Department of Transport., pp 171 pp.

Le Blond, P., and L. Mysak (1978), *Waves in the ocean*, Elsevier Science, New York.

Lemm, A. (1996), Offshore wave climate, Perth, Western Australia, University of Western Australia, Perth.

Lemm, A. J., B. J. Hegge, and G. Masselink (1999), Offshore wave climate, Perth (Western Australia), 1994-96, *Marine and Freshwater Research*, *50*(2), 95–102.

Lodge, J. P. (1989), *Methods of air sampling analysis*, Lewis, London, UK.

M J Paul and Associates Pty Ltd (2005), Port Geographe Coastal Management Study – an independent review of coastal aspects of the Port Geographe Marina Project. Report No. SW330-3301-056. Report prepared for Seaport Pty Ltd.

Mackey, P., C. Collier, and P. Lavery (2007), Effects of experimental reduction of light availability on the seagrass *Amphibolis griffithii*, *Marine Ecology Progress Series*, *342*, 117-126.

Marba, N., and D. I. Walker (1999), Growth, flowering, and population dynamics of temperate Western Australian seagrasses, *Marine Ecology-Progress Series*, *184*, 105-118.

Masselink, G., and C. B. Pattiaratchi (2001), Characteristics of the sea breeze system in Perth, Western Australia, and its effect on the nearshore wave climate, *Journal of Coastal Research*, *17*(1), 173–187.

McComb, A., and J. Davis (1993), Eutrophic waters of southwestern Australia, *Fertiliser Research*, *36*, 105-114.

McMahon, K., E. Young, S. Montgomery, J. Cosgrove, J. Wilshaw, and D. I. Walker (1997), Status of a shallow seagrass system, Geogrpahe Bay south-western Australia, *Journal of the Royal Society of Western Australia*, *80*, 255-262.

McMahon, K., and D. I. Walker (1998), Fate of seasonal, terrestrial nutrient inputs to a shallow seagrass dominated embayment, *Estuarine, Coastal and Shelf Science*, *46*, 15-25.

Noreika, S. (1995), Infragravity waves in Geographe Bay, Western Australia, University of Western Australia, Perth.

O'Callaghan, J., C. Pattiaratchi, and D. Hamilton (2007), The response of circulation and salinity in a micro-tidal estuary to sub-tidal oscillations in coastal sea surface elevation, *Continental Shelf Research*, *27*(14), 1947–1965.

Pariwono, J., J. Bye, and G. Lennon (1986), Long-period variations of sea-level in Australasia, *Geophysical Journal International*, *87*(1), 43–54.

Pattiaratchi, C., and S. Buchan (1991), Implications of long-term climate change for the Leeuwin current, *Journal of the Royal Society of Western Australia*, *74*, 133–140.

Pattiaratchi, C., B. Hegge, J. Gould, and I. Eliot (1997), Impact of sea-breeze activity on nearshore and foreshore processes in southwestern Australia, *Continental Shelf Research*, *17*(13), 1539–1560.

Pattiaratchi, C., and I. Eliot (2008), Sea level variability in south-west Australia: from hours to decades, paper presented at Thirty-first international coastal engineering conference, American Society of Civil Engineers.

Pearce, A., and C. Pattiaratchi (1999), The Capes Current: a summer countercurrent flowing past Cape Leeuwin and Cape Naturaliste, Western Australia, *Continental Shelf Research*, *19(*3), 401–420.

Porter, K. G., and Y. S. Feig (1980), The Use of DAPI for Identifying and Counting Aquatic Mircoflora, *Limnol. Oceanogr.*, *25*(5), 943-948.

Proudman, J. (1953), *Dynamical oceanography*, Methuen, London.

Provis, D., and R. Radok (1979), Sea-level oscillations along the Australian coast, *Australian Journal of Marine and Freshwater Research, 30*(3), 295–301.

Ridgway, K., and S. Condie (2004), The 5500-km-long boundary flow off western and southern Australia, *Journal of Geophysical Research—Oceans*, *109*.

Servais, P., C. Courties, P. Lebaron, and M. Troussellier (1999), Coupling Bacterial Activity Measurements with Cell Sorting by Flow Cytometry, *Mircobial Ecology*, *38,* 189-189.

Smagorinsky, J. (1963), General circulation experiments with the primitive equations, I. The basic experiment., *Monthly Weather Review*, *91*, 99-164.

Smith, R., A. Huyer, J. Godfrey, and J. Church (1991), The Leeuwin current off Western Australia, 1986–1987, *Journal of Physical Oceanography*, *21*(2), 323–345.

South West Development Commission (2009), Annual Report 2008-2009.

Steedman, R., and P. Craig (1983), Wind-driven circulation of Cockburn Sound, *Australian Journal of Marine and Freshwater Research*, *34(*1), 187–212.

Steudler, P. A., and B. J. Peterson (1984), Contribution of gaseous sulphur from salt marshes to the global sulphur cycle, *Nature*, *311*, 455-457.

Tang, Y., and R. Grimshaw (1995), A modal analysis of coastally trapped waves generated by tropical cyclones, *Journal of Physical Oceanography*, *25*(7), 1577–1598.

Thurman, E. M., and R. L. Malcolm (1981), Preparative isolation of aquatic humic substances, *Environmental Science and Technology*, *15*, 463-466.

UWA (2008), Flow Cytometric Analysis of Plankton Populations, 9 pp, University of Western Australia, Biomedical Imaging and Analysis Facility.

van Niel, K., K. Holmes, and B. Radford (2009), Seagrass Mapping Geographe Bay 2004-2007, 25 pp, University of Western Australia.

Walker, D., K. McMahon, J. Cosgrove, and R. Whittlemore (1995), Geographe Bay : Seagrass, algal and water quality studies. Summer 1993 - 1994. Report to Water Authority of Western Australia.

Walker, D. I., R. J. Lukatelich, and A. J. McComb (1987), Impacts of proposed developments on the benthic marine communities of Geographe Bay 12 pp, Environmental Protection Authority, Perth, Western Australia.

Walker, D. I., P. A. Hutchings, and F. E. Wells (1991), Seagrass, sediment and infauna - a comparison of *Posidonia australis*, *Posidonia sinuosa* and *Amphibolis antarctica* in Princess Royal Harbour, south-western Australia I. Seagrass biomass, productivity and contribution to sediments, In *The marine flora and fauna of Albany, Western Australia*, edited by F. W. Wells, *et al*., Western Australia Museum, Perth.

Wearne, G. (2000), The formation and maintenance of shoreface-attached sandbars in Geographe Bay, University of Western Australia, Perth.

Willmott, C. (1984), On the evaluation of model performance in physical geography, in *Spatial statistics and models,* edited by G. Gaile and C. Willmott, pp. 443–460, D Reidel Publishing Company, Dordrecht.

Seagrass Wrack Dynamics

The shallow waters of Geographe Bay support extensive seagrass beds that contribute large amounts of wrack (detached leaves and stems) to the local beaches, predominantly during winter. Along most of the coast, the wrack that collects on the beaches does not unduly affect the people that live close-by. However, at Port Geographe, a proportion of the wrack moving onshore is permanently trapped on the western side of the western training wall and in the two pocket beaches (Moonlight Bay). These accumulations, and the management interventions to remove them, have become major environmental and social issues, impacting severely on the amenity of the area for local residents. This study aimed to improve knowledge of seagrass wrack dynamics in Geographe Bay to inform the development of seagrass management approaches.